Utrecht University

Comparison of two-stage stochastic optimization and adaptive robust optimization for European day-ahead electricity market clearing

MASTER'S THESIS - MASTER ENERGY SCIENCE (GEO4-2510)

Joran van der Loo
Student number: 5696798| j.p.vanderloo@students.uu.nl

Supervisor & second reader :
Elena M. Fumagalli | e.m.fumagalli@uu.nl
Madeleine Gibescu | m.gibescu@uu.nl

Word count: 28,973 words

16-08-2023

Abstract

The current deterministic day ahead market clearing in wholesale electricity markets, which was constructed around dispatchable and controllable electricity from conventional producers, is in need of adaptation to address the increased uncertainty resulting from the integration of variable renewable energy sources. Through their stochastic nature, variable renewable energy sources are non-dispatchable and output cannot be controlled, potentially resulting in grid imbalances in cases of forecast errors. Two-stage stochastic optimization and Adaptive Robust optimization utilizing the Column-and-Constraint generation algorithm are proposed for the day ahead market clearing in a case study on the Dutch, French and German wholesale electricity markets. A framework of performance indicators is constructed to evaluate- and compare the models on their ability to maximize the social economic welfare, increase system security of supply and integrate variable renewable energy sources in the energy mix. The results of the case studies indicate an increased social economic welfare through improved system security by the proposed models, drastically reducing the occurrence of load shedding events. The stochastic model outperforms the robust formulation during the in-sample scenarios, however proving vulnerable to unexpected stochastic output realizations during the out-of-sample scenarios. The Robust model, showing the highest degree of system security of supply because of its conservative nature, significantly decreases the integration of variable renewable energy sources in the energy mix while requiring the highest amount of upward reserve capacity. Both proposed models indicate a need for increasing the upward reserve capacity in energy systems with high penetration of variable renewable energy sources, while decreasing the utilization of installed stochastic producer capacity. Results of the sensitivity analyses indicate an increased system security to unexpected output realizations of the stochastic model by increasing the in-sample size, although increasingly extended computational time was observed for solving the problem. The sensitivity analysis on the budget of uncertainty of the robust model showed a direct trade-off between integration of variable renewable energy sources and system security of supply, while a relationship between the distribution of installed stochastic producer capacity among the stochastic producers and the budget of uncertainty revealed potential market inequalities in real-world applications of this formulation.

Acknowledgments

I would like to express my special gratitude to my supervisor Dr. Elena M. Fumagalli for her direction and guidance during my master thesis. Your advice and comments helped me look critically through every part of my work and greatly improved my work.

In addition, I owe a great debt of gratitude to Lina Silva-Rodriguez, who invested a tremendous amount of time and effort to tutor me on uncertainty-based optimization techniques, provide feedback on my work and always be there for me to answer any questions I might have. I cannot underestimate the importance of your work during my thesis.

Finally, I would also like to give special thanks to my parents, brother and girlfriend for your listening ear, encouragement and support during my thesis. You all provided me with a solid foundation on which I could build and work.

Table of contents

1. Introduction

To mitigate the effects of climate change caused by the emission of greenhouse gasses, the electricity sector is transitioning from the use of fossil energy sources towards renewable energy sources (RES) [1]. After an initial slow start, signed commitments like the Paris Climate Agreement and the European New Green Deal have emphasized the need for implementation of RES and have committed to double the share of RES in the EU energy mix in the upcoming decade [2,3]. While the implementation of RES is becoming increasingly more cost competitive compared to fossil energy sources, the intermittent availability of variable renewable energy sources (VRES) provides challenges for the current electric power system [4].

To ensure a constant balance between supply and demand of electricity in a cost effective manner, the EU wholesale electricity market consists of interrelated sub-markets such as the forward market, the day-ahead (DA) market, the intraday (ID) market and the balancing market, each operating on an increasingly shorter time frame to real time (RT) [5]. Originally designed for conventional power plants, which can be readily scheduled and dispatched, the increased share of VRES brings along high degrees of uncertainty to the current deterministic electricity market. Renewable energy producers are unable to exactly predict power supply due to the variability and uncertainty of weather conditions, resulting in forecast errors. The scheduling programs made on the DA market need to be adjusted in the ID market or in the balancing market where expensive reserves are used, and, eventually leading to shedding demand or spilling renewable energy, with additional costs and market inefficiencies [6,7]. To successfully increase the share of VRES in the energy mix and ensure security of supply while offering affordable electricity for consumers, the current deterministic DA market clearing mechanism is in need of adaptation.

Several market clearing techniques have been proposed in literature to deal with the uncertainty of VRES. The first proposed uncertainty-based market clearing technique, stochastic optimization, aims to find an optimal solution by representing the probability distribution of the uncertain variables as a set of scenarios [7]. Two-stage stochastic optimization is a vastly applied optimization technique for DA market clearing under uncertainty [8-12], since the DA market clearing can be treated as a two-stage problem; the energy dispatch and reserve allocation corresponds to the first-stage (here-and-now decisions), while the second stage corresponds to the wait-and-see decisions made during real time operations when realization of uncertain output is known [13]. The use of two-stage stochastic optimization results in decreased operational costs [8,9] or increased social economic welfare (SEW) compared to the deterministic DA market clearing [11].

A second proposed uncertainty based market clearing technique utilizes robust optimization. Robust optimization addresses uncertainty by optimizing decision making while meeting requirements in the worst case scenario [13]. The conservative nature of this approach has limited the use of robust optimization mainly to unit commitment (UC) to ensure reliability of supply [14-16], however the technique has led to adaptations to apply adaptive robust optimization (ARO) to DA market clearing [17,18]. The main advantage of robust optimization is the flexibility in balancing conservativeness and performance, allowing the probabilistic protection of priori constraints to be decided. In addition, ARO ensures feasibility of the optimal solution for any realization of the uncertainty set, optimizing under realization of the worst-case scenario [19].

Several papers have utilized the combination of stochastic- and robust- optimization techniques [20-22], using the uncertainty distributions of VRES output for stochastic optimization while testing the risk probability of the results with robust optimization. By contrast, little research has focused on comparing the performance of stochastic- and robust optimization in DA market clearing [12]. More specifically, the existing body of literature is mainly focused on US electricity markets, which are

concerned with minimizing operational costs, compared to European electricity markets which are focused on maximizing SEW. Moreover, a clear framework of key performance indicators (KPIs) is currently missing in literature to compare both optimization techniques on different perspectives of performance. In order to compare and evaluate the performance of the Deterministic, Two-stage stochastic and ARO DA market clearing model in a real world application, three case studies will be conducted on the Dutch, French and German electricity wholesale markets. These countries are selected based on their different installed stochastic producer capacity, reserve capacities, market size and primary energy sources for electricity generation.

1.1 Aim and contributions

The aim of this study is to provide an overview and comparison of two-stage stochastic optimization and ARO for uncertainty-based DA market clearing in Europe. This work contributes to the state of the art by (1) formulating a two-stage stochastic and adaptive robust DA market clearing mechanism applicable to EU electricity markets, (2) developing a framework to compare uncertainty-based optimization techniques for application in the DA market and (3) implementing and comparing the aforementioned optimization techniques in a case study on the Dutch, French and German DA markets.

Specifically, the main research objective of this study is:

"to compare the performance of two-stage stochastic optimization and ARO for uncertainty-based DA market clearing in the Dutch, French and German electricity wholesale markets."

After describing the general characteristics of deterministic-, two-stage stochastic- and adaptive robust DA market clearing, this study will address the main research objective, by (i) providing a formulation of the proposed approaches suitable for the European DA markets, (ii) constructing a framework of key performance indicators (KPIs), (iii) collecting data and constructing scenarios representing the case studies and (iv) running the simulations and interpreting the results for the Dutch, French and German wholesale electricity markets.

2. Conceptual framework

This section provides a description of the current European electricity market in Section 2.1, followed by a description and literature review of the different DA market clearing optimization techniques in Section 2.2.

2.1 European electricity markets

In 1996, most EU member states initiated the liberalization of the electricity market to introduce market actors and competition. This shift from a vertically integrated market design allowed consumers to choose their suppliers and stimulated market actors to innovate to gain a competitive edge. EU electricity markets do not allow competition in transmission and distribution of electricity; a Transmission System Operator (TSO) has a legal monopoly position to utilize economies of scale and ensure reliable transmission and distribution of electricity [5].

While electricity can be sold on the forward market to ensure consumers and producers of reliable sources of electricity and revenue far ahead of RT, the first market mechanism to ensure balance between supply and demand starts in the DA market. Consumers and producers can submit bids to their region's power exchange (PX) containing the time, price and quantity of demand or supply of electricity. These bids are used to derive the market clearing price (MCP) after the gate closure time, which is set on 12:00 pm the day before.

For each time period, the PX places each demand bid on descending price order, while also placing each supply bid on ascending price order [23]. The intersection point at which demand and supply meet indicates the MCP; the uniform price that will be paid or received for each accepted bid. This market clearing mechanism ensures no market actor receives a lower- or pays a higher price compared to the submitted bidding price [23]. A visual representation is provided in Figure 1 below.

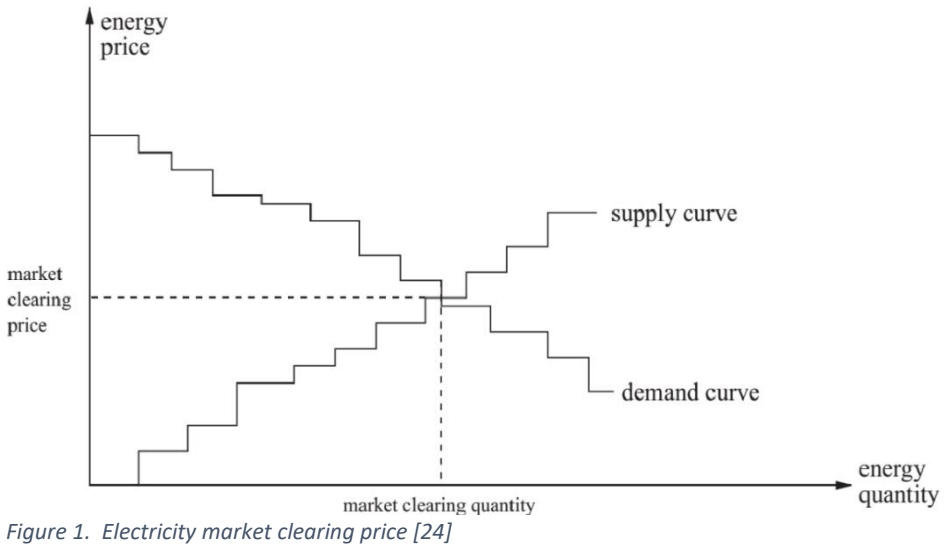

Figure 1. Electricity market clearing price [24]

While this market clearing mechanism ensures no market actor pays a higher price or receives a lower price for electricity compared to the submitted bid, the opposite however is true; the MCP can be lower than the accepted bid of buyers or higher than the accepted bid of sellers. Maximalization of this surplus of extra received value for market actors, called the SEW, is the primary objective of the

EU market clearing mechanism. After the MCP is known, the TSO computes the flows deriving from transmission- and generation dispatch to ensure system functioning [25].

In the intraday (ID) market, producers and consumers are able to optimize their schedule based on updated forecasts. The ID market, starting after gate closure of the DA market and closing up until an hour before RT, has seen a rise in prominence in recent years due to the increased implementation of VRES [26]. After gate closure of the ID market, the balancing market opens to ensure the balancing of supply and demand in RT to stabilize system frequency [27]. In EU electricity markets, balancing service providers (BSP's) are incentivized by the TSO to provide balancing services if ought necessary. Dispatchable producing units submit upward- or downward reserve procurement orders to signal their ability to increase or decrease their generation to the TSO. The TSO compensates BSPs for activating upward reserves, while BSPs reimburse the TSO when activating downward reserve capacity. Since the BSP's supply bid was initially accepted in the DA market, the BSP is compensated for its lost opportunity costs [28]. While a wide variety of different reserve-types exist, being able to activate on shorter time frames, extensive description of these reserves is beyond the scope of this research. The balancing market is the last of a sequence of the electricity markets to ensure security and stability of operations of the system.

2.1.1 Market integration: US vs. European markets

While a variety of operational differences between US and European electricity market exist, the differences in market integration underlie the focus in research on unit commitment (UC) in US markets and reserves allocation in European markets [29]. To support interpretation of the literature review in Section 2.2, this sub-section will highlight the beforementioned differences.

US DA market clearing is settled by pooling the energy- and reserve bids simultaneously, a joint market clearing, instead of the European sequential market clearing, which splits the two processes in different markets [30]. Joint markets are optimized by UC, which is used to determine the operation schedule of individual producing units to meet the varying demand loads. The system operator is responsible for determining the operation schedule based on the combined energy- and reserve bids [31]. Subsequentially, from the US system operator's perspective figuring out how to allocate supply and demand within the transmission boundaries in a cost effective manner is the main objective. In European markets, every connection to the electrical network is ought to have an appointed balance responsibility party (BRP), which is responsible for scheduling production capacities to balance demand and supply of their own portfolio. The schedules are communicated with the TSO, which is responsible for checking consistency in the planning. US electricity market based literature primarily focusses on UC and minimizing costs, while the literature on European markets is mainly focused on reserves allocation and maximizing SEW [29].

2.2 DA Market clearing mechanisms

In this section, a description and literature review of the market clearing techniques will be provided. Moreover, a general formulation of the two-stage stochastic- and adaptive robust market clearing models will be provided.

2.2.1 Deterministic DA market clearing

In a deterministic DA market, the demand- and supply bids are accepted to determine the MCP without taking into account deviations in output realization due to uncertainty [32]. Originally constructed for

controllable electricity generation from conventional producers, the deterministic DA market clearing model is still active in electricity markets [33]. Since deterministic DA market clearing does not take into account the uncertainty of realized output of RES, generation deviations in RT are addressed internally by stochastic producers in their market bids [17]. While the costs of imbalances are settled through financial penalties for liable market participants, grid stability issues result in additional costs for grid operators which lead to higher network charges for network users.

In this thesis, deterministic DA market clearing will be referred to as the Deterministic model and will be used as a baseline model to compare the robust- and two-stage stochastic DA market clearing models. The mathematical formulation of the deterministic model will be used as formulated by [17] and will be provided in Section 3.1.1.

2.2.2 Two-stage stochastic DA market clearing

As the name would likely suggest, a two stage stochastic optimization is applied in a situation in which decisions have to be made under uncertainty (the first stage), which result in the degree of corrective actions that have to be taken once all information is known (the second stage) [7]. Two-stage stochastic optimization is a widely applied optimization technique in DA market clearing, optimizing the energy- and reserve dispatch in the DA market (the first stage), taking into account the costs for imbalances during RT (the second stage). While high degrees of uncertainty are often limited to the output of stochastic producers, as is the case in [9,11], uncertainty in demand has been addressed in literature [34][35], as well as combining both short-term demand uncertainty and stochastic producer output uncertainty [8][36]. In this thesis, only uncertainty concerned with the output realization of stochastic producers will be addressed, a point which will be referred to later on in Section 3.3.1.3.

A general formulation of a two-stage stochastic optimization of European DA market clearing, derived from [7], is provided as follows:

$$\max\ b^T x - \sum_{\omega \in \Omega} \Phi_\omega c_\omega^T y_\omega \qquad (1.1)$$

In this general formulation (eq. 1.1), the objective function is trying to maximize the SEW (b^T) in the first stage minus the balancing costs (c_ω^T) during the second stage. While the decision variables of the first stage (accepted bid quantities and reserve capacities) are represented by vector x, which are deterministic in nature, the second stage decision variables (balancing reserves, wind spillage and demand shedding) are represented by vector y_ω, which are indeed subject to uncertainty. As mentioned earlier, the uncertainty of the output of the stochastic producers is accounted for by constructing a set of different scenarios (Ω). For each scenario in the set of scenarios $(\omega \in \Omega)$, a probability ϕ_ω is appointed, effectively acting like a weight for each scenario. Accordingly, realization of each scenario causes the second-stage decision variables y_ω to change, resulting in a different balancing cost c_ω^T. By summing the multiplication of the balance costs realized under the values of the second-stage decision variables with the scenario probability for each scenario, the solution will prove optimal under the weighted distribution of the possible scenarios. A detailed formulation of the two-stage stochastic model will be provided in Section 3.1.2.

Addressing both uncertainty in load demand and stochastic output realization, research by [8] found decreased operational costs and required reserve capacities when applying two-stage stochastic market clearing, while research by [10] observed reduced balancing costs. Noting a proposition for a

more structural change in DA market clearing, research by [12] found that the current market clearing mechanism should not clear expected stochastic production by default (i.e., the submitted bids), as this could lead to decrease market efficiency as well as diminished profits by stochastic producers. In this thesis, the two-stage stochastic model will be referred to as the Stochastic model.

2.2.3 Robust DA market clearing

Robust optimization is a field of optimization techniques applied for worst case analysis to realize the feasibility of uncertainty parameters or guarantee an objective value or distance from an objective value. While a diverse set of different techniques and applications of robust optimization are available in literature, the conservative nature of the technique (i.e., utilizing the worst case scenario) and the ability to apply parameter(s) to determine the degree of uncertainty to inspect the trade-off between system performance and protection against uncertainty are prevalent characteristics of the different techniques [37].

Robust optimization does not entail uncertainty according to a distribution of probabilities of scenarios, as is the case in stochastic optimization, but rather utilizes an uncertainty set, a range of uncertainty which can be flexibly parameterized to trade-off conservativeness and performance [15]. Unification of stochastic- and robust optimization techniques has been applied by [16], in which probability distributions have been used for scenario generation, which forms the adjustable boundaries of the uncertainty set.

Research by [18] introduced a two-stage robust optimization framework for DA market clearing, composing a *min-max-min* problem, minimizing the operating costs during the first decision phase, maximizing the realized uncertainty (the worst case) and again minimizing the dispatch costs in the second stage (RT). A reformulation of the robust optimization problem as provided by [18] will be proposed in this thesis. More specifically, the minimization of operating costs in the first decision stage will be reformulated to a maximization of SEW, as is the main objective of the EU electricity market. A general formulation is provided as:

$$min_x \; -B_x^T x - \; \mathfrak{D}_W(x) \tag{2.1}$$

In which:

$$\mathfrak{D}_W(x) = max_{\Delta W} \, min_y \, c_y^T y \tag{2.2}$$

In eq. 2.1, $B_x^T x$ indicates the SEW during the first decision stage representing the DA timeframe, entailing the decision variables in vector x. To remain close to the work by [18], please note that that the first stage is made negative to derive a min-problem, resulting likewise in a min-max-min problem. During the second stage, eq. 2.2, the uncertainty is realized under the max deviation of the realized stochastic output compared to the expected stochastic output ΔW. Under these maximized conditions, the worst case, balance costs are again minimized to maximize the resulting final SEW. A detailed formulation of the ARO model will be provided in Section 3.1.3.
In this thesis, the ARO model will be referred to as the Robust model.

3. Methodology

In this section, a description of the methodology used during this thesis is described. In Section 3.1, the mathematical formulation of the DA market clearing models is provided whereafter the KPIs used to measure the performance of the models are described in Section 3.2. The methods used for data collection and the construction of the datasets are provided in Section 3.3. Finally, a description of the approach to the data analysis and details on computational aspects are provided in Section 3.4 and Section 3.5.

3.1 Model formulation

The mathematical formulation of the deterministic model, stochastic model and Robust model will be provided in this sub-section.

3.1.1 Deterministic model formulation

The Deterministic model is formulated as follows:

$$max_{q^{DD}q^{DS}q^{DG}} \sum_{d\in D} q_d^{DD} * P_d - \sum_{g\in G} q_g^{DG} * P_g - \sum_{s\in S} q_s^{DS} * P_s - \sum_{g\in G} R_g^U * P_g^{RU} + R_g^D * P_g^{RD} \quad (3.1)$$

Subject to:

$$\sum_{d\in D} q_d^{DD} - \sum_{g\in G} q_g^{DG} - \sum_{s\in S} q_s^{DS} = 0, \quad (3.2)$$

$$q_g^{DG} + R_g^U \leq m_g^{DG}, \qquad \forall g \in \mathrm{G}, \quad (3.3)$$

$$q_g^{DG} \leq m_g^{DG}, \forall g \in \mathrm{G} \quad (3.4)$$

$$q_s^{DS} \leq m_s^{DS}, \forall s \in \mathrm{S} \quad (3.5)$$

$$q_g^{DG} - R_g^D \geq 0, \qquad \forall g \in \mathrm{G}, \quad (3.6)$$

$$R_g^U \leq R_g^{U,max}, \qquad \forall g \in \mathrm{G}, \quad (3.7)$$

$$R_g^D \leq R_g^{D,max}, \qquad \forall g \in \mathrm{G}, \quad (3.8)$$

$$\sum_{g \in G} R_g^U \geq Fixed_{country}^U, \qquad \forall g \in \mathrm{G},$$

(3.9)

$$\sum_{g \in G} R_g^D \geq Fixed_{country}^D, \quad \forall g \in \mathrm{G},$$

(3.10)

$$q_d^{DD} \geq 0 \; \forall d \in \mathrm{D}, q_g^{DG}, R_g^U, R_g^D \geq 0 \; \forall g \in \mathrm{G}, q_s^{DS} \geq 0 \; \forall s \in \mathrm{S}$$

(3.11)

Please note that some adaptations to the above provided formulation are made compared to the deterministic model as provided by [17]. The accepted demand quantities and conventional- and stochastic producer dispatch quantities are represented by q_d^{DS}, q_g^{DG}, q_s^{DS}. The parameters P_D, P_G, and P_S correspond to the bid prices, while m_d^{DD}, m_g^{DG} and m_s^{DS} are the submitted quantity bids of the market actors. The objective function eq. 3.1 maximizes the SEW, while equality constraint eq. 3.2 ensures balance between total supply and demand. A notable difference from [17] is the introduction of the upwards- and downwards reserve procurement represented by R_g^U and R_g^D, while the prices of reserve procurement are represented by P_g^{RU} and P_g^{RD}. Inequality constraints eq. 3.3-3.5 ensure that accepted bid quantities do not exceed submitted bid quantities for all market actors, while inequality constraints eq. 3.6-3.8 prevent reserve procurement exceeding the procurement capacities. Constraints eq. 3.9 and eq. 3.10 ensure the minimal amount of upward- and downward procurement of reserves. For each individual case study country, a fixed amount of upward- and downward reserve procurement will be determined (Section 3.3.2.1). Finally, non-negativity constraints for the accepted bids and procurement of reserves are represented in eq. 3.11.

Since the deterministic model does not take into account the possibility of imbalances, the model currently does not take into account reserve activation, wind spillage or load shedding events. After solving the objective function as provided in eq. 3.1, the solutions of the decision variables q_d^{DD}, q_g^{DG} and q_s^{DS} are inserted into the following second-stage deterministic model, which is formulated by:

$$min_{r_g^U, r_g^D, q_d^{shed}, q_s^{spill}} \sum_{g \epsilon G} r_g^U * P_g^{rU} - r_g^D * P_g^{rD} + \sum_{s \in S} P_s^{RS} * \left(q_{RT}^{DS} - q_s^{DS} - q_s^{spill}\right) + \sum_{d \in D} P_d^{shed} * q_d^{shed}$$

(3.12)

s.t.

$$\sum_{g \in G} r_g^U - r_g^D + \sum_{d \in D} q_d^{shed} + \sum_{s \in S} q_{RT}^{DS} - q_s^{DS} - q_s^{spill} = 0,$$

(3.13)

$$r_g^U \leq R_g^U, \qquad \forall g \in \mathrm{G},$$

(3.14)

$$r_g^D \leq R_g^D, \qquad \forall g \in \mathrm{G},$$

(3.15)

$$q_d^{shed} \leq q_d^{SD}, \qquad \forall d \in \mathrm{D},$$

(3.16)

$$q_{RT}^{spill} \leq q_s^{DS}, \qquad \forall s \in \mathrm{S},$$

(3.17)

$$R_g^U, R_g^D \geq 0, \forall g \in \mathrm{G};\ r_g^U, r_g^D \geq 0, \forall g \in \mathrm{G};\ q_s^{DS} \geq 0, \forall s \in \mathrm{S};$$
$$q_d^{shed} \geq 0, \forall d \in \mathrm{D};\ q_s^{spill} \geq 0, \forall s \in \mathrm{S}$$

(3.18)

In which decision variables r_g^U, r_g^D, q_d^{shed} and q_s^{spill} denote the quantities of upward- and downward reserve activation, shedding of demand and spillage of wind. Parameters P_g^{rU}, P_g^{rD} and P_d^{shed} represent the prices for upward- and downward reserve activation and the penalty for load shedding. Equality constraint eq. 3.13 balances supply and demand during RT. Inequality constraints eq. 3.14 and 3.15 ensure activation of reserves does not exceed procurement, while inequality constraints eq. 3.16 and 3.17 ensure load shedding- and wind spillage will not exceed the accepted quantities of demand bids and stochastic producer bids. Non-negativity constraints are represented in eq. 3.18. Finally, parameter q_{RT}^{DS} represents the realization of stochastic producer output. This value changes for each individual in-sample and out-of-sample scenario during the simulation runs.

3.1.2 Stochastic model formulation

The Stochastic model is formulated as follows:

$$max_{\delta_S} \sum_{d \in D} q_d^{SD} * P_d - \sum_{s \in S} q_s^{SS} * P_s^{SS} - \sum_{g \in G} \left[q_g^{SG} * P_g^{SG} + R_g^U * P_g^{RU} + R_g^D * P_g^{RD} \right] - \sum_{\omega \in \Omega} \Phi_\omega$$
$$* \left[\sum_g r_{g\omega}^U * P_g^{rU} - r_{g\omega}^D * P_g^{rD} + \sum_{s \in S} P_s^{SS} * \left[q_{s\omega}^{SS} - q_s^{SS} - q_{s\omega}^{spill} \right] + \sum_{d \in D} p_d^{shed} * q_{d\omega}^{shed} \right]$$

(4.1)

Subject to:

$$\sum_{d \in D} q_d^{SD} - \sum_{g \in G} q_g^{SG} - \sum_{s \in S} q_s^{SS} = 0,$$

(4.2)

$$q_d^{SD} \leq m_d^{SD}, \qquad \forall d \in \mathrm{D},$$

(4.3)

$$q_s^{SS} \leq m_s^{SS}, \qquad \forall s \in \mathrm{S},$$

(4.4)

$$q_g^{SG} + R_g^U \leq m_g^{SG}, \qquad \forall g \in \mathrm{G},$$

(4.5)

$$q_g^{SG} - R_g^D \geq 0, \qquad \forall g \in \mathrm{G},$$

(4.6)

$$R_g^U \leq R_g^{U,max}, \qquad \forall g \in \mathrm{G},$$

(4.7)

$$R_g^D \leq R_g^{D,max}, \qquad \forall g \in \mathrm{G},$$

(4.8)

$$r_{g\omega}^U \leq R_g^U, \qquad \forall \omega \in \Omega, \forall g \in \mathrm{G},$$

(4.9)

$$r_{g\omega}^D \leq R_g^D, \qquad \forall \omega \in \Omega, \forall g \in \mathrm{G},$$

(4.10)

$$q_{d\omega}^{shed} \leq q_d^{SD}, \qquad \forall \omega \in \Omega, \forall d \in \mathrm{D},$$

(4.11)

$$q_{s\omega}^{spill} \leq q_{s\omega}^{SS}, \qquad \forall \omega \in \Omega, \forall s \in \mathrm{S},$$

(4.12)

$$\sum_{g \in G} r_{g\omega}^U - r_{g\omega}^D + \sum_{d \in D} q_{d\omega}^{shed} + \sum_{s \in S} q_{s\omega}^{SS} - q_s^{SS} - q_{s\omega}^{spill} = 0, \qquad \forall \omega \in \Omega$$

(4.13)

$$q_d^{SD} \geq 0, \forall d \in \mathrm{D};\ q_g^{SG}, R_g^U, R_g^D \geq 0, \forall g \in \mathrm{G};\ r_{g\omega}^U, r_{g\omega}^D \geq 0, \forall g \in \mathrm{G}, \forall \omega \in \Omega;\ q_s^{SS} \geq 0, \forall s \in \mathrm{S};$$
$$q_{d\omega}^{shed} \geq 0, \forall d \in \mathrm{D}, \forall \omega \in \Omega;\ q_{s\omega}^{spill} \geq 0, \forall s \in \mathrm{S}, \forall \omega \in \Omega$$

(4.14)

The objective function (eq. 4.1) maximizes the SEW, having a similar framework as described in eq. 2.1. A notable difference from the robust optimization model is the notion of q_s^{SS} and $q_{s\omega}^{SS}$; while q_s^{SS} indicates the accepted bid quantity of stochastic producer s, $q_{s\omega}^{SS}$ indicates the realized output under scenario ω, which is indicated as the deviation Δq_s^{RS} in the robust model.

Constraints eq. 4.2-4.4 serve the same purpose as in the deterministic model, while constraints eq. 4.5 and 4.6 ensure submitted bids are not exceeded when using reserves. Additional costs subtracted from the SEW in the second stage constitute of the costs of the use of balance reserves r_g^U and r_g^D at their price P_g^r, deviations from stochastic producers minus the wind spillage q_s^{spill} and the cost of demand load shedding. Eq. 4.7-4.10 ensure the procurement and activation of reserves do not exceed the maximum reserve capacity, while eq. 4.11 and 4.12 ensure shedding- or spillage events do not exceed accepted bid demands of consumers or realized output of stochastic producers. Equality constraint eq. 4.13 ensures supply and demand are balanced during the second-stage. Non-negativity constraints are displayed in eq. 4.14.

The decision variables of the objective function constitute of:

$$\delta_S = \left\{R_g^U, R_g^D, r_{g\omega}^U, r_{g\omega}^D, q_d^{SD}, q_g^{SG}, q_s^{SS}, q_{s\omega}^{spill}, q_{d\omega}^{shed}, \forall \omega \in \Omega, \forall g \in \mathrm{G}, \forall d \in \mathrm{D}, \forall s \in \mathrm{S}\right\}$$

3.1.3 Robust model formulation

The Robust model is formulated as follows:

$$\begin{aligned} min_{\Xi^B} \sum_{s\in S} q_s^{RS} * P_s^{RS} + \sum_{g\in G} q_g^{RG} * P_g^{RG} + R_g^U * P_g^{RU} + R_g^D * P_g^{RD} - \sum_{d\in D} q_d^{RD} * P_d \\ - max_{\Delta q_s^{RS}} \; min_{\Xi^C} \sum_{g\in G} r_g^U * P_g^{rU} - r_g^D * P_g^{rD} \\ + \sum_{s\in S} P_s^{RS} * \left(\Delta q_s^{RS} - q_s^{spill}\right) + \sum_{d\in D} P_d^{shed} * q_d^{shed} \end{aligned} \quad (5.1)$$

Subject to:

$$\sum_{d\in D} q_d^{RD} - \sum_{g\in G} q_g^{RG} - \sum_{s\in S} q_s^{RS} = 0, \quad (5.2)$$

$$q_d^{RD} \leq m_d^{RD} \quad \forall d \in \mathrm{D}, \quad (5.3)$$

$$q_s^{RS} \leq m_s^{RS} \quad \forall s \in \mathrm{S}, \quad (5.4)$$

$$q_g^{RG} + R_g^U \leq m_g^{RG} \quad \forall g \in \mathrm{G}, \quad (5.5)$$

$$q_g^{RG} - R_g^D \geq 0 \quad \forall g \in \mathrm{G}, \quad (5.6)$$

$$R_g^U \leq R_g^{U,max} \quad \forall g \in \mathrm{G}, \quad (5.7)$$

$$R_g^D \leq R_g^{D,max} \quad \forall g \in \mathrm{G}, \quad (5.8)$$

$$r_g^U \leq R_g^U \quad \forall g \in \mathrm{G}, \quad (5.9)$$

$$r_g^D \leq R_g^D \quad \forall g \in \mathrm{G}, \quad (5.10)$$

$$q_d^{shed} \leq q_d^{RD} \quad \forall d \in \mathrm{D},$$

(5.11)

$$q_s^{spill} \leq q_s^{RS} + \Delta q_s^{RS} \quad \forall s \in \mathrm{S},$$

(5.12)

$$\sum_{g \in G} r_g^U + r_g^D + \sum_{s \in S} \Delta q_s^{RS} - q_s^{spill} + \sum_{d \in D} q_d^{shed} = 0$$

(5.13)

$$q_d^{SD} \geq 0, \forall d \in \mathrm{D};\ q_g^{SG}, R_g^U, R_g^D \geq 0, \forall g \in \mathrm{G};\ r_g^U, r_g^D \geq 0, \forall g \in \mathrm{G};\ q_s^{SS} \geq 0, \forall s \in \mathrm{S};$$
$$q_d^{shed} \geq 0, \forall d \in \mathrm{D};\ q_s^{spill} \geq 0, \forall s \in \mathrm{S};$$

(5.14)

The objective function (eq. 5.1), different as described in section 2.2.3, contains a *min-max-min* problem. The work by [18], which was used as a guideline for formulating the Robust model, is constructed to minimize the total costs of the production units in the dispatch problem. The resulting problem is therefore a *min-max-min* problem. To remain close to the used guideline, the first-stage of the objective function (eq. 5.1) is rewritten as a minimization problem by multiplying it by -1. The formulation of the adaptive robust model is similar to the formulation of the Stochastic model with one notable difference; the addition of Δq_s^{RS}, which represents the deviation of the realized output in RT compared to the expected output. The variables are used in the equality constraints eq. 5.2 and 5.13 and in the inequality constraint eq. 5.12.

The decision variables of the first- and second-stage constitute of:

$$\Xi^B = \{R_g^U, R_g^D, q_d^{RD}, q_g^{RG}, q_s^{RS}, \quad \forall g \in \mathrm{G}, \forall d \in \mathrm{D}, \forall s \in \mathrm{S}\}$$

$$\Xi^C = \{r_g^U, r_g^D, q_d^{shed}, q_s^{spill}, \ \forall g \in \mathrm{G}, \forall d \in \mathrm{D}, \forall s \in \mathrm{S}\}$$

The uncertainty set is characterized by:

$$|\Delta q_s^{RS}| \leq \Delta q_s^{RS,max} \quad \forall s \in \mathrm{S}$$

(5.15)

$$\sum_{q \in G} \frac{|\Delta q_s^{RS}|}{\Delta q_s^{RS,max}} \leq \Gamma$$

(5.16)

In which Γ acts as the budget of uncertainty, allowing the range of the uncertainty set to be manually determined (eq. 5.16). Constraint eq. 5.15 ensures that the realized deviation in stochastic output does not exceed the maximum deviation $\Delta q_s^{RS,max}$.

Despite including two stages in the model, namely the DA- and RT-stage, the ARO objective function as depicted in eq. 5.1 contains three optimization problems in the form of *min-max-min*, called a tri-level optimization problem. Solving a tri-level optimization problem is complex and computationally

challenging and established solution algorithms are only applicable to very restricted classes of problems, most not guaranteeing global optimality [41].
A solution algorithm to linear ARO problems was proposed in [42], dubbed the *column-and-constraint generation* (C&CG) algorithm, as an alternative to the already established Benders-dual cutting plane algorithm. The C&CG algorithm was found to require exponentially less computational time compared to the Benders-dual cutting plane algorithm with increasing problem size (i.e., size of the data to compute), making the algorithm more suitable for a market clearing optimization model with a large number of market participants.

A detailed general step-wise guide to formulating the C&CG algorithm is provided by both [42] and [43]. Being first published in [42], the C&CG algorithm is described in a more conceptual manner in the article; in [43], the C&CG algorithm is applied to a non-convex UC problem. Although both articles have established a mathematically sound description of applying the C&CG algorithm to different optimization problems, this section will follow with a step-wise guide to applying the C&CG algorithm to the EU market clearing problem without falling into repetition.

Step 1. Assigning dual variables to the inner min-problem

To distinguish between the three stages, the first-stage is referred to as the *outer-problem*, while the second- and third-stage problems are referred to as the *inner-problem*. Since the inner-problem is of a *max-min* form, it is not solvable within a single stage. A method to work around this problem is formulating the dual problem of the inner min-problem, which will become a max-problem. The first step in deriving the dual problem of the inner min-problem is assigning dual variables to the inequality constraints (μ) and equality constraints (λ) of the inner min problem, acting as penalty variables for exceedance of constraints. The inner min-problem is formulated as follows:

$$min_{\Xi^C} \sum_{g \epsilon G} r_g^U * P_g^{rU} - r_g^D * P_g^{rD} + \sum_{s \in S} P_s^{RS} * \left(\Delta q_s^{RS} - q_s^{spill}\right) + \sum_{d \in D} P_d^{shed} * q_d^{shed} \quad (5.17)$$

s.t.

$$r_g^U - R_g^U \leq 0 \quad \forall g \in \mathrm{G}, \quad : \mu_{1_g} \quad (5.18)$$

$$r_g^D - R_g^D \leq 0 \quad \forall g \in \mathrm{G}, \quad : \mu_{2_g} \quad (5.19)$$

$$q_d^{shed} - q_d^{RD} \leq 0 \quad \forall d \in \mathrm{D}, \quad : \mu_{3_d} \quad (5.20)$$

$$q_s^{spill} - (q_s^{RS} + \Delta q_s^{RS}) \leq 0 \quad : \mu_{4_s} \quad \forall s \in \mathrm{S}, \quad (5.21)$$

$$\sum_{g \in G} r_g^U - r_g^D + \sum_{s \in S} \Delta q_s^{RS} - q_s^{spill} + \sum_{d \in D} q_d^{shed} = 0 \quad : \lambda \quad (5.22)$$

$$-r_g^U, -r_g^D \leq 0 \quad : \mu_{5_g}, \mu_{6_g} \quad , \forall g \in \mathrm{G}$$

$$-q_d^{shed} \leq 0 \quad : \mu_{7_d} \quad , \forall d \in \mathrm{D}$$

$$-q_s^{spill} \leq 0 \quad : \mu_{8_s} \quad , \forall s \in \mathrm{S}$$

(5.23)

In which:

$$\Xi^C = \{r_g^U, r_g^D, q_d^{shed}, q_s^{spill}, \ \forall g \in \mathrm{G}, \forall d \in \mathrm{D}, \forall s \in \mathrm{S}\}$$

(5.24)

Please note that inequality constraints are made ≤ 0 when assigning their dual variables μ. Likewise, non-negativity constraints (eq. 5.23) are made negative.

Step 2. Formulating the Lagrangian function of the inner min-problem

The next step is to formulate the Lagrangian function, being denoted with $\mathcal{L}$. The Lagrangian function is derived by adding the multiplication of the dual variables with their respective constraints to the objective function, resulting in a single function to find local maxima and minima while being subject to the constraints. The Lagrangian function is formulated as follows:

$$\begin{aligned}\mathcal{L}\left(\Xi^C, \mu_{1_g}, \mu_{2_g}, \mu_{3_d}, \mu_{4_s}, \mu_{5_g}, \mu_{6_g}, \mu_{7_d}, \mu_{8_s}, \lambda\right) \\ = \sum_{g \epsilon G} r_g^U * P_g^{rU} - r_g^D * P_g^{rD} + \sum_{s \epsilon S} P_s^{RS} * \left(\Delta q_s^{RS} - q_s^{spill}\right) + \sum_{d \epsilon D} P_d^{shed} * q_d^{shed} \\ + \sum_{g \epsilon G} \mu_{1_g}\left(r_g^U - R_g^U\right) + \sum_{g \epsilon G} \mu_{2_g}\left(r_g^D - R_g^D\right) + \sum_{d \epsilon D} \mu_{3_d}\left(q_d^{shed} - q_d^{RD}\right) \\ + \sum_{s \epsilon S} \mu_{4_s}\left(q_s^{spill} - (q_s^{RS} + \Delta q_s^{RS})\right) - \sum_{g \epsilon G} \mu_{5_g} * r_g^U - \sum_{g \epsilon G} \mu_{6_g} * r_g^D - \sum_{d \epsilon D} \mu_{7_d} * q_d^{shed} \\ - \sum_{s \epsilon S} \mu_{8_s} * q_s^{spill} + \lambda(\sum_{g \epsilon G} r_g^U - r_g^D + \sum_{s \epsilon S} \Delta q_s^{RS} - q_s^{spill} + \sum_{d \epsilon D} q_d^{shed})\end{aligned}$$

(5.25)

Step 3. Derive the Karush-Kuhn-Tucker Conditions

The resulting eq. 5.25 is an unconstrained optimization problem, which can be used to find the maximum and minimum of a differentiable function and subsequently to find a saddle-point within the feasible set of solutions [44]. The Karush-Kuhn-Tucker (KKT) conditions, a set of first order derivative tests, can be used to prove an optimal solution in nonlinear-programming. Due to their extensive presence in literature, this research will not completely elaborate on the KKT conditions; a detailed explanation and proof on the KKT conditions can be found in [45], [46], [47].

The KKT conditions include *stationarity*, *primal feasibility*, *dual feasibility* and *complementary slackness* for the local optimum and the optimization problem. The first step in obtaining the KKT conditions is setting the Lagrangian gradients equal to zero. This results in the following stationary conditions:

$$\frac{\partial \mathcal{L}(\Xi^C, \mu_{1_g}, \mu_{2_g}, \mu_{3_d}, \mu_{4_s}, \mu_{5_g}, \mu_{6_g}, \mu_{7_d}, \mu_{8_s}, \lambda)}{\partial r_g^U} = P_g^{rU} + \mu_{1_g} - \mu_{5_g} + \lambda = 0, \quad \forall g \in \mathrm{G}$$

(5.26)

$$\frac{\partial \mathcal{L}(\Xi^C, \mu_{1_g}, \mu_{2_g}, \mu_{3_d}, \mu_{4_s}, \mu_{5_g}, \mu_{6_g}, \mu_{7_d}, \mu_{8_s}, \lambda)}{\partial r_g^D} = -P_g^{rD} + \mu_{2_g} - \mu_{6_g} - \lambda = 0, \quad \forall g \in \mathrm{G}$$

(5.27)

$$\frac{\partial \mathcal{L}(\Xi^C, \mu_{1_g}, \mu_{2_g}, \mu_{3_d}, \mu_{4_s}, \mu_{5_g}, \mu_{6_g}, \mu_{7_d}, \mu_{8_s}, \lambda)}{\partial q_d^{shed}} = P_d^{shed} + \mu_{3_d} - \mu_{7_d} + \lambda = 0, \quad \forall d \in \mathrm{D}$$

(5.28)

$$\frac{\partial \mathcal{L}(\Xi^C, \mu_{1_g}, \mu_{2_g}, \mu_{3_d}, \mu_{4_s}, \mu_{5_g}, \mu_{6_g}, \mu_{7_d}, \mu_{8_s}, \lambda)}{\partial q_s^{spill}} = -P_s^{RS} + \mu_{4_s} - \mu_{8_s} - \lambda = 0, \quad \forall s \in \mathrm{S}$$

(5.29)

Secondly, the complementary conditions have to be derived from inequality constraints eq. 5.18-5.23 and their respective dual variables. Also, the KKT condition *dual feasibility* implies non-negativity for all involved inequality constraints. From both conditions, the following complementary conditions can be derived:

$$0 \leq R_g^U - r_g^U \perp \mu_{1_g} \geq 0, \quad \forall g \in \mathrm{G}$$

(5.30)

$$0 \leq R_g^D - r_g^D \perp \mu_{2_g} \geq 0, \quad \forall g \in \mathrm{G}$$

(5.31)

$$0 \leq q_d^{RD} - q_d^{shed} \perp \mu_{3_d} \geq 0, \quad \forall d \in \mathrm{D}$$

(5.32)

$$0 \leq \left(\widehat{q_s^{RS}} + \Delta q_s^{RS}\right) - q_s^{spill} \perp \mu_{4_s} \geq 0, \quad \forall s \in \mathrm{S}$$

(5.33)

$$0 \leq r_g^U \perp \mu_{5_g} \geq 0, \quad \forall g \in \mathrm{G}$$

(5.34)

$$0 \leq r_g^D \perp \mu_{6_g} \geq 0, \quad \forall g \in \mathrm{G}$$

(5.35)

$$0 \leq q_d^{shed} \perp \mu_{7_d} \geq 0, \quad \forall d \in \mathrm{D}$$

(5.36)

$$0 \leq q_s^{spill} \perp \mu_{8_s} \geq 0, \quad \forall s \in \mathrm{S}$$

(5.37)

The total number of dual variables (and thus decision variables) in the dual problem can be reduced by rewriting the partial derivatives (eq. 5.26-5.29). The dual variables $\mu_{5_g}, \mu_{6_g}, \mu_{7_d}$ and μ_{8_s} can be rewritten as follows:

$$\mu_{5_g} = P_g^{rU} + \mu_{1_g} + \lambda, \quad \forall g \in \mathrm{G}$$

(5.38)

$$\mu_{6_g} = -P_g^{rD} + \mu_{2_g} - \lambda, \quad \forall g \in \mathrm{G}$$

(5.39)

$$\mu_{7_d} = P_d^{shed} + \mu_{3_d} + \lambda, \quad \forall d \in \mathrm{D}$$

(5.40)

$$\mu_{8_s} = -P_s^{RS} + \mu_{4_s} - \lambda, \quad \forall s \in \mathrm{S}$$

(5.41)

Since $\mu_{5_g}, \mu_{6_g}, \mu_{7_d}$ and μ_{8_s} are non-negative, as provided by eq. 5.34-5.37, they can be excluded from the model formulation as depicted in eq. 5.38-5.41 by simply making the equations non-negative as follows:

$$0 \leq r_g^U \perp P_g^{rU} + \mu_{1_g} + \lambda \geq 0, \quad \forall g \in \mathrm{G}$$

(5.42)

$$0 \leq r_g^D \perp -P_g^{rD} + \mu_{2_g} - \lambda \geq 0, \quad \forall g \in \mathrm{G}$$

(5.43)

$$0 \leq q_d^{shed} \perp P_d^{shed} + \mu_{3_d} + \lambda \geq 0, \quad \forall d \in \mathrm{D}$$

(5.44)

$$0 \leq q_s^{spill} \perp -P_s^{RS} + \mu_{4_s} - \lambda \geq 0, \quad \forall s \in \mathrm{S}$$

(5.45)

$$P_g^{rU} + \mu_{1_g} + \lambda \geq 0 \quad , \forall g \in G$$

(5.46)

$$-P_g^{rD} + \mu_{2_g} - \lambda \geq 0 \quad , \forall g \in G$$

(5.47)

$$P_d^{shed} + \mu_{3_d} + \lambda \geq 0 \quad , \forall d \in D$$

(5.48)

$$-P_s^{RS} + \mu_{4_s} - \lambda \geq 0 \quad , \forall s \in S$$

(5.49)

The final KKT condition, *primal feasibility* simply tells us that every solution must satisfy the constraints in the primal problem (eq. 5.2-5.14).

Step 4. derive the dual of the inner problem

Havin derived the KKT conditions, the next step involves deriving the dual problem (or simply *dual*) of the inner problem. The dual problem of the inner problem can be obtained by removing the decision variables and parameters of the *outer problem* from the Lagrangian function (eq. 5.25), which are seen in the inner problem as constants. Secondly, the complementary conditions eq. 5.46-5.49 are used as constraints of the dual problem, while the *dual feasibility* conditions ensure non-negativity for the inequality dual variables. This results in the following dual inner-problem:

$$max_{\mu_{1_g},\mu_{2_g},\mu_{3_d},\mu_{4_s},\lambda} \ \lambda \sum_{s\in S} \Delta q_s^{RS} - \sum_{g\in G} \mu_{1_g} * R_g^U + \mu_{2_g} * R_g^D - \sum_{d\in D} \mu_{3_d} * q_d^{RD} - \sum_{s\in S} \mu_{4_s}(q_s^{RS} + \Delta q_s^{RS}) \quad (5.50)$$

s.t.

$$P_g^{rU} + \mu_{1_g} + \lambda \geq 0 \quad , \forall g \in G \quad (5.51)$$

$$-P_g^{rD} + \mu_{2_g} - \lambda \geq 0 \quad , \forall g \in G \quad (5.52)$$

$$P_d^{shed} + \mu_{3_d} + \lambda \geq 0 \quad , \forall d \in D \quad (5.53)$$

$$-P_s^{RS} + \mu_{4_s} - \lambda \geq 0 \quad , \forall s \in S \quad (5.54)$$

$$\mu_{1_g}, \mu_{2_g}, \mu_{3_d}, \mu_{4_s} \geq 0, \forall s \in S \ \forall d \in D \ \forall g \in G \quad (5.55)$$

$$\lambda \ free \quad (5.56)$$

Now that the dual problem has been constructed in the form of a max-problem, hence it can simply be merged with the second-level decision stage of the same form. This merging results in the following inner-problem:

$$max_{\mu_{1_g},\mu_{2_g},\mu_{3_d},\mu_{4_s},\lambda,\Delta q_s^{RS}} \quad \lambda \sum_{s\in S} \Delta q_s^{RS} - \sum_{g\in G} \mu_{1_g} * R_g^U + \mu_{2_g} * R_g^D - \sum_{d\in D} \mu_{3_d} * q_d^{RD} - \sum_{s\in S} \mu_{4_s}(q_s^{RS} + \Delta q_s^{RS}) \quad (5.57)$$

s.t.

$$|\Delta q_s^{RS}| \leq \Delta q_s^{RS,max} \quad \forall s \in S$$

(5.58)

$$\sum_{q \in G} \frac{|\Delta q_s^{RS}|}{\Delta q_s^{RS,max}} \leq \Gamma$$

(5.59)

$$P_g^{rU} + \mu_{1_g} + \lambda \geq 0 \quad , \forall g \in G$$

(5.60)

$$-P_g^{rD} + \mu_{2_g} - \lambda \geq 0 \quad , \forall g \in G$$

(5.61)

$$P_d^{shed} + \mu_{3_d} + \lambda \geq 0 \quad , \forall d \in D$$

(5.62)

$$-P_s^{RS} + \mu_{4_s} - \lambda \geq 0 \quad , \forall s \in S$$

(5.63)

$$\mu_{1_g}, \mu_{2_g}, \mu_{3_d}, \mu_{4_s} \geq 0, \forall s \in S \; \forall d \in D \; \forall g \in G$$

(5.64)

$$\lambda \; free$$

(5.65)

Step 5. Linearize the bilinear terms

Now an inconvenience arises when looking at the objective function of the inner problem (eq. 5.57), as the following parts of the function contain bilinear terms:

$$\lambda \sum_{s \in S} \Delta q_s^{RS}$$

(5.66)

$$\sum_{s \in S} \mu_{4_s} (q_s^{RS} + \Delta q_s^{RS})$$

(5.67)

While bilinear optimization problems can be solved, finding optimal solutions is computationally demanding as the solution space increases exponentially with the problem size. In computational complexity theory, these problems are therefore generally classified as non-deterministic polynomial-time (NP) hard problems [48]. By linearization of the bilinear terms through an outer-approximation (OA) algorithm, the C&CG algorithm can solve the bilinear optimization problem with significantly reduced computational time without reducing solution optimality [43].

In the OA algorithm, the dual problem inner-problem as described in eq. 5.50-5.56 is solved for a fixed feasible value of Δq_s^{RS} (called u_1) such that $u_1 \in U$, in which U is the uncertainty set. In this first iteration j, the solution of the dual inner-problem is fixed as $\mu_{1_g}{}_j, \mu_{2_g}{}_j, \mu_{3_d}{}_j, \mu_{4_s}{}_j, \lambda_j, \Delta q_s^{RS}{}_j$. With the fixed values of the dual inner-problem solution, the bilinear terms in the inner-problem of eq. 5.66 and 5.67 are linearized as follows:

$$L1\left(\lambda, \lambda_j, \Delta q_s^{RS}, \Delta q_s^{RS}{}_j\right) = \lambda_j * \sum_{s \in S} \Delta q_s^{RS}{}_j + \left(\lambda - \lambda_j\right) * \sum_{s \in S} \Delta q_s^{RS}{}_j + \lambda_j * \sum_{\in S} (\Delta q_s^{RS} - \Delta q_s^{RS}{}_j)$$

(5.68)

$$\begin{aligned} L2\left(\mu_{4_s}, \mu_{4_s}{}_j, \Delta q_s^{RS}, \Delta q_s^{RS}{}_j, q_s^{RS}\right) \\ = \sum_{s \in S} \mu_{4_s}{}_j * (q_s^{RS} + \Delta q_s^{RS}{}_j) + (\sum_{s \in S} \mu_{4_s} - \mu_{4_s}{}_j) * (q_s^{RS} + \Delta q_s^{RS}{}_j) \\ + \sum_{s \in S} \mu_{4_s}{}_j * ((q_s^{RS} + \Delta q_s^{RS}) - (q_s^{RS} + \Delta q_s^{RS}{}_j)) \end{aligned}$$

(5.69)

s.t.

$$\beta \leq L1\left(\lambda, \lambda_j, \Delta q_s^{RS}, \Delta q_s^{RS}{}_j\right) \quad \forall j$$

(5.70)

$$\gamma \leq L2\left(\mu_{4_s}, \mu_{4_s}{}_j, \Delta q_s^{RS}, \Delta q_s^{RS}{}_j, q_s^{RS}\right) \quad \forall j$$

(5.71)

The terms as provided in eq. 5.68 and eq. 5.69 show the linearized terms of the bilinear terms eq. 5.66 and 5.67. The two constraints added to the problem, eq. 5.70 and 5.71, ensure that the inner-problem solution is at least equal or better than the solution of the dual inner-problem.

The resulting complete notation of inner-problem becomes:

$$max_{\mu_{1_g}, \mu_{2_g}, \mu_{3_d}, \mu_{4_s}, \lambda, \Delta q_s^{RS}} \quad \beta - \sum_{g \in G} \mu_{1_g} * R_g^U + \mu_{2_g} * R_g^D - \sum_{d \in D} \mu_{3_d} * q_d^{RD} - \gamma$$

(5.72)

s.t.

$$|\Delta q_s^{RS}| \leq \Delta q_s^{RS,max} \quad \forall s \in S$$

(5.73)

$$\sum_{q \in G} \frac{|\Delta q_s^{RS}|}{\Delta q_s^{RS,max}} \leq \Gamma$$

(5.74)

$$P_g^{rU} + \mu_{1_g} + \lambda \geq 0 \quad , \forall g \in G$$

(5.75)

$$-P_g^{rD} + \mu_{2_g} - \lambda \geq 0 \quad , \forall g \in G$$

(5.76)

$$P_d^{shed} + \mu_{3_d} + \lambda \geq 0 \quad , \forall d \in D$$

(5.77)

$$-P_s^{RS} + \mu_{4_s} - \lambda \geq 0 \quad , \forall s \in S$$

(5.78)

$$\mu_{1_g}, \mu_{2_g}, \mu_{3_d}, \mu_{4_s} \geq 0, \forall s \in S \; \forall d \in D \; \forall g \in G$$

(5.79)

$$\lambda \; free$$

(5.80)

$$\beta \leq \; L1\left(\lambda, \lambda_j, \Delta q_s^{RS}, \Delta q_s^{RS}{}_j\right) \quad , \forall j$$

(5.81)

$$\gamma \leq \; L2\left(\mu_{4_s}, \mu_{4_s}{}_j, \Delta q_s^{RS}, \Delta q_s^{RS}{}_j, q_s^{RS}\right) \quad , \forall j$$

(5.82)

In which

$$L1\left(\lambda, \lambda_j, \Delta q_s^{RS}, \Delta q_s^{RS}{}_j\right) = \lambda_j * \sum_{s \in S} \Delta q_s^{RS}{}_j + \left(\lambda - \lambda_j\right) * \sum_{s \in S} \Delta q_s^{RS}{}_j + \lambda_j * \sum_{\in S} (\Delta q_s^{RS} - \Delta q_s^{RS}{}_j)$$

(5.83)

$$\begin{aligned} L2\left(\mu_{4_s}, \mu_{4_s}{}_j, \Delta q_s^{RS}, \Delta q_s^{RS}{}_j, q_s^{RS}\right) \\ = \sum_{s \in S} \mu_{4_s}{}_j * (q_s^{RS} + \Delta q_s^{RS}{}_j) + (\sum_{s \in S} \mu_{4_s} - \mu_{4_s}{}_j) * (q_s^{RS} + \Delta q_s^{RS}{}_j) \\ + \sum_{s \in S} \mu_{4_s}{}_j * ((q_s^{RS} + \Delta q_s^{RS}) - (q_s^{RS} + \Delta q_s^{RS}{}_j)) \end{aligned}$$

(5.84)

After solving the inner-problem, the solution values of $\mu_{1_g}, \mu_{2_g}, \mu_{3_d}, \mu_{4_s}, \lambda, \Delta q_s^{RS}$ become $\mu_{1_g}{}_{j+1}, \mu_{2_g}{}_{j+1}, \mu_{3_d}{}_{j+1}, \mu_{4_s}{}_{j+1}, \lambda_{j+1}, \Delta q_s^{RS}{}_{j+1}$, and the next iteration is initiated. The solution values are again inserted in the dual inner-problem as provided in eq. 5.50-5.56. This process is repeated until the objective value of the dual inner-problem becomes equal to the objective value of the inner-problem, i.e. when convergence is met. When convergence is met, the (optimal) solution values of $\mu_{1_g}, \mu_{2_g}, \mu_{3_d}, \mu_{4_s}, \lambda, \Delta q_s^{RS}$ are provided to the outer-problem.

Step 6. Add constraint to the outer-problem

Figure 3 below provides a visualization of the working principles of the C&CG algorithm. In the graph, the outer-problem is dubbed the Bender's Decomposition (BD) Master Problem, while the OA

Subproblem and OA Master Problem are respectively the inner-problem and dual inner-problem. As can be seen from Figure 3, the C&CG algorithm is constituted of multiple loops; only the Outer Approximation loop has been treated thus far. The working principle of the BD Subproblem loop will be treated in Step 6.

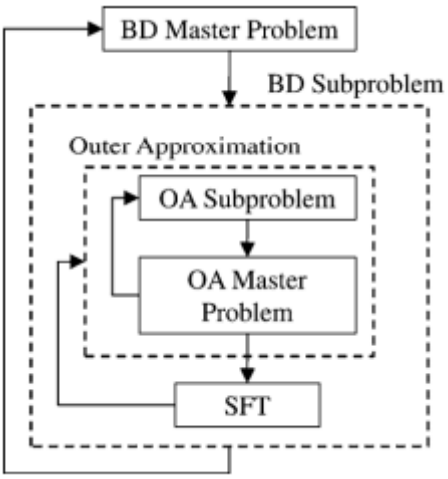

Figure 3. Flow chart of the proposed two-level algorithm. SFT stands for simultaneous feasibility test, where security constraints, such as N-1 constraints, are tested at current solutions and violated constraints are added sequentially [43].

An additional decision variable α is added to the *outer-problem* as provided in eq. 5.17-5.24, making use of the solution values $\mu_{1_g}, \mu_{2_g}, \mu_{3_d}, \mu_{4_s}, \lambda, \Delta q_s^{RS}$ of the optimal solution of the OA algorithm. The decision variable α is added to the objective function of the *outer-problem* as follows:

$$min_{\Xi^C} \sum_{g \in G} r_g^U * P_g^{rU} - r_g^D * P_g^{rD} + \sum_{s \in S} P_s^{RS} * \left(\Delta q_s^{RS} - q_s^{spill}\right) + \sum_{d \in D} P_d^{shed} * q_d^{shed} + \alpha$$

(5.85)

Whereafter α is subjected to the following constraint:

$$\alpha \geq \lambda_k \sum_{s \in S} \Delta q_s^{RS}{}_k - \sum_{g \in G} \mu_{1_{g_k}} * R_g^U + \mu_{2_{g_k}} * R_g^D - \sum_{d \in D} \mu_{3_{d_k}} * q_d^{RD} - \sum_{s \in S} \mu_{4_{s_k}} * \left(q_s^{RS} + \Delta q_s^{RS}{}_k\right) \quad k \forall K$$

(5.86)

By augmenting the outer problem objective function with the constrained α iteratively, it is ensured that for each iteration (k) of the BD subproblem loop an improved solution is found. This loop will continue until no further improvements are found by the augmented outer problem; the resulting first-stage decision variables as denoted by Ξ^B will be the optimal solution for the Robust model and will be subjected to the in-sample and out-of-sample scenarios to measure performance.

3.2 Key performance indicators

To compare the performance of robust- and two stage stochastic optimization in DA market clearing, a set of KPIs will be defined. While the objective functions of the optimization models are oriented

towards maximizing SEW, the KPIs offer insights in the nuances of each individual market clearing mechanism. The KPIs are selected on the basis of the following three different performance criteria: (1) maximizing SEW, (2) the integration of VRES in the system and (3) the system security of supply. Each performance criteria is assigned a sub-section in which the drafting of corresponding KPIs will be explained.

3.2.1 Maximizing SEW

The maximization of SEW is the main objective of EUPHEMIA, the algorithm used for coupling supply and demand in the European DA markets [39]. Maximizing SEW is ought to provide for affordable electricity for all market participants in a social- and cost effective manner, leading to long-term economic growth [5]. From the SEW resulting from the optimization of the DA market clearing, two performance indicators can clearly be identified; (i) the consumer surplus and (ii) the producer surplus. The consumer surplus can be described as the cumulative underbid of all accepted demand bids compared to the determined MCP, while the producer surplus can be described as the cumulative overbid of all accepted supply bids compared to the determined MCP. An adaptation of Figure 1 is made to visualize the consumer surplus and producer surplus in Figure 2 below.

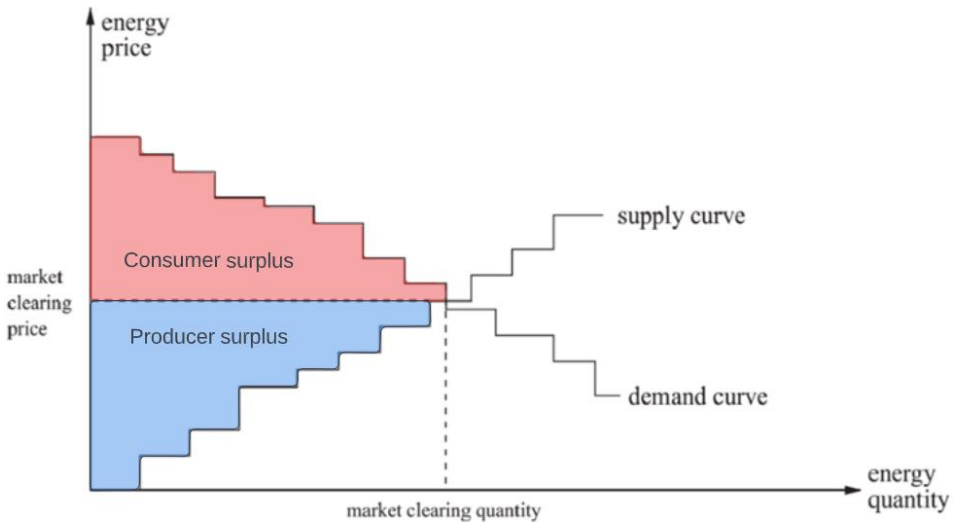

Figure 2. Visualization of the consumer surplus and producer surplus

While the SEW only describes the total welfare of the whole power system, the consumer surplus and producer surplus KPIs help to identify which group of market actors is benefiting under each DA market clearing model.

The formulas used to calculate the consumer surplus and producer surplus are as follows:

$$ConsumerSurplus = \sum_{d \in D} q_d^{DD} * P_d - \sum_{d \in D} q_d^{D} * MCP \qquad (6.1)$$

$$ProducerSurplus = \sum_{g \in G} q_g^{G} * MCP + \sum_{s \in S} q_s^{S} * MCP - \sum_{g \in G} q_g^{G} * P_g - \sum_{s \in S} q_s^{S} * P_s \qquad (6.2)$$

In which the MCP is set equal to the intersection point of the lowest accepted supply bid price and the highest accepted demand bid price. In case of an imparity between the two prices, the lowest supply bid price will be used as the MCP.

To account for the costs associated with balancing supply and demand, a third KPI is introduced. While the two above mentioned KPIs are determined the day before during DA market clearing, potential imbalances from realization of stochastic producer output bring along costs for liable market actors. Moreover, recurring grid imbalances raise costs of all network users, impacting the SEW over time.

3.2.2 Integration of VRES

As mentioned earlier, the integration of VRES in the energy mix of the European power system is one of the primary goals and challenges of the EU in the upcoming decades [3], substantiating its selection as a performance criterium. The integration of VRES in the energy mix will be evaluated on (i) the revenues of stochastic producers, (ii) the share of VRES in the energy mix and (iii) the utility of the investments of stochastic producers.

The first KPI corresponding to objective (i) is the producer surplus of stochastic producers. As mentioned in section 3.2.1, the producer surplus is an indicator of added value to producers; likewise, the stochastic producer surplus indicates the added value to stochastic producers. This KPI is presented both as the stochastic producer surplus after DA market clearing, as well as the resulting profits after having paid potential imbalance costs. The formulas used for calculating the Stochastic producer surplus and the stochastic producer profit are as follows:

$$StochProducerSurplus = \sum_{s \in S} q_s^S * MCP - \sum_{s \in S} q_s^S * P_s \qquad (6.3)$$

$$StochProducerProfits = \sum_{s \in S} q_s^S * MCP - \sum_{s \in S} q_s^S * P_s - \sum_{g \in G} r_g^U * P_g^{rU} - \sum_{d \in D} p_d^{shed} * q_d^{shed} \qquad (6.4)$$

Please note that only the costs resulting from imbalances are subtracted from the stochastic producer surplus, namely the activation of upward reserves and costs resulting from load shedding events.

Secondly, the KPI corresponding to objective (ii) is the share of VRES in the electricity mix. To calculate the share of VRES in the energy mix, the total amount of accepted stochastic supply bids is calculated, whereafter the amount of activated upward reserves and curtailed demand are subtracted and the amount of activated downward reserves is added. Finally, the used stochastic producer output is divided by the total *delivered* demand, which is equal to the amount of accepted demand bids minus the curtailed demand. The share of VRES is calculated as follows:

$$VRES = \ 100 * \frac{\sum_{s \in S} q_s^S + \sum_{g \in G} r_g^D - r_g^U - \sum_{d \in D} q_d^{shed}}{\sum_{d \in D} q_d^{DD} - q_d^{shed}} \qquad (6.5)$$

Finally, the amount of wind spillage in MWh is the KPI to measure (iii) the utilization of investments of stochastic producers. A low amount of wind spillage would indicate a higher degree utilization of stochastic producer investments. The total amount of wind spillage is equal to $\sum_{s \in S} q_s^{spill}$.

3.2.3 System security of supply

Given the vital role of electricity in societal functioning, reliability and security of supply of electricity is paramount. However due to uncertainty of stochastic producer output, events can occur in which demand cannot be met. The respective KPIs are needed to (i) indicate the frequency of load shedding events under the analyzed approaches and (ii) indicate the magnitude of load shedding events under the analyzed approaches. The first KPI is indicated by the percentage of simulated hours experiencing load shedding events, while the second KPI indicates the total amount of switched-off MWh electricity during the load shedding events. The following formulas are used:

$$Frequency^{shed} = \frac{\sum_{t\in \mathrm{T}} \sum_{\omega\in\Omega} \sum_{d\in D} [q_{d\omega t}^{shed} > 0]}{|T| * |\Omega| * |D|} \quad (6.6)$$

$$Magnitutde_{\omega\in\Omega}^{shed} = \sum_{t\in \mathrm{T}} \sum_{d\in D} q_{d\omega}^{shed} \quad (6.7)$$

An overview of the performance criteria and corresponding KPIs is provided in Table 1 below.

Performance criteria	Key performance indicator	Unit
Maximizing SEW	Consumer surplus	€
	Producer surplus	€
	Balancing costs	€
Integration of VRES	Stochastic producer surplus	€
	Share of VRES in electricity mix	%
	Amount of wind spillage	MWh
System security of supply	Frequency of load shedding events	%
	Magnitude of load shedding events	MWh

Table 1. Overview of performance criteria and KPIs

3.3 Data collection

While a big amount of data is freely available on the internet, collecting data for the purpose of electricity system modelling raises concerns on cost barriers and legal barriers from copyright- and privacy restrictions. An overview of available data sources for energy system modelling was provided by [49], also describing the limitations of the available data sources. In the clear absence of available data, assumptions will be made.

To replicate the DA electricity markets for the simulation runs, the constructed datasets need to include and resemble (1) the bidding quantities and prices of the demand- and supply bids, (2) the bidding quantities and prices of capacity reserves and (3) the uncertainty of output realization of stochastic producing units. For each objective, a sub-section will be provided to explain the method of creating the data for the country's respective dataset.

3.3.1 Day-ahead market bids

In this sub-section, the method of collecting the data and constructing the model datasets of the quantities and prices of the DA market bids will be treated. First, the methods of constructing the datasets of the market bids of the producers (Section 3.3.1.1) and consumers (Section 3.3.1.2) will be explained , whereafter Section 3.3.1.3 provides an overview of the made assumptions and limitations of the methods.

3.3.1.1 Supply bids

Both supply- and demand bids of individual market participants are sent for each timestep to the bidding area's PX, after which an order book is constructed to calculate the MCP. While market data of the DA wholesale electricity market is made available by the bidding area's PX, bidding data of individual market participants is disclosed in compliance with the Regulation on wholesale Energy Market Integrity and Transparency (REMIT) No. 1227/2011, Article 9.3. Among privacy regulatory reasons, bids of individual market participants are commercially sensitive information as it reveals a market participant's bidding strategy. Wholesale electricity market bidding strategies have been extensively covered in literature, explaining the market mechanics and motivations behind the strategies [50] and modelling bidding strategies in Multi-Agent models combined with reinforcement learning [51] [52]. However, reconstructing the supply bids while taking into account the bidding strategies of market participants is well beyond the scope of this research. Therefore, a point forecast bidding strategy will be used for the Stochastic producers, in which the forecasted amount of output determines the bidding quantity.

Due to the unavailability of the order book data, a different approach is used to reconstruct the supply bids of the different wholesale electricity markets. The technical nominal power (TNP) of generating units, which is openly available, is used to determine the quantities of the supply bids of the conventional producers, while the marginal costs are used as the prices of the supply bids. The marginal costs are calculated by adding the fuel costs in $\$/mWh_{electricity}$ to the costs of CO_2 in $\$/tonne_{CO_2}$. While this approach does not take into account the bidding strategy of the generating units, this approach will naturally reflect the actual merit order to economically optimize the supply of electricity.

The datasets of the active generating units in both the Netherlands, France and Germany are taken from the Open Power system Data (OPSD), a platform created for facilitating the collection of data for power system modelling from publicly available sources [53].

3.3.1.2 Demand bids

For each 15-minute timestep, the Entso-e Transparency platform provides the actual load in MW. However, this data only includes the accepted (and delivered) quantities of demand, not indicating unaccepted submitted bids. While EPEX, the PX responsible for the Dutch, French and German markets, does provide the aggregated curves for each individual hour, this data only includes the current- and previous day, not allowing to collect longitudinal data on demand bids. Moreover, the aggregated curve data is provided only as a readable graph, not allowing easy extraction of data in table form [54]. Due to the absence of the order book data of demand bids, certain assumptions have to be made in constructing the demand bid quantities and prices.

From the EPEX market data access platform, aggregated demand curve data is gathered from the period of May 19th 2023 until May 25th 2023. For this time period, the demand order bids are categorized in 49 price steps ranging from 4000 €/MWh to 0 €/MWh. The submitted demand bid for

each price category is expressed as a percentage of the total demand for each individual hour. While negative bids can be submitted in reality, the use of marginal costs as the supply bid prices in this thesis eliminates the possibility of negative supply bid prices; the negative demand bids from the aggregated demand curve data are added to the 0 €/MWh price step. In Appendix A, an overview of the demand bid distributions is provided.
From the Entso-e Transparency platform, the total amount of accepted (and delivered) demand is provided for each country in 15-minute timesteps. The hourly average (00:00 – 00:15 until 00:45-01:00 will be t = 1 for example) will be used to reconstruct the demand bids.

Four individual days will be simulated in the simulation runs. These days are picked at random, only being constraint to 1 day per season. The total accepted demand, as available from the Entso-e Transparancy platform, of these days will be used in the simulation runs. To take into account the unaccepted demand bids, the total submitted demand for each country is assumed to be 25% higher compared to the observed accepted demand from the aggregated demand curve data. Further information on the selected days will be provided in Section 3.3.4.

To provide an example; on a certain day, the total accepted demand will be equal to 10,000 MW at a certain hour. The 10,000 accepted demand will be equal to 12,500 MW in total submitted demand bids. For each individual case study 49 demand bids will be constructed (Appendix A), multiplying the percentage of each price range with the 12,500 MW total submitted demand bids.

Finally, the price of shedding events has to be determined. For the Netherlands, a study was conducted by the Autoriteit Consumenten Markt (ACM) which determined the Value of Lost Load (VoLL) at 68,887 €/MWh for consumers [55]. However, a notable difference is observable in the results from the study conducted by CEPA in 2018, indicating a VoLL of 22,940 €/MWh for the Netherlands, 6,920 €/MWh for France and 12,410 €/MWh for Germany as a domestic average [56]. While both studies have used different methods in the estimation of the VoLL for the different countries, the numbers as provided by CEPA will be used in this thesis because of the provision of both the Netherlands, France and Germany in a single study, ensuring consistency between the countries in the used method. Table 2 below provides an overview of the VoLL.

Country	The Netherlands	France	Germany
Shedding costs[€/MWh]	22,940	6,920	12,410

Table 2. Overview of the Value of Lost Load (VoLL) for the different case study countries

3.3.1.3 Assumptions and limitations

A first assumption made is setting the price of the supply bids equal to the marginal costs of each individual generating unit, excluding the plant operator's bidding strategy. Considering the exclusion of ramping costs and ramping rates in this thesis, generating units will not apply bidding strategies to gradually ramp-up their generation. The impact of this exclusion on the model results is rather unclear; while the inclusion of ramping costs would increase the marginal costs of electricity production, supply bid strategies have been found to affect demand bidding strategies through market oriented demand response, potentially leading to lower electricity prices [57][58].

A second assumption made is the uniformity of the demand bid distributions for each day and hourly timestep. In reality, demand bid distributions are heavily influenced by market responses. High forecasted yields of wind energy increase the amount of lower-price demand bids, while peaks in demand increase the amount of higher-cost demand bids. In this thesis, a uniform demand bid distribution is used for each different simulation day; only the quantities differ between the days.

A third assumption is the bidding quantity of stochastic producers, which is set equal to the DA initial forecast. In reality, stochastic producers would apply a more robust bidding strategy to decrease the chance of underproduction compared to the accepted bidding quantity, resulting in penalty costs due to imbalances. Considering the stochastic- and robust DA market clearing models make use of wind profile scenarios to address uncertainty, this assumption will have the most impact on the results of the deterministic DA market clearing model.

3.3.2 Reserve bids

In this section, the method of constructing the datasets of the reserve procurement bids and reserve activation prices will be treated. Section 3.3.2.1 explains the method of determining the quantities and prices of the reserve procurement bids, as well as the amount of reserve procurement for the countries in the case study, while the method used to determine the prices of the activation of the reserves is treated in Section 3.3.2.2. Finally, section 3.3.2.3 provides an overview of the made assumptions and limitations of the used methods.

3.3.2.1 Reserves procurement

While actual data on reserve procurement bids is limited to the Entso-e Transparancy platform, which only discloses averaged prices and cumulative bids for each 15 min timestep, the ancillary service market is heavily regulated which provides an opportunity for substantiated assumptions. Since the DA market clearing models operate on 1-hour timesteps, primary- and secondary control reserves are not accounted for in the data collection, only treating manual Frequency Restoration Reserves (mFFR). Due to differences in regulations, this section is divided for each individual country.

The Netherlands

In the Netherlands, each generating unit is obliged to submit reserve bids if they produce >60 MW, while smaller connections can voluntarily place bids. Bids are required to be 20 MW at minimum [59]. Due to the 1-hour timesteps used in the models, bids are placed (and consequently) paid in $€/\mathrm{MWh}$. Reserve procurement bids can be either upward (providing energy in case of shortages) or downward (in case of abundance). In actuality, a certain amount of mFFR reserves are contracted annually for a fixed price; in this thesis, we assume a bidding mechanism for each respective timestep.

As provided by Tennet, the TSO in the Dutch electricity market, the minimal amount of accepted upward mFRR procurement is settled at 350 MW, while accepted downward procurement is settled at 200 MW [60]. This minimal amount of procurement is settled to ensure reliability of the transmission of electricity in case of an unexpected drop in generation or demand.
To meet the above mentioned requirements, the upward- and downward mFRR bids are determined by assuming each generating unit >200 MW TNP will submit a bid equal to 10% of the TNP. The fixed amount of upward- and downward procured reserves for the Dutch case study is set equal to:

$$Fixed^{U}_{Netherlands} = 350 \qquad (7.1)$$

$$Fixed^{D}_{Netherlands} = 200 \qquad (7.2)$$

France

In France, mFRR bids are to be submitted to the RACOON platform in $€/\mathrm{MWh}$ for each time block. Notably, RTE makes a discrepancy for annually contracted mFRR capacities able to be activated in 13 minutes for a period of 2 hours (500 MW total) called *reserve rapide* and capacities able to be activated

in 30 minutes for 4 hours (250 MW total) called *reserve complementaire* [61]. The total amount of mFRR capacities required is totaled at 1000 MW, not specifying either upward- or downward as per Article L.321-11 of the French Energy code, with 750 MW annually contracted. Generating units are however to submit bids; in case of an increase in economical performance, submitted bids may be chosen over accepted annually contracted bids which are paid a compensation [62]. In this thesis, the 1000 MW is assumed either upward- and downward reserve procurement, without taking into consideration the annually contracted mFRR reserves; all reserves are procured from DA bids. Generating units are not obliged to submit reserve bids, however bidding quantities are obliged to total 10 MW at minimum [61]. Due to the absence of mFRR order book data, the assumption is made that each producing unit with a TNP of >200 MW submits a bid of 5% of their TNP as upward- and downward mFRR reserves. This assumption will provide enough reserve capacity for the market to comply to the 1000 MW upward- and downward reserve procurement requirement, leaves enough reserves to increase procurement if ought to be necessary by the TSO and complies to the 10 MW minimum reserve bid quantity. The fixed amount of upward- and downward procured reserves for the French case study is set equal to:

$$Fixed^{U}_{France} = 1000 \tag{7.3}$$

$$Fixed^{D}_{France} = 1000 \tag{7.4}$$

Germany

In Germany, mFRR bids are submitted in steps of 1 MW upward or downward in €/MWh, with a maximum of 9.999 MW. Bidding parties are allowed to declare their bid undividable up to 25 MW [63]. No requirements are set for generating units to submit a minimal bid. The assumption is made that every >100 MW TNP generating unit is submitting a reserve procurement bid for 5% of the total TNP.

The minimum amount of accepted upward mFRR procurement is settled at 2048 MW, while accepted downward procurement is settled at 1131 MW [60]. To meet the above mentioned requirements, the upward- and downward mFRR bids are determined by assuming each generating unit >200 MW TNP will submit a bid equal to 10% of the TNP. The fixed amount of upward- and downward procured reserves for the German case study is set equal to:

$$Fixed^{U}_{Germany} = 2048 \tag{7.5}$$

$$Fixed^{D}_{Germany} = 1131 \tag{7.6}$$

Please note that the above mentioned procurement constraint eq. 7.1-7.6 only apply to the deterministic DA market clearing model; the Stochastic and Robust DA market clearing models make use of the wind profile scenarios and uncertainty set to optimize dispatching of reserve procurement and activation.

3.3.2.2 Reserve capacity activation

The prices of reserve capacity activation are different for both the Netherlands, Germany and France. In the Netherlands, the price of reserve activation is contracted at either the generating unit's marginal

cost plus 10%, the EPEX day ahead market (DAM) price +200 €/MWh or at least +200 €/MWh whichever is higher [64]. For the French and German markets, reserve activation prices are included in the reserve bids, which are not openly available. Due to the absence of data on reserve capacity activation prices, the assumption will be made that upward- and downward reserve capacity activation costs are derived from the marginal costs of the generating units. For upward reserve procurement producers are receiving 60% of the marginal cost, while receiving an additional 60% of the marginal cost in the case of upward reserve activation. For downward reserve procurement producers are receiving 110% of the generating unit's marginal cost, while having to pay 90% of the marginal cost back to the TSO for downward reserve activation. Please note that in the case of downward reserve capacity activation a generating unit has already received at least their marginal cost + 10% as payment for electricity; 20% of the marginal costs are received at minimum for ramping down generation. This mechanism ensures an economic incentive for electricity producers to submit reserve bids.

An overview of the reserve bid quantities and prices is provided in Table 3 below.

Bid characteristics	The Netherlands	France	Germany
Reserve procurement quantity [MWh]	10% of TNP ($\geq$ 200 MW TNP)	5% of TNP ($\geq$ 200 MW TNP)	5% of TNP ($\geq$ 100 MW TNP)
Upward reserve procurement price [€/MWh]	80% of marginal cost	80% of marginal cost	80% of marginal cost
Downward reserve procurement price [€/MWh]	Marginal cost + 10%	Marginal cost + 10%	Marginal cost + 10%
Upward reserve activation price [€/MWh]	60% of marginal cost	60% of marginal cost	60% of marginal cost
Downward reserve activation recovery [€/MWh]	Marginal cost – 10%	Marginal cost – 10%	Marginal cost – 10%

Table 3. Overview of reserve procurement and reserve activation prices and quantities of the case study countries

3.3.2.3 Assumptions and limitations

The first assumption made is the exclusion of automatic Frequency Restoration Reserve (aFRR) and Frequency Control Reserves (FCR) from the DA market clearing models. Considering the timesteps used in the models are 1-hour, the inclusion of aFRR and FCR is not possible due to their respective operating timeframes. Additional costs for aFRR and FCR are not taken into consideration in this thesis.

The second assumption made is the price of the reserve procurement bids. In reality, conventional producers sent bids based on the amount of imbalance, bids of competitors and the costs of ramping up and down for the generator. Due to limiting uncertainty only to stochastic producers and the exclusion of ramping costs and -limits in this thesis, pursuing a method to replicate the reserve procurement bid prices would remain redundant.

The third assumption made in this thesis is the exclusion of reserve activation failure. In the case of reserve activation failure, contracted generating parties are obliged to pay a penalty sum to the area's TSO [61][60]. This assumption is in line with this research's general assumption to not take technical failures into account; uncertainty is limited to the realization of stochastic producer output (i.e., wind power). However, this causes a notable contradiction when looking at the minimum reserve procurement requirements for each individual country; these minima are determined based on the premise that, besides demand load uncertainty, reserves have to be procured for potential technical failures. A risk analysis will be performed to determine the impact of the different DA market clearing models on the amount of required reserve procurement.

3.3.3 Day-ahead wind power uncertainty

Despite improvements in forecasting of wind energy, DA forecasting accuracy is still far from satisfactory, leading to additional costs up to 10% of the generator income [65]. Forecasting errors have been observed to increase significantly with higher timeframes as close to four hours ahead [66]. While initial research focus was emphasized on improving forecasting wind power generation capabilities, the past decade has seen an increased interest in utilizing DA forecasting error distributions to averse financial risks for wind farms on the DA electricity market.

Research on DA forecasting errors has proven difficult due to the unavailability of forecasting data, as well as actual generation data which is usually disclosed by wind power farm operators. While data on generation forecasts is provided by TSOs, historical data on actual generation is only construed from accepted bids and delivered electricity, rather then the maximum (potential) yield by the wind farm during the time period. A platform created to tackle the problem of VRES profile generation was RESgen, described as 'an open-source platform for space-time forecasting of renewable energy generation' [67]. Initially designed for the Western part of the USA, work by [68] has added a list of applicable countries for RESgen including the Netherlands, France and Germany. A notable benefit of RESgen is the ability to generate forecast scenarios of up to 90 hours lead time, increasing the forecast uncertainty with the increasing amount of hours lead time. With gate closure time for the DA market at 12:00 pm in both the Netherlands, France and Germany, the lead time of wind power forecasts ranges from 12 hours to 36 hours lead time, which can be included in RESgen's scenario generation. The amount of wind-farm locations for each individual country will be determined in Section 4 in the case study descriptions.

The wind profile scenarios created by RESgen can be directly inserted into the Stochastic DA market clearing model. However, the budget of uncertainty for the ARO DA market clearing model has to be determined, trying to find a trade-off between conservativeness, risk and opportunity [69]. As mentioned by [70], the budget of uncertainty can vary widely between different purposes, ranging from very tight budgets in construction engineering or somewhat more loose budgets for commercial inventory management. Determining the budget of uncertainty for stochastic producer output evokes a duality; due to the stochastic nature of weather forecasting a statistical approach with a large number of scenarios can be utilized to determine the risk factor and thus the budget of uncertainty [71], or a sensitivity analysis can be performed to observe the effect of the budget of uncertainty on the model results [72].

In this thesis, the uncertainty set will be derived from the generated stochastic output scenarios by the same mehtod as conducted by [16]. For each individual timestep, the highest- and lowest stochastic output realization will be taken ($\widehat{q_{RT}^{DS}}$ and $\widecheck{q_{RT}^{DS}}$) which will be used to determine the range of deviation in stochastic producer output to $\left\{\Delta q_s^{RS} \in \mathbb{R} \;\middle|\; \widecheck{q_{RT}^{DS}} - q_s^{RS} \leq \Delta q_s^{RS} \leq \widehat{q_{RT}^{DS}} - q_s^{RS}\right\}$ $\forall s \in \mathrm{S}$.

The budget of uncertainty will be determined using the following equation:

$$\Gamma = \frac{N_s}{2} \qquad (7.7)$$

In which N_s indicates the total number of wind farms for each individual case study. This budget of uncertainty will be used during the case studies. After, a sensitivity analysis will be performed (Section 4.4.1) to test the effect of the budget of uncertainty on the KPI results.

3.3.3.1 Assumptions and limitations

The main limitation of the use of RESgen is its inability to specify exact locations with their latitudes and longitudes. While RESgen does have a limited number of default locations in its source data containing coordinates to utilize the spatial characteristics of each location, it does not, however, offer the option to choose specific locations. It only allows for selecting the quantity of locations for which scenarios will be generated. RESgen is not able to differentiate between off-shore and on-shore wind farm locations in its scenario generation, therefore not taking into account the higher degree of uncertainty in on-shore wind power forecasting due to physical interference with objects on land or the higher observed wind speeds over water surfaces [73].

3.3.4 Seasonality

To include seasonality in the datasets, for each season one day will be selected at random using a random number generator from the python Random-library. The selected days are May 8th 2023, December 20th 2022, September 13th 2022 and March 2nd 2023 for both the Netherlands, France and Germany. In each case study description, a short overview will be provided of the demand load- and wind profile patterns for each of the four simulation days.

3.4 Data analysis

In this section, the methods of conducting and analyzing the model simulations will be provided. The total number of generated wind profile scenarios will be divided in two sets; the in-sample forecasts and out-of-sample forecasts. No general rule is constructed in setting the amount of scenarios for either stochastic- and robust optimization, however work by [74],[75],[76],[77] and [78] applied a range of 10 to 250 scenarios. For the simulation runs in this research, a total of 105 scenarios will be generated using the RESgen platform, divided into the in-sample scenarios (53 scenarios) and the out-of-sample scenarios (52 scenarios). After providing the case study results, a sensitivity analysis will be performed on the in-sample size for the Stochastic model.

The stochastic- and ARO Da market clearing models will run on the in-sample scenarios to retrieve an optimal solution. After the optimal solution has been found, it will be tested iteratively through all in-sample scenarios and out-of-sample scenarios to retrieve the KPI results; the results of both the in-sample and out-of-sample runs will be provided separately.

3.5 Model computation

The Deterministic-, Stochastic- and Robust DA market clearing models are written in Python 3.9 using the Spyder v5.1.5 Integrated Development Environment (IDE) in the Anaconda v23.3.1 Graphical User Interface (GUI). The solver used in the models is the Gurobi solver available in the *gurobipy* library made by Gurobi TM using the full academic license [79]. The model simulations are performed with an Intel(R) Core(TM) i5-10400 CPU 2.90GHz.

4. Results

In this section, the descriptive results of the case studies can be found in Section 4.1 (The Netherlands), Section 4.2 (France) and Section 4.3 (Germany). After, the results of the sensitivity analyses are provided in Section 4.4. A comparison of the results of the case studies and sensitivity analyses is provided in Section 4.5, which provides an interpretation of the observed case study results and the working principles of the models.

4.1 Case Study 1: The Netherlands

Covering a size area of 41,543 km^2 and having a population of roughly 17.8 million inhabitants, the Netherlands is one of the most densely populated countries in Europe [80]. Despite its relative small size, the Netherlands has the 5^{th} highest GDP of all EU members and the 7^{th} highest total annual electricity consumption [81][82]. As of 2021, electricity generation was mainly sourced by coal (14%) and natural gas (46%), although use of fossil sources has been declining due to the shift to renewable energy sources [83]. The historical high share of natural gas in the Dutch electricity mix can be allocated to a negative public opinion on the use of nuclear energy, (recent) policies limiting the use of coal sourced power generation and the availability of cheap natural gas due to the exploitation of large natural gas reserves underneath the country's surface [84].

4.1.1 Input data - The Netherlands

In this case study, the Dutch electricity wholesale market is simulated with 52 conventional producers, 48 demand loads from consumers and 5 wind farms (stochastic producers) for 24 consecutive hours to test the different DA market clearing models. An overview and description of the wind farm locations and the simulation days will be provided in sub-sections 4.1.1.1 and 4.1.1.2 below.

4.1.1.1 Wind farm locations - The Netherlands

As of 2023, the Netherlands has a total of 5,745 MW installed wind capacity on land and 2,987 MW installed wind capacity off-shore [85], although tenders have already been submitted for a large amount of off-shore wind farms [86]. To limit the amount of different locations of wind farms or even individual wind turbines in the model simulations, the installed wind capacity will be subdivided into 5 different proximate spatial locations. An overview of the locations is provided in Figure 4 below:

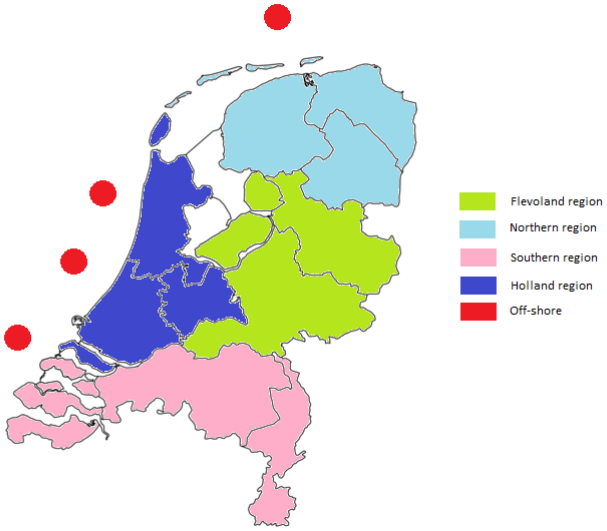

Figure 4. Overview of stochastic production locations – The Netherlands

A description of the five wind locations is provided below:

Flevoland region

As per [b], a total of 1,647 MW installed on-shore wind capacity is placed in the province of Flevoland. To limit the amount of different wind farm locations, the installed capacity of the provinces Gelderland (235 MW) and Overijssel (88 MW) will be added to the Flevoland region, adding up to a total installed wind capacity of 1,970 MW.

Northern region

The installed wind capacities in the provinces of Friesland (618 MW), Groningen (830 MW) and Drenthe (271 MW) are added together to form the second location, the Northern region with a total installed capacity of 1,719 MW [85].

Southern region

The Southern region constitutes of the provinces of Zeeland (573 MW), Noord-Brabant (427 MW) and Limburg (120 MW) with a total installed wind capacity of 1,120 MW [85].

Holland region

The provinces of North-Holland (720 MW), South-Holland (770 MW) and Utrecht (34 MW) form the Holland region with a total installed capacity of 1,524 MW [85].

Off-shore

To simplify the process of determining the wind farm locations, all off-shore wind capacity will be allocated in a single location. This off-shore wind capacity will include the Wind farm locations Egmond aan Zee, Princess Amalia, Luchterduinen, Gemini, Borssele I-II and Borssele III-IV, having a cumulative share of roughly 28% of the total installed wind capacity (2,460 MW) [85].

An overview of the wind farm locations of the Netherlands is provided in Table 4 below.

Region name	Installed wind capacity (MW)	Share of total capacity
Flevoland region (W1)	1,970	22.4%
Northern region (W2)	1,719	19.5%
Southern region (W3)	1,120	12.7%
Holland region (W4)	1,524	17.3%
Off-shore (W5)	2,460	28.0%
Total	8,793	100%

Table 4. Overview of wind farm locations – The Netherlands

4.1.1.2 Simulation days - The Netherlands

In this sub-section, an overview of the demand load profiles and the DA wind generation forecasts of the Dutch case study will be provided.

Demand load patterns

The demand load patterns of the four selected simulation days are presented below in Graph 1. As can be seen, the demand load patterns of May 8th 2023, December 20th 2022 and September 13th 2022 are quite similar except for the total electricity consumption, which can be explained by increased consumption for heating or cooling and seasonal differences in photovoltaic generation. The different demand load pattern of March 2nd 2023 can be explained by the Dutch spring break.

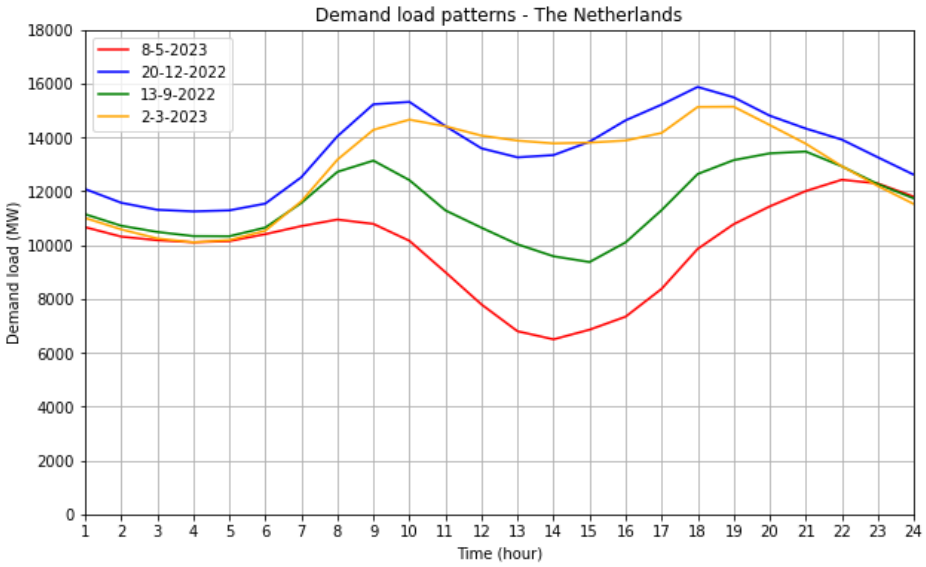

Graph 1. Demand load patterns of selected simulation days (MW) – The Netherlands

Forecasted stochastic output profile

The cumulative DA forecasted stochastic output profiles of the 5 wind farm locations are presented in Graph 2 below. The profiles range from low- to high expected outputs and from moderate intraday deviations to high intermittent profiles. Please note the forecasted generation profile of December 20th 2022; due to the high forecasted wind speeds, output production is expected to be near the nominal capacity. However, these high wind speeds have an increased chance of nearing the cut-off speed, i.e. the point at which wind turbines are shut-off to avoid potential damage of equipment.

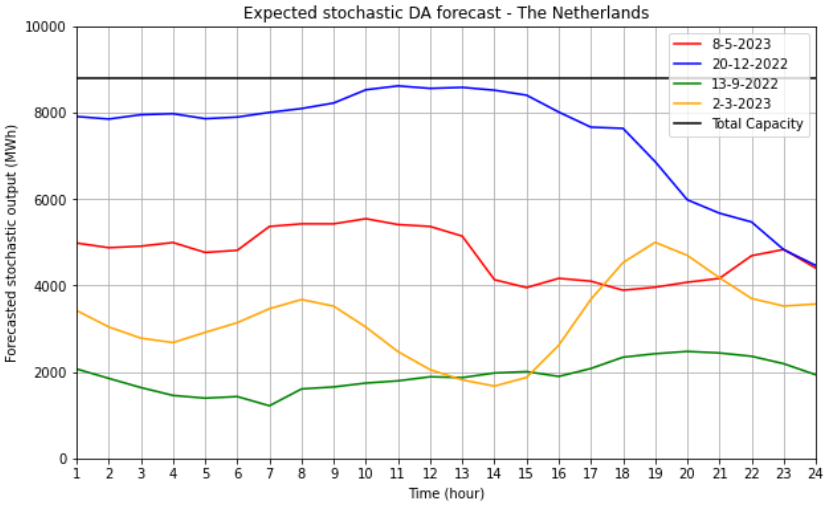

Graph 2. DA forecasted stochastic generation profiles of the four simulation days – The Netherlands

When comparing both the demand load patterns and the forecasted wind profiles of the simulation days, as is provided in Graph 3 below, some notable observations can be made for the different simulation days. For May 8th 2023, the forecasted wind output nears the demand load during the mid-day, while having a much smaller share during the morning, afternoon and night. For December 20th 2022, the demand load pattern as well as the forecasted wind output profile are the highest among the simulation days. For September 13th 2022 and March 2nd 2023, the low forecasted wind output is expected to only fulfill a small share of the demand load.

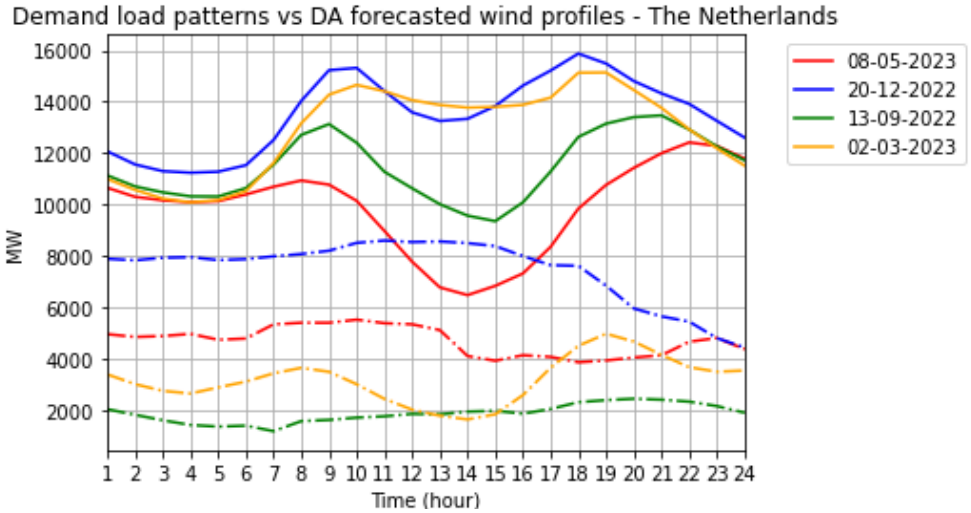

Graph 3. Demand load patterns (solid) vs DA forecasted wind profiles (dash-dotted) - The Netherlands

4.1.2 Model results - The Netherlands

In this section, the model results of the DA market clearing models during the four simulation days are presented for both the in-sample scenarios and out-of- sample scenarios for the Dutch case study. The performance criteria as described in Section 3.2 will be treated in separate sub-sections.

4.1.2.1 Maximizing SEW - The Netherlands

The results of the four simulations of the Dutch case study indicate an increased total SEW when applying the Robust model and the Stochastic model compared to the existing deterministic model. For the Deterministic model, the simulation days of May 8th 2023 and December 20th 2022, which are characterized by highly deviating stochastic output realizations for the in-sample scenarios, resulted in the lowest observed SEW because the fixed amount of reserve procurement proved unable to address the imbalances. Resulting load shedding events heavily affected the SEW, even resulting in a negative SEW for December 20th 2022. The Stochastic DA market clearing model resulted in the highest SEW for the in-sample analysis, followed closely by the Robust model. An overview of the in-sample scenario SEW results is provided in Graph 4 below.

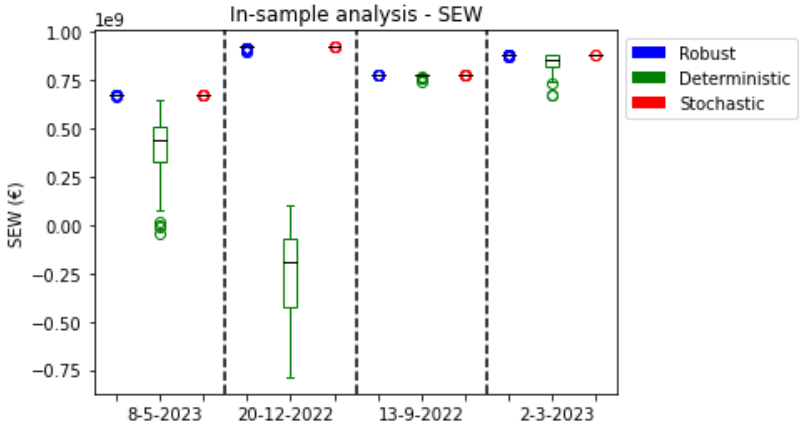

Graph 4. SEW of in-sample scenarios for simulation days – The Netherlands

When observing the results of the out-of-sample simulation runs, some notable observations can be made: the results of the deterministic model and Robust model are quite similar compared to the results of the in-sample analysis, while the performance of the Stochastic model is decreased by 0.01%,

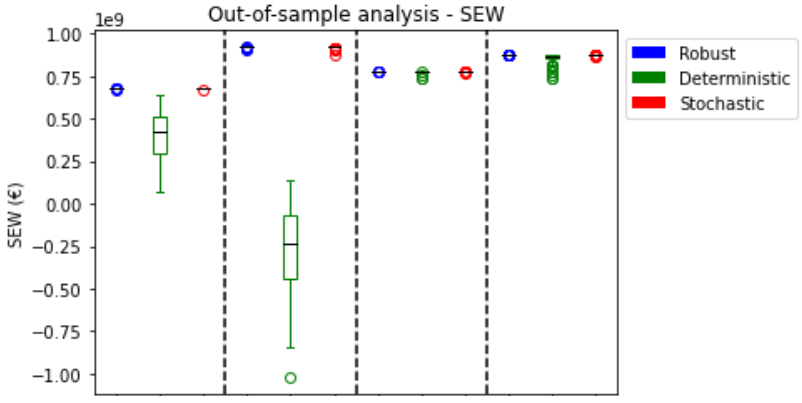

Graph 5. SEW of out-of-sample scenarios for simulation days – The Netherlands

0.3%, 0.08% and 0.1% during the four simulation days. An overview of the resulting SEW of the out-of-sample scenarios is provided in Graph 5 below.

Consumer surplus

Looking at the results of the consumer surplus, rather small differences are observable between the different DA market clearing models, as can be seen from Graph 6 below. Table 5 below provides a numerical overview of the consumer surplus results of the different models.

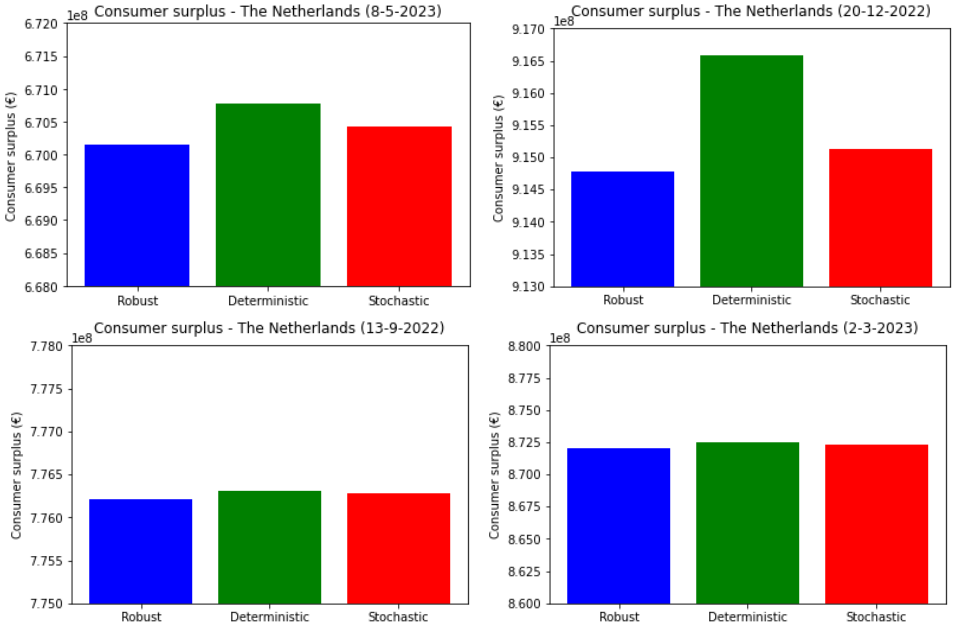

Graph 6. DA Consumer surplus for simulation days – The Netherlands

Simulation day	Robust	Deterministic	Stochastic
08-05-2023	€6.701 * 10^8	€6.708 * 10^8	€6.704 * 10^8
20-12-2022	€9.148 * 10^8	€9.167 * 10^8	€9.152 * 10^8
13-09-2022	€7.762 * 10^8	€7.763 * 10^8	€7.763 * 10^8
02-03-2023	€8.720 * 10^8	€8.725 * 10^8	€8.723 * 10^8

Table 5. Overview of DA Consumer surplus during the simulation days – The Netherlands

The Deterministic model results in the highest consumer surplus. The Stochastic model results in an average decrease of 0.06% in the consumer surplus, while the Robust model yields the lowest consumer surplus with an average decrease of 0.09%. The differences in consumer surplus are mainly caused by the differing quantities of accepted stochastic producer bids between the models. The stochastic producer supply bids are placed first on the merit order because of their low marginal cost (which is set to zero). Therefore, the Deterministic model accepts all submitted stochastic producer bids, while the Stochastic model and Robust model take into account the potential costs due to imbalances, resulting in a lower amount of accepted stochastic producer bids. This lower amount of accepted stochastic producer bids result in i) accepting more expensive conventional producer bids, which could result in a higher MCP or ii) rejecting otherwise accepted demand bids due to changes in the merit order, which would both decrease the total consumer surplus. Although the more conservative working principles of the Stochastic and Robust models result in a lower consumer

surplus, the observed differences are considerably low (>1%), as can be seen from the numerical overview as provided in Table 5.

Producer surplus

Looking at the producer surplus after DA market clearing, the Deterministic model significantly outperforms the Stochastic and Robust model for the simulation days May 8th 2023 and December 20th 2022, which were characterized by high amounts of forecasted wind output, while the differences are far smaller for the simulation days September 13th 2022 and March 2nd 2023, which were characterized by low amounts of forecasted wind output. An overview of the DA Producer surplus results is provided in Graph 7 below.

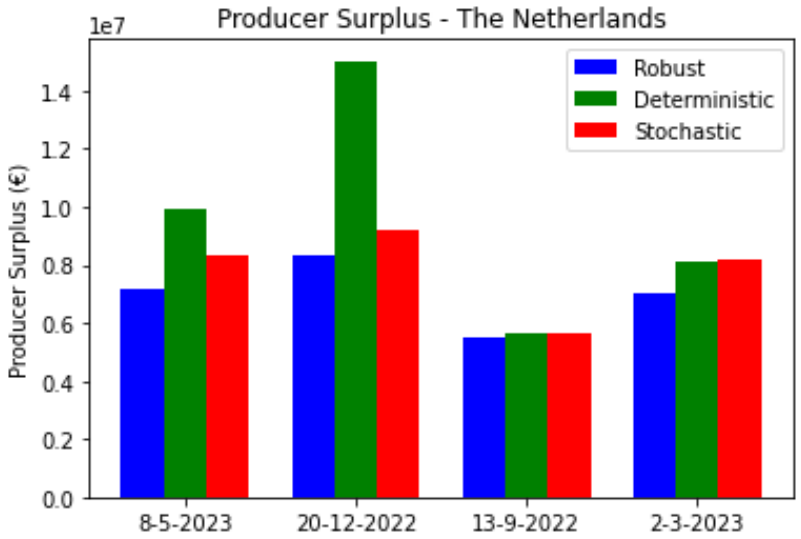

Graph 7. DA Producer surplus for simulation days – The Netherlands

The higher amount of accepted stochastic producer bids by the Deterministic model results in a higher producer surplus. The producer surplus resulting from the Stochastic model is heavily influenced by the output realizations from the in-sample scenarios, resulting in an average decrease of 13.2% of the producer surplus due to a decreased amount of accepted stochastic producer bids. The Robust model, constraining the amount of accepted stochastic producer bids to the amount of procured upwards reserves to account for the worst-case realization, results in a relatively stable producer surplus during the simulation days. However, an average decrease of 22.1% of the producer surplus is observed compared to the Deterministic model, with the highest decrease during the simulation day of December 20th 2022 with an observed decrease of 44.6% due to the high potential deviations in stochastic producer realization from the forecast.

Balancing costs

The highest balancing costs result from the Deterministic model due to the occurrence of expensive load shedding events. Interestingly, the Robust model and Stochastic model have higher average reserve procurement costs compared to the deterministic model, while resulting in significantly lower average costs from upward reserve activation. Moreover, the Robust model yields the highest reserve procurement costs, while bringing about the lowest average upward reserve activation costs. The average results of the in-sample and out-of-sample analysis for simulation day May 8th 2023 are provided in Table 6 and Table 7 below.

Model	Robust	Deterministic	Stochastic
Upward reserve procurement	€1,722,645.96	€385,942.73	€1,590,537.08
Downward reserve expenses	€0.00	€255,405.55	€0.00
Upward reserve activation	€54,780.40	€278,225.04	€205,487.08
Demand load shedding	€136,712.15	€284,419,352.51	€0.00

Table 6. Average balancing costs May 8th 2023 in-sample scenarios – The Netherlands

Model	Robust	Deterministic	Stochastic
Upward reserve procurement	€1,722,645.96	€385,942.73	€1,590,537.08
Downward reserve expenses	€0.00	€255,405.55	€0.00
Upward reserve activation	€52,809.96	€281,788.97	€196,157.39
Demand load shedding	€139,341.22	€280,011,641.37	€88,173.84

Table 7. Average balancing costs May 8th 2023 out-of-sample scenarios – The Netherlands

While the performance of the Stochastic model decreases when applying the out-of-sample scenarios during the simulation day, balancing costs still decrease 2.1% compared to the out-of-sample balancing results of the Robust model.

A complete overview of the average balancing costs is provided in Appendix B.1 and Appendix B.2.

4.1.2.2 Integration of VRES - The Netherlands

Stochastic producer surplus

The results of the stochastic producer surplus are quite comparable to the results of the producer surplus treated in the previous sub-section 4.1.2.1. An overview of the results is provided in Graph 8 below. When comparing the results from Graph 7 and Graph 8, it can be observed that the results for the producer surplus and stochastic producer surplus are quite similar during the simulation days. The main difference can be observed during the simulation days with rather high stochastic output forecasts, May 8th 2023 and December 20th 2022, in which the Deterministic model is outperforming the Robust model with an increased stochastic producer profit of 52.2% and 122.2% and the Stochastic model with 23.5% and 87.3%.

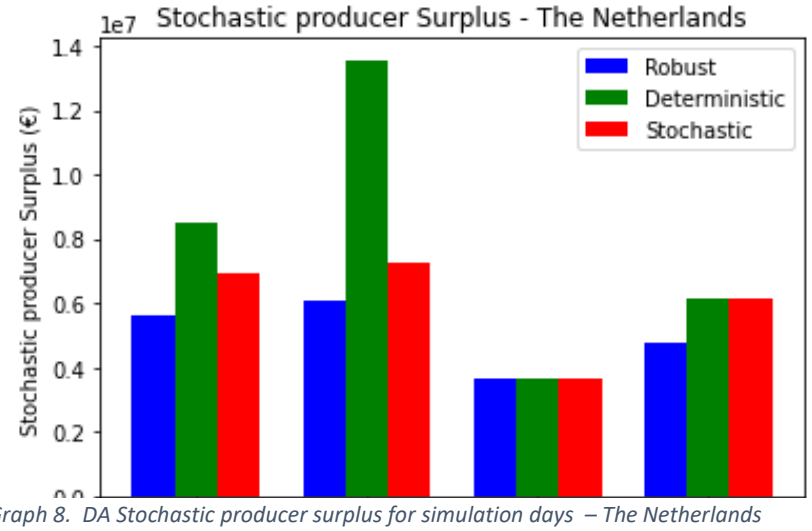

Graph 8. DA Stochastic producer surplus for simulation days – The Netherlands

However, when taking into account the balancing costs as provided in Section 4.1.2.1, the resulting profits for stochastic producers are quite different for both the in-sample and out-of-sample scenarios. Although the Deterministic model realizes a much higher stochastic producer surplus after DA market clearing (Graph 7), balancing costs are significantly outweighing this surplus, leading to extreme net losses for stochastic producers. A numerical overview of the balancing costs is provided in Appendix B.

Comparing the results of the Robust model and the Stochastic model, the Stochastic model yields higher profits for stochastic producers on average. Despite showing a higher degree of robustness in stochastic producer profits when applying the Robust model to the out-of-sample scenarios, the Stochastic model yields 3.7% higher stochastic producer profits on average. An overview of the stochastic producer profits of the Robust model and Stochastic model is provided in Graph 9 and Graph 10 below. The results of the Deterministic model are left out for proper scaling of the y-axis, considering they are significantly lower for the simulation days May 8th 2023, December 20th 2022 and March 2nd 2023.

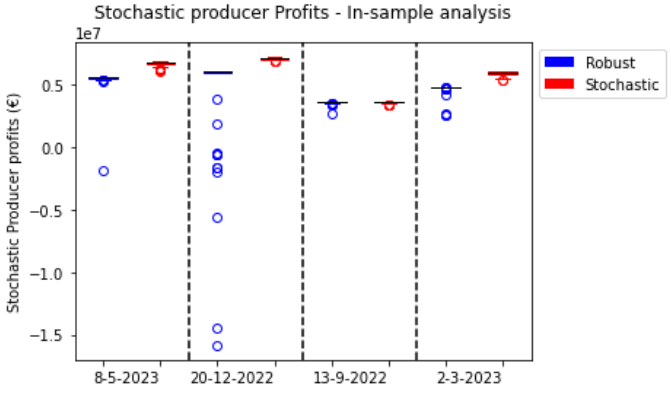

Graph 9. Stochastic producer profits from in-sample scenarios – The Netherlands

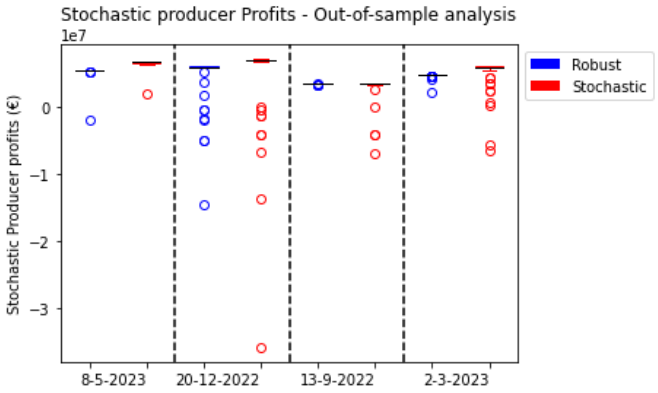

Graph 10. Stochastic producer profits from out-of-sample scenarios – The Netherlands

Share of VRES in energy mix

Looking at the share of VRES in the energy mix, the Deterministic model is clearly outperforming the Robust model and Stochastic model due to the higher amount of accepted stochastic producer bids. A second explanation can be found when taking into account the amount of curtailed demand, which would increase the share of VRES in the energy mix during the day, a point which will be referred back to in Section 4.1.2.3. During the simulation day of May 8th 2023, which was characterized by a low demand and high forecasted stochastic output (Graph 3), the Deterministic model averages its share of VRES in the energy mix at 47.4% during the day, while the Stochastic model averages its share of VRES in the energy mix at 39.7%. The Robust model yields the lowest average share of VRES in the energy mix at 33.9%. The daily profiles of VRES share of the three models are provided in Graph 11-13 below.

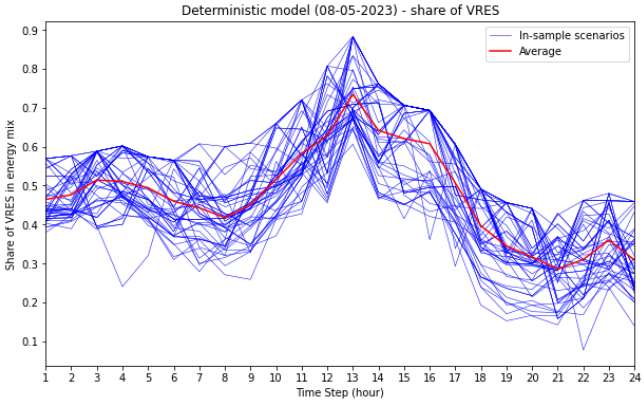

Graph 11. Deterministic model share of VRES in energy mix (08-05-2023) in-sample scenarios – The Netherlands

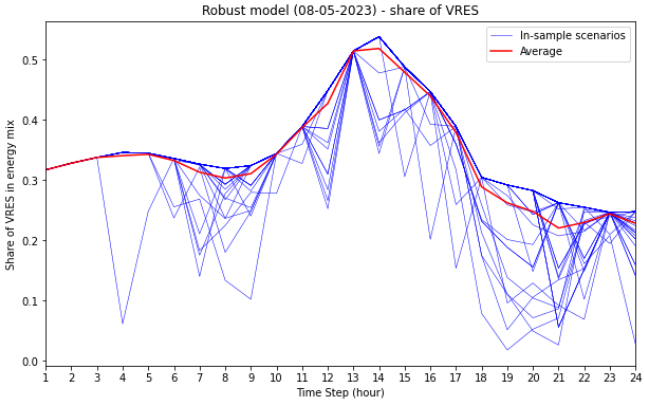

Graph 12. Robust model share of VRES in energy mix (08-05-2023) in-sample scenarios – The Netherlands

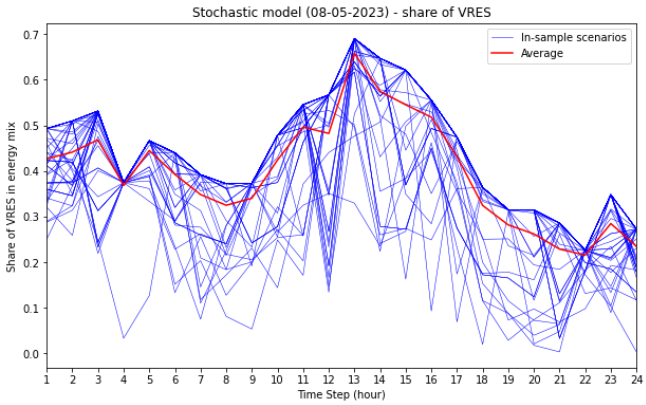

Graph 13. Stochastic model share of VRES in energy mix (08-05-2023) in-sample scenarios – The Netherlands

Due to the fixed amount of procured downward reserves, the Deterministic model is able to increase the stochastic producer output in the energy mix in case of under-forecasting, as can be clearly observed from the amount of scenarios above the average line in Graph 11. Due to the smaller amount of accepted stochastic supply bids, the daily profile of the Robust model appears much less susceptible to deviations in output realization compared to the other models.

Interestingly, the average share of VRES in the energy mix of the Stochastic model is higher when running the out-of-sample scenarios, averaging 25.9% compared to 25.0% during the in-sample scenarios. However looking at the balancing costs as provided in Appendix B.2, higher upward reserve procurement and load shedding costs are resulting from the out-of-sample scenarios, indicating the Stochastic model performance decreased during the out-of-sample scenarios by fitting the optimal solution to the in-sample scenarios. The daily profiles are presented in Graph 14 and Graph 15.

A complete overview of the share of RES daily profiles for the different market clearing models for the simulation days can be found in Appendix C.1 (in-sample) and Appendix C.2 (out-of-sample).

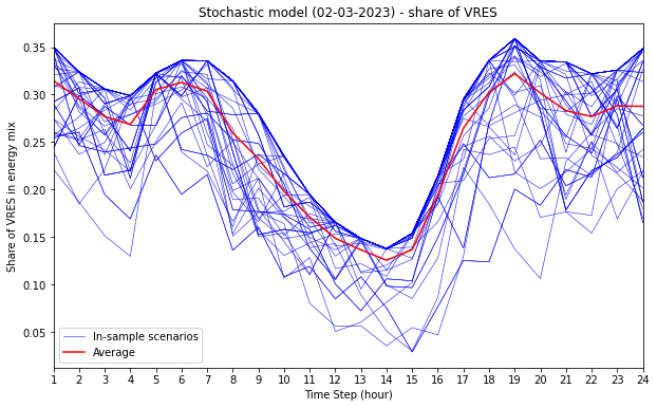

Graph 14. Stochastic model share of VRES in energy mix (13-09-2022) in-sample scenarios – The Netherlands

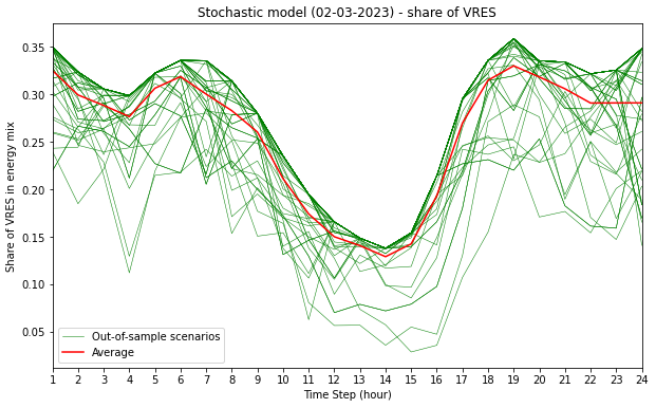

Graph 15. Stochastic model share of VRES in energy mix (13-09-2022) out-of-sample scenarios – The Netherlands

Amount of wind spillage

Inversely proportional to the results of the integration of RES in the energy mix are the results of the amount of wind spillage. The Deterministic model, accepting higher amounts of stochastic supply bids, is averaging much lower amounts of wind spillage in both the in-sample as out-of-sample scenarios, specifically in the simulation days September 8th 2023 and December 20th 2022. Due to this higher amount of accepted stochastic producer bids, less scenarios occur in which an excess of stochastic producer output is realized to cause spillage of wind. Comparing the results of the Deterministic model and Stochastic model for simulation day December 20th 2022 (Graph 16 and Graph 17), the Deterministic model is clearly activating upward reserves during a large part of the day, while the Stochastic model has rather decreased the amount of accepted stochastic producer bids to save costs on upward reserve procurement and activation, resulting in an increased SEW.

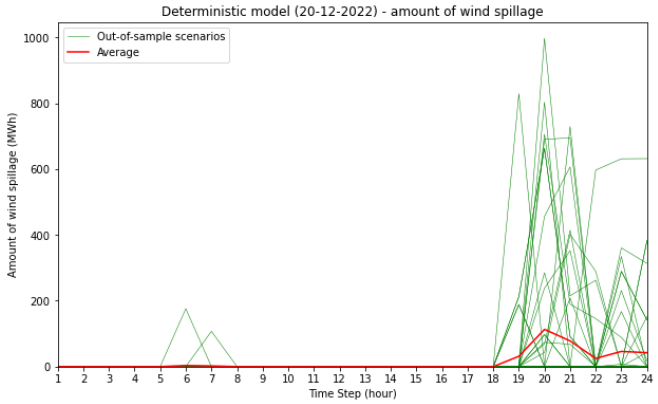

Graph 16. Deterministic model - Amount of wind spillage (20-12-2022) out-of-sample scenarios – The Netherlands

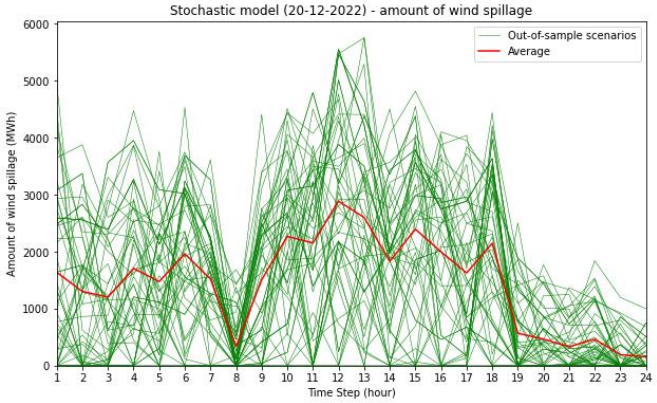

Graph 17. Stochastic model - Amount of wind spillage (20-12-2022) out-of-sample scenarios – The Netherlands

The Robust model shows the highest amounts of wind spillage during all simulation days, as could be expected from the low share of RES in the energy mix mentioned before. The conservativeness of the Robust model results in the lowest amount of accepted stochastic producer bids, which increases the occurrences and amounts of wind spillage during the scenarios. A table overview of the daily average amount of wind spillage during the simulation days is provided in Table 8 (in-sample) and Table 9 (out-of-sample) below.

Simulation day	Robust	Deterministic	Stochastic
08-05-2023	63,992	4,671	36,582
20-12-2022	107,700	785	77,602
13-09-2022	17,328	9,363	16,335
02-03-2023	38,700	3,967	8,423

Table 8. Daily average amount of wind spillage (MWh) for in-sample scenarios – The Netherlands

Simulation day	Robust	Deterministic	Stochastic
08-05-2023	62,478	4,164	29,460
20-12-2022	104,036	752	75,260
13-09-2022	15,845	8,721	14,956
02-03-2023	41,807	4,324	9,703

Table 9. Daily average amount of wind spillage (MWh) for out-of-sample scenarios – The Netherlands

The amounts of wind spillage differ vastly between the different simulation days. Especially during the simulation days with lower amounts of forecasted stochastic producer output, namely May 8th 2023 and December 20th 2022, the Robust model stands out with much higher amounts of wind spillage compared to the Deterministic model and Stochastic model due to its conservativeness.

A complete overview of the amount of wind spillage for the different market clearing models for the simulation days can be found in Appendix D.1 (in-sample) and Appendix D.2 (out-of-sample).

4.1.2.3 System security of supply - The Netherlands

Frequency of load shedding events

The Stochastic model and Robust model are trying to minimize the occurrences of load shedding events due to the high VoLL of demand curtailment by increasing the amount of procured reserves and decreasing the amount of accepted stochastic supply bids. This results in decreased frequencies of load shedding events, as can be seen from Table 10 below. The Deterministic model, being bound to a fixed amount of procured reserves, is particularly prone to load shedding events during the simulation day of December 20th 2022, which is characterized by high degrees of wind-uncertainty.

Simulation day	Deterministic	Robust	Stochastic
08-05-2023	9.90%	0.0096%	0.00%
20-12-2022	18.35%	0.074%	0.00%
13-09-2022	0.016%	0.0032%	0.00%
02-03-2023	1.51%	0.0064%	0.00%

Table 10. Frequency of load shedding events from in-sample analysis – The Netherlands

The results from the out-of-sample analysis show an approximately even performing Deterministic model. The Robust model shows a high degree of robustness to load shedding events, for both the in-sample and out-of-sample scenarios, only experiencing load shedding events during a fraction of the in-sample and out-of-sample scenarios. The Stochastic model, not experiencing a single load shedding event during the in-sample scenarios, performs significantly worse during the out-of-sample scenarios, as can be seen from the results in Table 11.

Simulation day	Deterministic	Robust	Stochastic
08-05-2023	9.33%	0.0098%	0.018%
20-12-2022	18.60%	0.067%	0.10%
13-09-2022	0.18%	0.00%	0.046%
02-03-2023	1.04%	0.0033%	0.070%

Table 11. Frequency of load shedding events from out-of-sample analysis – The Netherlands

Magnitude of load shedding events

When looking at the amount of load shedding during the different simulation days, a perspective on the severity of the load shedding events is provided. As can be seen from Graph 18 and Graph 19 below, showing the daily amount of load shedding events during the simulation runs, the stochastic model and Robust model are experiencing relatively small load shedding events compared to the Deterministic model.

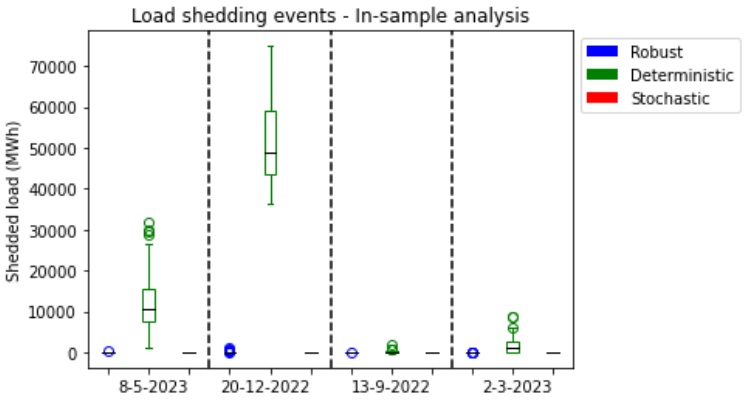

Graph 18. Amount of load shedding from in-sample scenarios – The Netherlands

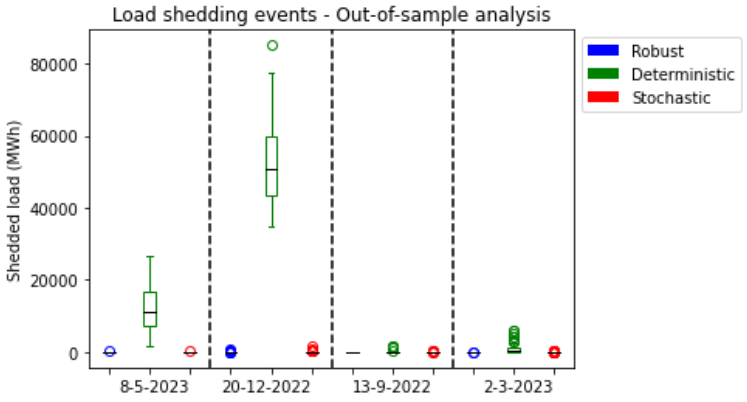

Graph 19. Amount of load shedding from out-of-sample scenarios – The Netherlands

During the simulation runs of December 20th 2022, the Stochastic model and Robust model are experiencing a daily amount of around 900 MWh at maximum during the out-of-sample scenarios, while the Deterministic model is averaging an amount of 50,979 MWh and 50,346 MWh when running the in-sample and out-of-sample scenarios. During the out-of-sample scenarios, the Robust model is decreasing the amount of curtailed demand by 40.7% compared to the Stochastic model.

4.1.2.4 Results summary – The Netherlands

The Stochastic model and Robust model result in a significantly higher SEW compared to the Deterministic model due to the decrease of load shedding events. The Stochastic model has the highest performance during the in-sample scenarios as a result of a smaller amount of procured upward reserves compared to the Robust model; as a consequence, the Robust model yields a slightly higher SEW during the out-of-sample scenarios.

The Stochastic model yields the highest stochastic producer profits in both the in-sample and out-of-sample scenarios, followed closely by the Robust model. While the Deterministic model brings forth the highest share of RES in the energy mix, the high costs to address imbalances result in the lowest stochastic producer profits. The Stochastic model decreases the share of RES in the energy mix significantly with around 8%, although the Robust model decreases the share of RES in the energy mix by roughly 13%. These results are reflected in the amount of wind spillage, which is significantly higher

for the Robust model, while differences between the Deterministic model and Stochastic model are comparable, although substantial.

Finally, the results of the system security of supply indicate a big increase in performance from both the Stochastic model and Robust model compared to the existing Deterministic model. While the differences are most notable during simulation days with high stochastic output forecasts, the amount of curtailed electricity during load shedding events is limited to <1000 MWh during a single scenario. Performance of the Stochastic model is higher compared to the Robust model during the in-sample scenarios, while the Robust model is the best performing model during the out-of-sample scenarios.

4.2 Case Study 2: France

The second case study, France, covers a land area of 549,970 km^2 and inhabits a population of 62,814,233 people [87]. Compared to other EU countries, France's GDP and annual electricity consumption both rank second. As of 2021, the majority of electricity generation was sourced from nuclear energy (68%), while fossil energy sources like gas (7%) and coal (2%) have a marginal share in the energy mix. A share of 23% of the total electricity generation was sourced by wind (8%), hydro (12%), solar (1%), biofuels/biomass (1%) and other sources (1%) [88]. The dependence on nuclear energy emerged from the 1973 oil crisis, after which the country, not possessing over domestically located reserves of fossil energy sources, wanted to decrease its reliance on imports [89].

4.2.1 Input data - France

In this case study, the French electricity wholesale market is simulated with 138 conventional producers, 44 demand loads from consumers and 7 wind farms (stochastic producers) for 24 consecutive hours to test the different DA market clearing models. An overview and description of the wind farm locations and the simulation days will be provided in sub-sections 4.2.1.1 and 4.2.1.2 below.

4.2.1.1 Wind farm locations – France

As of 2021, France had a total of 18,908 MW installed wind capacity, of which all located onshore [90]. Although many offshore wind farms are currently under construction to be completed in the near future, none of these have yet been operational and connected to the power grid. The installed wind capacity of France will be divided into 7 locations. An overview of the locations is provided in Figure 5 below:

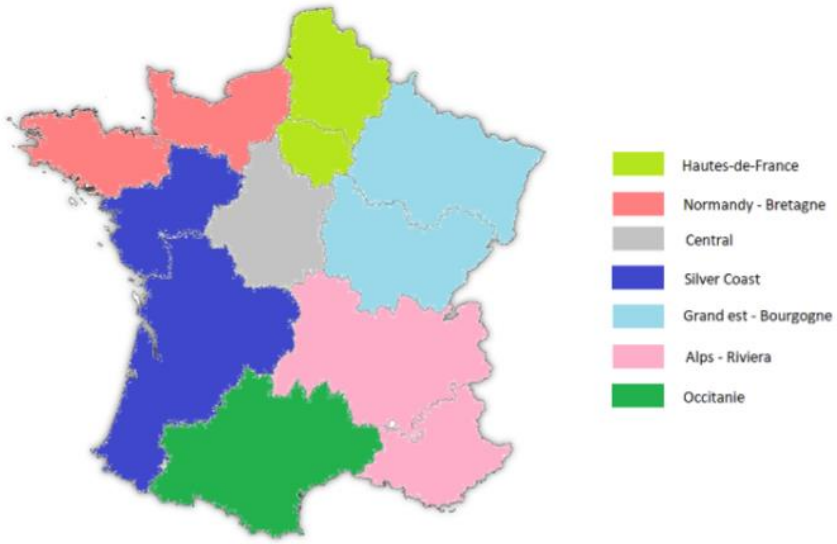

Figure 5. Overview of stochastic production locations – France

The values of installed wind capacity are retrieved from [89]. A description of the different wind locations is provided below:

Hautes-de-France region

The first location includes the installed wind capacity of both the northern regions of Hautes-de-France (5,307 MW) and Île-de-France (127 MW), cumulating to an installed wind capacity of 5,434 MW.

Normandy – Bretagne

The second location includes the regions of Normandy (905 MW) and Bretagne (1,164 MW) with a combined installed wind capacity of 2,069 MW.

Central region

The third location refers to the region of Centre Val de Loire with an installed wind capacity of 1,392 MW.

Silver Coast region

The fourth location, named the Silver Coast region, constitutes the newly established region of Nouvelle-Aquitaine with an installed capacity of 2,507 MW.

Grand est – Bourgogne region

The fifth location includes both the regions of Grand est (4,198 MW) and Bourgogne-Franche-Comté (940 MW) with a combined installed capacity of 5,138 MW.

Alps - Riviera

The sixth location includes both the regions of Auvergne-Rhone-Alpes (600 MW) and Provence-Alpes-Côte-d'Azur (113 MW) with a combined installed capacity of 713 MW.

Occitanie region

The final location is the region Occitaine with an installed capacity of 1,655 MW.

An overview of the wind farm locations of France is provided in Table 12 below.

Region name	Installed wind capacity (MW)	Percentage of total
Hautes-de-France (W1)	5,434	28.7%
Normandy – Bretagne (W2)	2,069	10.9%
Central (W3)	1,392	7.4%
Silver Coast (W4)	2,507	13.3%
Grand est – Bourgogne (W5)	5,138	27.2%
Alps – Riviera (W6)	713	3.7%
Occitanie (W7)	1,655	8.8%
Total	18,908	100%

Table 12. Overview of wind farm locations – France

4.2.1.2 Simulation days - France

In this sub-section, an overview of the demand load profiles and the DA wind generation forecasts will be provided.

Demand load patterns

The demand load patterns of the four selected simulation days are presented below in Graph 20. As can be seen, the demand load patterns of the simulation days stay somewhat stable during the day. The simulation days during the winter (December 20th 2022) and early spring (March 2nd 2023) bear the highest demand of electricity compared to the late spring (May 8th 2023) and autumn (September 13th 2022) simulation days.

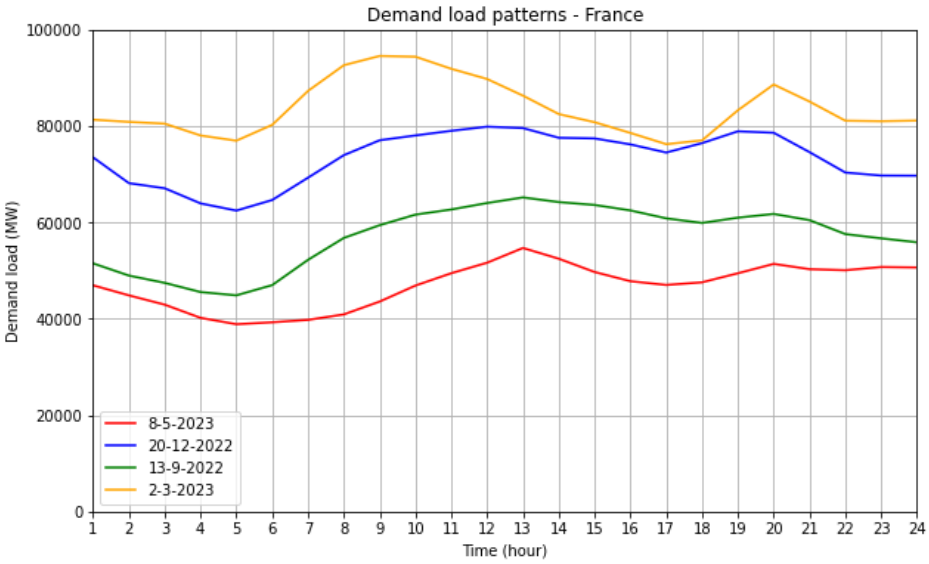

Graph 20. Demand load patterns of selected simulation days (MW) – France

Forecasted stochastic output profile

The cumulative forecasted stochastic output profiles of the 7 wind farms locations are presented in Graph 21 below. While the forecasted stochastic output of three of the simulation days are somewhat in line with the demand load patterns as shown in Graph 20, a notable difference is made during the day May 8th 2023, yielding the highest forecasted stochastic producer output.

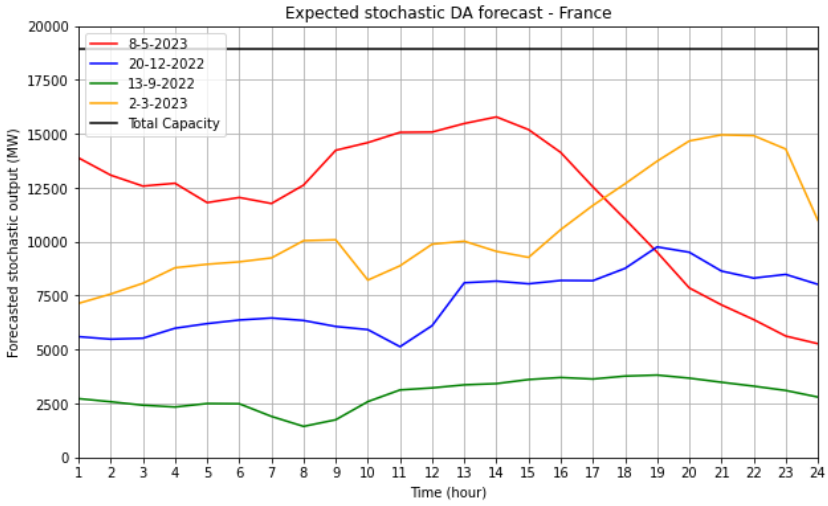

Graph 21. DA forecasted stochastic generation profiles of the four simulation days – France

When looking at a comparison of the demand load patterns and the forecasted wind profiles of the simulation days, as provided in Graph 22 below, a relatively small share of stochastic output in the energy mix is expected for all simulation days.

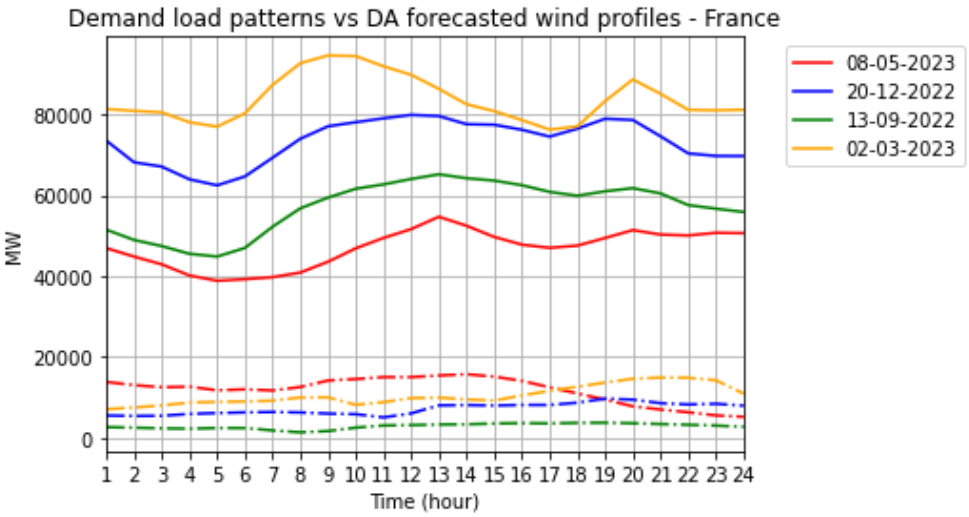

Graph 22. Demand load patterns (solid) vs DA forecasted wind profiles (dash-dotted) - France

4.2.2 model results - France

In this section, the model results of the DA market clearing models during the four simulation days are presented for both the in-sample scenarios and out-of- sample scenarios for the French case study. The performance criteria as described in Section 3.2 will be treated in separate sub-sections.

4.2.2.1 Maximizing SEW – France

The resulting SEW from the simulation runs of the different models is quite comparable, as can be seen from the results in Graph 23 and Graph 24 below.

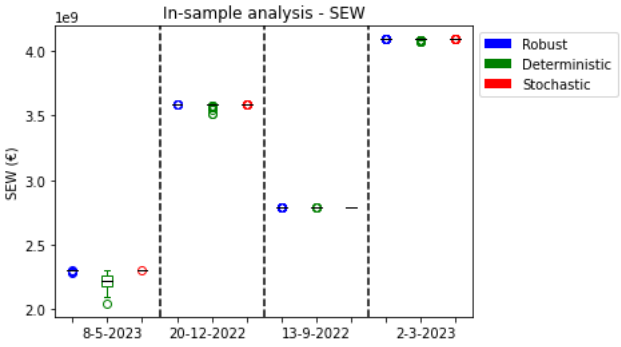

Graph 23. SEW of in-sample scenarios for simulation days – France

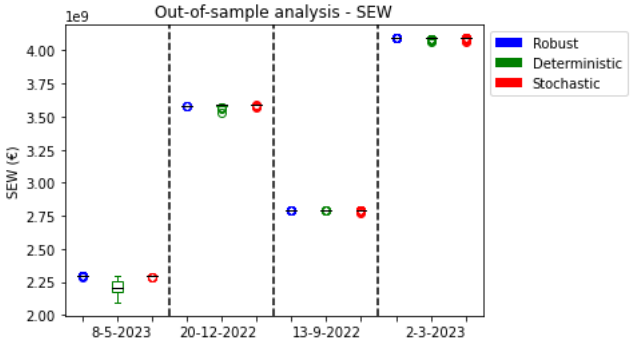

Graph 24. SEW of out-of-sample scenarios for simulation days – France

For the in-sample and out-of-sample scenario runs of May 8th 2023, the simulation day with the highest forecasted stochastic producer output, the resulting SEW of the deterministic model is the lowest with the highest deviation between the results due to higher costs resulting from imbalances. The Stochastic model slightly outperforms the robust model during the in-sample scenarios by 0.024%, while the Robust model slightly outperforms the stochastic model by 0.017% during the out-of-sample scenarios due to significantly increased balancing costs resulting from the Stochastic model during the out-of-sample scenarios. During the simulation run December 20th 2022, characterized by a low forecasted stochastic producer output, the Stochastic model slightly outperforms the Robust model, as is the case for the simulation run of March 2nd 2023. The SEW results from the simulation run of September 13th 2022 are extremely comparable due to low amounts of deviations in stochastic output realization from the DA forecast. A numerical overview of the average SEW during the simulation runs is provided in Table 12 below.

Simulation	Robust	Deterministic	Stochastic
May 8th 2023 (in-sample)	€2.297 * 10^9	€2.211 * 10^9	€2.298 * 10^9
May 8th 2023 (out-of-sample)	€2.298 * 10^9	€2.207 * 10^9	€2.297 * 10^9
December 20th 2022 (in-sample)	€3.585 * 10^9	€3.581 * 10^9	€3.586 * 10^9
December 20th 2022 (out-of-sample)	€3.585 * 10^9	€3.582 * 10^9	€3.585 * 10^9
September 13th 2022 (in-sample)	€2.794 * 10^9	€2.794 * 10^9	€2.794 * 10^9
September 13th 2022 (out-of-sample)	€2.794 * 10^9	€2.794 * 10^9	€2.794 * 10^9
March 2nd 2023 (in-sample)	€4.091 * 10^9	€4.090 * 10^9	€4.093 * 10^9
March 2nd 2023 (out-of-sample)	€4.092 * 10^9	€4.090 * 10^9	€4.091 * 10^9

Table 12. Numerical overview of average SEW - France

Consumer surplus

The consumer surplus resulting from the different DA market clearing models is comparable within a 0.01% range for the simulation days of May 8th 2023, December 20th 2022 and September 13th 2022. Due to the high amount of nuclear conventional producers, and thus, a high amount of supply bids with the same bid price, a small increase or decrease in the amount of accepted stochastic supply bids will not have a large effect on the MCP and the consumer surplus. However, due to the high demand of electricity for simulation day March 2nd 2023, the MCP is determined further up the merit order, impacting the MCP. The decrease in MCP for the Stochastic model, resulting from less amounts of accepted stochastic supply bids and less procured upward reserves, causes a drop in the consumer surplus, a point which will be treated in the *producer surplus* section. A numerical overview of the Consumer surplus results is provided in Table 13 below.

Simulation day	Robust	Deterministic	Stochastic
08-05-2023	€2.291 * 10^7	€2.291 * 10^7	€2.291 * 10^7
20-12-2022	€3.578 * 10^7	€3.578 * 10^7	€3.578 * 10^7
13-09-2022	€2.788 * 10^7	€2.788 * 10^7	€2.788 * 10^7
02-03-2023	€4.074 * 10^7	€4.077 * 10^7	€4.077 * 10^7

Table 13. Overview of DA Consumer surplus for simulation days – The Netherlands

Producer surplus

While the results of the simulation days May 8th 2023, December 20th 2022 and September 13th 2022 are as could be expected, namely the highest producer surplus for the Deterministic model, followed by the Stochastic model due to an increased amount of accepted stochastic producer output for these models, the results of March 2nd 2023 are opposed to these expectations, as can be seen from the results in Graph 25.

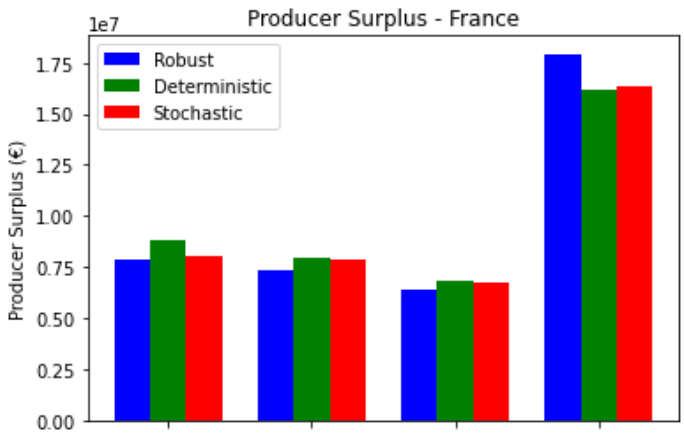

Graph 25. DA Producer surplus for simulation days – France

The Robust model results in the highest producer surplus, increasing the producer surplus 10.7% compared to the Deterministic model, which would seem contradicting given the conservative nature of the Robust model. However, the producer surplus is not higher due to an increased amount of accepted stochastic producer output, but rather because of the high amount of procured upward reserves; these upward procured reserves retain a part of the conventional producer capacity which leads to the use of more expensive conventional producers to meet demand. As can be seen from the results shown in Graph 26, the MCP is higher for the Robust model, resulting in the higher producer surplus. Recalling the consumer surplus results as depicted in Table 13, the higher MCP negatively affects the consumer surplus, resulting in the lowest consumer surplus when applying the Robust model.

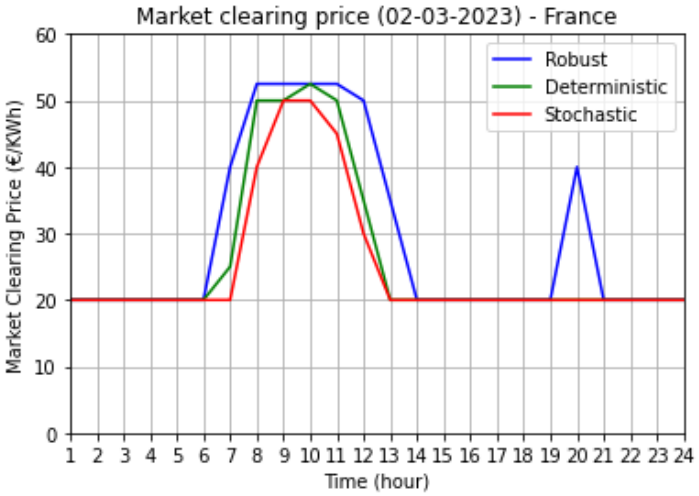

Graph 26. Market clearing price of March 2nd 2023 - France

Balancing costs

The balancing costs resulting from imbalances are differing significantly between the simulation days, with the highest balancing costs occurring during the simulation day May 8th 2023. During this simulation day, characterized with the highest forecasted stochastic producer output, the Deterministic model yields the highest balancing costs for both the in-sample and out-of-sample analysis due to high load shedding costs. The same, albeit more moderately, applies for the results of the simulation days December 20th 2022 and March 2nd 2023. An overview of the balancing costs is provided in Graph 27 and Graph 28.

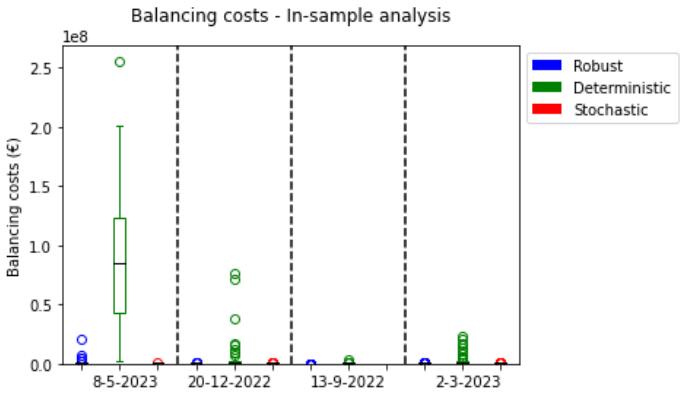

Graph 27. Daily balancing costs in-sample scenarios - France

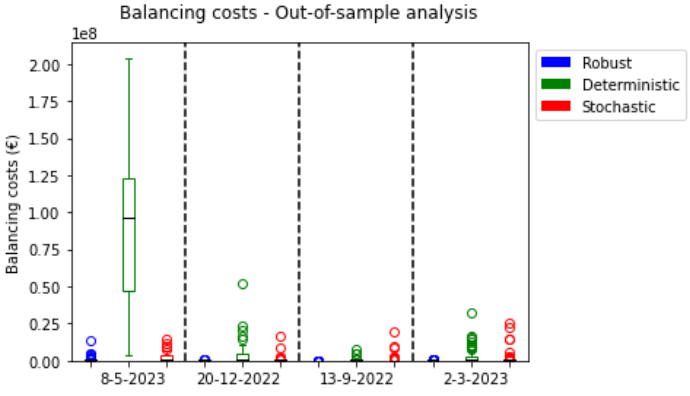

Graph 28. Daily balancing costs out-of-sample scenarios - France

A noteworthy observation can be made when comparing the in-sample and out-of-sample results of the Stochastic model. During the in-sample scenarios the Stochastic model decreases the balancing costs by 63.8% on average compared to the Robust model. However, during the out-of-sample analysis the Robust model decreases the balancing costs by 42.1% on average compared to the stochastic model. This difference is due to the decreased performance of the Stochastic model during the out-of-sample scenarios compared to the in-sample scenarios; the Robust model performs quite evenly during the simulations.

A Complete overview of the average balancing costs is provided in Appendix B.3 and Appendix B.4.

4.2.2.2 Integration of RES - France

Stochastic producer surplus

The stochastic producer surplus turns out the highest for the Deterministic model, although very slightly compared to the Stochastic model for the simulation day September 13th 2022, as can be seen from the results in Graph 29. The Robust model is yielding the lowest stochastic producer surplus for each simulation day, despite having the stochastic producers benefitting from an increased MCP (Graph 26). Overall, the Deterministic model results in an average increase of the stochastic producer surplus of 10.8% compared to the Stochastic model and 55.9% compared to the Robust model.

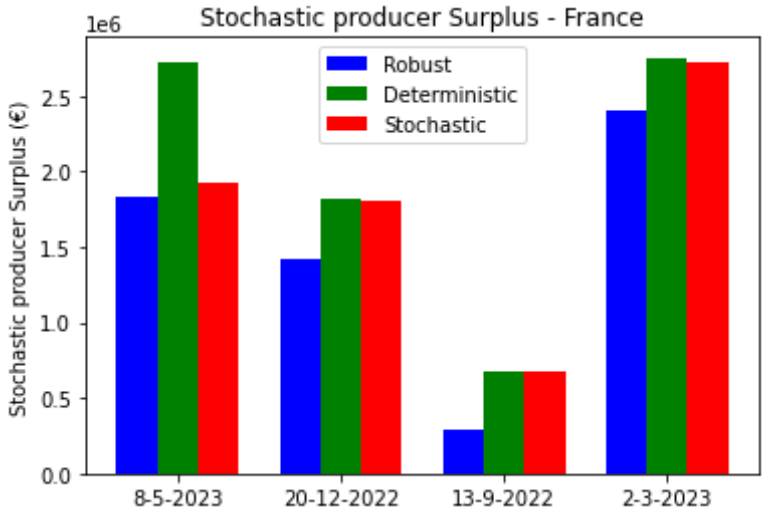

Graph 29. DA Stochastic producer surplus for simulation days – France

However, when subtracting the balancing costs (Appendix B.3) from the stochastic producer surplus to retrieve the stochastic producer profits, a different picture is drawn, as can be seen from Graph 30 and Graph 31. With the exception of simulation day September 13th 2022, which only experiences moderately deviating stochastic output realization scenarios, the Stochastic- and Robust model yield the highest profits for stochastic producers.

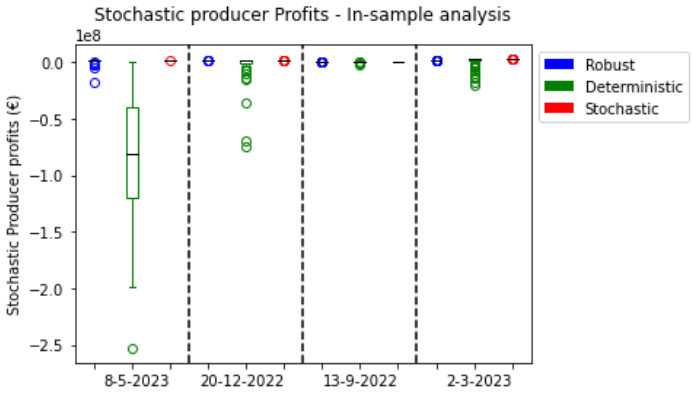

Graph 30. Stochastic producer profits from in-sample scenarios – France

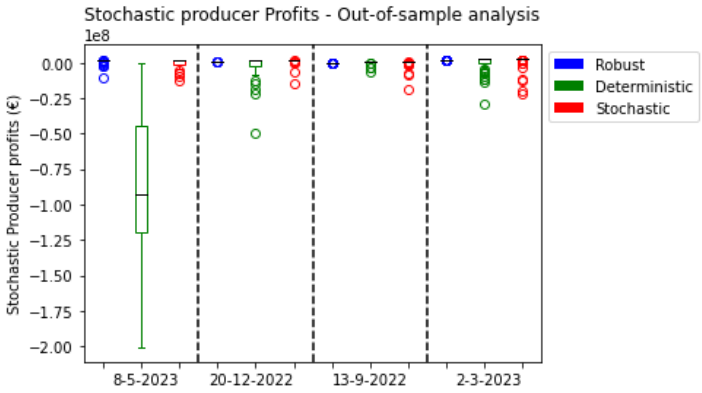

Graph 31. Stochastic producer profits from out-of-sample scenarios – France

While the stochastic producer profits from applying the Stochastic model are 58.6% higher on average compared to the Robust model during the in-sample scenarios, the out-of-sample analysis results indicate potential net losses during the out-of-sample analysis for each individual simulation day.

Share of RES in energy mix

The Deterministic model is the model yielding the highest share of VRES in the energy mix. Looking at the in-sample daily profiles of the share of VRES in the energy mix of May 8th 2023 (Graph 32-34), the Deterministic model yields a share of 15.9%, followed by the Stochastic model with a share of 12.5%, while the Robust model yields the lowest share at 11.8%. During the simulation days, the Deterministic model averages a share of 9.8% VRES in the energy mix, while the Stochastic model (7.8%) and Robust model (5.9%) have a significantly lower share. Note that the averages are brought down by the low forecast scenario September 13th 2022, in which the Deterministic model averaged a share of 4.1% VRES.

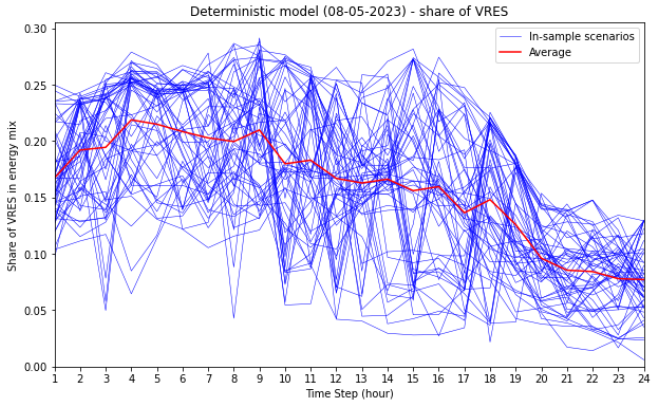

Graph 32. Deterministic model share of VRES in energy mix (08-05-2023) in-sample scenarios – The Netherlands

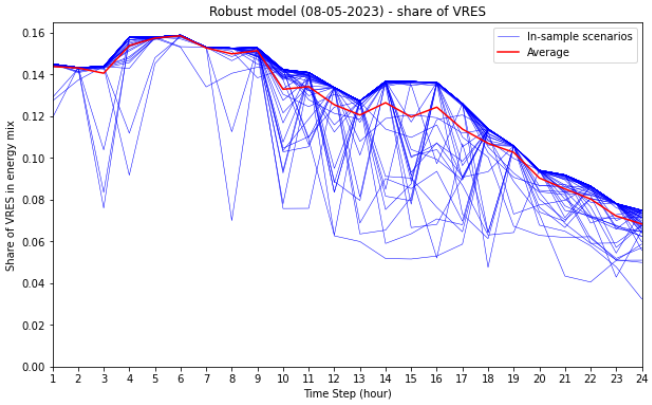

Graph 33. Robustc model share of VRES in energy mix (08-05-2023) in-sample scenarios – The Netherlands

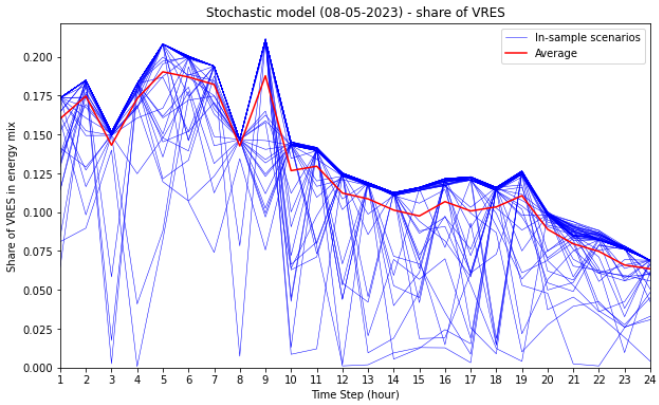

Graph 34. Stochastic model share of VRES in energy mix (08-05-2023) in-sample scenarios – France

Besides a higher amount of accepted stochastic supply bids, another reason for the higher share of VRES in the energy mix of the Deterministic model is the fixed amount of procured upward reserves. These reserves enable the Deterministic model to ramp down conventional producers in case of under-forecasted stochastic producer output and increase generation of stochastic producers. The Stochastic model and Robust model, not procuring upward reserves, are constrained by the amount of accepted stochastic producer bids, regardless of output realization.

Looking at the results of simulation day September 13th 2022, an interesting difference between the Stochastic model and Robust model can be made. Given the low forecasted stochastic output realization, the Stochastic model allows for more frequent activation of upward reserves due to the relatively smaller activated amounts of reserves, as can be seen from Graph 35. The Robust model rather decreases the amount of stochastic producer bids to prepare for the worst-case scenario, resulting in significantly less activation of upward reserves (Graph 36).

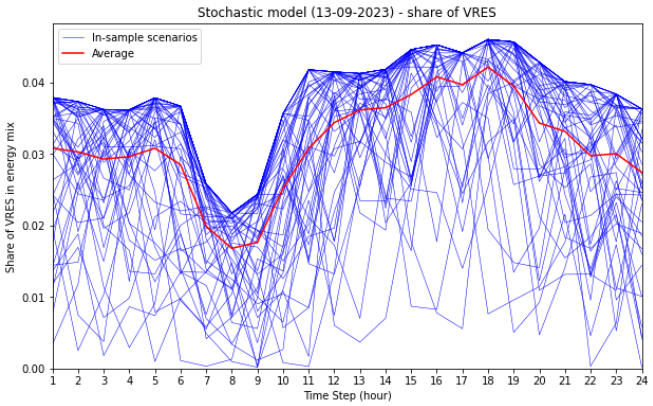

Graph 35. Stochastic model share of VRES in energy mix (13-09-2022) in-sample scenarios – France

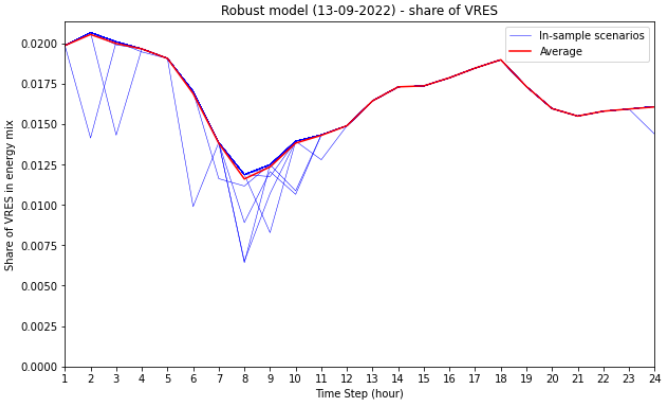

Graph 36. Robust model share of VRES in energy mix (13-09-2022) in-sample scenarios – France

The difference between the in-sample and out-of-sample scenario results from the Stochastic model and Robust model are very similar. Only during simulation day May 8th 2023 the Stochastic model decreases its share of VRES to 12.4%, a decrease of 0.8% compared to the in-sample scenarios. Despite highly differing balancing costs resulting from the Stochastic model during the in-sample scenarios and out-of-sample scenarios, the results of the Stochastic model are notably similar, as can be observed from Graph 37 and Graph 38 below.

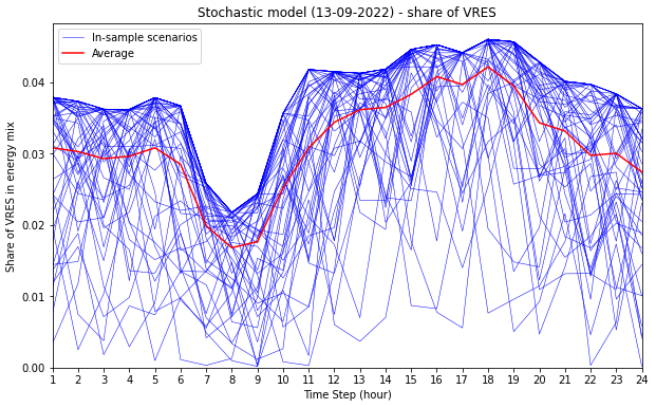

Graph 38. Graph 39. Stochastic model share of VRES in energy mix (31-09-2022) in-sample scenarios – France

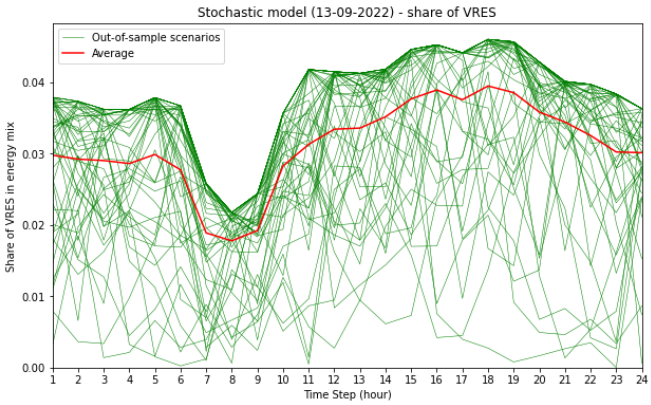

Graph 37. Stochastic model share of VRES in energy mix (13-09-2022) out-of-sample scenarios – France

A complete overview of the daily profiles of the share of VRES for the different market clearing models during the simulation days can be found in Appendix C.3 (in-sample) and Appendix C.4 (out-of-sample).

Amount of wind spillage

Compared to the Robust model and Stochastic model, the Deterministic model results in the least amount of wind spillage during the simulation days. Looking at the results of simulation day December 20th 2022, the Robust model is experiencing the highest amount of wind spillage, followed by the Stochastic model. The daily profile of amount of wind spillage of the in-sample scenarios is provided in Graph 39-41 below. During this simulation day, the Deterministic model is averaging a daily amount of 12,707 MWh of wind spillage, followed by the Stochastic model (22,678 MWh) and Robust model (42,916 MWh).

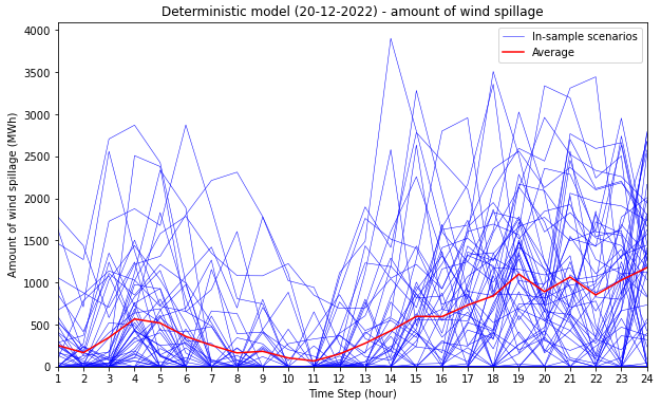

Graph 39. Deterministic model - Amount of wind spillage (20-12-2022) in-sample scenarios – France

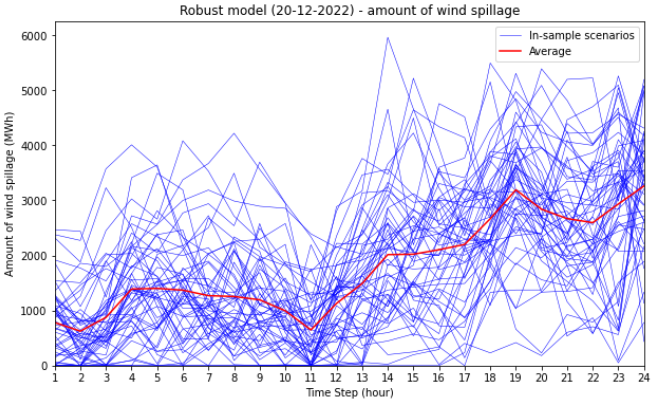

Graph 40. Robust model - Amount of wind spillage (20-12-2022) in-sample scenarios – France

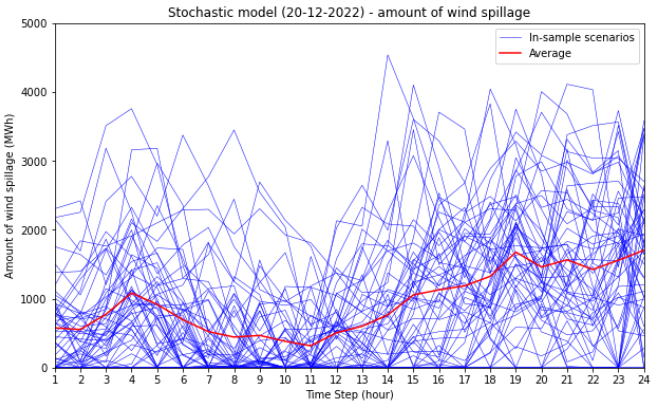

Graph 41. Stochastic model - Amount of wind spillage (20-12-2022) in-sample scenarios – France

Comparing the in-sample and out-of-sample results, the Stochastic model is providing rather similar results. Looking at the results of the simulation day May 8th 2023 as can be seen from Graph 42 and Graph 43, characterized with the highest forecasted amount of stochastic producer output, the average amount of wind spillage is even decreasing with 6.7% during the out-of-sample scenarios. However, this increase in share of VRES can be attributed to the amount of curtailed demand during the out-of-sample scenarios, decreasing the total amount of delivered demand.

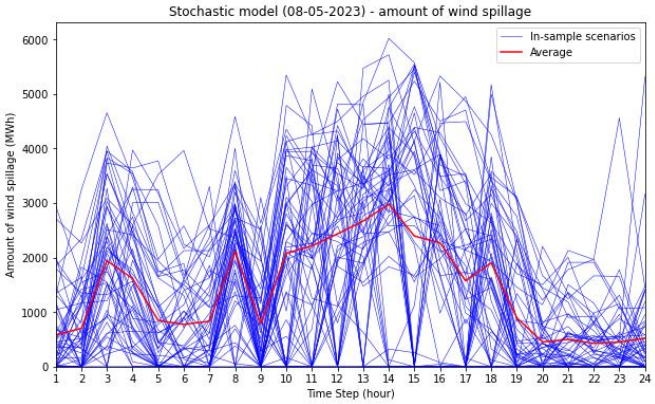

Graph 42. Stochastic model Amount of wind spillage (08-05-2023) in-sample scenarios – France

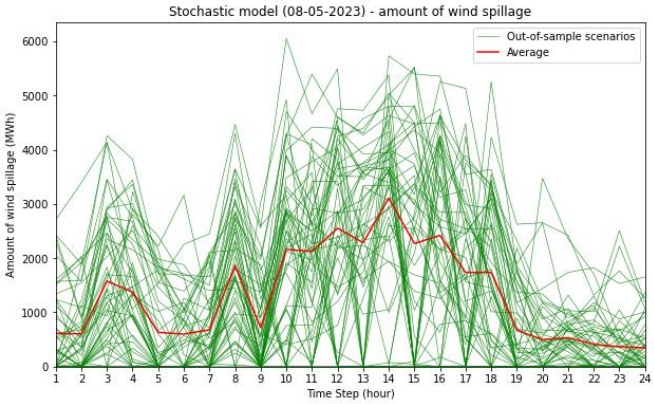

Graph 43. Stochastic model Amount of wind spillage (08-05-2023) in-sample scenarios – France

A complete overview of the amount of wind spillage for the different market clearing models for the simulation days can be found in Appendix D.3 (in-sample) and Appendix D.4 (out-of-sample).

4.2.2.3 System security of supply - France

Chance of load shedding events

The Deterministic model is experiencing load shedding events during all simulation days for both the in-sample and out-of-sample scenarios, mainly during the simulation day March 5th 2023. The Robust model is experiencing load shedding events during the simulation day March 5th 2023. The Stochastic model is outperforming the other models during the in-sample scenarios, not experiencing a single load shedding event. On the contrary, during the out-of-sample analysis the Stochastic model its performance decreases significantly, resulting in load shedding events during all simulation days. An overview of the chance of load shedding events is provided in Table 14 and Table 15 below.

Simulation day	Deterministic	Robust	Stochastic
08-05-2023	3.91%	0.05%	0.00%
20-12-2022	0.25%	0.00%	0.00%
13-09-2022	0.01%	0.00%	0.00%
02-03-2023	0.12%	0.00%	0.00%

Table 14. Chance of load shedding events from in-sample analysis – France

Simulation day	Deterministic	Robust	Stochastic
08-05-2023	4.191%	0.038%	0.111%
20-12-2022	0.231%	0.000%	0.025%
13-09-2022	0.028%	0.002%	0.078%
02-03-2023	0.124%	0.000%	0.070%

Table 15. Chance of load shedding events from out-of-sample analysis – France

Magnitude of load shedding events

Looking at the amount of electricity curtailed during load shedding events, the Deterministic model is clearly underperforming, averaging an amount of 12,802 MWh (in-sample) and 13,358 MWh (out-of-sample) of curtailed demand during the simulation day of May 8th 2023. Although clearly underperforming during the in-sample scenarios, the out-of-sample results of the Deterministic model and Stochastic model are quite comparable during the three other simulation days. During the simulation day September 13th 2022, the Stochastic model causes 123 MWh of curtailed demand on average during the out-of-sample scenarios, compared to zero from the Robust model. Although the Robust model is only experiencing rather small load shedding events during the majority of the scenarios, a maximum amount of 2,856 MWh (in-sample) and 1,816 MWh (out-of-sample) of demand is curtailed in outlying scenarios. An overview of the magnitude of the load shedding events during the simulation days is provided in Graph 44 and Graph 45.

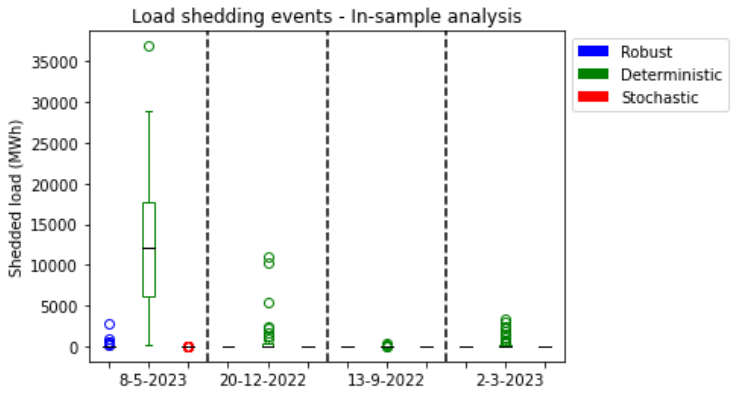

Graph 44. Amount of load shedding from in-sample scenarios – France

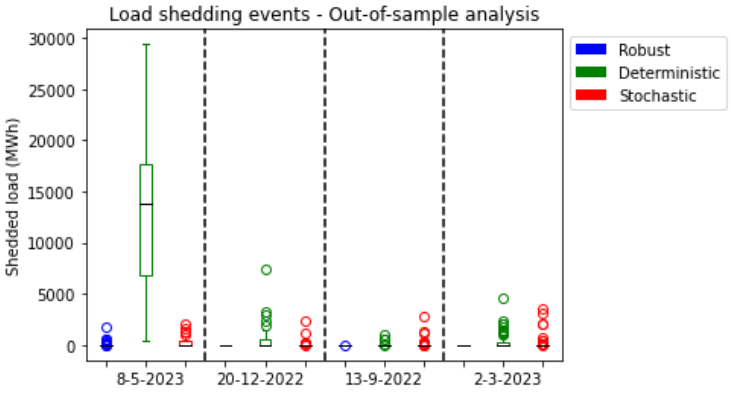

Graph 45. Amount of load shedding from out-of-sample scenarios – France

4.2.2.4 Results summary – France

The SEW results of the three models show quite comparable performance, safe for the simulation day May 8th 2023 characterized by the highest forecasted stochastic producer output. The results of the producer surplus indicate a significantly increase in the producer surplus for the Robust model due to an increased MCP because of higher amounts of upward reserve procurement, although this producer surplus is directly subtracted from the consumer surplus.

Despite accepting higher amounts of stochastic producer bids, as could be seen from the higher share of VRES in the energy mix, the stochastic producers experience net losses on average when applying the Deterministic model. The Stochastic model and Robust model average with net profits for Stochastic producers, while negative outlying results are appearing more frequently for the Stochastic model during the out-of-sample scenarios. The Robust model resulted in the lowest share of VRES in the energy mix with the highest amount of wind spillage.

Looking at the results of the system security of supply, the Robust model is outperforming both the Deterministic model and Stochastic model. The occurrence of load shedding events during the simulation day May 8th 2023 for the Robust model indicate a too high degree of lenience in the budget of uncertainty during this simulation day. The performance of the Stochastic model, not experiencing a single load shedding event during the in-sample scenarios, significantly decreases during the out-of-sample scenarios during all simulation days.

4.3 Case Study 3: Germany

Germany, the third case study, is the most populated country of the three case studies with a total of over 84 million inhabitants while covering an land size area of 348,672 km^2. As of 2022, the German energy mix for electricity generation is already heavily sourced by renewable energy sources with a share of 48.3% in the electricity mix, of which 25.9% offshore and onshore wind, 11.4% solar PV, 2.8% hydropower and 8.6% biomass. Despite heavily decreasing the use of coal and nuclear energy for electricity generation, the share of coal (32.8%), natural gas (11.5%) and nuclear (8.0%) still had a high share in the energy mix. The last remaining three nuclear power plants are planned to be decommissioned on April 15th 2023 [91]. To draw even the results between the simulation days, these nuclear power plants are left out from all simulation runs in this research.

4.3.1 Input data - Germany

In this case study, the French electricity wholesale market is simulated with 671 conventional producers, 48 demand loads from consumers and 7 wind farms (stochastic producers) for 24 consecutive hours to test the different DA market clearing models. An overview and description of the wind farm locations and the simulation days will be provided in sub-sections 4.3.1.1 and 4.3.1.2 below.

4.3.1.1 wind farm locations - Germany

As of 2023, Germany has an installed wind capacity of 64,303 MW of which 56,848 MW placed on land and 7,455 MW placed offshore in the Baltic sea and North sea [92][93]. The installed wind capacity of Germany will be divided into 7 locations. An overview of the locations is provided in Figure 6 below:

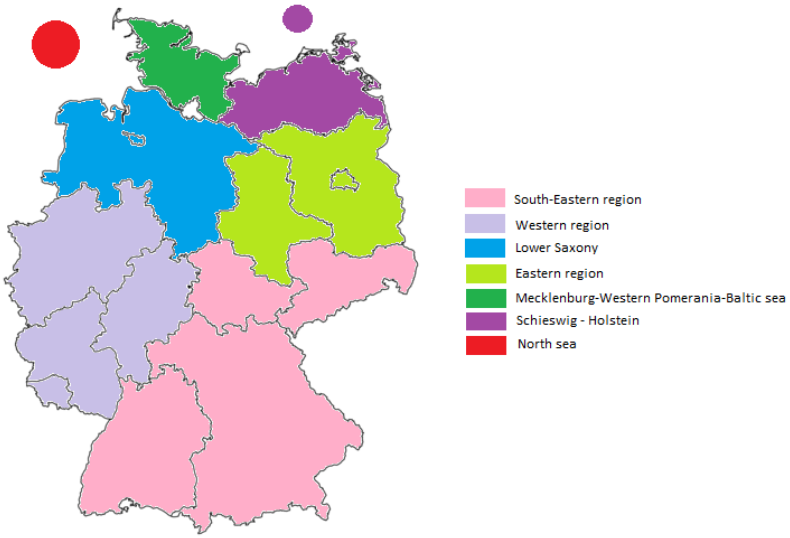

Figure 6. Overview of stochastic production locations – Germany

The values of installed wind capacity are retrieved from [92] and [93]. A description of the different wind locations is provided below:

South-Eastern region

The first region represents the installed wind capacity of Bavaria (2,575 MW), Baden-Württemberg (1,729 MW), Thüringen (1,733 MW) and Saxony (1,273 MW) with a combined wind capacity of 7,310 MW.

Western region

The second region represents the installed wind capacity of Saarland (520 MW), Rhineland-Palatinate (3,862 MW), Hesee (2,337 MW) and North Rhine-Westphalia (6,548 MW) with a combined wind capacity of 13,267 MW.

Lower Saxony

The third region is the northern state of Lower Saxony with an installed wind capacity of 11,785 MW.

Eastern region

The Eastern region represents the states of Brandenburg (8,067 MW) and Saxony-Anhalt (5,309 MW) with an installed capacity of 13,376 MW.

Mecklenburg-Western Pomerania-Baltic sea region

The fifth region represents the installed wind capacity of Mecklenburg-Western Pomerania (3,556 MW) and the installed offshore wind capacity on the Baltic sea (1,096 MW) with a combined installed capacity of 4,652MW.

Schleswig-Holstein

The sixth region is the state of Schleswig-Holstein with an installed wind-capacity of 7,215 MW.

North sea

The final region represents the 6,698 MW of installed offshore wind capacity in the North sea.

An overview of the wind farm locations of the Netherlands is provided in Table 15 below.

Region name	Installed wind capacity (MW)	Share of total capacity
South-Eastern region (W1)	7,310	11.4%
Western region (W2)	13,267	20.6%
Lower Saxony (W3)	11,785	18.4%
Eastern region (W4)	13,376	20.8%
Mecklenburg-Western Pomerania-Baltic sea region (W5)	4,652	7.2%
Schleswig-Holstein (W6)	7,215	11.2%
North sea (W7)	6,698	10.4%
Total	64,303	100%

Table 15. Overview of wind farm locations – Germany

4.3.1.2 Simulation days - Germany

In this sub-section, an overview of the demand load profiles and the DA wind generation forecasts will be provided.

Demand load patterns

The demand load patterns of the German case study simulation days are showing en extremely corresponding path, as can be seen from Graph 46. Although interseasonal differences are observable, the demand load patterns are differing no more than 27.5% at any given moment during the simulation days. Moreover, the simulation days during the colder months period (December 20th 2022 and March 2nd 2023) are experiencing nearly identical amounts of demand load during a large part of the day, which can also be said for the simulation days of May 8th 2023 and September 13th 2022.

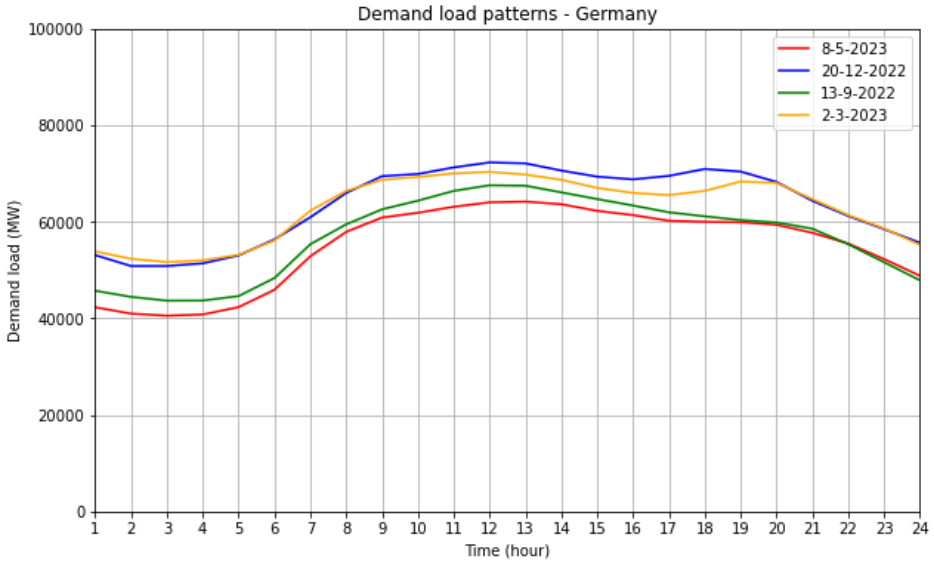

Graph 46. Demand load patterns of selected simulation days (MW) – Germany

Forecasted stochastic output profile

The cumulative forecasted stochastic output profiles of the 7 wind farms locations are presented in Graph 47 below. The simulation day of May 8th 2023 has the highest forecasted stochastic producer output, averaging around 50% of the total installed capacity of the whole day. The second highest forecast is made for March 2nd 2023, followed by September 13th 2022 and December 20th 2022.

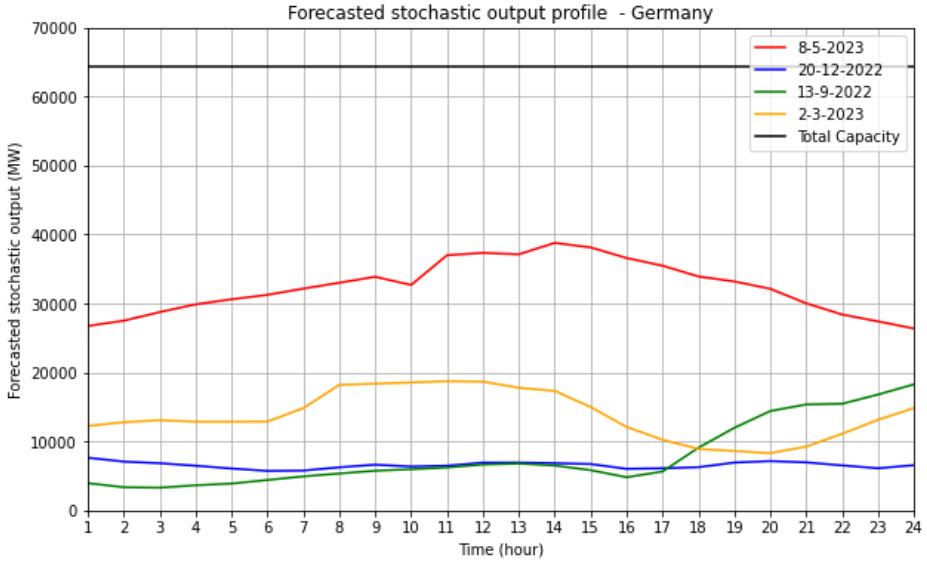

Graph 47. DA forecasted stochastic generation profiles of the four simulation days – Germany

When comparing the demand load profiles and stochastic producer forecasts, it can be expected that the simulation day of May 8th 2023 will experience the highest degree of uncertainty due to the higher share of forecasted stochastic producer output in the energy mix. During the simulation days September 13th 2022 and December 20th 2022, stochastic producer output will only source a small fraction of the demand load. An overview is provided in Graph 48 below.

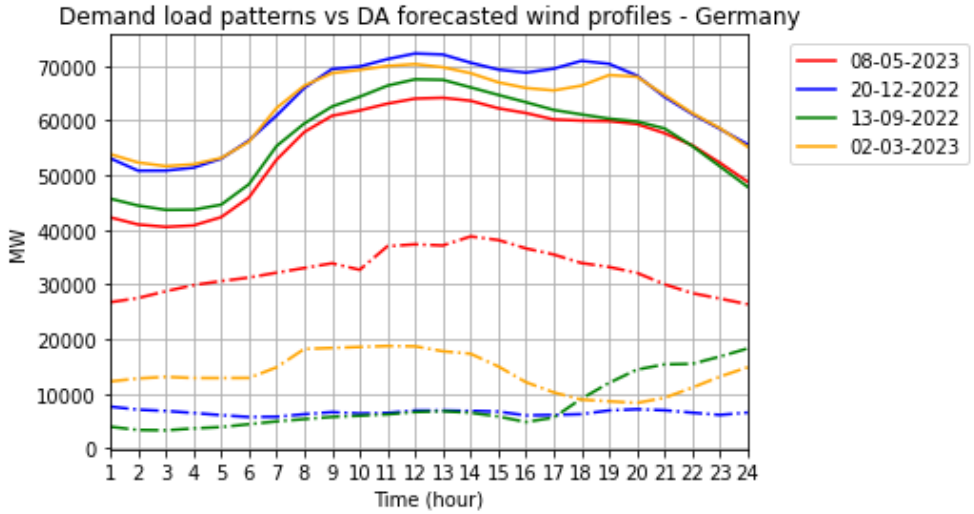

Graph 48. Demand load patterns (solid) vs DA forecasted wind profiles (dash-dotted) – Germany

4.3.2 model results - Germany

In this section, the model results of the DA market clearing models during the four simulation days are presented for both the in-sample scenarios and out-of-sample scenarios for the German case study. The performance criteria as described in Section 3.2 will be treated in separate sub-sections.

4.3.2.1 Maximizing SEW - Germany

From the in-sample results, the Stochastic model yields the highest SEW of the models in all simulation days, followed closely by the Robust model. The Deterministic model is performing nearly equal during the simulation days December 20th 2022 and March 2nd 2023 compared to the Stochastic model and Robust model, while performing much worse during the other two simulation days, resulting in a negative SEW during all simulations of simulation day May 8th 2023. During the simulation day September 13th 2023, a decrease of 33.6% in SEW compared to the Stochastic model and 25.7% compared to the Robust model is observed. On average, the Stochastic model increases the SEW by 0.27% compared to the Robust model. A boxplot overview is provided in Graph 49 below.

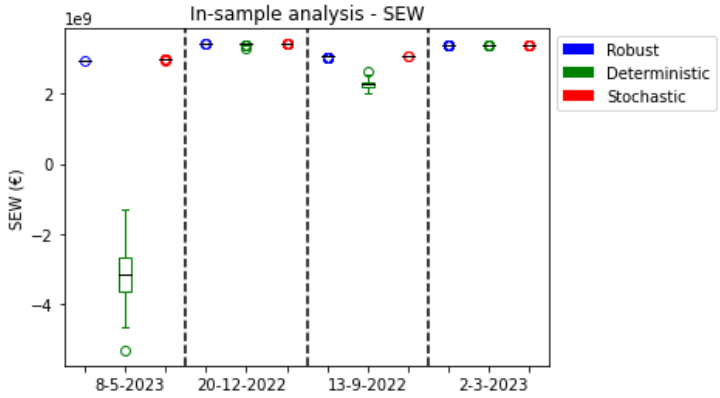

Graph 49. SEW of in-sample scenarios for simulation days – Germany

Looking at the results of the out-of-sample scenarios, the Stochastic model is performing slightly worse compared to the in-sample scenario runs with an average decrease in SEW of 0.17%, while the change in performance of the Robust model is within <0.01%. The Deterministic model, yet again, is the lowest performing model, showing a higher degree of negative deviations in SEW during the simulation day March 2nd 2023. The out-of-sample scenario results are provided in Graph 50.

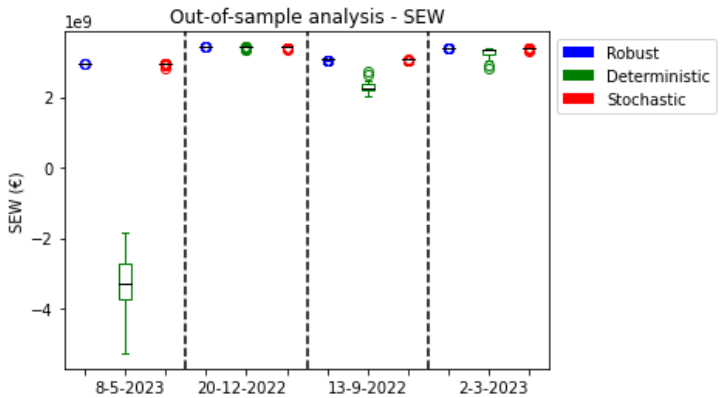

Graph 50. SEW of out-of-sample scenarios for simulation days – Germany

Consumer surplus

The Deterministic model yields the highest consumer surplus during three of the four simulation days by accepting the highest amount of stochastic producer bids. However, during simulation day May 8th 2023, the Deterministic model is yielding the lowest consumer surplus, outperformed by the Robust model and Stochastic model, as can be shown in Table 16.

Simulation day	Robust	Deterministic	Stochastic
08-05-2023	€2.925 * 10^9	€2.921* 10^9	€2.928* 10^9
20-12-2022	€3.376 * 10^9	€3.380* 10^9	€3.379* 10^9
13-09-2022	€3.025* 10^9	€3.027* 10^9	€3.026* 10^9
02-03-2023	€3.334* 10^9	€3.388* 10^9	€3.337* 10^9

Table 16. Overview of DA Consumer surplus for simulation days – Germany

Recalling the demand load profile and stochastic producer output forecast as provided in Graph 48, a high share of VRES in the energy mix was forecasted during the simulation day of May 8th 2023. One would argue that because of the higher amount of accepted stochastic supply bids, a recurring characteristic of the Deterministic model, the consumer surplus would by higher. However due to the fixed amount of upward reserve procurement, for which the cheapest conventional producers are used, the capacity of these cheap conventional producers to meet the demand load is decreased, raising the MCP during these time hours. As can be seen from the results in Graph 51, the Stochastic model yields a lower MCP during $t = \{1, 2, 3, 4, 5, 6, 7, 8, 24\}$, resulting in a higher consumer surplus.

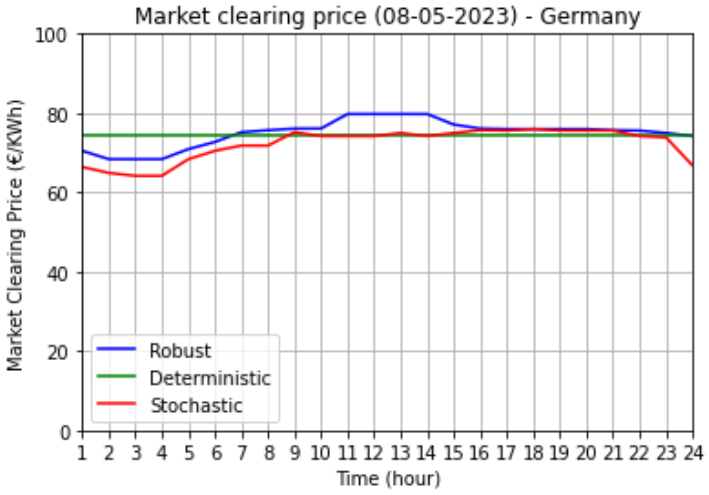

Graph 51. Market clearing price of May 8th 2023 - Germany

Producer surplus

The producer surplus results are quite in line with expectations, indicating the highest producer surplus for the Deterministic model, followed by the Stochastic model with an average decrease of 23.5% and the Robust model yielding the lowest producer surplus with a decrease of 31.3% compared to the Deterministic model. Recalling the observations regarding the MCP made in Graph 51, the significantly higher consumer surplus of the Deterministic model during simulation day May 8th 2023 is a direct consequence of the higher MCP during this day. The producer surplus results are provided in Graph 52 below.

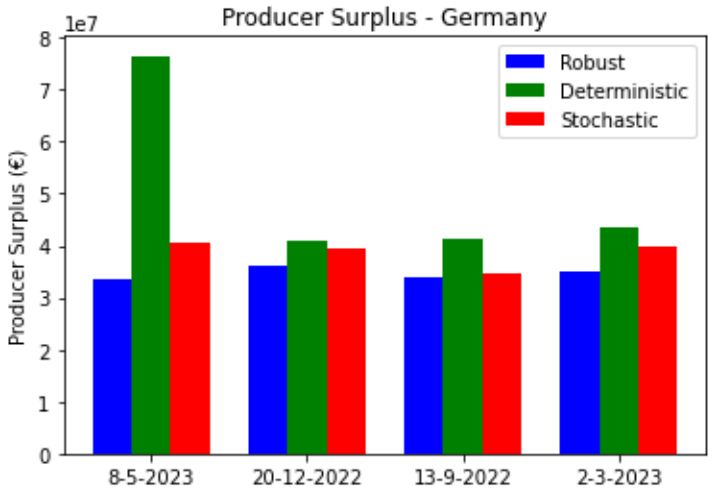

Graph 52. DA Producer surplus for simulation days – Germany

Balancing costs

Looking at the balancing costs, the Deterministic model results are indicating much higher balancing costs compared to the Stochastic model and Robust model. More specifically, the results of simulation day May 8th 2023 indicate high losses, as could also be seen from the Sew results in Graph 49 and Graph 50. The Stochastic model and Robust model are both resulting in much lower balancing costs during the in-sample scenarios, although the Stochastic model results in 52.9% lower costs compared to the Robust model. During the out-of-sample results, the balancing costs resulting from the Stochastic model increase by 276.1%, although a positive SEW on average is provided. The Robust model is performing nearly identical during the out-of-sample analysis, with balancing costs even decreasing by 1.4% on average, decreasing balancing costs by 49.6% compared to the Stochastic model. An overview of the balancing costs is provided in Graph 53 (in-sample) and Graph 54 (out-of-sample).

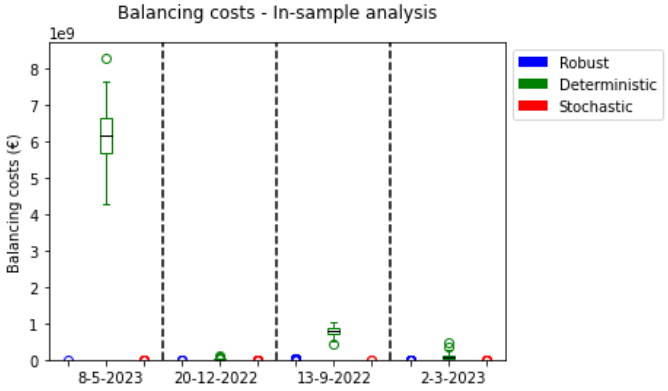

Graph 53. Daily balancing costs in-sample scenarios - Germany

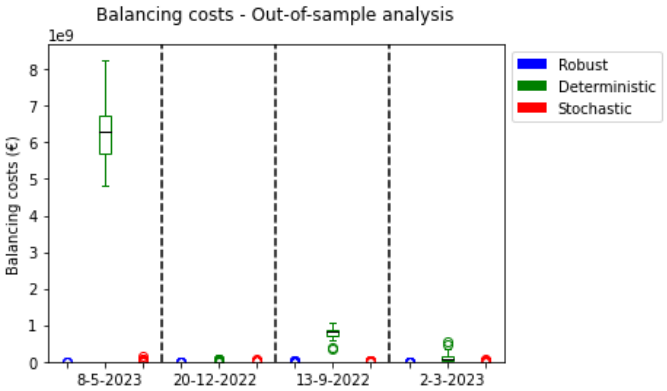

Graph 54. Daily balancing costs out-of-sample scenarios - Germany

A Complete overview of the average balancing costs is provided in Appendix B.5 and Appendix B.6.

4.3.2.2 Integration of VRES - Germany

Stochastic producer surplus

Showing many similarities with the producer surplus results as provided in Graph 52, the DA stochastic producer surplus results are the highest for the Deterministic model during all simulation days. The results of simulation day May 8th 2023 show a much higher stochastic producer surplus in particular, as can be seen from the results in Graph 55.

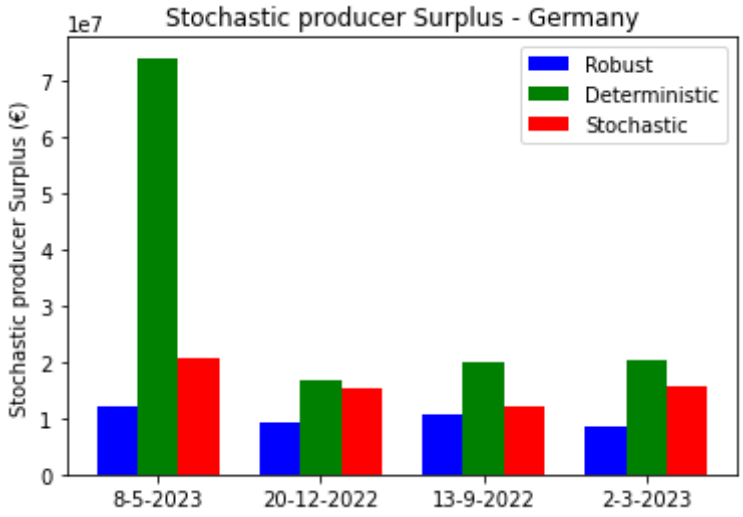

Graph 55. DA Stochastic producer surplus for simulation days – Germany

When taking into account the balancing costs (Appendix B.5-B.6), the Deterministic model results in stochastic producer net losses during the simulation days May 8th 2023, September 13th 2022 and March 2nd 2023 in both the in-sample analysis and out-of-sample analysis. The stochastic model averages profits during all in-sample and out-of-sample scenarios, although the out-of-sample scenarios indicate frequently occurring losses for stochastic producers. notably, the Robust model yields losses when running the out-of-sample scenarios of simulation day September 13th 2022. The stochastic producer profit results are provided in Graph 56 and Graph 57.

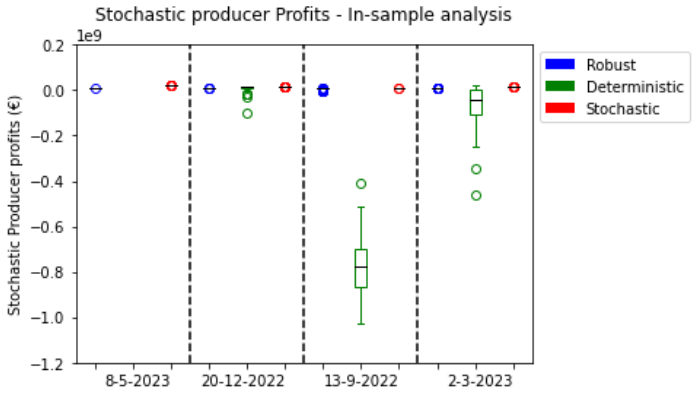

Graph 56. Stochastic producer profits from in-sample scenarios – Germany

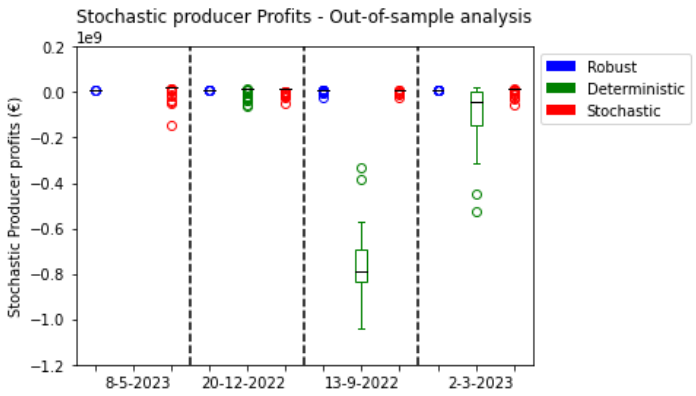

Graph 57. Stochastic producer profits from out-of-sample scenarios – Germany

Note that the Deterministic model results of simulation day May 8th 2023 are withheld from Graph 56 and Graph 57 to compensate for the scaling of the y-axis. The stochastic producer profits average €-6.093 * 10^9 (in-sample) and €-6.225 * 10^9 (out-of-sample) for the Deterministic model during this simulation day.

Share of VRES in energy mix

The results of the share of VRES in the energy mix show substantial differences between the models. Looking at the in-sample scenario simulations of May 8th 2023, the Deterministic model shows the highest share of VRES by a large margin at 71.2%, although a standard deviation of over 5% share of VRES in the energy mix is observable. The Stochastic model, yielding the second highest share of 31.2% of VRES in the energy mix, followed by the Robust model with a share of 18.2%. Save for a single scenario at $t = 18$, the Robust model shows an exorbitant stability in the share of VRES in the energy mix during the simulation day. An overview of the daily profiles of the share of VRES in the energy mix is provided in Graph 58-60 below.

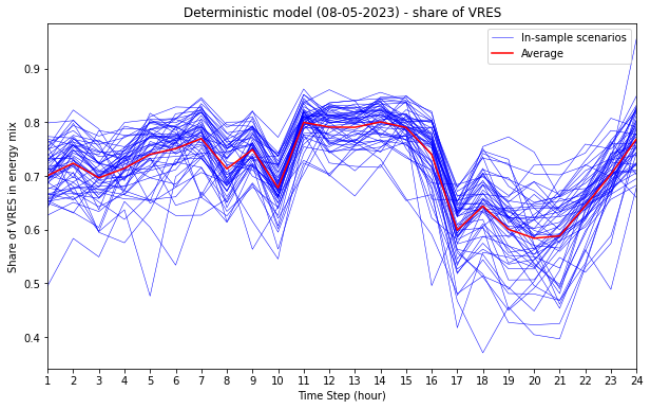

Graph 58. Deterministic model share of RES in energy mix (08-05-2023) in-sample scenarios – Germany

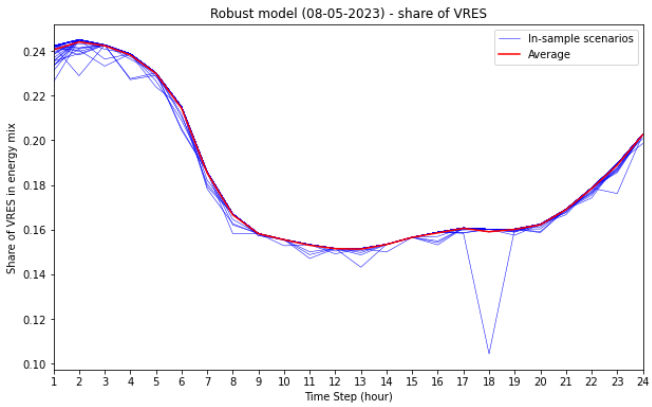

Graph 59. Robust model share of RES in energy mix (08-05-2023) in-sample scenarios – Germany

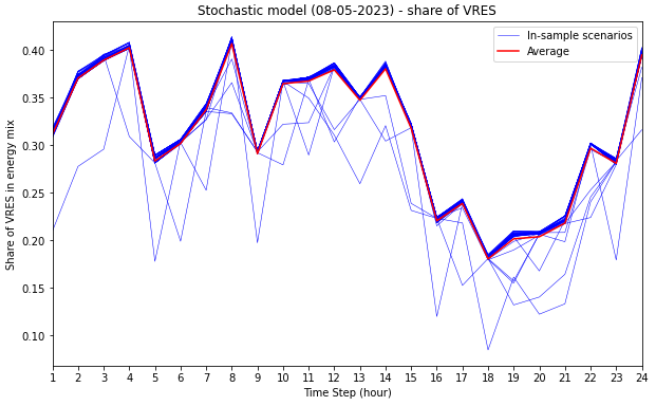

Graph 60. Stochastic model share of RES in energy mix (08-05-2023) in-sample scenarios – Germany

Looking at the daily profile of the Deterministic model in Graph 58, an inconsistency is observable from the demand load and forecasted stochastic output profile as provided in Graph 48; the forecasted amount of stochastic production is not nearly as high as the share of VRES as provided in Graph 58. Note that the results provided above indicate the share of VRES in the energy mix of the total *accepted demand* minus the curtailed electricity during load shedding events (i.e., *delivered demand*).

The results of the in-sample and out-of-sample are similar for both the Stochastic model and the Robust model. Comparing these results of the Stochastic model of simulation days May 8th 2023 and March 2nd 2023 as provided in Graph 60-63 below, the average share of VRES in the energy mix is nearly identical, decreasing the share of VRES in the energy mix by only 0.18% for the Stochastic model and 0.01% for the Robust model.

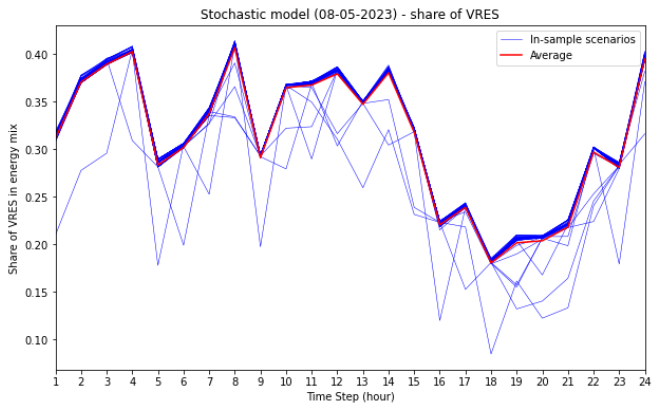

Graph 60. Stochastic model share of RES in energy mix (08-05-2023) in-sample scenarios – Germany

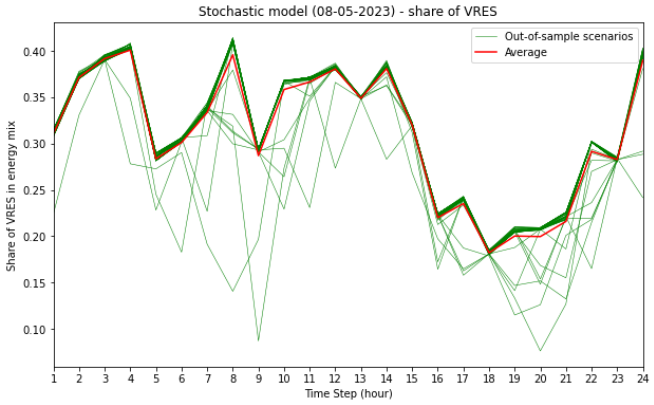

Graph 61. Stochastic model share of RES in energy mix (08-05-2023) out-of-sample scenarios – Germany

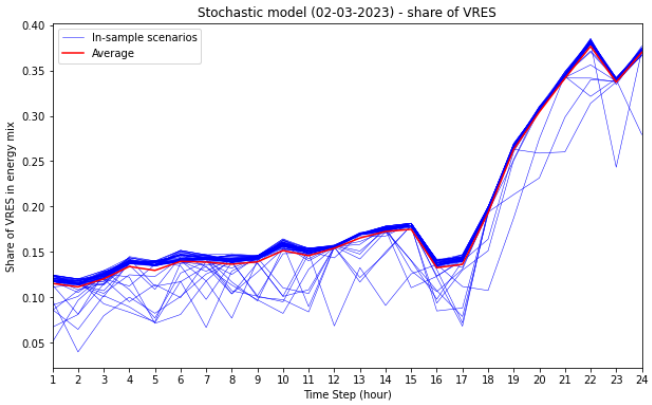

Graph 62. Stochastic model share of RES in energy mix (02-03-2023) in-sample scenarios – Germany

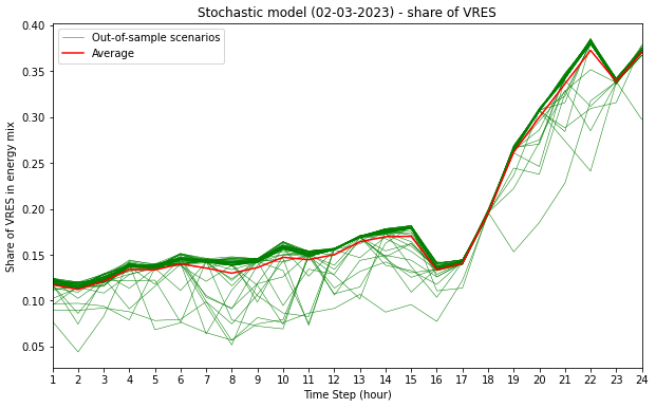

Graph 63. Stochastic model share of RES in energy mix (02-03-2023) out-of-sample scenarios – Germany

A complete overview of the share of VRES daily profiles for the different market clearing models for the simulation days can be found in Appendix C.5 (in-sample) and Appendix C.6 (out-of-sample).

Amount of wind spillage

Quite in line with the results in the previous section, the Deterministic model causes the least amount of wind spillage. As could be expected from the high share of VRES in the energy mix as shown in Graph 58, the amount of wind spillage during simulation day May 8th 2023 is equal to zero, save for a single in-sample scenario. An overview of the amount of wind spillage of May 8th 2023 is provided in Graph 64 below. Note that this also indicate a high frequency of negative net imbalances due to shortages in stochastic output realization, which have to be addresses by either upward reserve activation or curtailment of demand.

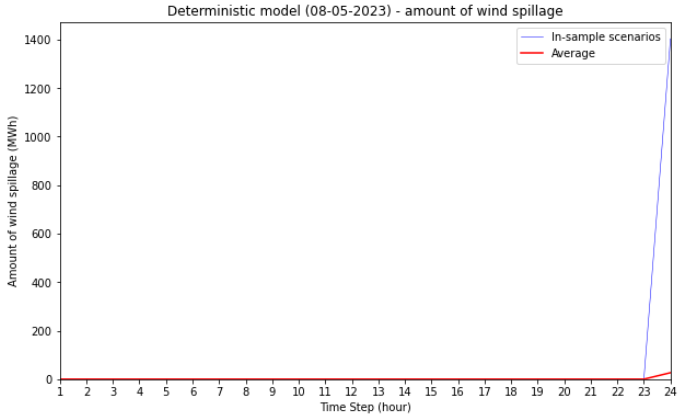

Graph 64. Determinstic model - Amount of wind spillage (08-05-2023) in-sample scenarios – Germany

However, the other simulation days do not provide such extreme results. Comparing the amount of wind spillage of the different models during simulation day December 20th 2022, the results are much closer to one another as can be seen from Graph 65-67 below. An important difference between the Deterministic-, Stochastic- and Robust model are the amount of scenarios with an amount of wind spillage equal to zero, which is significantly higher for the Deterministic model. These moments indicate a higher frequency of shortages of stochastic output realization, as described earlier.

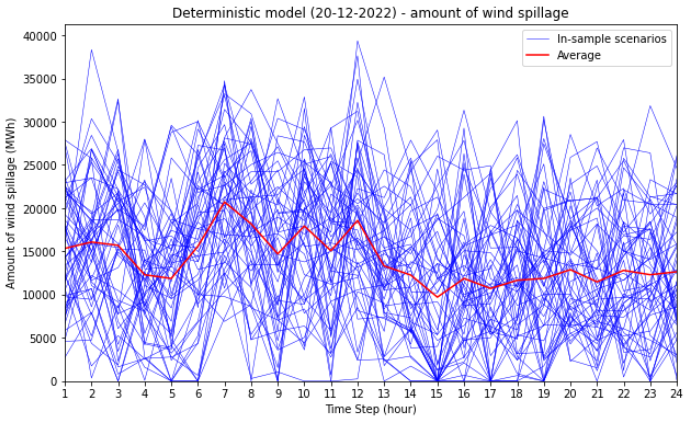

Graph 65. Deterministic model - Amount of wind spillage (20-12-2022) in-sample scenarios – Germany

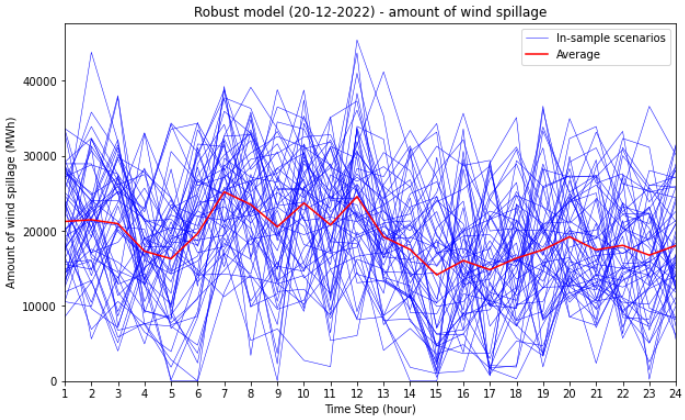

Graph 66. Robust model - Amount of wind spillage (20-12-2022) in-sample scenarios – Germany

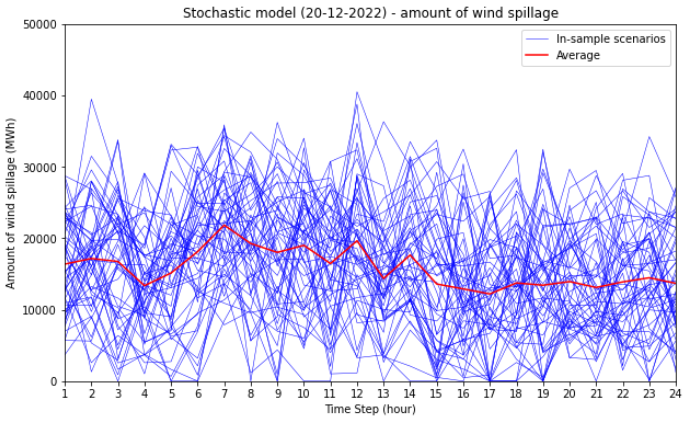

Graph 67. Stochasticc model - Amount of wind spillage (20-12-2022) in-sample scenarios – Germany

A complete overview of the amount of wind spillage for the different market clearing models for the simulation days can be found in Appendix D.5 (in-sample) and Appendix D.6 (out-of-sample).

4.2.3.3 System security of supply - Germany

The percentage of simulated hours experiencing load shedding events is provided for the in-sample scenarios in Table 17 and for the out-of-sample scenarios in Table 18.

Simulation day	Deterministic	Robust	Stochastic
08-05-2023	93.11%	0.00%	0.00%
20-12-2022	0.17%	0.0016%	0.00%
13-09-2022	3.50%	0.072%	0.00%
02-03-2023	1.72%	0.00%	0.00%

Table 17. Chance of load shedding events from in-sample analysis – Germany

Simulation day	Deterministic	Robust	Stochastic
08-05-2023	93.32%	0.00%	0.24%
20-12-2022	0.19%	0.00%	0.098%
13-09-2022	2.90%	0.074%	0.069%
02-03-2023	2.01%	0.00%	0.13%

Table 18. Chance of load shedding events from out-of-sample analysis – Germany

The first observation to address is the extreme chance of load shedding events experienced by the Deterministic model during simulation day May 8th 2023. While this percentage seems unconceivable, it can be explained by looking at the forecasted and realized amount of stochastic producer output, as is shown in Graph 68 below. The simulation day had an extremely case of over-forecasting for nearly all scenarios, clarifying the high amount of load shedding events.

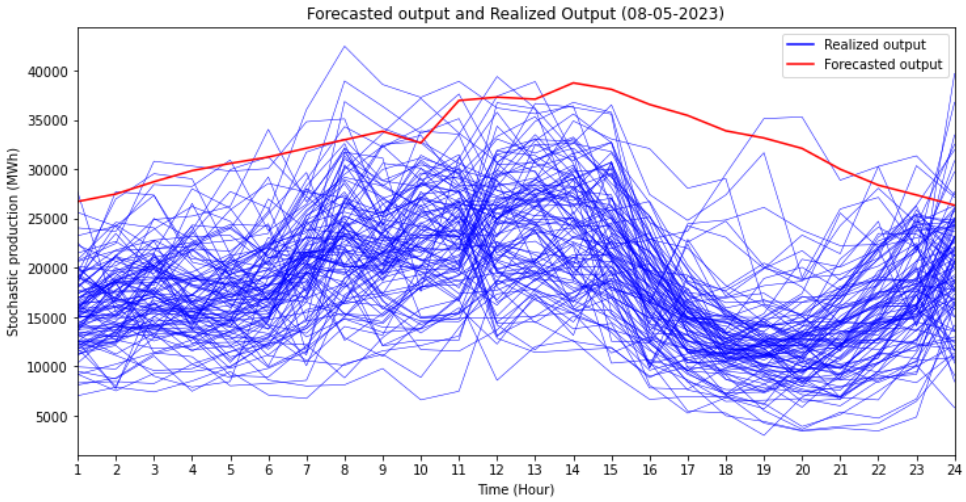

Graph 68. Day profile of Forecasted- and realized stochsatic producer output (08-05-2023) - Germany

A second observation is difference in performance of the Stochastic model between the in-sample scenarios and out-of-sample scenarios. During all out-of-sample simulation days, load shedding events are experienced when applying the Stochastic model, albeit during only a small percentage of the simulated running time. A sensitivity analysis will be performed to test the effect of increasing the in-sample size on the system security of supply for May 8th 2023, the simulation day with the highest percentage of load shedding events during the out-of-sample analysis.

Magnitude of load shedding events

Looking at the amount of curtailed electricity during the load shedding events (Graph 69 and Graph 70), it becomes evident that the Stochastic model and Robust model are experiencing relatively small load shedding events compared to the Deterministic model. During the out-of-sample scenarios of simulation day December 20th 2022, the highest daily amount of curtailed demand is 2,528 MWh for the Robust model, 5,159 MWh for the Stochastic model and over 292,000 MWh in a single scenario for the Deterministic model.

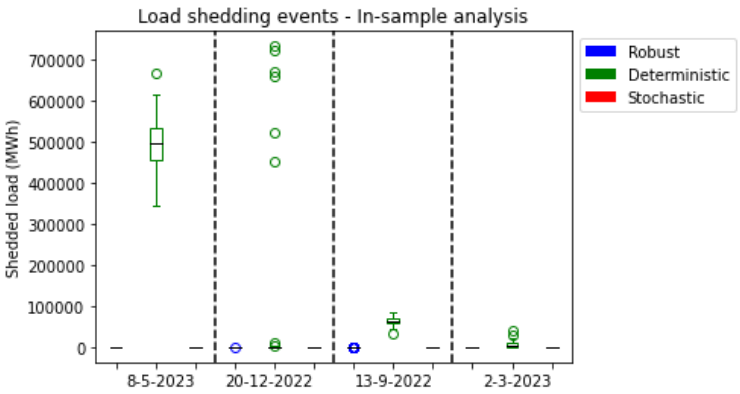

Graph 69. Amount of load shedding from in-sample scenarios – Germany

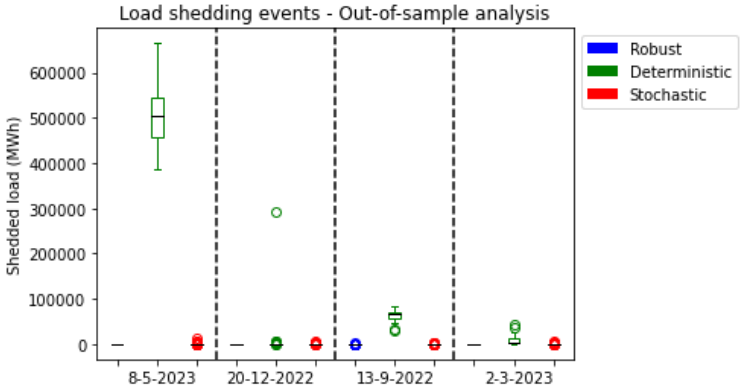

Graph 70. Amount of load shedding from in-sample scenarios – Germany

Looking at the results of simulation day May 8th 2023, the high share of VRES in the energy mix can clearly be assigned to the high amount of curtailed electricity, decreasing the total amount of delivered demand for electricity. With a total amount of 1,048 GWh of accepted demand bids, the average amount of 496 GWh of load shedding events nearly doubles the share of VRES in the Energy mix.

4.3.2.4 Results summary – Germany

The Stochastic model yielded the highest SEW, followed by the Robust model. The Deterministic model observed extreme amounts of balancing costs during the simulation day May 8th 2023, which was characterized by a high degree of over-forecasting of stochastic producer output. Overall, the Deterministic model resulted in the highest consumer- and producer surplus.

The Stochastic model yielded the highest stochastic producer profits during the in-sample scenarios, although the Robust model resulted in the highest security of stochastic producer profits during the out-of-sample scenarios. The results of the share of VRES in the energy mix extremely favored the Deterministic model, although high amounts of shedding events heavily affected these results as a significant part of the demand was curtailed.

The results on the system security of supply show an extremely high reduction in load shedding events for both the Stochastic model and Robust model in the case of over-forecasting, as was the case in simulation day May 8th 2023. The Deterministic model observed extreme high frequencies and amounts of load shedding events during this simulation day. The Stochastic model saw a slight increase

in the frequency of load shedding events during the out-of-sample scenarios, although these events were still rather small in magnitude.

4.4 Sensitivity analysis

A sensitivity analysis is performed on both the budget of uncertainty for the Robust model and the in-sample size of the Stochastic model to test the relationship between the resulting SEW, risk-averseness of load shedding events and integration of VRES in the energy mix. Section 4.4.1 provides the results of the sensitivity analysis on the budget of uncertainty, while Section 4.4.2 provides the results of the in-sample size sensitivity analysis.

4.4.1 Budget of uncertainty

During the simulation runs of the Robust model, the budget of uncertainty was set equal to eq. 7.7:

$$\Gamma = \frac{N_s}{2} \qquad (7.7)$$

As was shown during the case studies, the Robust model yielded the lowest chance of load shedding events, while also yielding the lowest share of VRES in the energy mix. To measure the trade-off between system security of supply, financial performance and integration of VRES, a sensitivity analysis is conducted in which the results of the SEW, chance of load shedding events and share of VRES in the energy mix are used to assess model performance. During the sensitivity analysis, the budget of uncertainty is set equal to:

$$\Gamma = \frac{N_s}{\rho} \qquad (8.1)$$

In which $\rho = \{1.5,\ 2.0,\ 2.5,\ 3.0,\ 3.5,\ 4.0\}$. Table 19 provides an overview of the budget of uncertainty (Γ) with changing ρ values for the different case studies.

ρ value	1.5	2.0	2.5	3.0	3.5	4.0
The Netherlands	3.33	2.50	2.00	1.67	1.43	1.25
France	4.67	3.50	2.80	2.33	2.00	1.75
Germany	4.67	3.50	2.80	2.33	2.00	1.75

Table 19. Overview of ρ value and budget of uncertainty values of the case studies

The simulation days December 20th 2022 (The Netherlands), May 8th 2023 (France) and September 13th 2022 (Germany) will be subjected to the sensitivity analysis. During the French and German simulation days load shedding events were experienced by the Robust model during these simulation day, while for the Dutch case study this particular simulation day possessed the highest degree of uncertainty due to the high amount of forecasted stochastic producer output.

The SEW results indicate similar effects of increases in the budget of uncertainty between the case studies. For the Dutch case study, increasing the ρ value to 2.5 slightly decreases the average SEW, whereafter the average SEW significantly decreases and the amount of outlying results rapidly increase. The results of the French case study indicate a higher degree of robustness with a ρ value of 1.5, limiting the effect of an increased budget of uncertainty to a few outlying scenarios. Even after increasing the ρ value to 4.0, the spread of the resulting SEW of both the in-sample and out-of-sample scenarios only moderately increases. The results of the German case study are quite comparable to the results of the Dutch case study, although large deviations in the results are mainly observable at a ρ value of 3.5. The graph results are provided in Graph 71-76 below.

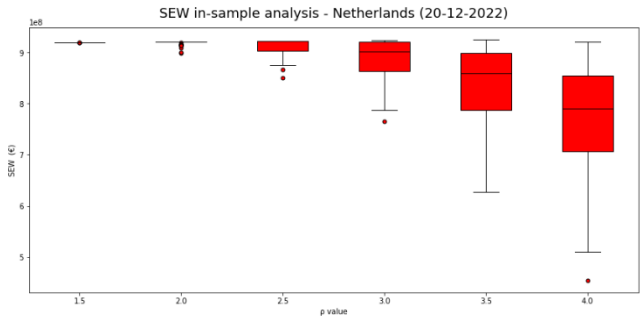

Graph 71. SEW in-sample sensitivity analysis – The Netherlands (20-12-2022)

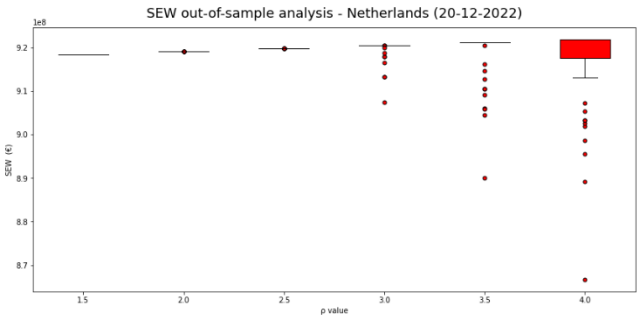

Graph 72. SEW out-of-sample sensitivity analysis – The Netherlands (20-12-2022)

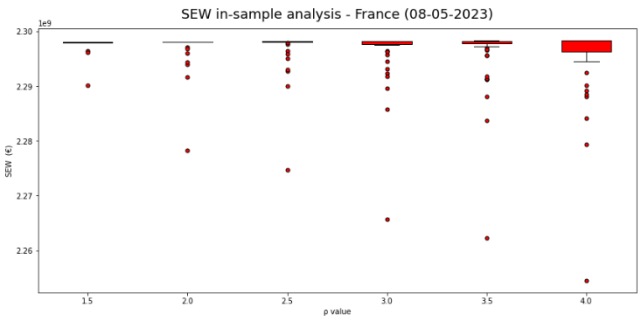

Graph 73. SEW in-sample sensitivity analysis – France (08-05-2023)

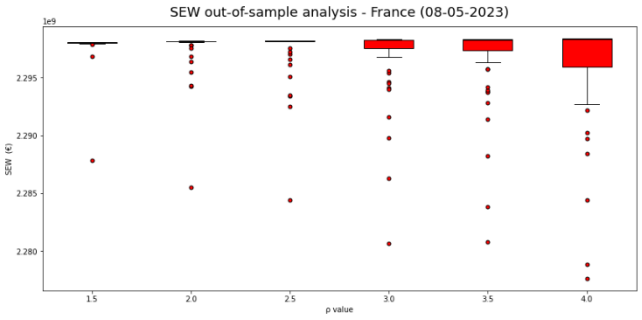

Graph 74. SEW out-of-sample sensitivity analysis – France (08-05-2023)

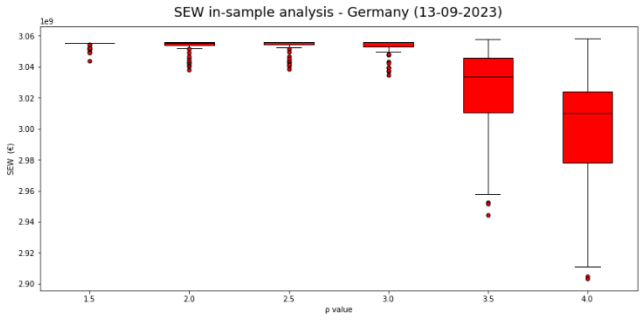

Graph 75. SEW in-sample sensitivity analysis – Germany (13-09-2022)

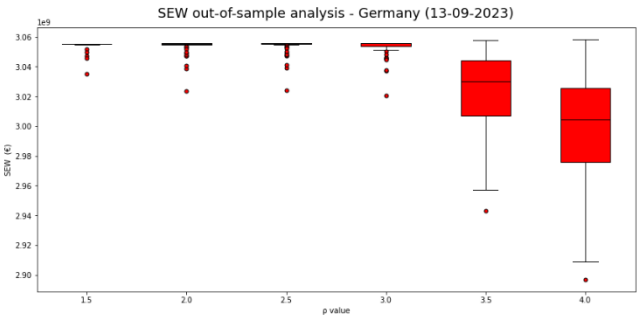

Graph 76. SEW out-of-sample sensitivity analysis – Germany 13-09-2022)

While a general theme is observable from these results, namely the increase in deviating outliers when increasing the ρ value (and consequently, decreasing the budget of uncertainty), the degree of deviation is much smaller for the French case study. At a first glance, an argument could be made that this is due to the higher relative share of installed wind capacity in the Dutch and German case studies,

resulting in a higher degree of uncertainty during this case studies. However, looking at the forecasted stochastic output, the average output realization and average maximum deviation in stochastic output realization of the in-sample case study scenarios during the above mentioned simulation days, as provided in Table 20, it can be observed that the Dutch case study endures the highest relative deviation in output realization compared to the forecasted output, indicating the prepared for worst-case scenario for the Dutch case study would result in a higher degree of conservativeness.

Case study	The Netherlands	France	Germany
Forecasted output	7,479.24	6,626.69	18,506.26
Mean output realization	5,029.36	7,204.25	18,343.41
Average $\sum_{s \in S} \Delta q_s^{RS,max}$	5,166.75	3,006,95	5,166.75

Table 20. Overview of average forecasted output, output realization and worst-case maximum output deviation of in-sample scenarios (MWh)

An explanation of the conservativeness of the French case study can be found when looking at the distribution of the installed stochastic capacity over the different wind farm locations, as provided in Table 21 below. The installed stochastic capacity is distributed much more evenly for the Dutch and German case study, while for the French case study only 2 locations already make up for 55.9% of the installed wind capacity. Given the working mechanism of the budget of uncertainty, which chooses a value ranging from 0 to 1 for each individual location (read; stochastic producer) based on the relative deviation of stochastic output realization compared to the maximum deviation, a maximal deviation in stochastic output realization for W1 and W6 during the French case study is both appointed a value of 1, whilst implications on the system balance can widely differ.

Case study	The Netherlands	France	Germany
W1	22.4%	28.7%	11.4%
W2	19.5%	10.9%	20.6%
W3	12.7%	7.4%	18.4%
W4	17.3%	13.3%	20.8%
W5	28.0%	27.2%	7.2%
W6	-	3.7%	11.2%
W7	-	8.8%	10.4%

Table 21. Overview of distribution of installed stochastic capacity over wind farm locations of the Dutch, French and German case study

Increasing the ρ value and decreasing the budget of uncertainty results in an increasingly higher share of VRES in the energy mix. By decreasing the amount of output deviations in the worst-case scenario, the Robust model accepts higher amounts of stochastic supply bids during the DA market clearing stage. For the Dutch case study, decreasing the ρ value to 1.5 decreases the average share of VRES during the simulation day from 25.7% to 19.4%. Increases in the ρ value result in diminishing increases in the share of VRES, as can be seen form the Results in Graph 77 below. The results of the French case study (Graph 78) indicate a far lesser effect of the ρ value on the share of VRES. Interestingly, a higher increase in the share of VRES is observable for greater values of ρ. Recalling the corresponding uncertainty budget as provided in Table 19 and the found relationship between the budget of uncertainty and the distribution of stochastic capacity, it can be deduced that when $\Gamma < 2$ a relatively much larger amount of supply bids from stochastic producers W1 and W5 can be accepted, thus increasing the average share of VRES in the energy mix.

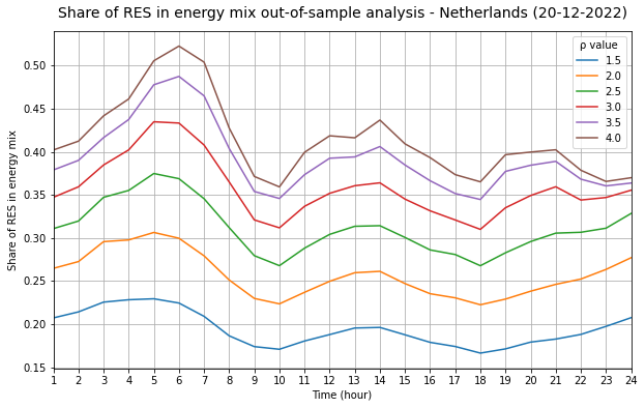

Graph 77. Average share of RES in energy mix under varying budgets of uncertainty – The Netherlands (20-12-2022)

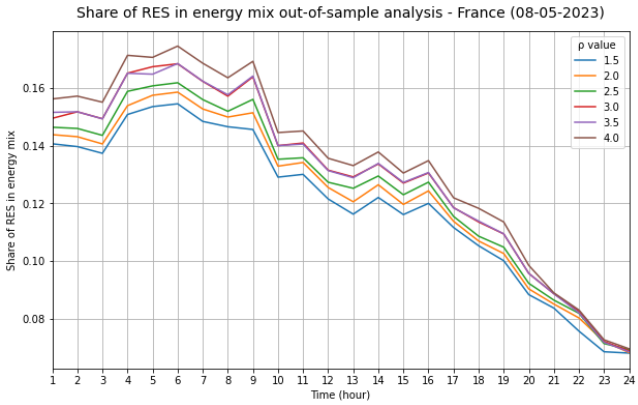

Graph 78. Average share of RES in energy mix under varying budgets of uncertainty – France (08-05-2023)

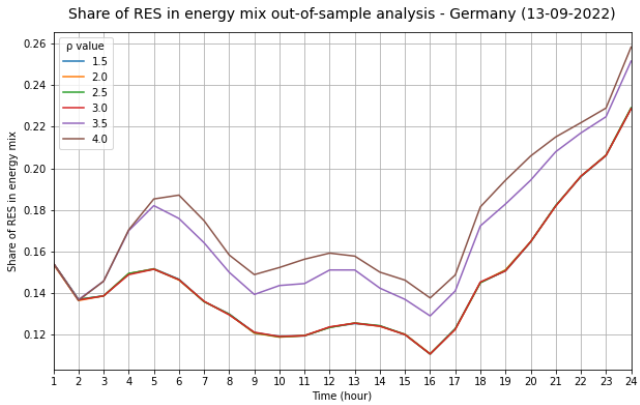

Graph 79. Average share of RES in energy mix under varying budgets of uncertainty – Germany (13-09-2022)

Looking at the results for the German case study, an interesting pattern in the results is observable; changing the ρ value from 1.5 to 3.0 does not result in substantial differences in the share of VRES, while after changing the ρ value to 3.5 onwards significantly increases the share of VRES. An explanation of this observation can be found by looking at the amount of curtailed demand after increasing the ρ value above 3.0, as can be seen from Graph 80 below. These large amounts of curtailed demand increase the share of VRES in the energy mix, although the total amount of accepted stochastic supply bids do not increase significantly because of the limited amount of available upward reserve capacity.

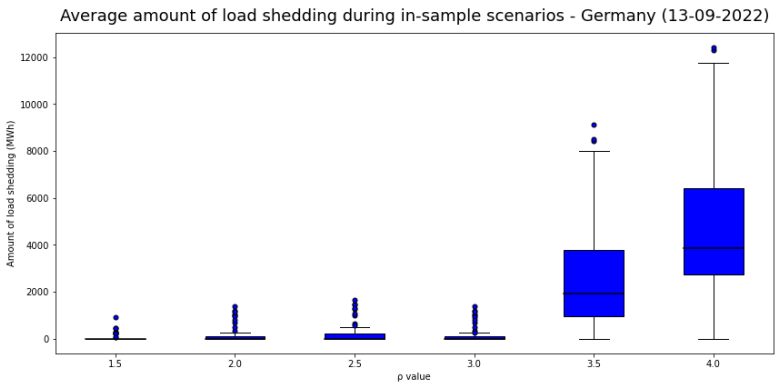

Graph 80. Amount of load shedding during in-sample scenarios under varying budgets of uncertainty – Germany (13-09-2022)

The observed increase in curtailed demand is reflected in the occurrence of load shedding events for the German case study, increasing almost a ten-fold after increasing the ρ value to 3.5. The Dutch case study shows a more gradual increase in load shedding events relatively, although exponentially in absolute percentages. The French case study, being subjected to the lowest amount of forecasted stochastic producer output, only experiences relatively minor occurrences of load shedding events. The numerical results are provided in Table 22 (in-sample) and Table 23 (out-of-sample).

ρ value	1.5	2.0	2.5	3.0	3.5	4.0
The Netherlands	0.00%	0.010%	0.42%	1.18%	2.13%	3.45%
France	0.010%	0.051%	0.056%	0.079%	0.11%	0.14%
Germany	0.032%	0.071%	0.072%	0.095%	0.714%	1.47%

Table 22. Frequencies of load shedding events under varying budgets of uncertainty (in-sample scenarios)

ρ value	1.5	2.0	2.5	3.0	3.5	4.0
The Netherlands	0.00%	0.0098%	0.32%	1.23%	2.43%	3.99%
France	0.016%	0.038%	0.061%	0.078%	0.096%	0.13%
Germany	0.021%	0.072%	0.074%	0.085%	0.79%	1.45%

Table 23. Frequencies of load shedding events under varying budgets of uncertainty (out-of-sample scenarios)

4.4.2 In-sample size

In this research, an in-sample size of 53 scenarios was used for both the Stochastic model, as well as for deriving the area of uncertainty for the Robust model. Given the large differences in performance of the Stochastic model when running the in-sample scenarios and out-of-sample scenarios, a sensitivity analysis is performed to observe the effects of an increased in-sample size on the out-of-sample scenarios. During the sensitivity analysis, the amount of in-sample scenarios $N_{in-sample}$ will chance to 100, 200, 300, 400 and 500 scenarios. The newly found solution will be tested against 53 out-of-sample scenarios.

The worst performing simulation days of the Stochastic model will be subjected to the sensitivity analysis, namely the simulation day December 20th 2022. During this simulation run, the out-of-sample analysis resulted in a chance of load shedding events of well over 1%, despite having a high share of VRES in the energy mix during the day. The sensitivity analysis will test the effects of an increased in-sample size on both KPIs for this simulation day, a well as the SEW (the objective function).

Looking at the SEW results of the sensitivity analysis in Graph 81 and Graph 82, an interesting pattern can be observed. During the in-sample scenarios, an increased size of in-sample scenarios causes a larger spread of outliers, increasing significantly at a sample size of $N_{in-sample} = 300$. On the contrary, the increased in-sample size provides robustness during the out-of-sample analysis, increasing out-of-sample performance significantly at a sample size of $N_{in-sample} = 100$.

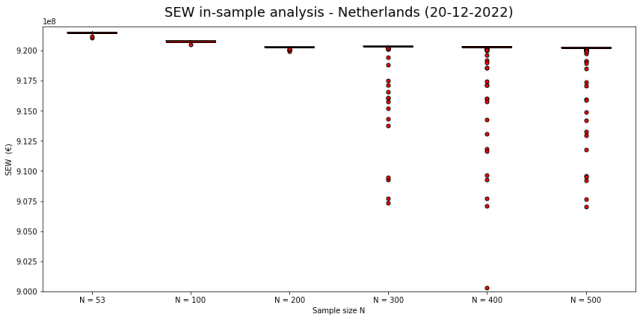

Graph 81. SEW in-sample sensitivity analysis – The Netherlands (20-12-2022)

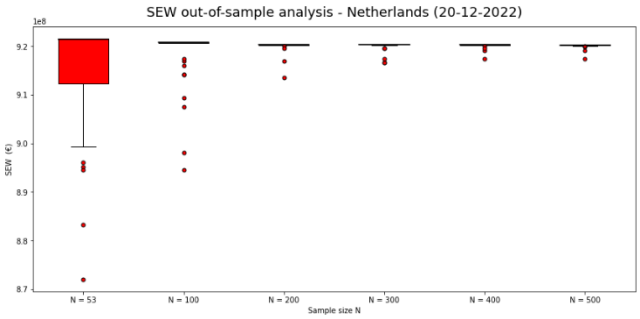

Graph 82. SEW out-of-sample sensitivity analysis – The Netherlands (20-12-2022)

The increased amount of outlying SEW results during the in-sample scenarios can be explained by the decreasing weight factor of each individual scenario, which is equal to $\frac{1}{N_{in-sample}}$. When applying a small in-sample size, occurring load shedding events would heavily impact the average found solution. The results of the simulation runs with $N_{in-sample} = \{300,\ 400,\ 500\}$ indicate an increased average SEW when allowing for certain in-sample scenarios which experience load shedding events.

This explanation is supported by the results of the amount of curtailed electricity during load shedding events, as provided in Graph 83 and Graph 84, which a re invertedly nearly identical to the SEW results. From these results it can be deduced that the outlying SEW results can be appointed to load shedding events. Interestingly, the $N_{in-sample} = 500$ simulation run results in slightly greater load shedding events compared to an in-sample size of $N_{in-sample} = 400$. While increasing the in-sample size of the Stochastic model does increase the system security of supply significantly, a great increase in in-sample size can arise the problem of overfitting, potentially negatively affecting the system security of supply.

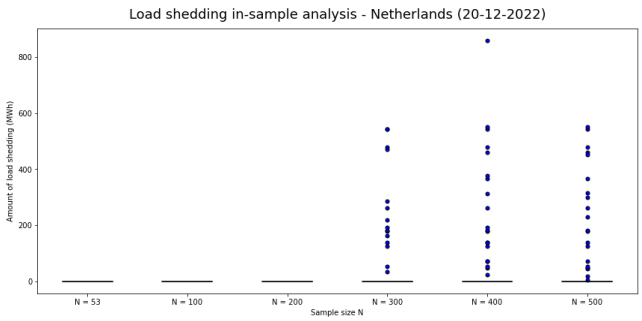

Graph 83. Amount of load shedding in-sample sensitivity analysis – The Netherlands (20-12-2022)

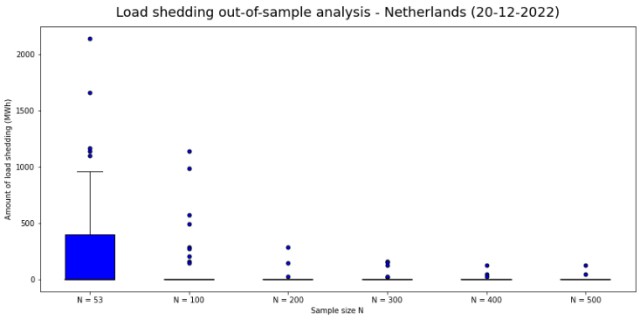

Graph 84. Amount of load shedding out-of-sample sensitivity analysis – The Netherlands (20-12-2022)

The results of the share of VRES in the energy mix indicate a negative impact of an increased in-sample size on the amount of accepted stochastic producer bids. Looking at the results of the average share of VRES in the energy mix during the out-of-sample scenarios as provided in Graph 85, the share of VRES in the energy mix is gradually decreasing with an increased sample size, although stabilizing after 300 in-sample scenarios.

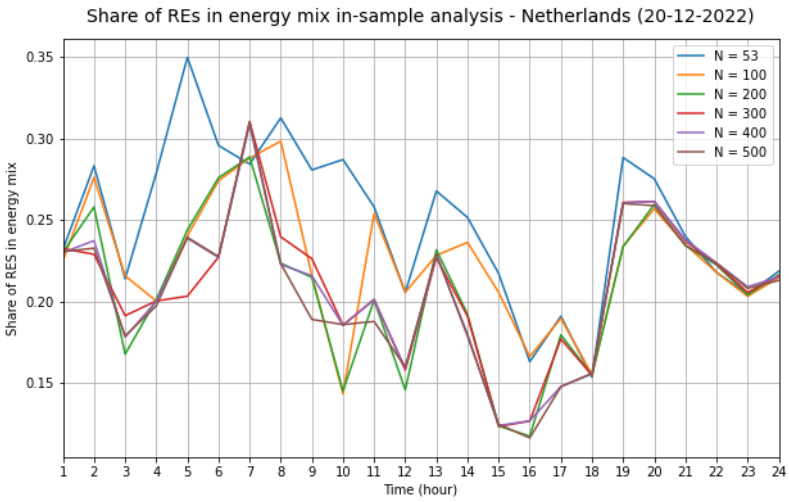

Graph 85. Average share of RES in energy mix out-of-sample sensitivity analysis – The Netherlands (20-12-2022)

Looking back at the SEW results of the sensitivity analysis, a notable shift in the results is observable in between $N_{in-sample} = 200$ and $N_{in-sample} = 300$. Even more interestingly, this exact pattern re-occurred when replicating the sensitivity analysis with a different set of randomized in-sample and out-of-sample scenarios. As the SEW results show in Graph 86 and Graph 87, again the results of the in-sample analysis are heavily changing after increasing the in-sample size to 300 scenarios, while the average SEW of the out-of-sample scenarios increases slightly after this point.

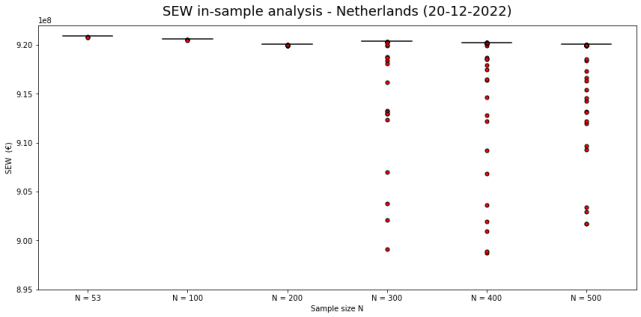

Graph 86. SEW second in-sample sensitivity analysis – The Netherlands (20-12-2022)

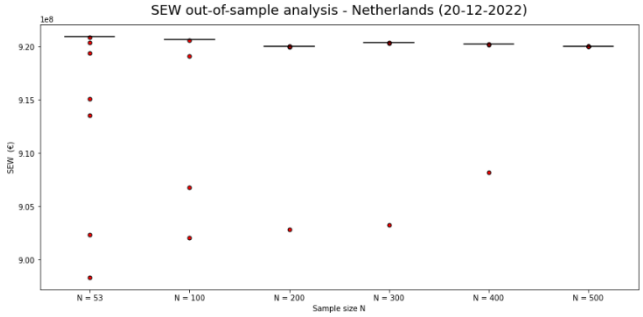

Graph 87. SEW second out-of-sample sensitivity analysis – The Netherlands (20-12-2022)

Upon closer inspection, an explanation can be found by looking at the relationship between the MCP, the VoLL and the size of $N_{in-sample}$. In above mentioned scenarios, a MCP was calculated ranging from 80-90 €/MWh with a p_d^{shed} set equal to 22,940 €/MWh. By dividing p_d^{shed} with the MCP, resulting in a value range of $\{254.89,\ 286.75\}$, it can be argued that this exact moment during the sensitivity analysis shifts the optimal solution towards allowing 1 MWh of load shedding to occur when an increase of 1 MWh of accepted stochastic producer bids can be realized during the first stage of the optimization problem. Changing the value of p_d^{shed} to €18,000 confirms this hypothesis, as can be seen from the results in Graph 88 below. Clearly, the shifting point in spread of in-sample SEW results starts after increasing the in-sample size to 200 scenarios.

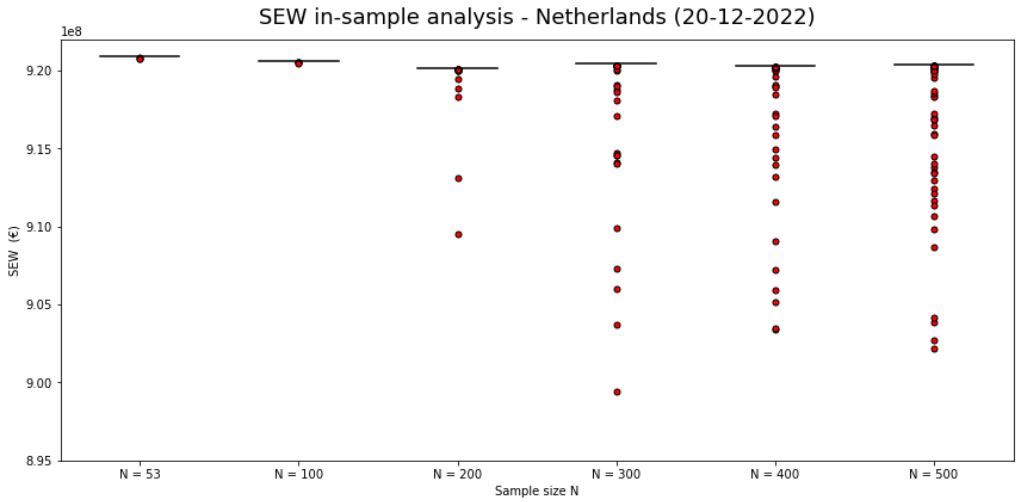

Graph 88. SEW in-sample sensitivity analysis ($p_a^{shed} = 18{,}000$) – The Netherlands (20-12-2022)

Comparing the out-of-sample results of the Stochastic model with $N_{in-sample} = 500$ to the results of the Robust model, an increase of €314,698.82 (0.03%) in average SEW is observed using the Stochastic model, while also showing more robustness with a standard deviation of €422,811 compared to €3,840,453 for the Robust model. Load shedding events occurred during two scenarios when applying the Stochastic model, totaling an amount of 48 MWh and 127 MWh, compared to 10 scenarios with occurring load shedding events totaling 3,331 MWh from the Robust model. Finally, the Stochastic model averages a daily share of VRES in the energy mix of 20.3% compared to 25.3% from the Robust mode. From these results it can be observed that the Stochastic model becomes increasingly more conservative with increased in-sample size, even surpassing the degree of conservativeness of the Robust model with an uncertainty budget of $\Gamma = \frac{N_s}{2}$.

4.5 Case study comparison

Considering the DA market clearing models have been subjected to different input data (market bids, installed wind capacity and stochastic producer realization), this provides difficulties in evaluating the performance of the models through a direct comparison of the three case studies. However, considering each case study was subjected to a simulation day with a rather high- or low amount of forecasted stochastic producer output, the case study results of the simulation day with the highest- and lowest forecasted share of stochastic producer output are compared in this section.

4.5.1 High-forecast simulation day

During the three case studies, the simulation days with the highest forecasted stochastic producer output as a share of the total demand load were December 20th 2022 for the Netherlands and May 8th 2023 for both France and Germany. Showing a rather similar share between the Dutch and German case study, the French case study did see a much smaller share considering the much smaller share of installed wind capacity in this country, as can be seen from Graph 89.

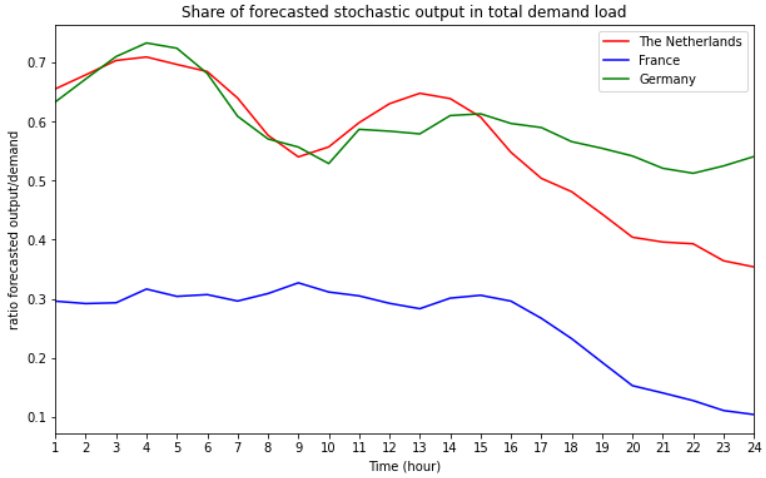

Graph 89. Ratio of forecasted stochastic output and total demand load of The Netherlands (20-12-2022), France (08-05-2023) and Germany (08-05-2023)

The higher share of forecasted stochastic producer output in the Dutch and German case studies results in a relative higher amount of stochastic producer bids and consequently, an increased degree of uncertainty during the balancing stage. Recalling the in-sample scenario results of the SEW during the case studies, the Deterministic model provided SEW results with a lower average and a higher deviation compared to the Stochastic model and Robust model as can be seen from the results in Graph 4, Graph 23 and Graph 49 below.

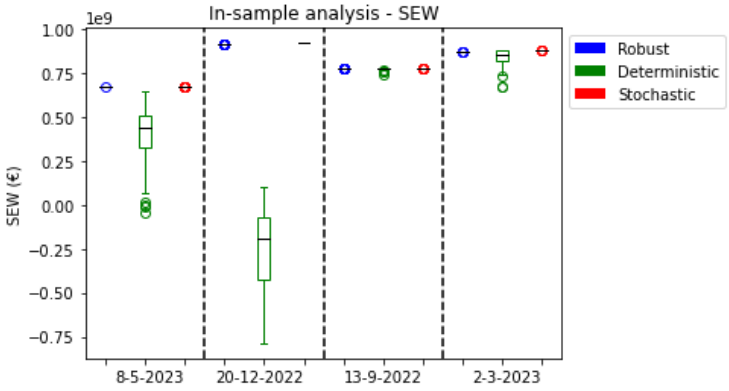

Graph 4. SEW of in-sample scenarios for simulation days – The Netherlands

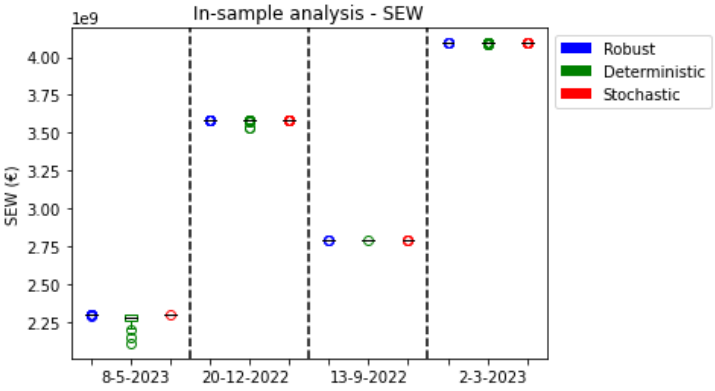

Graph 23. SEW of in-sample scenarios for simulation days – France

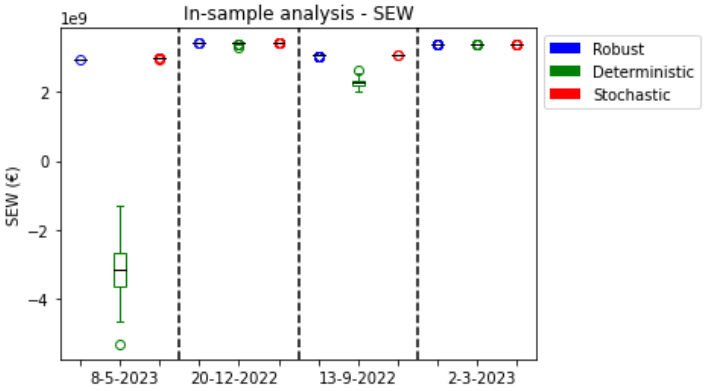

Graph 49. SEW of in-sample scenarios for simulation days – Germany

A second explanation for the results of the French case study can be found by looking at the ratio between the fixed amount of procured upward reserves and the forecasted stochastic producer output in MWh for the Deterministic model, which averaged around 0.053 for the French case study, 0.039 for the Dutch case study and 0.032 for the German case study. A low ratio results in both a higher risk of load shedding events, as well as a greater amount of curtailed electricity during these events.

A recurring resemblance between the three case studies is the varying performance of the Stochastic model between the in-sample and out-of-sample scenarios. The optimal solution resulting from the Stochastic model is tightly bound to the in-sample scenarios, therefore accepting stochastic producer bids and procuring upward reserves just barely sufficient to address potential imbalances for maximization of SEW. During the Dutch case study, the average SEW resulting from the Stochastic model decreased by 0.23%, while a decrease of 0.07% % and 0.32% where observed during the high-forecast simulation day of the French and German case studies.
The Robust model performs comparable during the out-of-sample scenarios. While the constructed uncertainty set of the robust model is susceptible to outlying extreme deviations in output realization during the out-of-sample scenarios, the preparation for the worst-case scenario provides significantly more conservatism during the out-of-sample scenarios. This conservatism drastically reduces the deviations in SEW form the out-of-sample scenarios. Compared to the Stochastic model, the Robust model increases the average SEW 0.038% during the out-of-sample scenarios in the French case study, although still an average reduction of 0.22% and 0.04% is observed during the Dutch and German case studies.

Due to the relatively high cost of load shedding events and the small in-sample size, as mentioned earlier in Section 4.4.2, the Stochastic model did not once experience a single load shedding event

during the in-sample scenarios. The penalty cost for curtailment of demand turned out higher compared to the costs for increased procurement- and activation of upward reserves and added SEW by increasing the amount of accepted stochastic producer bids. However, load shedding events did occur during the out-of-sample scenarios of each individual simulation day. This demonstrates a clear weakness of the working mechanism of the Stochastic model with the currently used in-sample size of 53 scenarios; the found optimal solution is often found *just* at the point at which an imbalance occurs which cannot be addressed by upward reserve activation, leaving a high vulnerability for outlying moments found in the out-of-sample scenario. The results of the sensitivity analysis on the in-sample size as provided in Section 4.4.2 confirmed this finding, indicating an increase in robustness during the out-of-sample analysis when increasing the in-sample size to 400 scenarios. Further increases of the in-sample size indicated signs of overfitting, resulting in decreased performance of the Stochastic model.
The results of the Stochastic model from the out-of-sample scenarios stress the importance of conducting an out-of-sample analysis in evaluating the performance of applying stochastic optimization to address uncertainty in DA market clearing. Work by [11], which compared a similar two-stage stochastic optimization market clearing model with the conventional deterministic market clearing model, explicitly stated that out-of-sample scenarios were not considered during the comparison and all possible outcomes were contained within the in-sample scenarios, admitting this assumption would prove unrealistic in reality. Especially considering a comparison of Stochastic optimization and Robust optimization in DA market clearing, leaving out an out-of-sample analysis drastically favors the performance of Stochastic optimization, which excels in goodness-of-fit of the in-sample scenarios rather than robustness of the optimal solution to unaccounted possibilities during the out-of-sample analysis.

The case study results of the consumer surplus indicate a decrease of <1% when applying the Stochastic model or Robust model to the DA market clearing, while the results of the producer surplus show a large decrease of over 15-50% of the producer surplus during the three case studies due to lower amounts of accepted stochastic producer bids and a decrease in the MCP. However, the higher balancing costs and frequent load shedding events resulting from the Deterministic model during the balancing stage raise doubts on the validity and value of using the producer surplus and consumer surplus as performance criteria for the DA market clearing models. Especially during the high-forecast simulation days, the Deterministic model resulted in a significantly higher consumer surplus and producer surplus after the DA market clearing, while balancing costs and load shedding events also increased accordingly.

When comparing the results of the share of VRES in the energy mix between the three case studies, as provided in Table 24 below, two main observations can be made: 1) the Deterministic model results in the highest share of VRES, followed by the Stochastic model while applying the Robust model results in the lowest share and 2) the differences in share of VRES are widely differing between the case studies, being much smaller for the French case study compared to the Dutch and German results.

Simulation day	NL (20-12-2022)		FR (08-05-2023)		GE (08-05-2023)	
In-sample/out-of-sample	InS	OoS	InS	OoS	InS	OoS
Deterministic	48.0%	47.8%	15.9%	15.6%	71.2%	70.4%
Robust	25.5%	25.3%	11.8%	11.8%	18.2%	18.2%
Stochastic	29.4%	29.0%	12.5%	12.4%	31.2%	31.0%

Table 24. Average share of VRES in energy mix during in-sample scenarios and out-of-sample scenarios

A first explanation can be found by looking at the amount of accepted stochastic producer bids, which is the highest for the Deterministic model. Besides increasing the amount of procured upward reserves

to deal with the uncertainty, the Stochastic model and Robust model also decrease the amount of accepted stochastic producer bids to decrease the amount of uncertainty. The higher amount of accepted stochastic producer bids also affects the amount of curtailed demand for the Deterministic model. During the Dutch and German case studies, an average daily amount of 50,979 MWh and 496,669 MWh of electricity demand was curtailed, a share of 17.7% and 47.3% of the total amount of accepted demand bids. Recalling the formula used for calculating the share of VRES (eq. 6.5):

$$VRES = 100 * \frac{\sum_{s \in S} q_s^S + \sum_{g \in G} r_g^D - r_g^U - \sum_{d \in D} q_d^{shed}}{\sum_{d \in D} q_d^{DD} - q_d^{shed}}$$

(6.5)

The increased total amount of curtailed demand decreases both the numerator and denominator equal, which will result in a relative increase in share of VRES. Compared to the French case study, which only resulted in an average 1.52% of curtailment of the total amount of accepted demand bids, a relatively much smaller amount of actually delivered electricity remains during the Dutch and German case studies during the high-forecast simulation day, for which consequently a larger share of stochastic output will be provided.

Comparing the results of the Robust model and Stochastic model, a larger difference is observable during the German case study. A main explanation can be found by looking at the maximum upward reserve capacity and the total installed wind capacity. Recalling the ratio between the fixed amount of procured upward reserves and the forecasted stochastic producer output in MWh, the German case study has a total maximum amount of 3,295 MWh upward reserve capacity while the forecasted stochastic output averages around 32,429 MWh (10.2%). Comparatively, the Dutch case study has a total maximum amount of 1,572 MWh upward reserve capacity for an average forecasted stochastic output of 7,479 MWh (21.0%). Due to the smaller amount of upward reserve capacity during the German case study, the amount of accepted stochastic producer bids is decreased to diminish the deviations in output realization during the worst-case scenario to an amount for which the upward reserve capacity can account for. A deeper look into this observation will be provided in Section 5.1.3.1.

Finally, the results on the system security of supply heavily indicate an increased system performance from applying uncertainty-based optimization techniques to the DA market clearing during days with high-forecasted stochastic producer output. The Deterministic encountered a frequency of load shedding events of over 9% and 3% during the Dutch and French case studies, while the Robust model and Stochastic model decreased these frequencies below 0.25%. The results of the German case study indicated the robustness of both the Robust model and Stochastic model during a situation of severe over-forecasting (Graph 68), in which the use of the Deterministic model resulted in load shedding frequencies well over 90% (i.e., complete system failure). The Stochastic model showed improved system security, although the frequency of load shedding events was 0.24% during the out-of-sample analysis. The Robust model did not experience any load shedding events during both the in-sample scenarios and out-of-sample scenarios, indicating extreme resilience from over-forecasting.

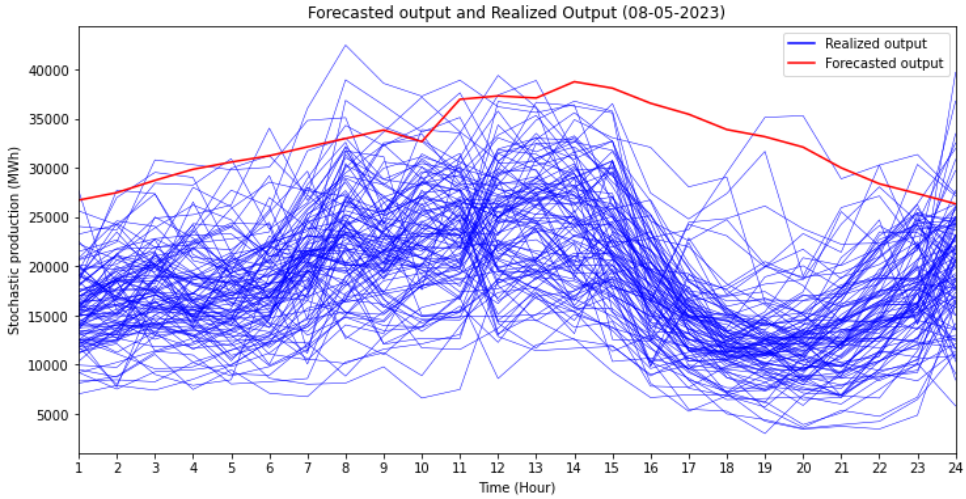

Graph 68. Day profile of Forecasted- and realized stochsatic producer output (08-05-2023) - Germany

4.5.2 Low forecast simulation day

The simulation days with the lowest amount of forecasted stochastic producer output were September 13th 2022 for both the Dutch- and French case study and December 20th for the German case study. The Dutch case study still had an average forecasted share of VRES of 16.7% compared to the total demand load during this simulation day, while France (5.2%) and Germany (10.5%) both had a much lower forecast, as can be seen from the daily profiles in Graph 90 below.

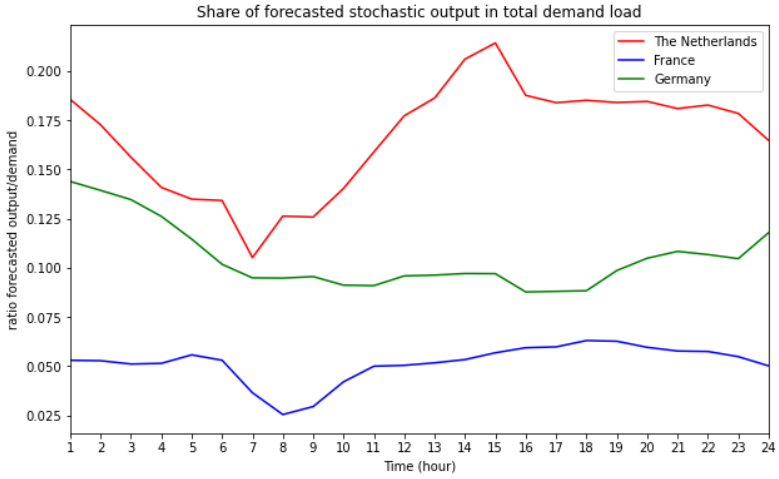

Graph 90. Ratio of forecasted stochastic output and total demand load of The Netherlands (13-09-2022), France (13-09-2022) and Germany (20-12-2022)

During the low-forecast simulation runs, the Stochastic model is the best-performing model by a slight margin during the in-sample scenarios, as can be seen from the results of Graph 91-93 below. The SEW results of the low-forecast simulation day indicate a reduced increase in SEW by applying uncertainty based optimization on the DA market clearing. In the German case study, application of ARO even results in a reduction of SEW compared to the current deterministic model due to the much higher reserve costs. The Stochastic model slightly improves the average SEW during the in-sample scenarios with 0.37% (NL), 0.14% (FR) and 0.22% (GE).

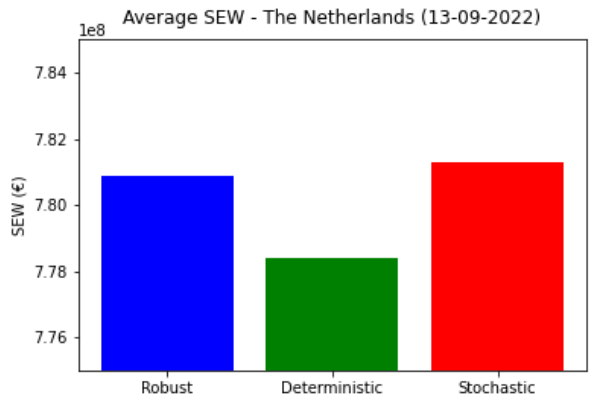

Graph 91. Average SEW of in-sample scenarios – The Netherlands (13-09-2022)

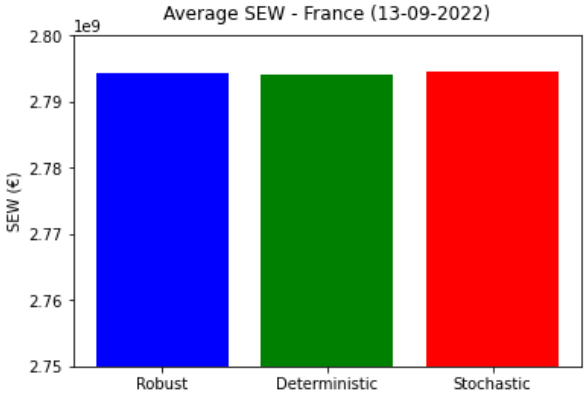

Graph 92. Average SEW of in-sample scenarios – France (13-09-2022)

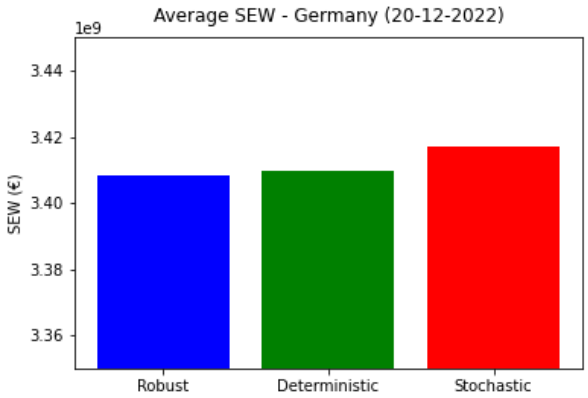

Graph 93. Average SEW of in-sample scenarios – Germany (20-12-2022)

During the out-of-sample scenarios, the SEW resulting from the Stochastic model decreased for each case study low-forecast simulation day compared to the in-sample scenarios, resulting in an average reduction of 0.07% (NL), 0.031% (FR) and 0.17% (GE). Despite these average reductions, the Stochastic model yielded the highest SEW during the low-forecast simulation days of The Netherlands and Germany. During the French low-cast simulation day, the Stochastic model yielded the lowest SEW, resulting in a reduction of 0.013% compared to the Deterministic model.

The balancing costs of during the simulation days indicate a high reduction of balancing costs during the low-forecast simulation days by the Stochastic model and Robust model. While the costs of upward reserve procurement are significantly higher for the Robust model, costs resulting from load shedding events are extremely reduced to an average maximum of €13,878, compared to €8,659,267 from the Deterministic model and €5,717,343 from the Stochastic model. The balancing costs of the Stochastic model vary widely between the in-sample scenarios and out-of-sample scenarios. While load shedding events are absent during the in-sample scenarios, average curtailment costs increase to €573,093 (NL), €851,292 (FR) and €5,717,343 (GE).

Application of the Stochastic model and Robust model result in a decreased share of VRES in the energy mix compared to the Deterministic model. The Robust model results in a significantly higher decrease in the share of VRES compared to the Stochastic model, although occurrences of load shedding events can create a distorted picture of this claim. The relatively highest difference between the Stochastic model and Robust model is observable in the French case study, as can be seen from the results in Graph 35 and Graph 36. Despite the relatively low forecasted amount of stochastic producer output, the heavily deviating results of the Stochastic model indicate high probabilities of extremely low-realization scenarios. The Robust model, preparing exactly for these worst-case scenarios, is significantly less affected by these scenarios by decreasing the amount of accepted stochastic supply bids resulting in a low share of VRES in the energy mix.

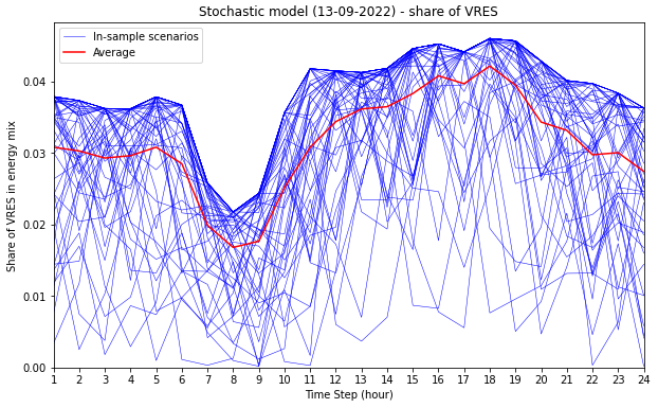

Graph 35. Stochastic model share of VRES in energy mix (13-09-2022) in-sample scenarios – France

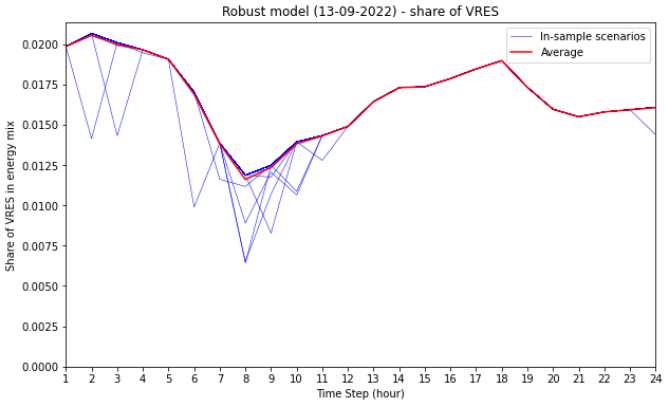

Graph 36. Robust model share of VRES in energy mix (13-09-2022) in-sample scenarios – France

Given the low amount of forecasted stochastic producer output and thus the relatively minor impact extreme deviations in output realization could make on the system security, one could argue that the conservativeness of the Robust model seems rather unnecessary during days with low amounts of forecasted stochastic output in energy systems with rather small penetration of VRES in the energy mix.

The results of the system security of supply indicate a significantly lower frequency of load shedding events for the Deterministic model during the low-forecast simulation days compared to the other simulation days for each case study. The lower amount of accepted stochastic producer bids result in a relatively higher amount of fixed reserve procurement to deal with this uncertainty, drastically reducing the occurrence of load shedding events. Despite these smaller amounts of accepted stochastic supply bids, the Robust model results in higher frequencies of load shedding events compared to high-forecasted simulation days. Preparing for the realization of a rather 'minor' worst-case scenario, average procurement of upward reserves is significantly decreased compared to upward reserve procurement of the Deterministic model, decreasing system security. Due to the tendency to narrowly fit the in-sample scenarios, the Stochastic model indicates vulnerability of system security to unexpected output realizations during the out-of-sample scenarios.

5. Discussion

The aim of this study was to formulate a Stochastic and Robust market clearing model applicable to EU electricity markets, develop a framework of KPIs to compare the performance of the different optimization techniques for application in the DA market and implement the DA market clearing models on the Dutch, French and German case study. An evaluation and comparison of the performance of the DA market clearing models will be provided in Section 5.1, followed by a deeper look into notable observations made during the results analysis in section 5.2. After, Section 5.3 provides an evaluation of the proposed KPI framework used to measure model performance. Limitations of this research will be discussed in Section 5.4. Finally, recommendations for future research will be proposed in Section 5.5.

5.1. Model performance evaluation

The Deterministic model accepted the highest amount of stochastic producer bids, resulting in a higher consumer surplus, (stochastic) producer surplus and share of VRES in the energy mix, while experiencing the lowest amount of wind spillage during the scenarios on average. However, by not addressing the uncertainty in output realization of stochastic producers with increased reserve procurement or a decrease in the amount of accepted stochastic producer bids, the Deterministic model becomes susceptible to significant imbalances which have to be addressed by load shedding events, especially during days with high-forecasted stochastic producer output. The frequent load shedding events heavily affect the system security of supply and impact profits for stochastic producers, for which net losses were observed despite the high amounts of accepted stochastic producer bids and low amounts of wind spillage. The high balancing costs resulted in the lowest SEW results for the Deterministic model during both the in-sample and out-of-sample scenarios.

During the in-sample scenarios, the Stochastic model yielded the highest SEW by heavily reducing the balancing costs compared to the Deterministic model. By finding an average optimal solution for the in-sample scenarios, the Stochastic model showed a high degree of goodness-of-fit to these scenarios with tightly amounts of accepted stochastic producers bids and procured upward reserves resulting in zero load shedding events. However, this goodness-of-fit proved susceptible to unexpected output realizations during the out-of-sample scenarios, in which a slight decrease (<0.5%) in SEW was observed during each individual simulation day. Although varying for each simulation day, the Stochastic model required an increased capacity of upward reserves to address uncertainty during simulation days with high amounts of forecasted stochastic producer output, although the amount of accepted stochastic producer bids decreased. This resulted in a significant decrease in the share of VRES in the energy mix and stochastic producer surplus, as well as an increase in the total amount of wind spillage. However, increased system security of supply drastically reduced the amount and magnitude of load shedding events, resulting in higher stochastic producer profits.
The results of the sensitivity analysis on the number of in-sample scenarios indicated an improved performance of the Stochastic model during the out-of-sample scenarios, along with a decrease in performance during the in-sample scenarios. However, the amount of load shedding events started to slightly increase when increasing the in-sample size from 400 to 500 scenarios, potentially indicating signs of over-fitting.

Finally, the Robust model proved the most conservative model with the least amount of accepted stochastic producer bids and highest amount of procured upward reserves compared to the Deterministic model and Stochastic model. Despite occurrences of load shedding events during 3 out of the 12 simulation days, the Robust model resulted in the highest system security of supply during

the out-of-sample scenarios, indicating increased robustness to unexpected stochastic producer outputs compared to the Stochastic model. The high reduction in balancing costs compared to the Deterministic model resulted in an increased SEW, however reduced integration of VRES and high amounts of upward procured reserves resulted in a lower SEW compared to the Stochastic model. Application of the Robust model resulted in the lowest share of VRES in the energy mix and high amounts of wind spillage, although stochastic producer profits became significantly more stable during the in-sample and out-of-sample scenarios compared to the Deterministic model and Stochastic model. Application of the Robust model resulted in the highest required amount of upward reserve capacity to address the worst-case scenario of the uncertainty from stochastic output realization. The results of the sensitivity analysis showed a trade-off between the system security of supply and integration of VRES in the energy system. A decrease in the budget of uncertainty resulted in a higher amount of accepted stochastic producer bids because of a reduction in the worst-case scenario, although frequency and magnitude of load shedding events increased significantly during both the in-sample and out-of-sample scenarios. Interestingly, the results of the French case study indicated a strong relationship with the distribution of installed wind capacity among the stochastic producers and the effect of changes in the budget of uncertainty, potentially leading to market inequalities between stochastic producers, a point which will be further elaborated on in Section 5.2.3.

The case study results indicated an increased system security of supply through the application of uncertainty-based optimization techniques in the DA market clearing. However, trade-offs were observed between financial performance, integration of VRES and system security of supply between the models.
Performance of the Stochastic model in the DA market clearing is strongly dependent on the accuracy of DA stochastic producer forecasts, and even more to the ability of DA forecasts to excluded unexpected highly deviating output realizations. Despite vulnerability of these unexpected output realizations, the Stochastic model provided increased system security of supply and SEW through a reduction of imbalances. However, a reduction in the share of VRES in the energy mix and an increased use in the amount of upward reserve capacity stress the importance of increasing the installed capacity of stochastic producers and installed reserve capacity of conventional producers despite significant changes in their revenue streams.
Implementation of the Robust model would result in increased system security of supply, in which the degree of conservatism could easily be parameterized through the budget of uncertainty. A strong relationship was observed between the total amount of accepted stochastic producer bids and the amount of upward reserve capacity in the system. Specifically during the German case study, in which a high amount of installed wind capacity and a relatively low amount of upward reserve capacity are available in the system, application of the Robust model drastically decreases the integration of VRES and reduces the stochastic producer profits compared to the Stochastic model.

The results of the sensitivity analysis indicate optimality in changing values for both the in-sample size and budget of uncertainty on the performance of the Stochastic model and the Robust model dependent of the case study and DA forecast of the stochastic producer output. While a one-fits-all approach would facilitate implementation of stochastic- and robust optimization in the DA market clearing in the real world, more research needs to be conducted on the relationship between case study-specific input parameters (installed wind capacity and upward reserve capacity, for example) and the optimal in-sample size and budget of uncertainty to increase system security of supply and SEW, while limiting the reduction in integration of VRES in the energy mix.

5.2 Observations

During the analysis of the simulation run results, some notable observations were made. This section provides a deeper look on these observations to shed light on the working mechanisms of the Stochastic model and Robust model and to provide comments for potential real-life application of uncertainty based optimization techniques for the DA market clearing.

5.2.1 Maximum upward reserves procurement constraint

As mentioned earlier, the Robust model anticipates on the worst case scenario, which is determined by the tightness of the budget of uncertainty. The robust model identifies if the risk of an increase in accepted stochastic supply bids can be mitigated by upward reserve procurement- and activation in a cost-effective manner (i.e., increasing the SEW overall). In case of cost-effectiveness of procuring reserves and increasing the amount of stochastic producer bids, this constraints the maximum allowed amount of stochastic output realization to $\sum_{s\in S} \Delta q_s^{RS} \leq \sum_{g\in G} R_g^{U,max}$. This observation was also noted in the work of [43] applying ARO to the UC, in which extremely high balancing costs were observed when increasing the budget of uncertainty due to an insufficient amount of reserves in the system to preserve system balance without load shedding events.

Extrapolating the current trends in newly installed wind capacity in both the Netherlands, France and Germany, this limitation could constrain the integration of VRES in the energy mix or could limit the level of uncertainty which could be applied using ARO if the system reserve capacity is not significantly increased. As work by [30] and [94] stated, research on the applicability of flexible reserve integration in energy systems or demand response is needed to prepare current energy systems for the transformation to high VRES penetrated energy systems in a cost effective manner.

5.2.2 Downward reserve procurement for VRES integration

The Deterministic model yielded the highest share of VRES in the energy mix because of both the higher amount of accepted stochastic demand bids and the fixed amount of procured downward reserves. In case of a realized scenario in which under-forecasting has occurred, these downward reserves activated can switch over generation from conventional producers to stochastic producers, consequently increasing the share of VRES in the energy mix.

However, the Robust model and Stochastic model proposed in this thesis do not make use of any downward reserves, even in the case of R_g^D = 0. Looking at the mathematical formulation of the Stochastic model, the second-stage balancing constraint

$$\sum_{g\in G} r_{g\omega}^U - r_{g\omega}^D + \sum_{d\in D} q_{d\omega}^{shed} + \sum_{s\in S} q_{s\omega}^{SS} - q_s^{SS} - q_{s\omega}^{spill} = 0, \qquad \forall \omega \in \Omega$$

(4.13)

ensures balance of supply and demand during the RT balancing stage. Given the cost associated with procurement- and activation of downward reserves, which is 20% of the marginal costs (Table 3), the most cost-effective solution will be to spill excess wind production for which no costs are associated. The Robust model on the other hand will prepare for the worst-case realization, which will include shortages of stochastic producer output realization leading to high-cost imbalances. Preparing for over-realization of stochastic producer output will not be accounted for by the model as it is not a

viable worst-case scenario, therefore no downward reserves are procured during the DA stage of the market clearing.

To tackle this problem in research on the application of uncertainty based optimization techniques in the DA market clearing, a hypothetical wind spillage penalty is introduced. This penalization of wind spillage deters from being overly conservative and aims for a form of Pareto-efficiency between the objective function and utilization of stochastic producer capacity. While a penalty for wind spillage is not currently applied in the Dutch, French and German wholesale electricity markets, hence the reason for not including it during the case studies in this thesis, the above described observation does point out the potential benefits (and perhaps necessity) of including such a penalty. However, this does raise the question as to how to determine the penalty cost for wind spillage in real-life applications. In experimental case studies as conducted by [8], [13], [15] and [18], the penalty cost for wind spillage is arbitrarily chosen. Given the relationship between the penalty cost for wind spillage to the amount of accepted stochastic supply bids, downward reserve procurement and security of system stability, more research is needed on wind spillage penalty cost assessment in real-life applications.

5.2.3 Budget of uncertainty and stochastic capacity distribution

A point raised during the sensitivity analysis on the budget of uncertainty in Section 4.4.1 is the relationship between the distribution of stochastic capacity on different wind farm locations and the budget of uncertainty as applied in this thesis. The rationale of applying the budget of uncertainty can be supported by the impact of weather phenomena on specific locations, less much affecting the production output of the whole system compared to the use of a boxed uncertainty set or polyhedral uncertainty set, a claim also mentioned by [18]. However, due to differences in installed wind capacity between wind farm locations, the Robust model is inclined to realize the worst-case scenario for locations with higher installed capacity to maximize the second-stage balancing costs.

Research on the utilization of ARO with a budget of uncertainty as provided by [15] and [18] do not note this observation because of two main reasons. First, a penalty for wind spillage is introduced to deter the optimal solution from large amounts of wind spillage due to increased costs. Second, and perhaps most important, in [15] three wind farm locations of equal capacity are used, while in [18] two wind farm locations with rather comparable capacity are used during the case study. Interestingly, research by [16] compared ARO using a box of uncertainty and a budget of uncertainty using a case study with three wind units with varying size. Using lower values for both the budget of uncertainty and the box of uncertainty, significantly increased conservativeness was observed using the budget of uncertainty, supporting the above mentioned relationship between the capacity distribution and the budget of uncertainty.

While this observation does not provide insight into the appropriateness of using either a box of uncertainty or budget of uncertainty for applying ARO in the DA market clearing, it does shed a light on the possible implications of using a budget of uncertainty. When wind farms with large capacities are more targeted to be part of the worst-case scenario, consequently relatively decreasing the amount of accepted supply bids from these producers, market inequalities can arise in which smaller wind farms are heavily favored.

5.2.4 Computational performance

The application of two-stage stochastic optimization and ARO to solve multi-dimensional problems requires a large amount of computing power and can result in a long computation time. The computational performance of such models is a widely discussed topic in research, especially considering the increased computational time and computational power required for solving NP problems with increased problem size. Contrary to comparable research on implementation of two-stage stochastic optimization and ARO, the computational performance of the models is not included in the KPI framework during this thesis, which focused on the market performance and implications of the different DA market clearing models. Providing an evaluation of the performance of solving algorithms proved beyond the scope of this thesis. However, given the practical implications in terms of required computational power and time constraints for solving the optimal solution, some insight into the computational performance of the DA market clearing model is provided.

Given the low-complex nature of the Deterministic model, optimal solutions are found within <0.01 for the Dutch case study, <0.015 for the French case study and <0.2 seconds for the German case study due to the increasing amount of market actors, increasing the problem size. Comparatively, the Stochastic model required 2.4 seconds (The Netherlands), 4.33 seconds (France) and 6.71 seconds (Germany) to find the optimal solution, while the Robust model required computational times of 100-250 seconds depending on the required amount of iterations needed in both the OA master problem and subproblem. Please note that the computational time of the Robust model is also heavily impacted by inefficiencies in the coding of the solving algorithm due to personal computational limitations and will therefore not be discussed in detail in this thesis.

The results on the computational performance of the Stochastic model during the sensitivity analysis also indicated a high increase in computational time with increased in-sample size, as can be seen from the results in Table 25 below. The CPU load increases with increasing in-sample size, albeit relatively slowly. With increased in-sample size, the number of computational iterations required indicates a diminishing rate of increase as well. Finally, the computational time is incrementally increasing with increased in-sample size. The increased computational time required indicates potential problems during real world applications of two-stage stochastic optimization with a high number of in-sample scenarios.

$N_{in-sample}$	53	100	200	300	400	500
CPU load [%]	1.7	2.7	4.0	4.6	4.6	4.8
Iterations [n]	77,848	113,660	186,402	248,726	294,952	351,491
Computational time [sec]	2.580	5.103	11.648	23.411	34.011	44.419

Table 25. Overview of computational performance of Stochastic model with varying in-sample size

5.3 Evaluation of KPI framework

One of the aims of this thesis was to develop a framework of KPIs to compare the performance of the different DA market clearing models. This section provides an evaluation of the established framework used during this thesis.

Initially established to capture a wide range of performance indicators regarding financial performance, integration of VRES and system security of supply, some of the selected KPIs did fall victim to an indirect form of double counting due to their interdependencies.
A first notable example is the relationship between the KPIs *balancing costs* and *Stochastic producer profits*. Since uncertainty is only limited to output realization of stochastic producers, balancing costs

are inherently appointed to stochastic producers. As a consequence, high balancing costs directly lead to lower stochastic producer profits, rendering the necessity of including both KPIs ambiguous. A second example can be found in the relationship between the share of VRES in the energy mix and the amount of wind spillage. Besides from the decreased total demand from possible load shedding events affecting the share of VRES, a direct linear relationship is observable between both KPIs.

Another point of discussion arises from the perceived usefulness of such a KPI framework. While the established framework proved useful as tool to keep track of model performance in widely different aspects of performance, the observed trade-offs between economic performance, system security and integration of VRES cannot provide an objective interpretation of overall performance. A suggestion for future research suggestion would be to shift the research perspective from the TSO towards different market actor perspectives to better understand the implications of including uncertainty-based optimization techniques to the DA market clearing.

5.4 Research assumptions & limitations

The first major assumption of this study is the applied quantity of the stochastic producer bids during the model simulations, which is assumed to be equal to the forecast due to absence of order book data. This assumption most heavily impacted the results of the Deterministic model, considering stochastic producers would reasonably not be assumed to take such heavy risk in their bidding strategies, while the Deterministic model does not increase the amount of procured upward reserves to address this increased risk of under-realization of stochastic producer output. The results of the Deterministic model indicated large amounts of curtailed electricity during load shedding events, far surpassing the amounts that occur in reality. While the Stochastic and Robust model are not affected by the bidding quantities to this extend, in the case of under-forecasting the bidding quantities can potentially constrain the optimal amount of accepted stochastic producer bids. Looking at an overview of stochastic producer bidding strategies as provided in [95], flaws can be identified in each individual bidding strategy; an optimal bidding strategy utilizing perfect forecasting does not only seem highly unrealistic, it renders the application of Stochastic- and Robust optimization techniques completely useless. A moving average bidding strategy and a one-price system both are both focused on the optimal bidding price, not taking into account the optimal bidding quantity. The last described bidding strategy, named Multivariate Interdependence Minimizing Imbalance Cost Strategy (MIMICS), applies stochastic optimization to determine the optimal bidding quantity of a single stochastic producer, although not taking into account anticipating bidding strategies of other market actors. Moreover, no literature is yet made on the effects of stochastic bidding strategies of stochastic producers on the performance of stochastic optimization techniques in DA market clearing, bearing the risk of heavily skewed results in favor of the Stochastic model. Given the high amount of used assumptions during this research, the choice for a point forecast bidding strategy, commonly recognized as the ‘default’ bidding strategy can be considered a safe and neutral choice.

A limitation of this research is the exclusion of transmission capacities of network lines and ramping rates of the conventional power plants in the models. Inclusion of the transmission capacities and ramping rates creates non-convexity in the feasible region of the problem through addition of binary variables, drastically increasing the complexity of finding the optimal solution. Moreover, addition of transmission capacities would heavily diversify possibilities for the outer-problem to realize a worst-case scenario; instead of targeting stochastic producers with high installed capacities to maximize the deviation in stochastic output realization, stochastic producers could become targeted by the worst-case scenario to cause the system unable to meet demand of certain loads, resulting in shedding events. Comparable research on this topic by [9] found improved system security of supply through

optimal dispatching of producing units and reserves through the application of two-stage stochastic optimization, while research by [10] found improved system security in case of contingencies. While this research did also indicate improved system security through the application of uncertainty-based optimization techniques, including transmission capacities and ramping rates in future work could increase the observed benefits from the proposed market clearing formulations, as well as providing a better representation for real-world applications.

6. Conclusion

In this thesis, a comparison was made between a deterministic-, two-stage stochastic and ARO DA market clearing model using a newly established framework of performance indicators on the Dutch, French and German wholesale electricity markets. The proposed models were compared and evaluated based on their ability to maximize SEW, integrate VRES in the energy mix and maintain system security of supply of electricity.

The results of the case studies indicate an increased SEW from the application of two-stage stochastic optimization and ARO to the DA market clearing compared to the current deterministic model due to a heavy decrease in balancing costs because of improved system security of supply. The Stochastic model is performing better during the in-sample results due to its goodness-of-fit, while the Robust model is better able to control unexpected output profiles during the out-of-sample scenarios. Implementation of the proposed Stochastic model results in a decreased integration of VRES in the energy mix, while the Robust model showed a relationship between the total system reserve capacity and the maximum allowed integration of VRES, stressing the need for increased reserve capacity for future energy systems with a high penetration of VRES.
The two-stage stochastic model showed a higher degree of conservativeness with increased in-sample size to unexpected stochastic output profiles, although occurrences of permitted load shedding events for increased SEW raises ethical doubts on real-life implementation in the DA market clearing. Furthermore, the use of the budget of uncertainty to parameterize the level of conservatism allowed to the ARO model indicates potential market inequalities by disproportionately affecting stochastic producers with high amounts of installed capacities.

To conclude, the results of this thesis provide insight in the performance of two-stage stochastic optimization and ARO in the DA market clearing of the Dutch, French and German electricity wholesale market. Moreover, points of discussion are evoked on the implications of an adaptation of the DA market clearing mechanism on the computational burden, market design, market actors and system capacities. Future research suggestions would include a focus on the implications of adaptations to the current DA market clearing mechanism for different market actors and a deeper look into the effects of in-sample size and the budget of uncertainty to the system security and integration of VRES in the energy mix.

References

[1] Markard, Jochen (2018). The next phase of the energy transition and its implications for research and policy. Nature Energy, doi:10.1038/s41560-018-0171-7

[2] UNFCCC. Adoption of the Paris Agreement, proposal by the President, Draft decision -/CP.21. United Nations Framework Convention on Climate Change (UNFCCC), FCCC/CP/2015/L.9/Rev.1; 12 December 2015.

[3] European Commission (2021, July 14). Commission presents Renewable Energy Directive revision. https://commission.europa.eu/news/commission-presents-renewable-energy-directive-revision-2021-07-14_en

[4] Dmitrii Bogdanov;Manish Ram;Arman Aghahosseini;Ashish Gulagi;Ayobami Solomon Oyewo;Michael Child;Upeksha Caldera;Kristina Sadovskaia;Javier Farfan;Larissa De Souza Noel Simas Barbosa;Mahdi Fasihi;Siavash Khalili;Thure Traber;Christian Breyer; (2021). Low-cost renewable electricity as the key driver of the global energy transition towards sustainability . Energy, (), –. doi:10.1016/j.energy.2021.120467

[5] Pepermans, Guido (2019). European energy market liberalization: experiences and challenges. International Journal of Economic Policy Studies, 13(1), 3–26., doi:10.1007/s42495-018-0009-0

[6] Goodarzi, S., Perera, H. N., & Bunn, D. (2019). The impact of renewable energy forecast errors on imbalance volumes and electricity spot prices. Energy Policy, 134, 110827.

[7] Birge, J. R., & Louveaux, F. (2011). Introduction to stochastic programming. Springer Science & Business Media.

[8] Reddy, S. S.; Abhyankar, A. R.; Bijwe, P. R. (2012). [IEEE 2012 IEEE Power & Energy Society General Meeting. New Energy Horizons - Opportunities and Challenges - San Diego, CA (2012.07.22-2012.07.26)] 2012 IEEE Power and Energy Society General Meeting - Market clearing for a wind-thermal power system incorporating wind generation and load forecast uncertainties. , (), 1–8. doi:10.1109/PESGM.2012.6345335

[9] Liu, Yang; Nair, Nirmal-Kumar C. (2015). A Two-Stage Stochastic Dynamic Economic Dispatch Model Considering Wind Uncertainty. IEEE Transactions on Sustainable Energy, (), 1–11. doi:10.1109/TSTE.2015.2498614

[10] Saric, A.T.; Murphy, F.H.; Soyster, A.L.; Stankovic, A.M. (2009). Two-Stage Stochastic Programming Model for Market Clearing With Contingencies. IEEE Transactions on Power Systems, 24(3), 1266–1278., doi:10.1109/TPWRS.2009.2023267

[11] Bjørndal, Endre; Bjørndal, Mette; Midthun, Kjetil; Tomasgard, Asgeir (2018). Stochastic electricity dispatch: A challenge for market design. Energy, (), S0360544218302834–. doi:10.1016/j.energy.2018.02.055

[12] Morales, Juan M.; Zugno, Marco; Pineda, Salvador; Pinson, Pierre (2014). Electricity market clearing with improved scheduling of stochastic production. European Journal of Operational Research, 235(3), 765–774., doi:10.1016/j.ejor.2013.11.013

[13] Morales, J. M., Conejo, A. J., Madsen, H., Pinson, P., & Zugno, M. (2013). Integrating renewables in electricity markets: operational problems (Vol. 205). Springer Science & Business Media.

[14] Wang, Qianfan; Watson, Jean-Paul; Guan, Yongpei (2013). Two-stage robust optimization for N-k contingency-constrained unit commitment. IEEE Transactions on Power Systems, 28(3), 2366–2375. doi:10.1109/TPWRS.2013.2244619

[15] Kazemzadeh, Narges; Ryan, Sarah M.; Hamzeei, Mahdi (2017). Robust optimization vs. stochastic programming incorporating risk measures for unit commitment with uncertain variable renewable generation. Energy Systems, doi:10.1007/s12667-017-0265-5

[16] Morales-España, Germán; Lorca, Álvaro; de Weerdt, Mathijs M. (2018). Robust unit commitment with dispatchable wind power. Electric Power Systems Research, 155(), 58–66. doi:10.1016/j.epsr.2017.10.002

[17] Silva-Rodriguez, L., Sanjab, A., Fumagalli, E., Virag, A., & Gibescu, M. (2022). A light robust optimization approach for uncertainty-based day-ahead electricity markets. Electric Power Systems Research, 212, 108281.

[18] Zugno, Marco; Conejo, Antonio J. (2015). A robust optimization approach to energy and reserve dispatch in electricity markets. European Journal of Operational Research, 247(2), 659–671. doi:10.1016/j.ejor.2015.05.081

[19] Bertsimas, Dimitris; Brown, David B.; Caramanis, Constantine (2011). Theory and Applications of Robust Optimization. , 53(3), 464–0., doi:10.1137/080734510

[20] Kim, H.J.; Kim, M.K.; Lee, J.W. (2021). A two-stage stochastic p-robust optimal energy trading management in microgrid operation considering uncertainty with hybrid demand response. International Journal of Electrical Power & Energy Systems, 124(), 106422–. doi:10.1016/j.ijepes.2020.106422

[21] Kena Zhao;Tsan Sheng Ng;Chin Hon Tan;Chee Khiang Pang; (2021). An almost robust model for minimizing disruption exposures in supply systems . European Journal of Operational Research, (), –. doi:10.1016/j.ejor.2021.03.003

[22] Panpan Li;Liangyun Song;Jixian Qu;Yuehui Huang;Xiaoyun Wu;Xi Lu;Shiwei Xia; (2021). A Two-Stage Distributionally Robust Optimization Model for Wind Farms and Storage Units Jointly Operated Power Systems . IEEE Access, (), doi:10.1109/access.2021.3101569

[23] Herrero, Ignacio; Rodilla, Pablo; Batlle, Carlos (2015). Electricity market-clearing prices and investment incentives: The role of pricing rules. Energy Economics, 47(), 42–51. doi:10.1016/j.eneco.2014.10.024

[24] Yan, X. (2014). Forecasting Mid-Term Electricity Market Clearing Price Using Support Vector Machines (Doctoral dissertation, University of Saskatchewan).

[25] Hong Lam, Le; Ilea, Valentin; Bovo, Cristian (2020). New Clearing Model to Mitigate the Non-Convexity in European Day-ahead Electricity Market. Energies, 13(18), 4716–. doi:10.3390/en13184716

[26] Shinde, Priyanka; Amelin, Mikael (2019). [IEEE 2019 IEEE Milan PowerTech - Milan, Italy (2019.6.23-2019.6.27)] 2019 IEEE Milan PowerTech - A Literature Review of Intraday Electricity Markets and Prices. , doi:10.1109/ptc.2019.8810752

[27] van der Veen, Reinier A.C.; Hakvoort, Rudi A. (2016). The electricity balancing market: Exploring the design challenge. Utilities Policy, (), S0957178716303125–., doi:10.1016/j.jup.2016.10.008

[28] Roumkos, C., Biskas, P. N., & Marneris, I. G. (2022). Integration of European Electricity Balancing Markets. Energies, 15(6), 2240.

[29] Divényi, Dániel; Polgári, Beáta; Sleisz, Ádám; Sőrés, Péter; Raisz, Dávid (2019). Algorithm design for European electricity market clearing with joint allocation of energy and control reserves. International Journal of Electrical Power & Energy Systems, 111(), 269–285. doi:10.1016/j.ijepes.2019.04.006

[30] Van den Bergh, Kenneth; Delarue, Erik (2020). Energy and reserve markets: interdependency in electricity systems with a high share of renewables. Electric Power Systems Research, 189(), 106537–., doi:10.1016/j.epsr.2020.106537

[31] Saravanan, B.; Das, Siddharth; Sikri, Surbhi; Kothari, D. P. (2013). A solution to the unit commitment problem—a review. Frontiers in Energy, 7(2), 223–236. doi:10.1007/s11708-013-0240-3

[32] Abbaspourtorbati, Farzaneh; Conejo, Antonio J.; Wang, Jianhui; Cherkaoui, Rachid (2016). Three- or Two-stage Stochastic Market-Clearing Algorithm?. IEEE Transactions on Power Systems, (), 1–1., doi:10.1109/TPWRS.2016.2621069

[33] Jiarong Cai;Weiwei Lai;Zhenghao Qian;Kang Huang;Rui Zhou;Zhisheng Huang; (2021). An Optimal Decision-Making Method for Power Market Transaction Based on Renewable Energy Multi-Scenario Forecast . Journal of Physics: Conference Series, (), –. doi:10.1088/1742-6596/1754/1/012063

[34] Khazaei, Javad; Zakeri, Golbon; Oren, Shmuel S. (2017). Single and Multisettlement Approaches to Market Clearing Under Demand Uncertainty. Operations Research, (), opre.2017.1610–. doi:10.1287/opre.2017.1610

[35] Huang, Y.-H., Wu, J.-H., & Hsu, Y.-J. (2016). Two-stage stochastic programming model for the regional-scale electricity planning under demand uncertainty. Energy, 116, 1145–1157. doi:10.1016/j.energy.2016.09.112

[36] Alnowibet, K. A., & El-Meligy, M. A. (2022). A stochastic programming approach using multiple uncertainty sets for AC robust transmission expansion planning. Sustainable Energy, Grids and Networks, 30, 100648.

[37] Gabrel, Virginie; Murat, Cécile; Thiele, Aurélie (2014). Recent advances in robust optimization: An overview. European Journal of Operational Research, 235(3), 471–483. doi:10.1016/j.ejor.2013.09.036

[38] Atamtürk, Alper; Zhang, Muhong (2007). Two-Stage Robust Network Flow and Design Under Demand Uncertainty. Operations Research, 55(4), 662–673. doi:10.1287/opre.1070.0428

[39] Single Price Coupling Algorithm. EUPHEMIA Public Description. 2020. Available online: https://www.nordpoolgroup.com/globalassets/download-center/single-day-ahead-coupling/euphemia-public-description.pdf (accessed on 3 March 2023).

[40] Ghiasi, Mohammad; Ghadimi, Noradin; Ahmadinia, Esmaeil (2019). An analytical methodology for reliability assessment and failure analysis in distributed power system. SN Applied Sciences, 1(1), 44–., doi:10.1007/s42452-018-0049-0

[41] Avraamidou, S., & Pistikopoulos, E. N. (2020). A global optimization algorithm for the solution of tri-level mixed-integer quadratic programming problems. In *Optimization of Complex Systems: Theory, Models, Algorithms and Applications* (pp. 579-588). Springer International Publishing.

[42] Zeng, Bo; Zhao, Long (2013). Solving two-stage robust optimization problems using a column-and-constraint generation method. Operations Research Letters, 41(5), 457–461. doi:10.1016/j.orl.2013.05.003

[43] Bertsimas, Dimitris; Litvinov, Eugene; Sun, Xu Andy; Zhao, Jinye; Zheng, Tongxin (2013). Adaptive Robust Optimization for the Security Constrained Unit Commitment Problem. IEEE Transactions on Power Systems, 28(1), 52–63., doi:10.1109/tpwrs.2012.2205021

[44] Meerschaert, Mark M. (2013). Mathematical Modeling || Multivariable Optimization. , (), 21–55. doi:10.1016/B978-0-12-386912-8.50002-6

[45] Ruszczynski, A. (2011). Nonlinear optimization. Princeton university press.

[46] Birbil, Ş. İ., Frenk, J. B. G., & Still, G. J. (2007). An elementary proof of the Fritz-John and Karush–Kuhn–Tucker conditions in nonlinear programming. European journal of operational research, 180(1), 479-484.

[47] Zhang, M., Wang, G., & Fu, L. (2004, November). Robustness enhancement for proximal support vector machines. In Proceedings of the 2004 IEEE International Conference on Information Reuse and Integration, 2004. IRI 2004. (pp. 290-295). IEEE.

[48] Gronski, J. (2019). Non-convex optimization and applications to bilinear programming and super-resolution imaging (Doctoral dissertation, University of Colorado at Boulder).

[49] Hirth, L. (2020). Open data for electricity modeling: Legal aspects. Energy Strategy Reviews, 27, 100433.

[50] F.S Wen; A.K David (2001). Strategic bidding for electricity supply in a day-ahead energy market. , 59(3), 197–206. doi:10.1016/s0378-7796(01)00154-7

[51] Bajo, Javier; Vale, Zita; Hallenborg, Kasper; Rocha, Ana Paula; Mathieu, Philippe; Pawlewski, Pawel; Del Val, Elena; Novais, Paulo; Lopes, Fernando; Duque Méndez, Nestor D.; Julián, Vicente; Holmgren, Johan (2017). [Communications in Computer and Information Science] Highlights of Practical Applications of Cyber-Physical Multi-Agent Systems Volume 722 || Multi-agent Wholesale Electricity Markets with High Penetrations of Variable Generation: A Case-Study on Multivariate Forecast Bidding Strategies. , 10.1007/978-3-319-60285-1(Chapter 29), 340–349. doi:10.1007/978-3-319-60285-1_29

[52] Kebriaei, Hamed; Tajeddini, Mohammad Amin; Rashedi, Navid (2016). Markov game approach for multi-agent competitive bidding strategies in electricity market. IET Generation, Transmission & Distribution, (), –.doi:10.1049/iet-gtd.2016.0075

[53] Wiese, F., Schlecht, I., Bunke, W. D., Gerbaulet, C., Hirth, L., Jahn, M., ... & Schill, W. P. (2019). Open Power System Data–Frictionless data for electricity system modelling. Applied Energy, 236, 401-409.

[54] EPEX Spot. (2023). Market Data | EPEX SPOT. Retrieved May 26, 2023, from https://www.epexspot.com/en/market-data

[55] Autoriteit Consumenten Markt. (2022). Besluit TenneT vaststelling Value of Lost Load (ACM/22/178437). ACM. Retrieved May 19, 2023, from https://www.acm.nl/system/files/documents/vaststelling-value-of-lost-load.pdf

[56] CEPA & Agency for the Cooperation of Energy Regulators. (2022). STUDY ON THE ESTIMATION OF THE VALUE OF LOST LOAD OF ELECTRICITY SUPPLY IN EUROPE (ACER/OP/DIR/08/2013/LOT 2/RFS 10.). Cambridge Economic Policy Associates (CEPA). Retrieved May 23, 2023, from https://www.acer.europa.eu/en/Electricity/Infrastructure_and_network%20development/Infrastructure/Documents/CEPA%20study%20on%20the%20Value%20of%20Lost%20Load%20in%20the%20electricity%20supply.pdf

[57] Wang, Yao; Ai, Xin; Tan, Zhongfu; Yan, Lei; Liu, Shuting (2015). Interactive Dispatch Modes and Bidding Strategy of Multiple Virtual Power Plants Based on Demand Response and Game Theory. IEEE Transactions on Smart Grid, (), 1–1., doi:10.1109/tsg.2015.2409121

[58] Zare, Kazem; Nojavan, Sayyad; Mohammadi-Ivatloo, Behnam (2015). Optimal bidding strategy of electricity retailers using robust optimisation approach considering time-of-use rate demand response programs under market price uncertainties. IET Generation, Transmission & Distribution, 9(4), 328–338., doi:10.1049/iet-gtd.2014.0548

[59] Lampropoulos, Ioannis; Frunt, Jasper; Nobel, Frank A.; Virag, Ana; van den Bosch, Paul P. J.; Kling, Wil L. (2012). [IEEE 2012 9th International Conference on the European Energy Market (EEM 2012) - Florence, Italy (2012.05.10-2012.05.12)] 2012 9th International Conference on the European Energy Market - Analysis of the market-based service provision for operating reserves in the Netherlands. , (), 1–8. doi:10.1109/eem.2012.6254735

[60] Brinkel, N. (2018). A Balancing Act: Developments in Dutch and German balancing markets and the impact of variable renewable generation. [MA Thesis]. Utrecht University.

[61] RTE. (2022, July 21). Modalités de sélection des offres au sein de l'appel d'offres annuel RR/RC. Retrieved June 1, 2023, from https://www.services-rte.com/files/live/sites/services-rte/files/pdf/RRRC/RRRC2023_Description%20interclassement_vf.pdf

[62] RTE. (2023, January 1). Manual frequency restoration reserve and replacement reserve terms and conditions. Retrieved June 1, 2023, from https://www.services-rte.com/files/live//sites/services-rte/files/documentsLibrary/2023-01-01_MFRR-RR_TERMS_AND_CONDITIONS_4507_en

[63] 50Hertz, Tennet, Transet BW, & Ampion. (2022, December 8). Modalitaten für Regelreserveanbieter. Retrieved June 1, 2023, from https://www.regelleistung.net/Portals/1/downloads/modalit%C3%A4ten_rahmenvertraege/modalitaeten_regelreserveanbieter_en/1__MfRRA%20Stand%2008.12.2022.pdf?ver=TT6f7lPsGHUYQvNa5TKkDw%3d%3d

[64] Lampropoulos, Ioannis; van den Broek, Machteld; van der Hoofd, Erik; Hommes, Klaas; van Sark, Wilfried (2018). A system perspective to the deployment of flexibility through aggregator companies in the Netherlands. Energy Policy, 118(), 534–551. doi:10.1016/j.enpol.2018.03.073

[65] Wu, Junli; Zhang, Buhan; Li, Hang; Li, Zhongcheng; Chen, Yi; Miao, Xiaogang (2014). Statistical distribution for wind power forecast error and its application to determine optimal size of energy storage system. International Journal of Electrical Power & Energy Systems, 55(), 100–107. doi:10.1016/j.ijepes.2013.09.003

[66] Bielecki, M. F. (2010). Statistical characterization of errors in wind power forecasting (Doctoral dissertation, Northern Arizona University).

[67] Iversen, J. E. B., & Pinson, P. (2016). Resgen: Renewable energy scenario generation platform. In 2016 IEEE Power Engineering Society General Meeting. IEEE.

[68] Arduin, I. (2016). Development of an Open-source Platform for Wind and Solar Probabilistic Forecasting [MA Thesis]. Danmarks Tekniske Universitet.

[69] Bertsimas, D., & Thiele, A. (2006). Robust and data-driven optimization: modern decision making under uncertainty. In Models, methods, and applications for innovative decision making (pp. 95-122). INFORMS.

[70] Ben-Tal, A., El Ghaoui, L., & Nemirovski, A. (2009). Robust optimization (Vol. 28). Princeton university press.

[71] Wang, Cheng; Liu, Feng; Wang, Jianhui; Qiu, Feng; Wei, Wei; Mei, Shengwei; Lei, Shunbo (2016). Robust Risk-Constrained Unit Commitment with Large-scale Wind Generation: An Adjustable Uncertainty Set Approach. IEEE Transactions on Power Systems, (), 1–1. doi:10.1109/TPWRS.2016.2564422

[72] Li, Zhigang; Wu, Wenchuan; Shahidehpour, Mohammad; Zhang, Boming (2015). Adaptive Robust Tie-Line Scheduling Considering Wind Power Uncertainty for Interconnected Power Systems. IEEE Transactions on Power Systems, (), 1–1., doi:10.1109/TPWRS.2015.2466546

[73] Tuinema, Bart W.; Rueda, Jose L.; van der Meijden, Mart A.M.M. (2015). [IEEE 2015 IEEE Eindhoven PowerTech - Eindhoven, Netherlands (2015.6.29-2015.7.2)] 2015 IEEE Eindhoven PowerTech - Network redundancy versus generation reserve in combined onshore-offshore transmission networks. , (), 1–6., doi:10.1109/PTC.2015.7232416

[74] Wang, Jianhui, Mohammad Shahidehpour, and Zuyi Li. "Security-constrained unit commitment with volatile wind power generation." IEEE Transactions on Power Systems 23.3 (2008): 1319-1327.

[75] Wang, J., Wang, J., Liu, C., & Ruiz, J. P. (2013). Stochastic unit commitment with sub-hourly dispatch constraints. Applied energy, 105, 418-422.

[76] Papavasiliou, A., Oren, S. S., & O'Neill, R. P. (2011). Reserve requirements for wind power integration: A scenario-based stochastic programming framework. IEEE Transactions on Power Systems, 26(4), 2197-2206.

[77] Zhao, C., & Guan, Y. (2013). Unified stochastic and robust unit commitment. IEEE Transactions on Power Systems, 28(3), 3353-3361.

[78] Dvorkin, Y., Pandžić, H., Ortega-Vazquez, M. A., & Kirschen, D. S. (2014). A hybrid stochastic/interval approach to transmission-constrained unit commitment. IEEE Transactions on Power Systems, 30(2), 621-631.

[79] Optimization for Academics - Gurobi Optimization. (2023, March 28). Gurobi Optimization. https://www.gurobi.com/personas/optimization-for-academics/

[80] Gallego, F. J. (2010). A population density grid of the European Union. Population and Environment, 31(6), 460-473.

[81] Statista. (2023, February 28). GDP of European countries 2021. https://www.statista.com/statistics/685925/gdp-of-european-countries/

[82] Statista. (2023, January 25). Power demand in the European Union (EU) 2021, by country. https://www.statista.com/statistics/1260553/eu-power-demand-country/

[83] The Netherlands - Countries & Regions - IEA. (n.d.). IEA. https://www.iea.org/countries/the-netherlands

[84] Wouter Biesiot; Klaas Jan Noorman (1999). Energy requirements of household consumption: a case study of The Netherlands. , 28(3), 0–383., doi:10.1016/s0921-8009(98)00113-x

[85] Windstats. (2023). Gegevens. Retrieved from https://windstats.nl/statistieken/#data_results

[86] The Netherlands on track with approach to offshore wind energy | RVO.nl. (n.d.). https://english.rvo.nl/news/netherlands-track-approach-offshore-wind-energy#:~:text=The%20Dutch%20Offshore%20Wind%20Energy,by%20the%20end%20of%202023.

[87] France - The World Factbook. (2023). https://www.cia.gov/the-world-factbook/countries/france/

[88] France - Countries & Regions - IEA. (2023). IEA. https://www.iea.org/countries/france

[89] IEA. (2023, January 23). Nuclear power plants generated 68% of France's electricity in 2021. https://www.eia.gov/todayinenergy/detail.php?id=55259#:~:text=France%20has%20few%20fossil%20fuel,it%20turned%20to%20nuclear%20power.

[90] Averbuch, D. & IFP Energies Nouvelles. (2022). IEA Wind TCP - France 2021. IEA. https://usercontent.one/wp/iea-wind.org/wp-content/uploads/2022/12/IEA_Wind_TCP_AR2021_France.pdf

[91] Bundesnetzagentur. (2022). Monitoringbericht 2022. BUNDESNETZAGENTUR. https://www.bundeskartellamt.de/SharedDocs/Publikation/DE/Berichte/Energie-Monitoring-2022.pdf?__blob=publicationFile&v=5

[92] BWE & VDMA. (2023). Status des Windenergieausbaus an Land in Deutschland Erstes Halbjahr 2023. Deutsche WindGaurd. https://www.windguard.de/veroeffentlichungen.html?file=files/cto_layout/img/unternehmen/veroeffentlichungen/2023/Status%20des%20Windenergieausbaus%20an%20Land_Halbjahr%202023.pdf

[93] BWE, BWO, VDMA, & WAB. (2023). Status des Offshore-Windenergieausbaus in Deutschland Erstes Halbjahr 2023. Deutsche WindGuard. https://www.windguard.de/veroeffentlichungen.html?file=files/cto_layout/img/unternehmen/veroeffentlichungen/2023/Status%20des%20Offshore-Windenergieausbaus_Halbjahr%202023.pdf

[94] van Stiphout, Arne; De Vos, Kristof; Deconinck, Geert (2016). The Impact of Operating Reserves on Investment Planning of Renewable Power Systems. IEEE Transactions on Power Systems, (), 1–1. doi:10.1109/TPWRS.2016.2565058

[95] Vilim, Michael; Botterud, Audun (2014). Wind power bidding in electricity markets with high wind penetration. Applied Energy, 118(), 141–155., doi:10.1016/j.apenergy.2013.11.055

Appendix A – Demand bid distributions

Bidding ID	Bid Price [€/MWh]	NL	FR	DE
1	4000	55,00%	50,00%	55,00%
2	3000	1,59%	0,00%	0,00%
3	2000	1,14%	0,00%	0,70%
4	1500	0,51%	0,00%	1,50%
5	1000	0,26%	0,93%	0,60%
6	750	0,26%	0,00%	0,30%
7	650	0,00%	0,75%	0,15%
8	500	0,52%	0,43%	0,31%
9	450	1,30%	1,02%	1,86%
10	400	0,88%	1,85%	1,36%
11	350	1,30%	0,46%	0,18%
12	300	1,51%	0,46%	0,25%
13	250	0,52%	0,63%	0,43%
14	200	0,52%	0,99%	0,32%
15	150	0,52%	0,00%	0,77%
16	140	0,22%	0,23%	0,50%
17	130	0,32%	0,23%	0,31%
18	125	0,36%	0,42%	0,64%
19	120	0,67%	0,34%	0,23%
20	115	0,29%	0,37%	0,48%
21	110	0,31%	0,03%	0,19%
22	105	0,48%	1,46%	0,31%
23	100	0,36%	0,32%	0,72%
24	95	0,55%	1,16%	0,42%
25	90	0,52%	0,21%	0,12%
26	85	0,41%	0,30%	0,23%
27	80	0,61%	0,60%	0,85%
28	77,5	0,52%	0,44%	0,40%
29	75	0,32%	0,62%	0,52%
30	72,5	0,11%	0,56%	0,23%
31	70	0,52%	0,28%	0,08%
32	67,5	0,14%	0,21%	0,21%
33	65	0,42%	0,31%	0,46%
34	62,5	0,36%	0,13%	0,62%
35	60	0,52%	1,06%	0,89%
36	57,5	0,30%	0,43%	0,62%
37	55	0,56%	0,21%	0,24%
38	52,5	0,65%	0,67%	0,32%
39	50	0,19%	1,13%	0,22%
40	45	0,52%	0,78%	0,46%
41	40	0,22%	0,81%	0,91%
42	35	0,89%	0,65%	0,10%
43	30	0,81%	0,78%	0,67%
44	25	0,36%	1,32%	1,02%

45	20	0,52%	1,06%	0,51%
46	15	0,53%	0,87%	0,34%
47	10	1,21%	6,55%	0,65%
48	5	1,30%	4,80%	0,74%
49	0	18,05%	13,14%	21,06%

Appendix B – Average balancing costs

B.1 In-sample analysis results – The Netherlands

Model	Robust model			
Day	**08-05-2023**	**20-12-2022**	**13-09-2022**	**02-03-2023**
Upward reserve procurement	€720,665.56	€661,234.52	€109,456.91	€755,816.51
Downward reserve procurement	€0.00	€0.00	€0.00	€0.00
Upward reserve activation	€37,388.62	€6,262.79	€210.32	€1,993.84
Load shedding	€694,137.78	€0.00	€0.00	€0.00

Model	Deterministic model			
Day	**08-05-2023**	**20-12-2022**	**13-09-2022**	**02-03-2023**
Upward reserve procurement	€329,142.86	€329,142.86	€329,142.86	€354,098.26
Downward reserve procurement	€213,518.67	€213,518.67	€213,518.67	€213,518.67
Upward reserve activation	€159,324.51	€65,886.56	€108,307.50	€20,339.79
Load shedding	€88,588,598.72	€5,091,988.97	€80,849.63	€2,541,728.07

Model	Stochastic model			
Day	**08-05-2023**	**20-12-2022**	**13-09-2022**	**02-03-2023**
Upward reserve procurement	€658,150.79	€528,043.86	€215,484.97	€390,306.56
Downward reserve procurement	€0.00	€0.00	€0.00	€0.00
Upward reserve activation	€51,568.04	€31,984.53	€19,015.33	€10,454.48
Load shedding	€0.00	€0.00	€0.00	€0.00

B.2 Out-of-sample analysis results – The Netherlands

Model	Robust model			
Day	**08-05-2023**	**20-12-2022**	**13-09-2022**	**02-03-2023**
Upward reserve procurement	€720,665.56	€661,234.52	€109,456.91	€755,816.51
Downward reserve procurement	€0.00	€0.00	€0.00	€0.00
Upward reserve activation	€35,415.41	€4,465.81	€731.76	€1,619.51
Load shedding	€515,812.52	€0.00	€1,169.98	€0.00

Model	Deterministic model			
Day	08-05-2023	20-12-2022	13-09-2022	02-03-2023
Upward reserve procurement	€329,142.86	€329,142.86	€329,142.86	€354,098.26
Downward reserve procurement	€213,518.67	€213,518.67	€213,518.67	€213,518.67
Upward reserve activation	€166,342.80	€65,013.00	€105,605.87	€23,951.07
Load shedding	€92,436,443.40	€4,008,645.30	€296,849.75	€2,966,535.93

Model	Stochastic model			
Day	08-05-2023	20-12-2022	13-09-2022	02-03-2023
Upward reserve procurement	€658,150.79	€528,043.86	€215,484.97	€390,306.56
Downward reserve procurement	€0.00	€0.00	€0.00	€0.00
Upward reserve activation	€55,394.75	€30,140.02	€21,240.21	€10,530.66
Load shedding	€1,614,785.82	€537,171.13	€851,291.75	€1,750,765.24

B.3 In-sample analysis results - France

Model	Robust model			
Day	08-05-2023	20-12-2022	13-09-2022	02-03-2023
Upward reserve procurement	€653,880.18	€633,233.15	€109,456.91	€708,390.51
Downward reserve procurement	€0.00	€0.00	€0.00	€0.00
Upward reserve activation	€6,969.61	€3,324.97	€18.50	€585.07
Load shedding	€0.00	€0.00	€0.00	€0.00

Model	Deterministic model			
Day	08-05-2023	20-12-2022	13-09-2022	02-03-2023
Upward reserve procurement	€329,142.86	€329,142.86	€329,142.86	€354,098.26
Downward reserve procurement	€213,518.67	€213,518.67	€213,518.67	€213,518.67
Upward reserve activation	€65,738.59	€24,603.09	€47,406.77	€1,895.03
Load shedding	€65,738.59	€24,603.09	€47,406.77	€1,895.03

Model	Stochastic model			
Day	08-05-2023	20-12-2022	13-09-2022	02-03-2023

Upward reserve procurement	€589,771.65	€438,069.17	€176,771.74	€82,580.91
Downward reserve procurement	€0.00	€0.00	€0.00	€0.00
Upward reserve activation	€27,522.19	€14,441.78	€9,900.21	€1,812.64
Load shedding	€0.00	€0.00	€0.00	€0.00

B.4 Out-of-sample analysis results – France

Model	**Robust model**			
Day	**08-05-2023**	**20-12-2022**	**13-09-2022**	**02-03-2023**
Upward reserve procurement	€653,880.18	€633,233.15	€109,456.91	€708,390.51
Downward reserve procurement	€0.00	€0.00	€0.00	€0.00
Upward reserve activation	€6,864.17	€708.50	€197.27	€274.99
Load shedding	€0.00	€0.00	€0.00	€0.00

Model	**Deterministic model**			
Day	**08-05-2023**	**20-12-2022**	**13-09-2022**	**02-03-2023**
Upward reserve procurement	€329,142.86	€329,142.86	€329,142.86	€354,098.26
Downward reserve procurement	€213,518.67	€213,518.67	€213,518.67	€213,518.67
Upward reserve activation	€81,344.18	€23,314.76	€47,878.58	€4,092.48
Load shedding	€95,175.49	€113,372.31	€115,249.97	€115,714.22

Model	**Stochastic model**			
Day	**08-05-2023**	**20-12-2022**	**13-09-2022**	**02-03-2023**
Upward reserve procurement	€589,771.65	€438,069.17	€176,771.74	€82,580.91
Downward reserve procurement	€0.00	€0.00	€0.00	€0.00
Upward reserve activation	€31,807.63	€10,067.68	€10,575.91	€1,296.12
Load shedding	€0.00	€0.00	€0.00	€0.00

B.5 In-sample analysis results - Germany

Model	Robust model			
Day	**08-05-2023**	**20-12-2022**	**13-09-2022**	**02-03-2023**
Upward reserve procurement	€3,430,699.41	€3,578,359.12	€2,777,032.68	€2,979,771.54
Downward reserve procurement	€0.00	€0.00	€0.00	€0.00
Upward reserve activation	€1,478.34	€8,008.10	€126,257.81	€4,955.14
Load shedding	€0.00	€2,756.67	€2,288,420.10	€0.00

Model	Deterministic model			
Day	**08-05-2023**	**20-12-2022**	**13-09-2022**	**02-03-2023**
Upward reserve procurement	€2,461,583.25	€2,915,434.13	€2,753,829.35	€2,855,938.04
Downward reserve procurement	€1,202,220.45	€1,202,220.45	€1,202,220.45	€1,202,220.45
Upward reserve activation	€3,382,016.06	€124,094.53	€1,348,655.90	€1,059,991.39
Load shedding	€6,163,666,815.62	€7,486,428.30	€794,359,104.98	€86,267,771.87

Model	Stochastic model			
Day	**08-05-2023**	**20-12-2022**	**13-09-2022**	**02-03-2023**
Upward reserve procurement	€2,273,463.567	€1,690,894.67	€1,604,073.98	€2,049,316.43
Downward reserve procurement	€0.00	€0.00	€0.00	€0.00
Upward reserve activation	€91,010.99	€60,173.08	€115,821.78	€150,850.82
Load shedding	€0.00	€0.00	€0.00	€0.00

B.6 Out-of-sample analysis results – Germany

Model	Robust model			
Day	**08-05-2023**	**20-12-2022**	**13-09-2022**	**02-03-2023**
Upward reserve procurement	€3,430,699.41	€3,578,359.12	€2,777,032.68	€2,979,771.54
Downward reserve procurement	€0.00	€0.00	€0.00	€0.00
Upward reserve activation	€4,230.23	€10,042.80	€128,583.81	€2,481.80

Load shedding	€0.00	€0.00	€2,067,264.67	€0.00

Model	Deterministic model			
Day	**08-05-2023**	**20-12-2022**	**13-09-2022**	**02-03-2023**
Upward reserve procurement	€2,461,583.25	€2,915,434.13	€2,753,829.35	€2,855,938.04
Downward reserve procurement	€1,202,220.45	€1,202,220.45	€1,202,220.45	€1,202,220.45
Upward reserve activation	€3,384,676.97	€94,040.72	€1,333,182.56	€1,087,022.63
Load shedding	€6,295,652,765.98	€8,659,267.03	€786,479,948.03	€108,542,265.38

Model	Stochastic model			
Day	**08-05-2023**	**20-12-2022**	**13-09-2022**	**02-03-2023**
Upward reserve procurement	€2,273,463.57	€1,690,894.67	€1,604,073.98	€2,049,316.43
Downward reserve procurement	€0.00	€0.00	€0.00	€0.00
Upward reserve activation	€118,378.48	€48,317.05	€109,441.20	€183,243.08
Load shedding	€9,331,434.21	€5,717,343.00	€2,012,711.52	€5,081,002.61

Appendix C – Share of VRES in energy mix

C.1 In-sample analysis results – The Netherlands

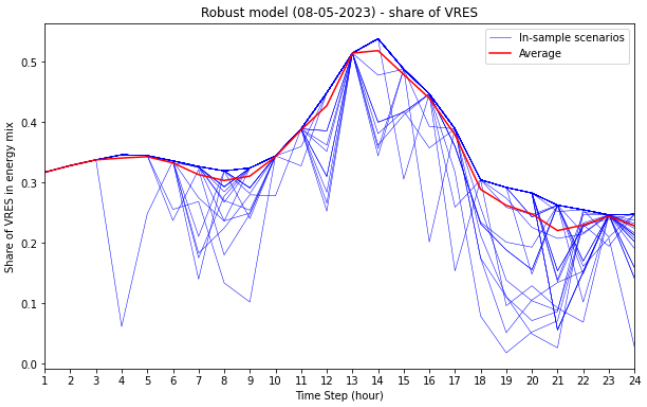

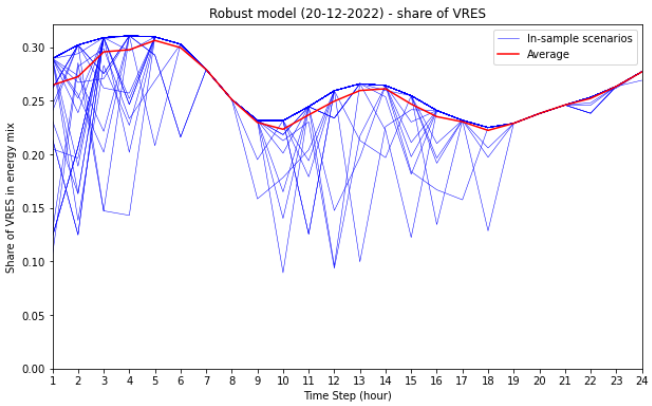

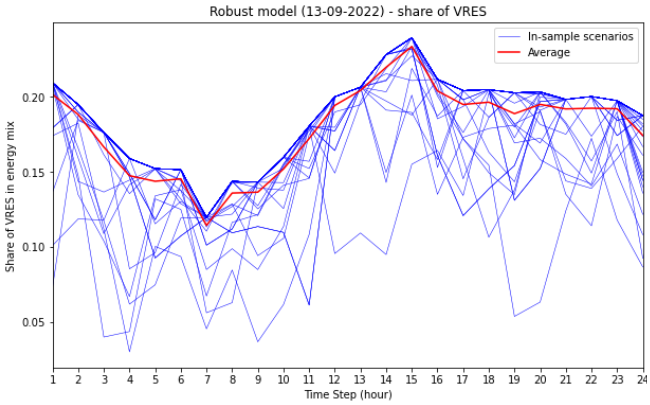

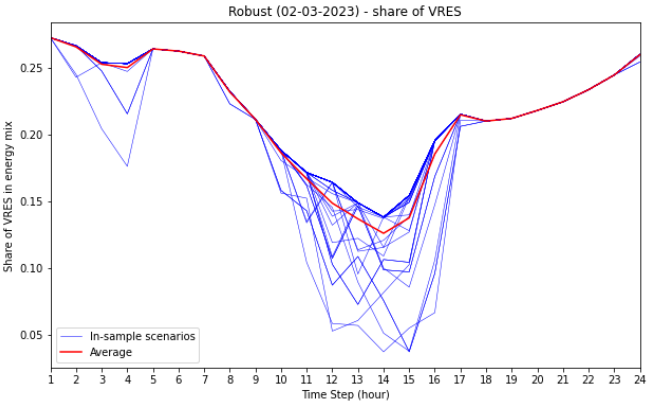

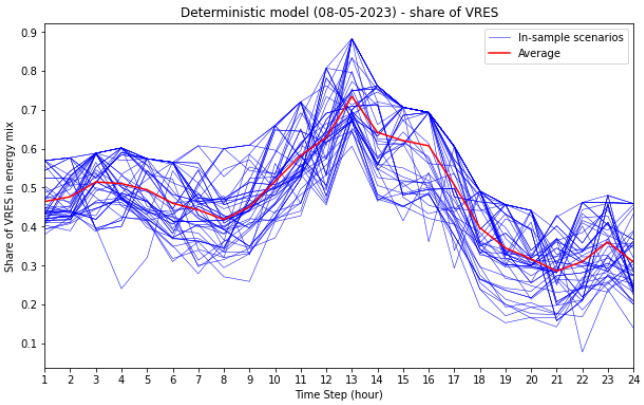

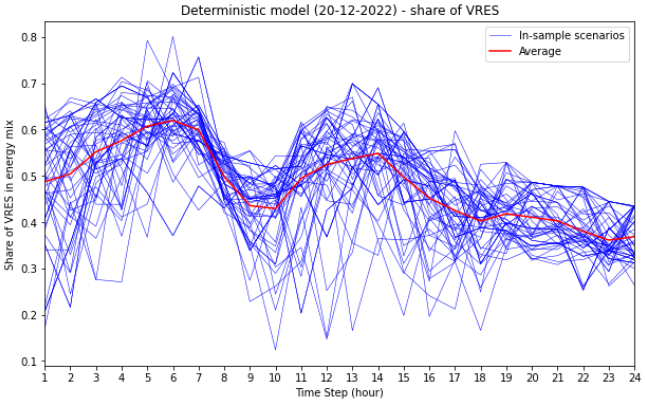

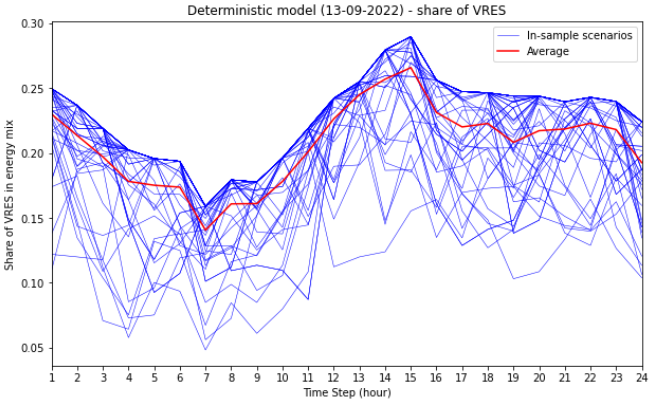

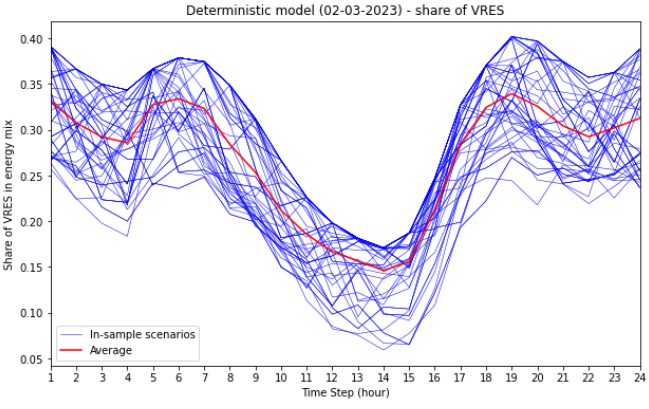

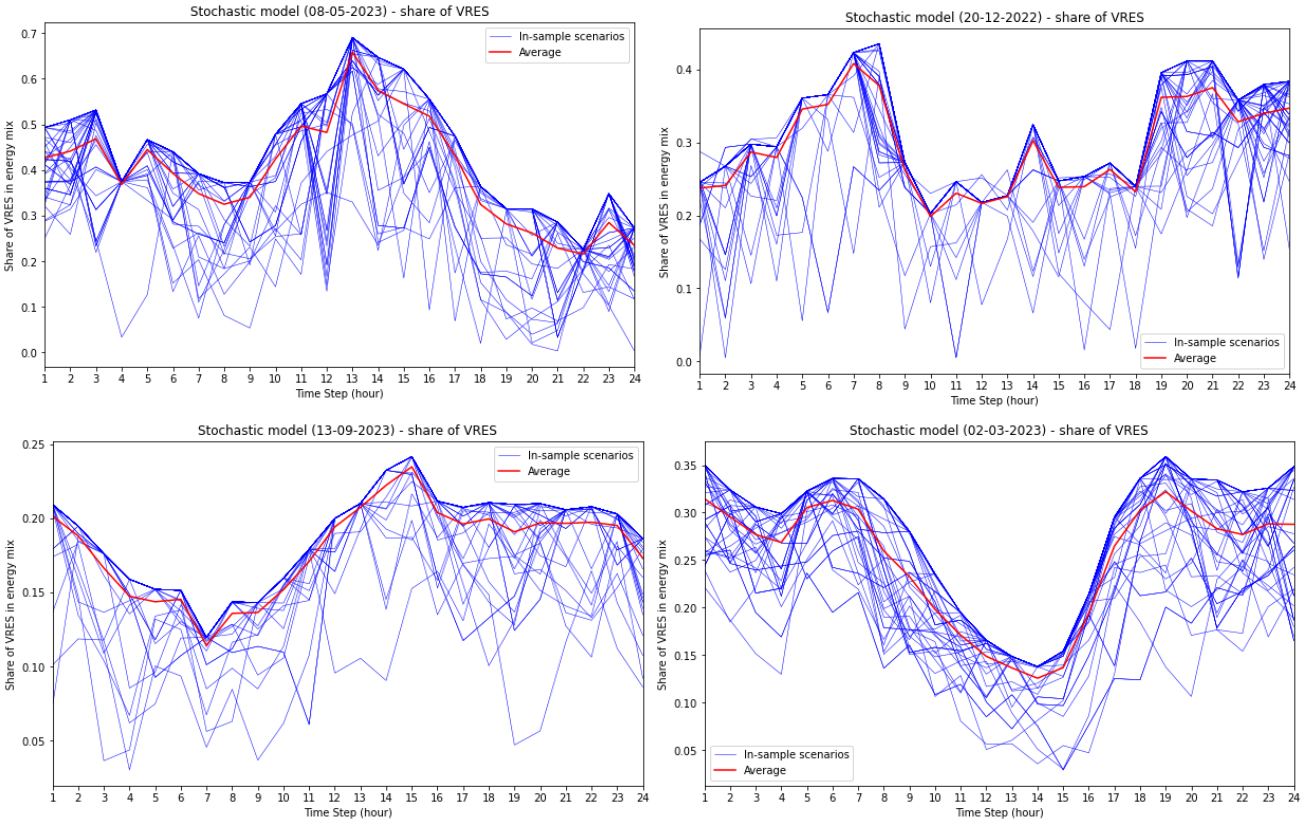

C.2 Out-of-sample analysis results – The Netherlands

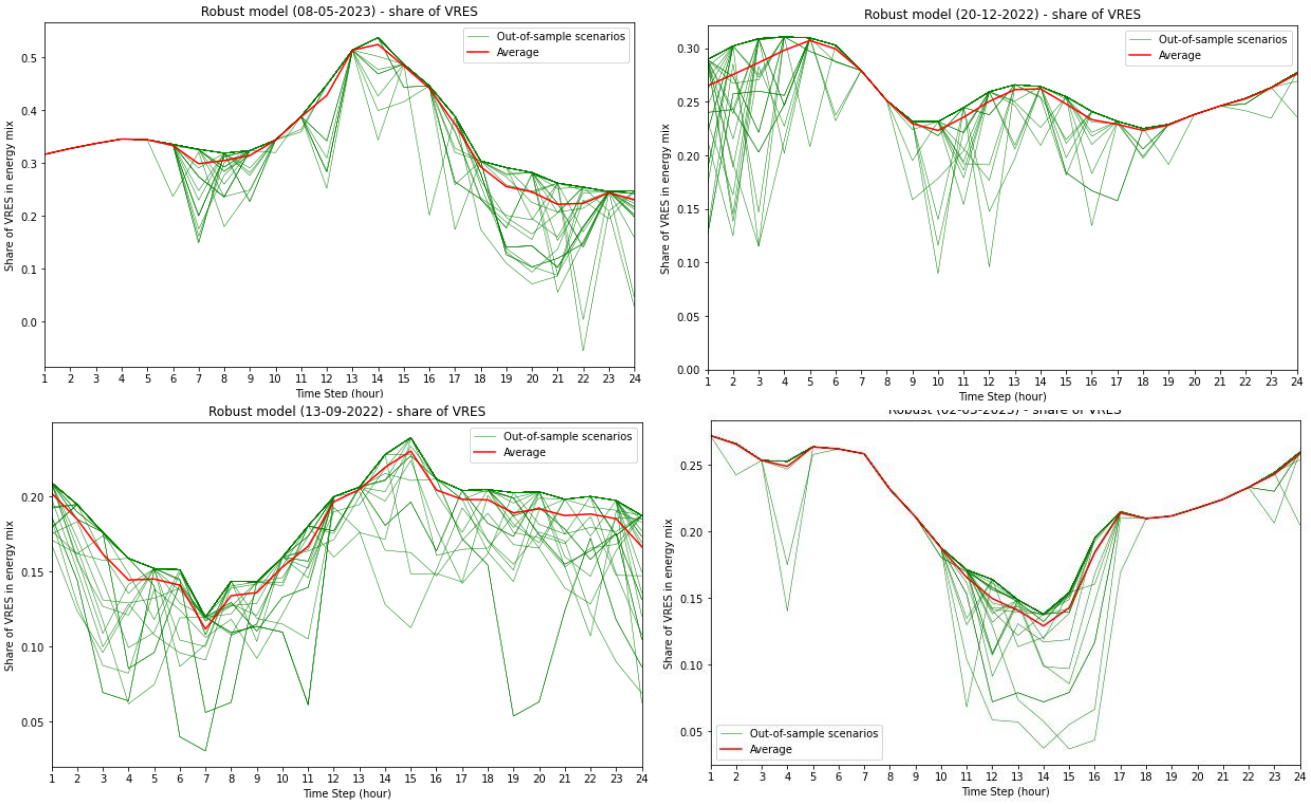

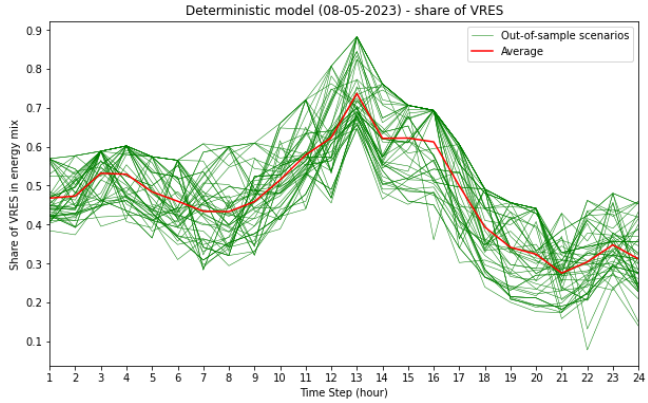
Deterministic model (08-05-2023) - share of VRES
Out-of-sample scenarios
Average
Share of VRES in energy mix
Time Step (hour)

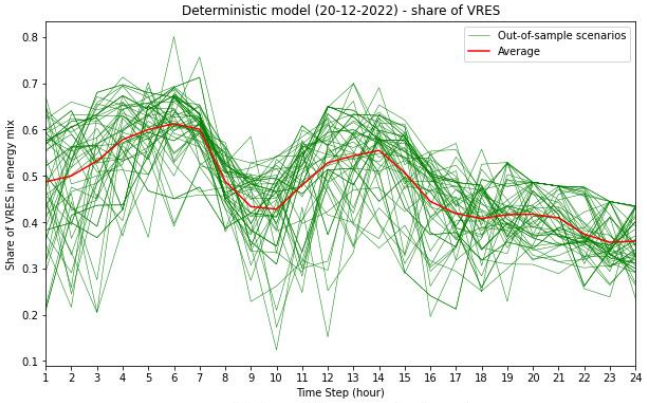
Deterministic model (20-12-2022) - share of VRES
Out-of-sample scenarios
Average
Share of VRES in energy mix
Time Step (hour)

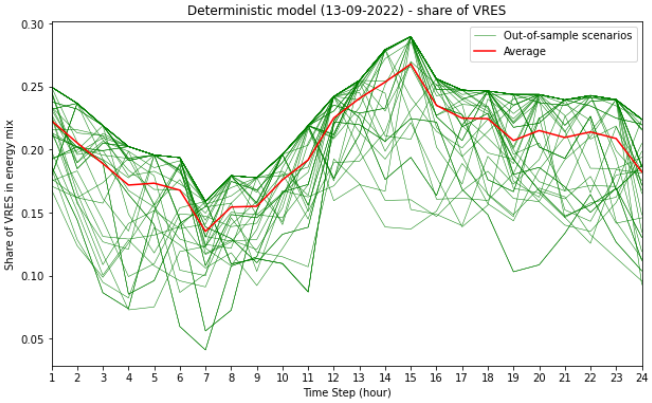
Deterministic model (13-09-2022) - share of VRES
Out-of-sample scenarios
Average
Share of VRES in energy mix
Time Step (hour)

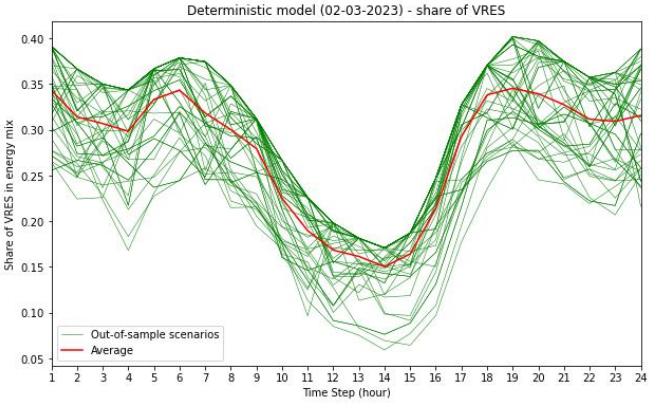
Deterministic model (02-03-2023) - share of VRES
Out-of-sample scenarios
Average
Share of VRES in energy mix
Time Step (hour)

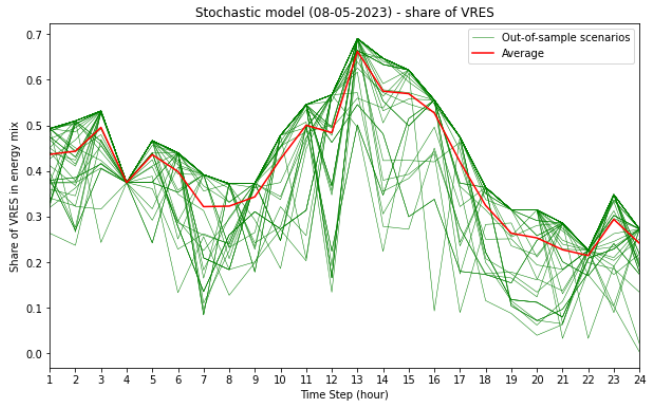
Stochastic model (08-05-2023) - share of VRES
Out-of-sample scenarios
Average
Share of VRES in energy mix
Time Step (hour)

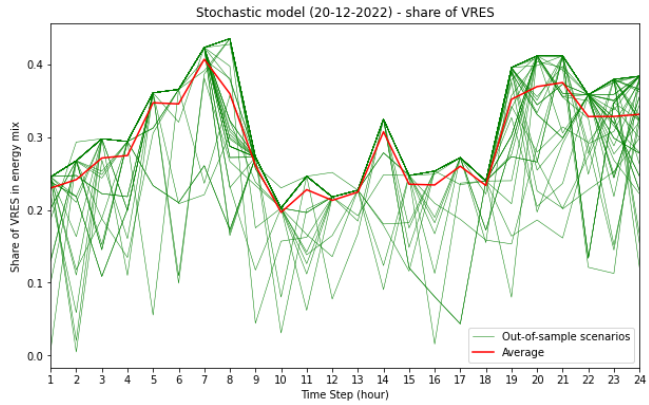
Stochastic model (20-12-2022) - share of VRES
Out-of-sample scenarios
Average
Share of VRES in energy mix
Time Step (hour)

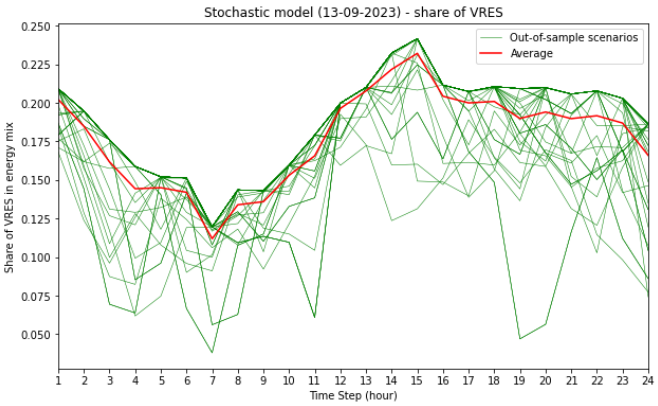
Stochastic model (13-09-2023) - share of VRES
Out-of-sample scenarios
Average
Share of VRES in energy mix
Time Step (hour)

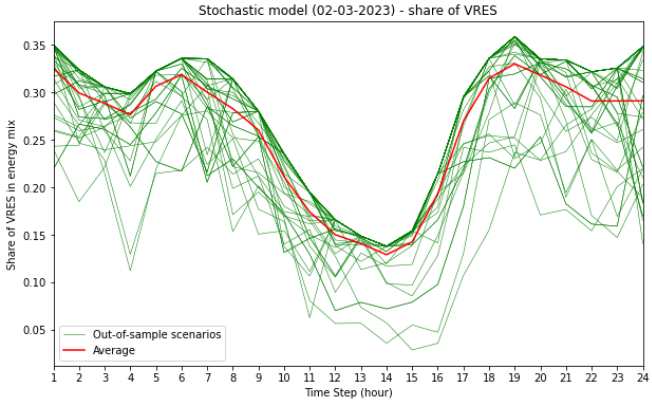
Stochastic model (02-03-2023) - share of VRES
Out-of-sample scenarios
Average
Share of VRES in energy mix
Time Step (hour)

C.3 In-sample analysis results – France

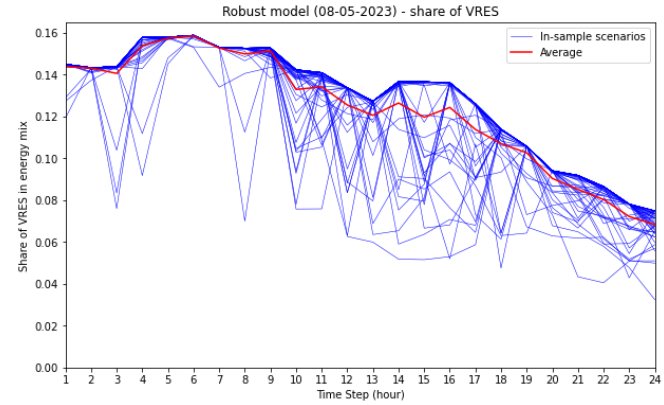

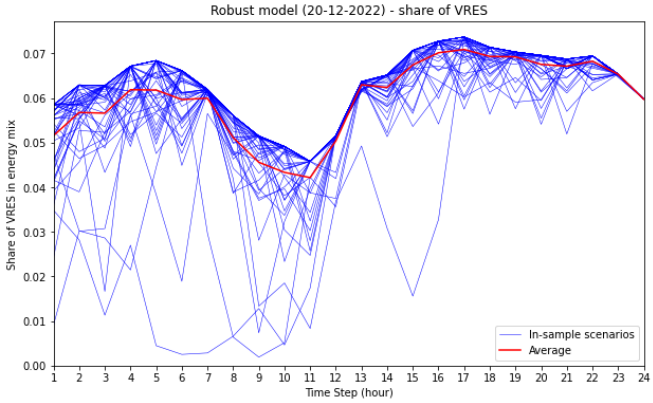

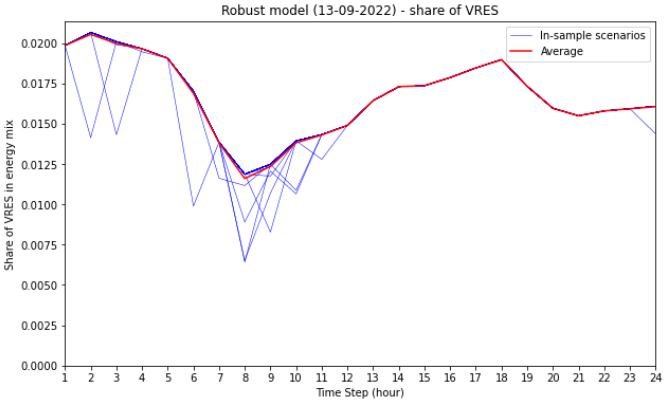

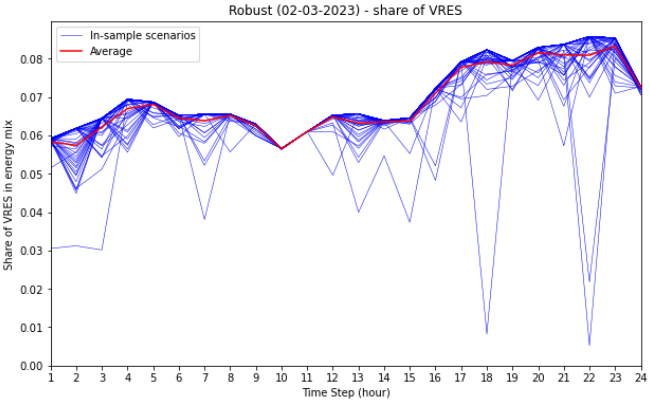

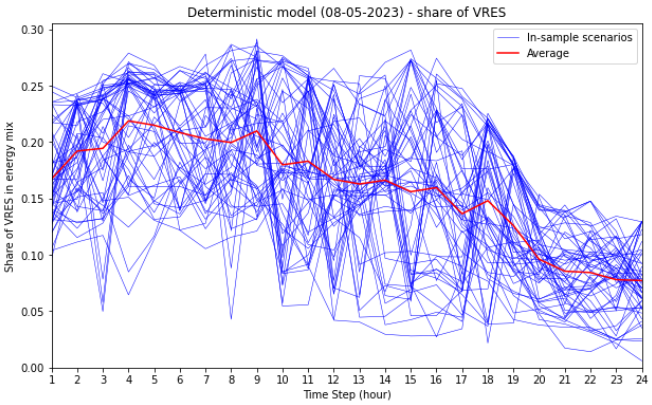

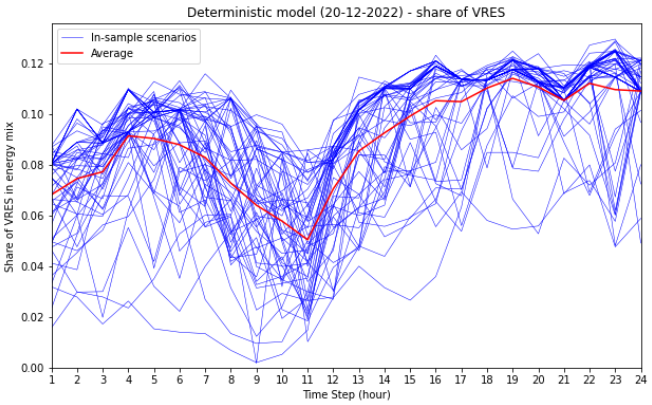

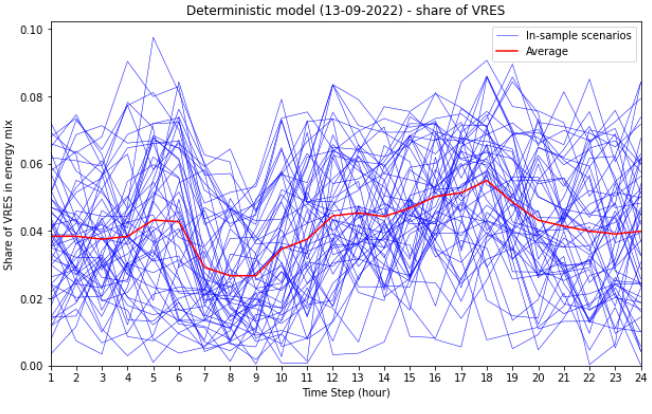

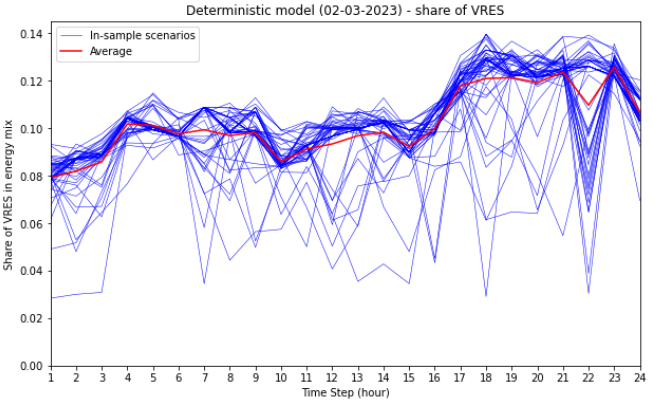

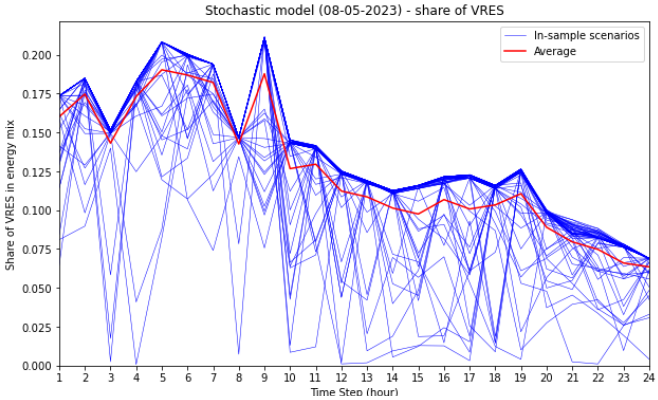

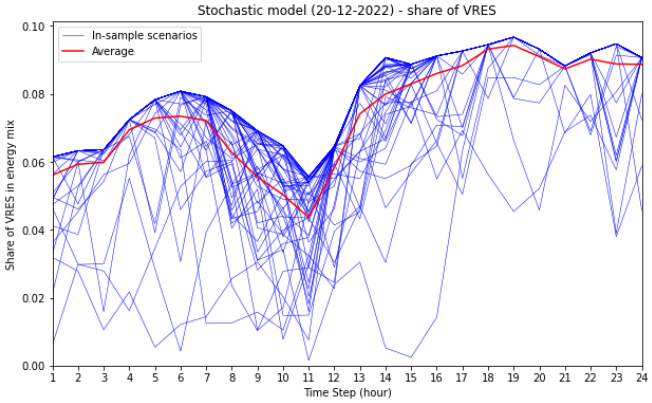

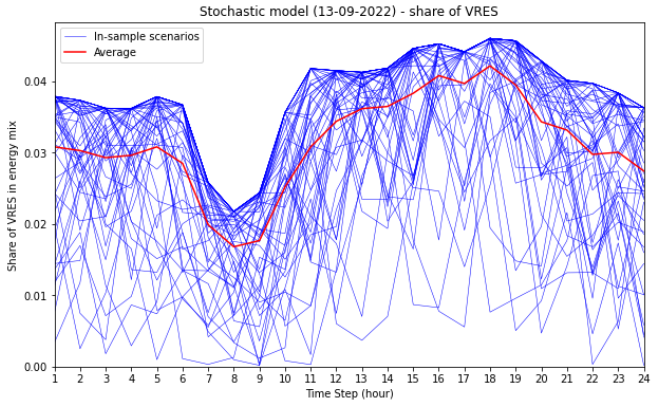

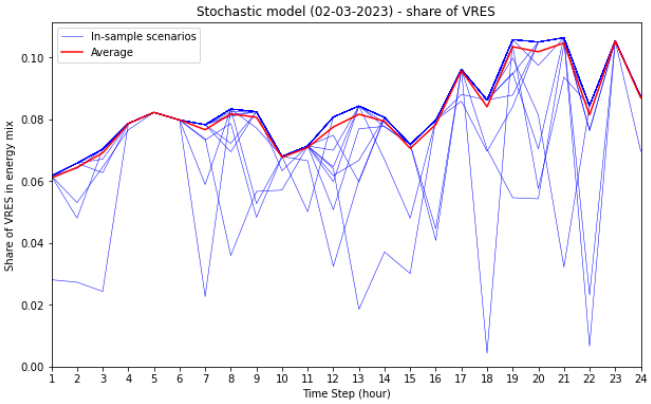

C.4 Out-of-sample analysis results – France

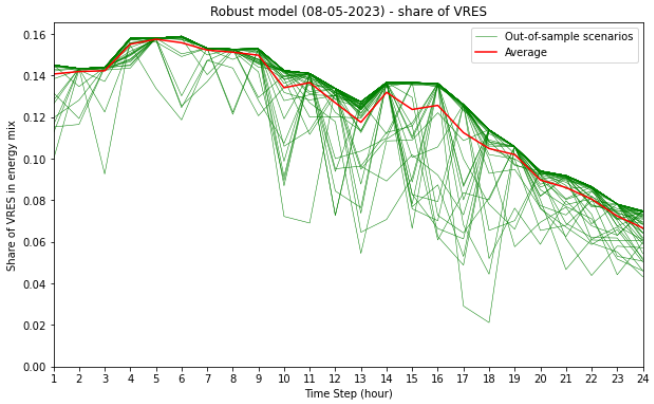

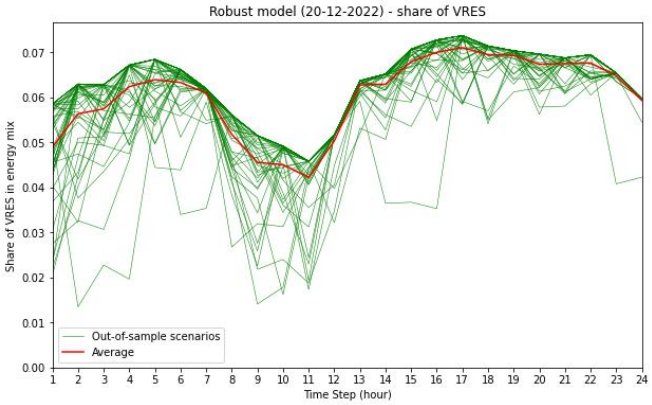

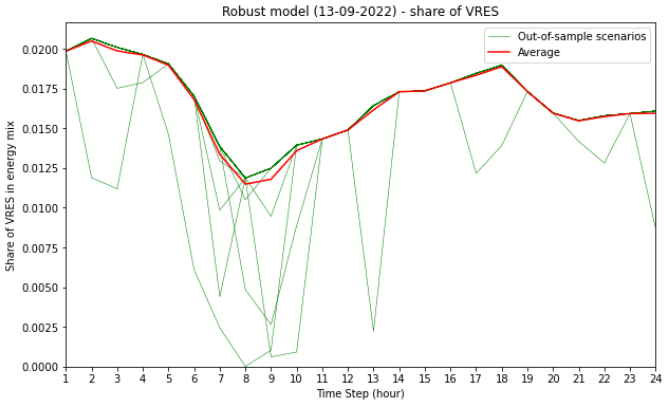

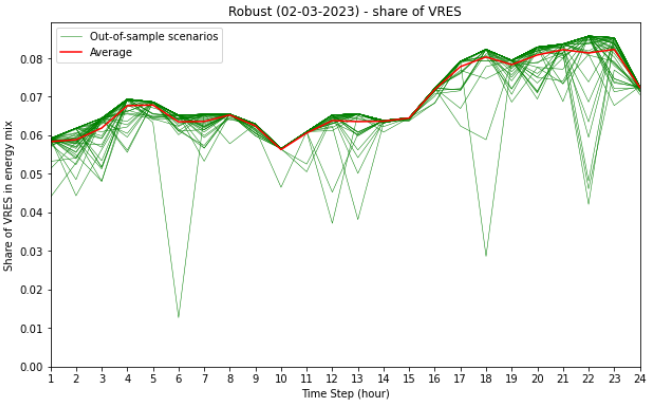

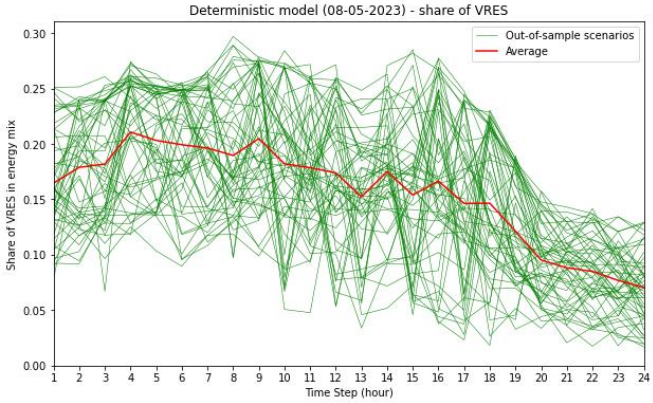
Deterministic model (08-05-2023) - share of VRES
Out-of-sample scenarios
Average
Share of VRES in energy mix
Time Step (hour)

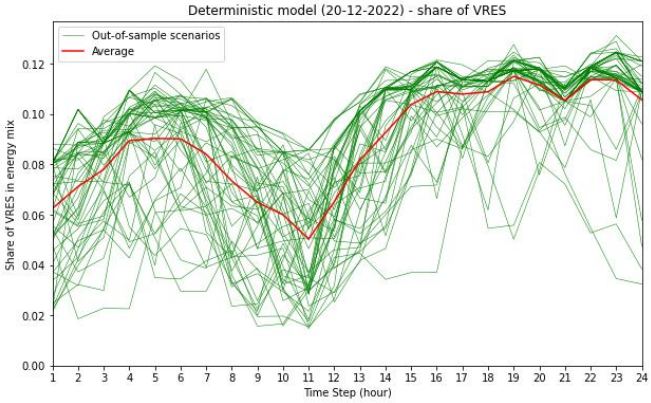
Deterministic model (20-12-2022) - share of VRES
Out-of-sample scenarios
Average
Share of VRES in energy mix
Time Step (hour)

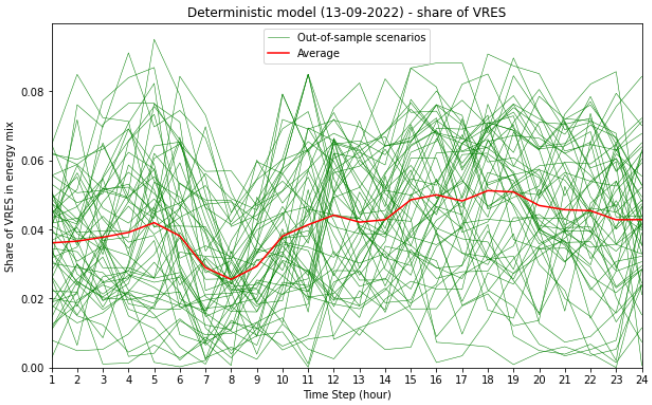
Deterministic model (13-09-2022) - share of VRES
Out-of-sample scenarios
Average
Share of VRES in energy mix
Time Step (hour)

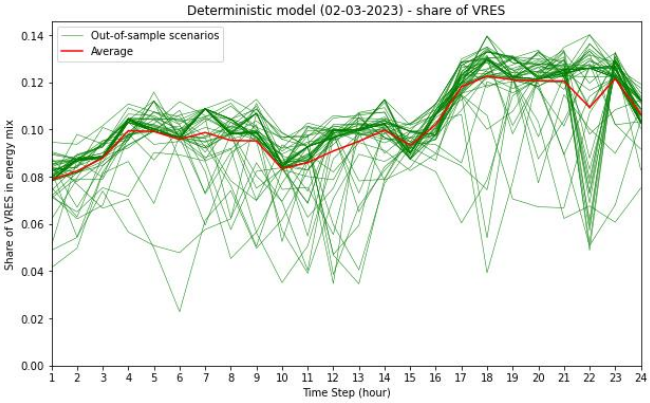
Deterministic model (02-03-2023) - share of VRES
Out-of-sample scenarios
Average
Share of VRES in energy mix
Time Step (hour)

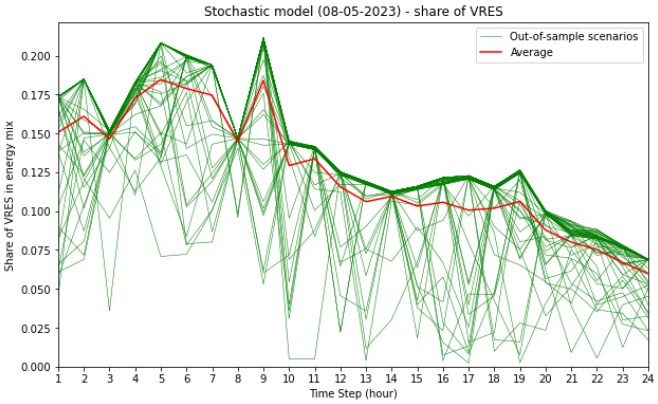
Stochastic model (08-05-2023) - share of VRES
Out-of-sample scenarios
Average
Share of VRES in energy mix
Time Step (hour)

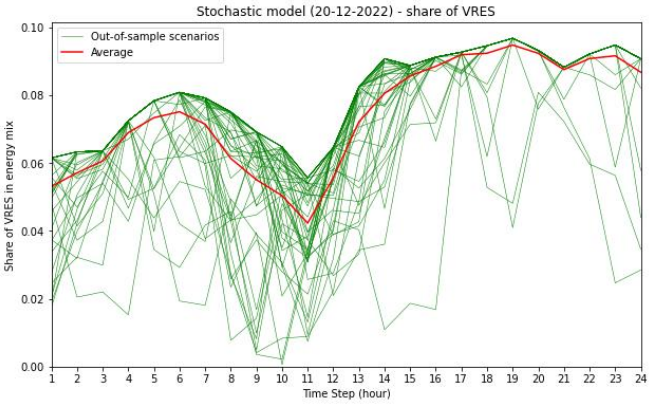
Stochastic model (20-12-2022) - share of VRES
Out-of-sample scenarios
Average
Share of VRES in energy mix
Time Step (hour)

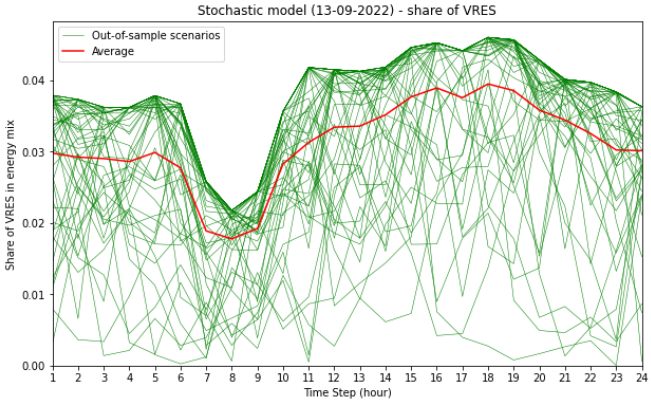
Stochastic model (13-09-2022) - share of VRES
Out-of-sample scenarios
Average
Share of VRES in energy mix
Time Step (hour)

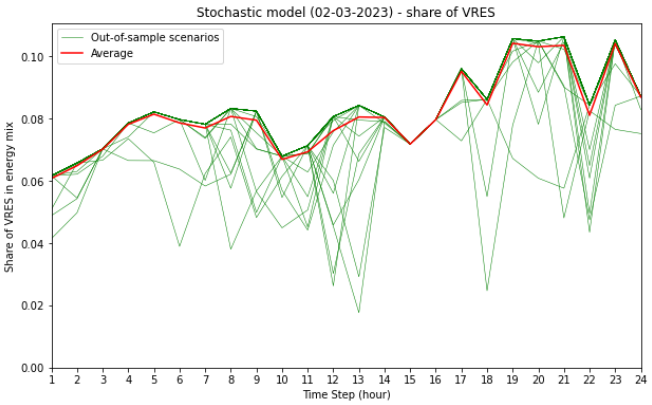
Stochastic model (02-03-2023) - share of VRES
Out-of-sample scenarios
Average
Share of VRES in energy mix
Time Step (hour)

C.5 In-sample analysis results – Germany

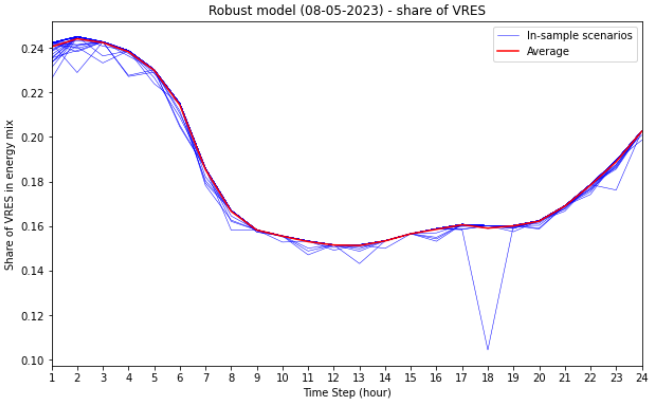

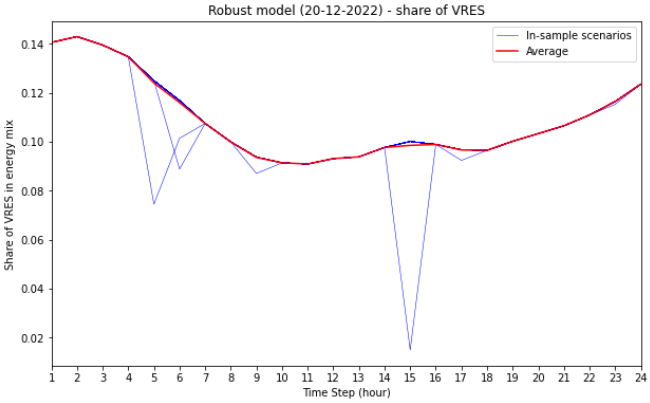

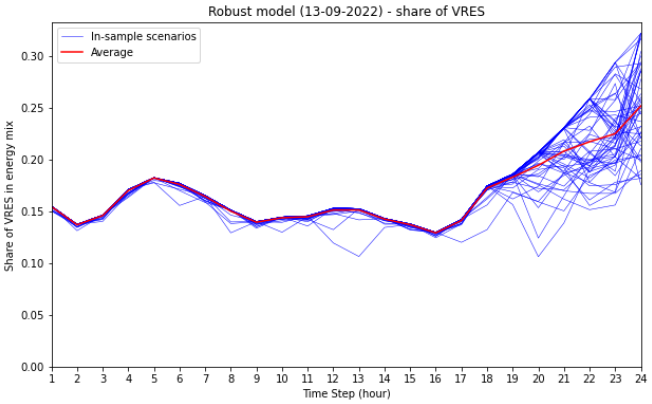

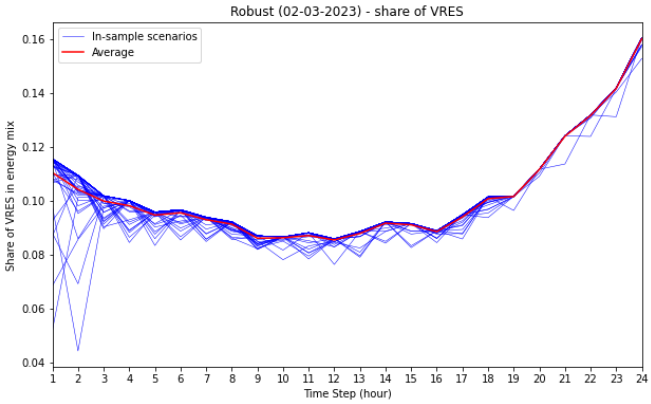

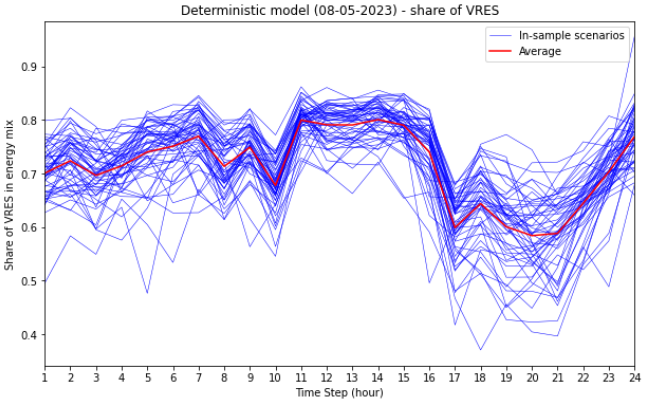

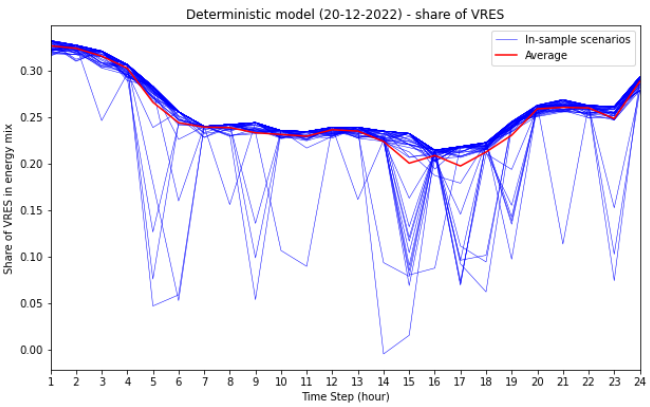

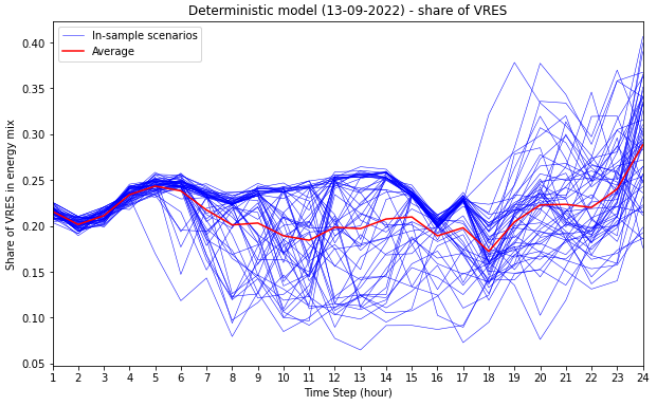

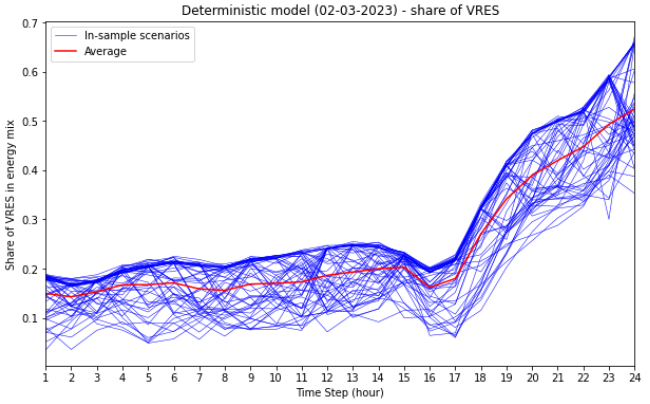

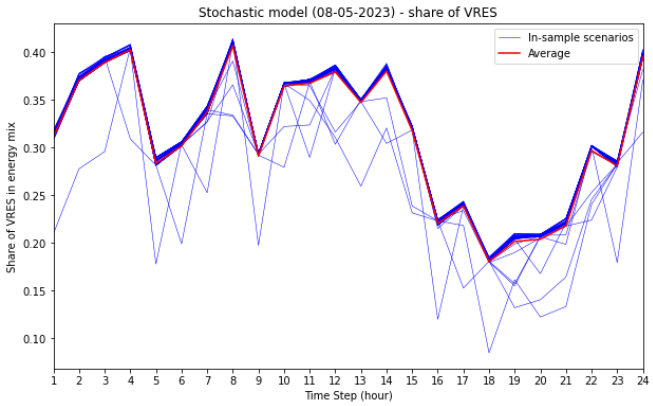

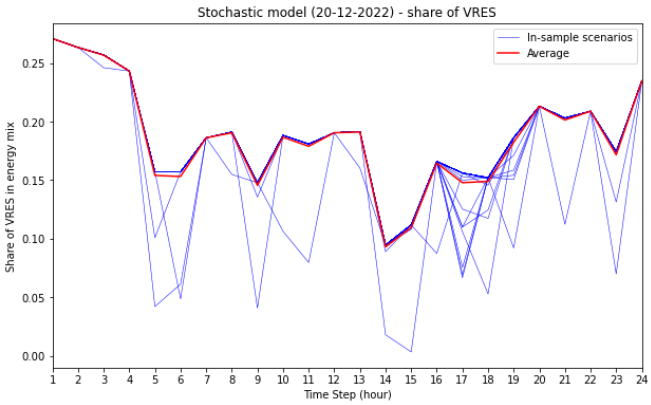

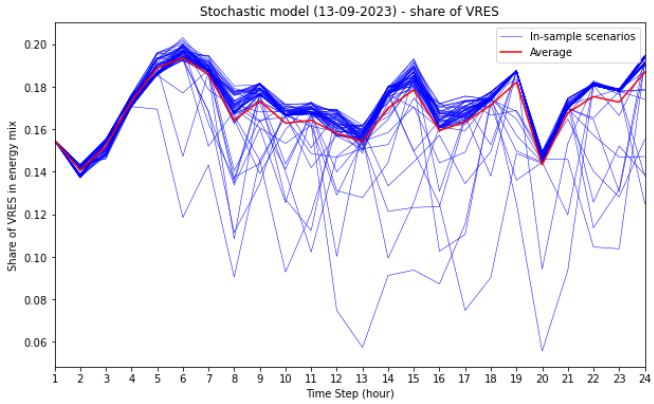

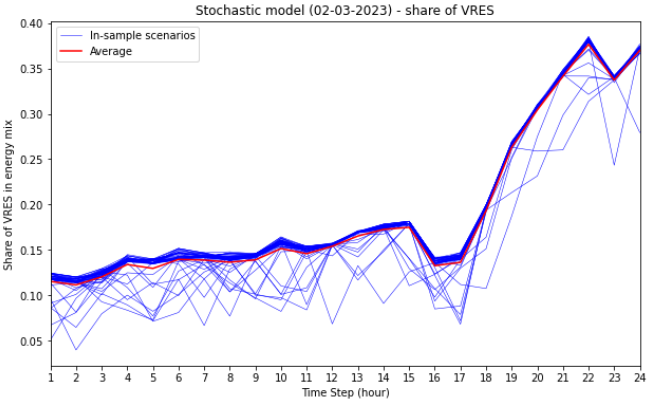

C.6 Out-of-sample analysis results – Germany

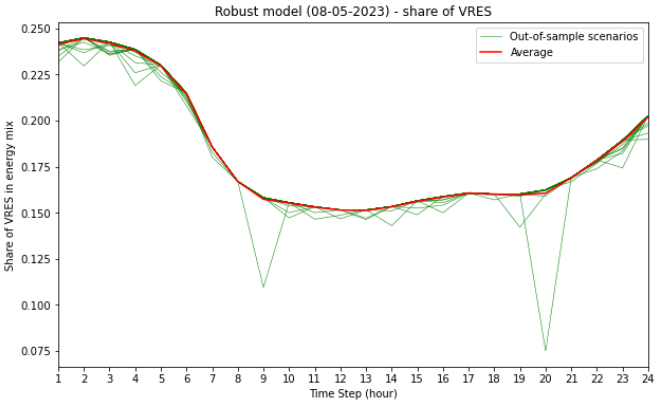

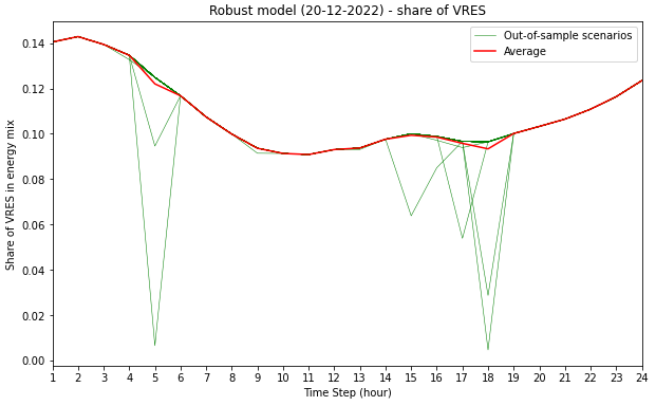

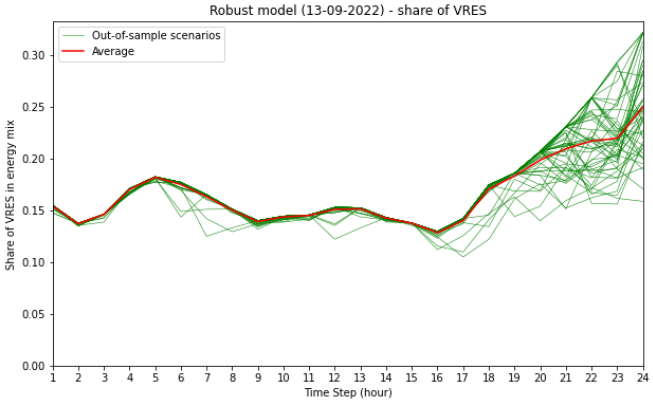

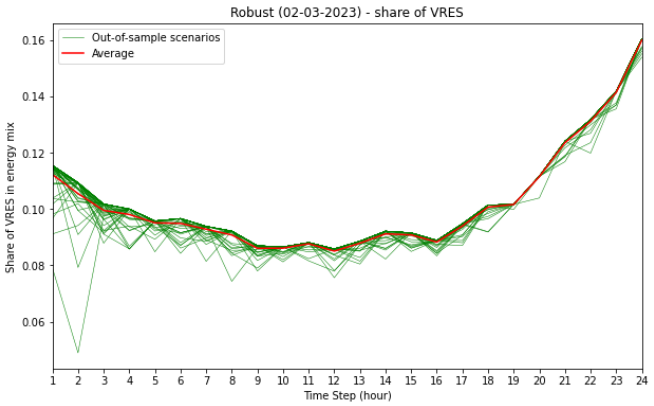

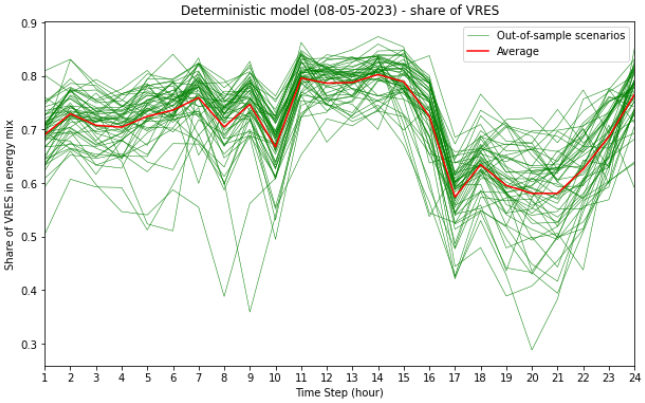
Deterministic model (08-05-2023) - share of VRES
Out-of-sample scenarios
Average
Share of VRES in energy mix
Time Step (hour)

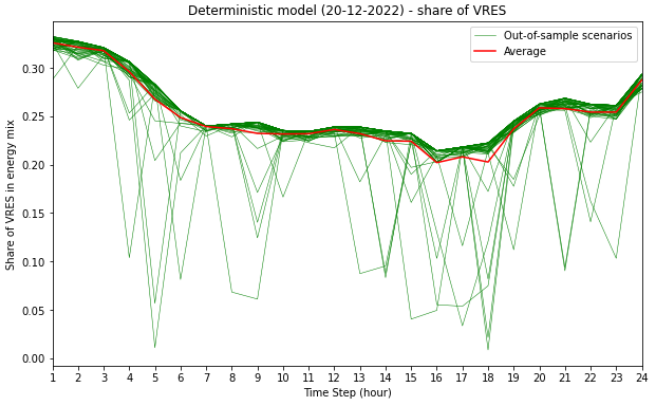
Deterministic model (20-12-2022) - share of VRES
Out-of-sample scenarios
Average
Share of VRES in energy mix
Time Step (hour)

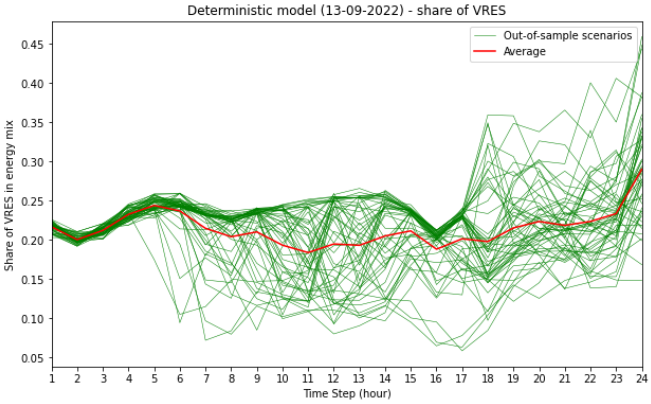
Deterministic model (13-09-2022) - share of VRES
Out-of-sample scenarios
Average
Share of VRES in energy mix
Time Step (hour)

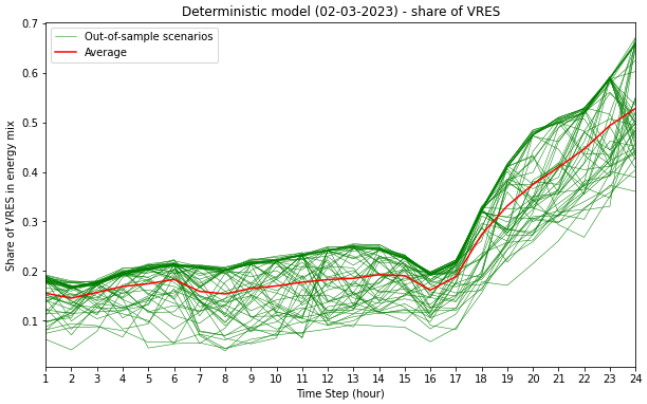
Deterministic model (02-03-2023) - share of VRES
Out-of-sample scenarios
Average
Share of VRES in energy mix
Time Step (hour)

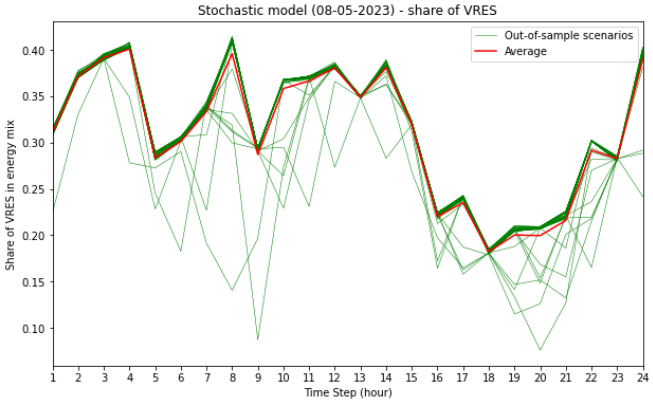
Stochastic model (08-05-2023) - share of VRES
Out-of-sample scenarios
Average
Share of VRES in energy mix
Time Step (hour)

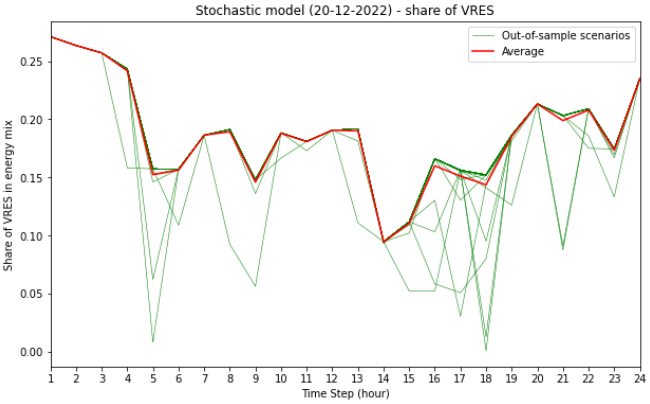
Stochastic model (20-12-2022) - share of VRES
Out-of-sample scenarios
Average
Share of VRES in energy mix
Time Step (hour)

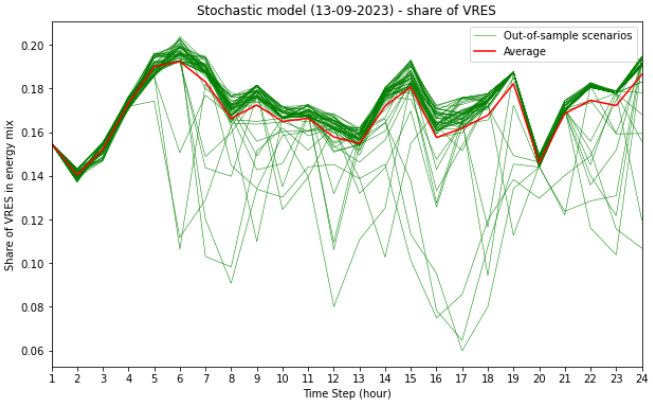
Stochastic model (13-09-2023) - share of VRES
Out-of-sample scenarios
Average
Share of VRES in energy mix
Time Step (hour)

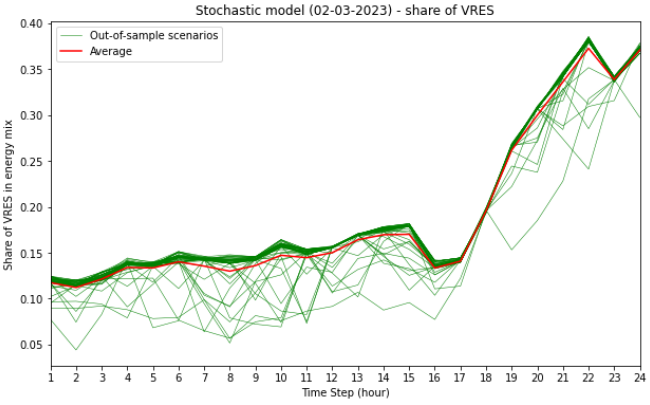
Stochastic model (02-03-2023) - share of VRES
Out-of-sample scenarios
Average
Share of VRES in energy mix
Time Step (hour)

Appendix D – Amount of wind spillage

D.1 In-sample analysis results – The Netherlands

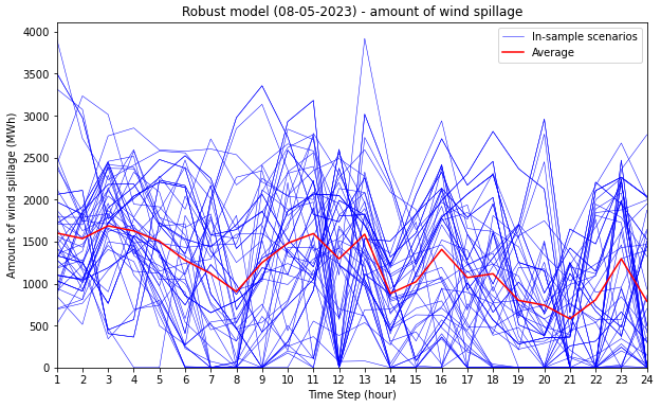

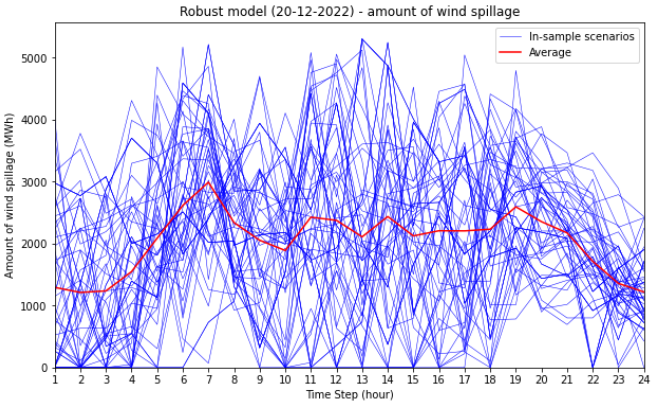

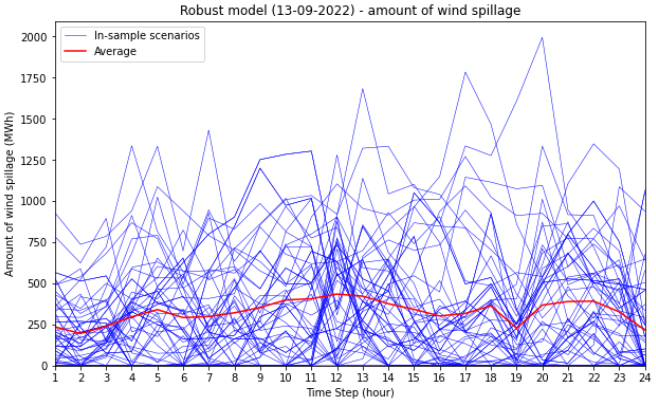

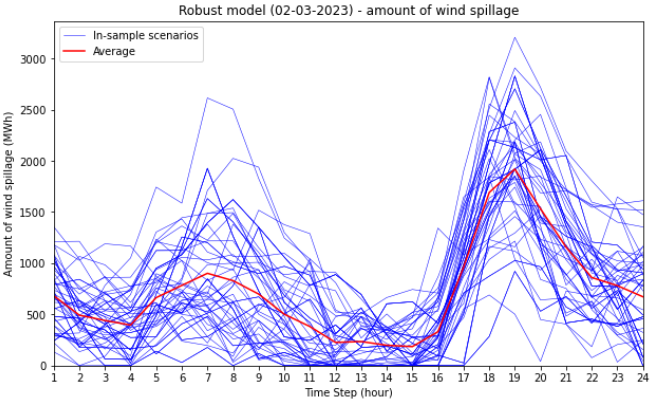

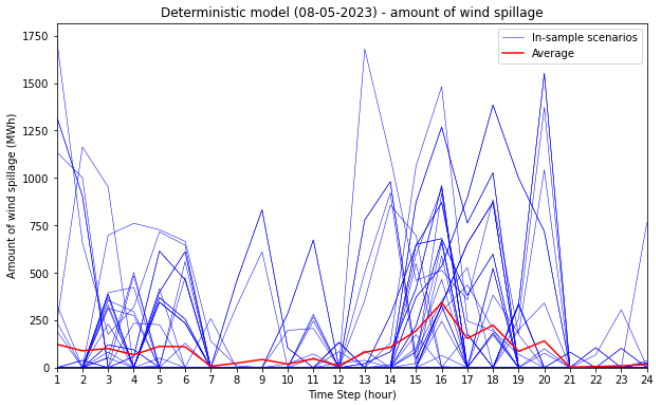

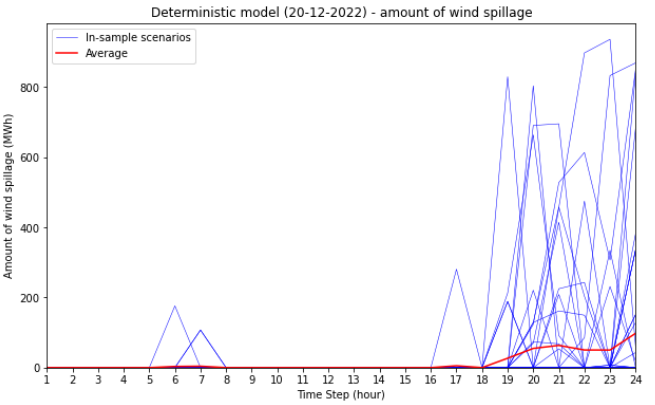

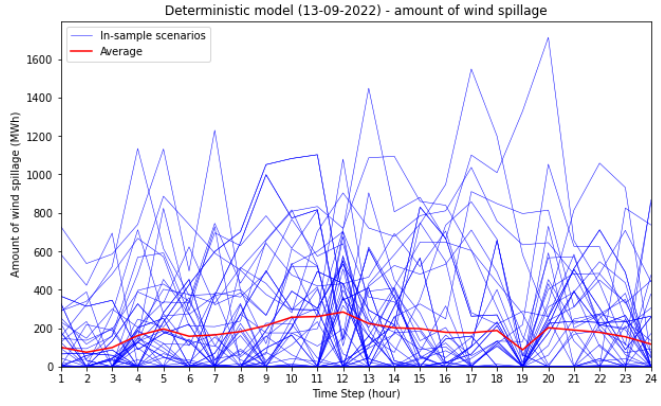

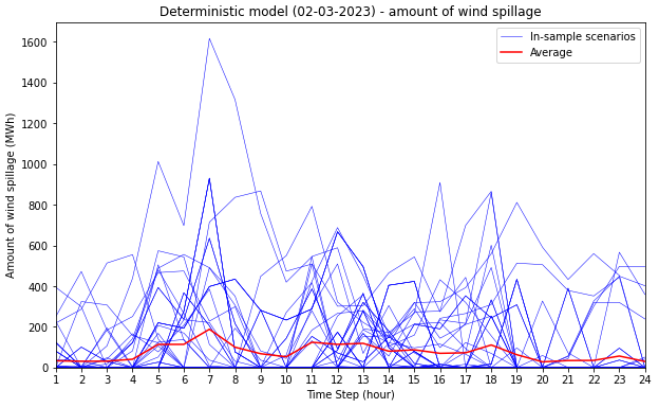

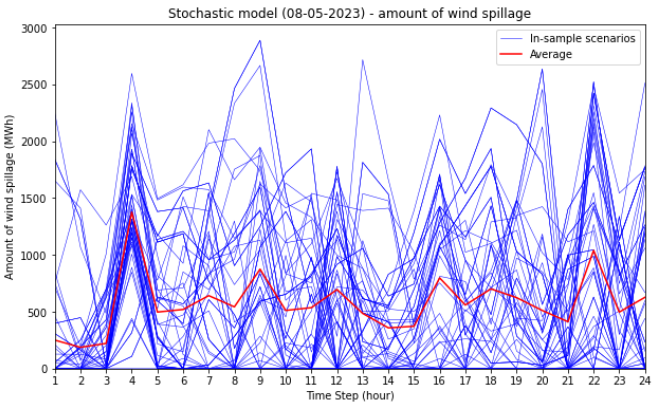

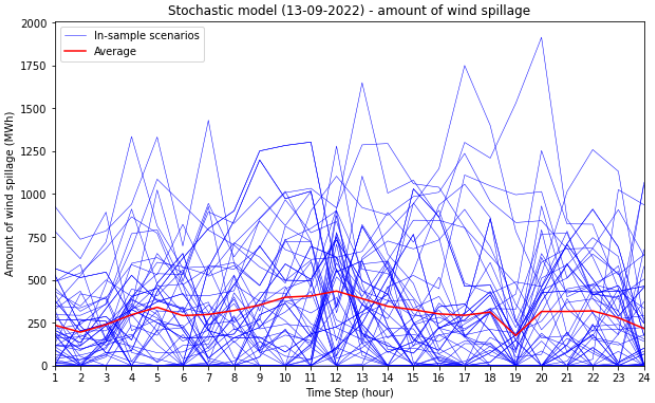

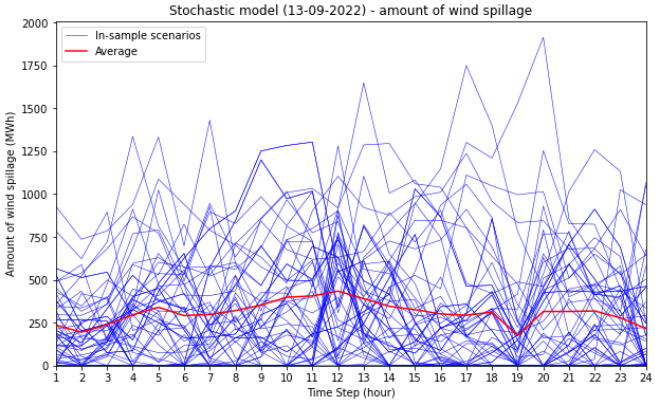

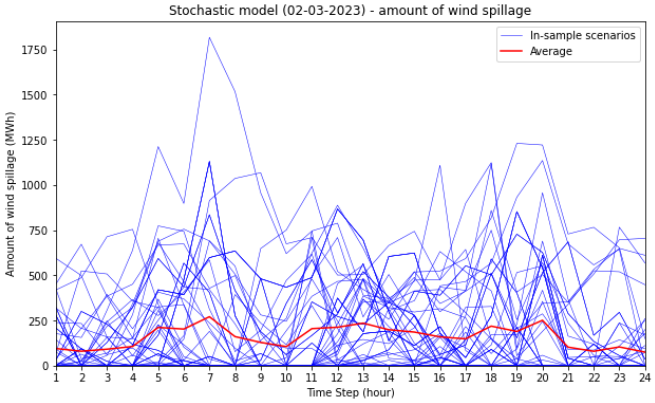

D.2 Out-of-sample analysis results – The Netherlands

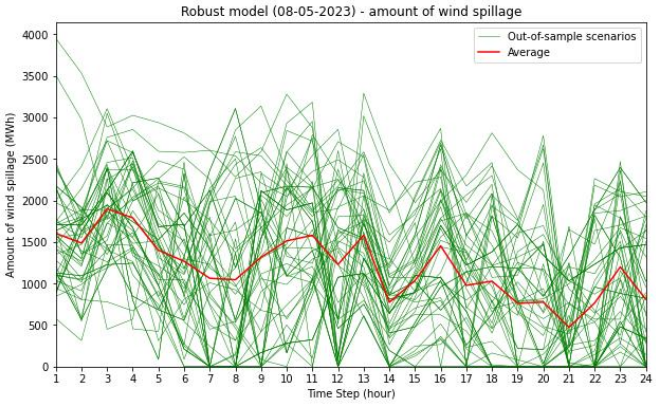

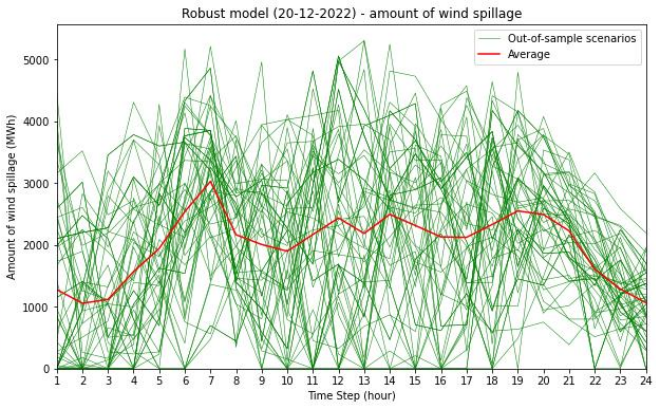

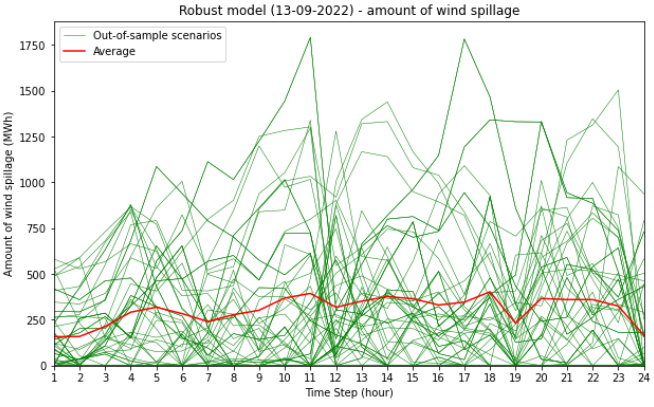

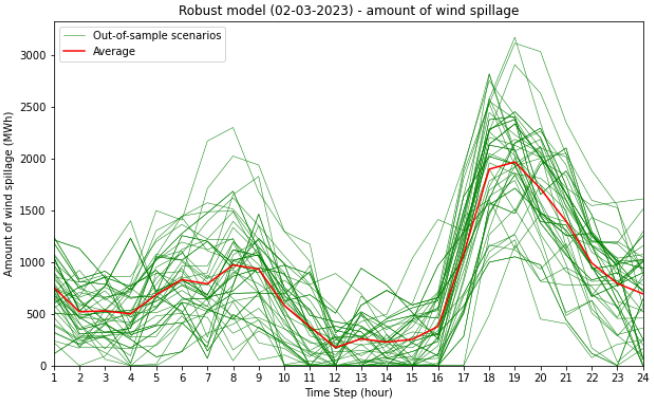

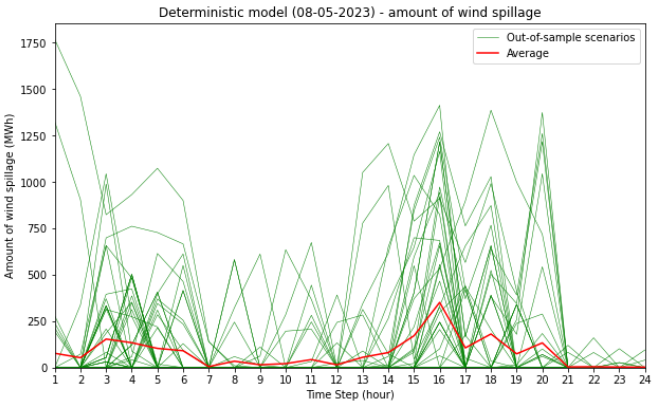
Deterministic model (08-05-2023) - amount of wind spillage
Out-of-sample scenarios
Average
Amount of wind spillage (MWh)
Time Step (hour)

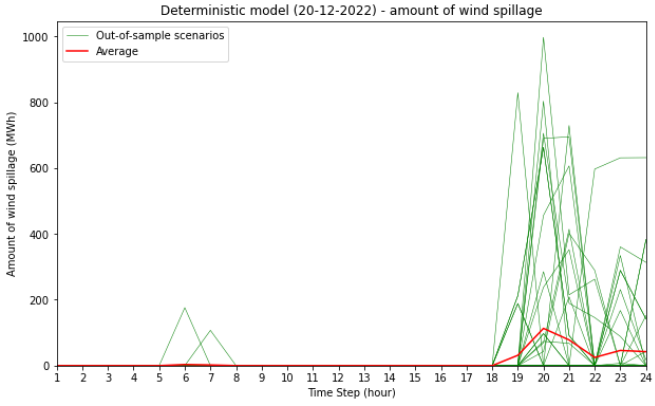
Deterministic model (20-12-2022) - amount of wind spillage
Out-of-sample scenarios
Average
Amount of wind spillage (MWh)
Time Step (hour)

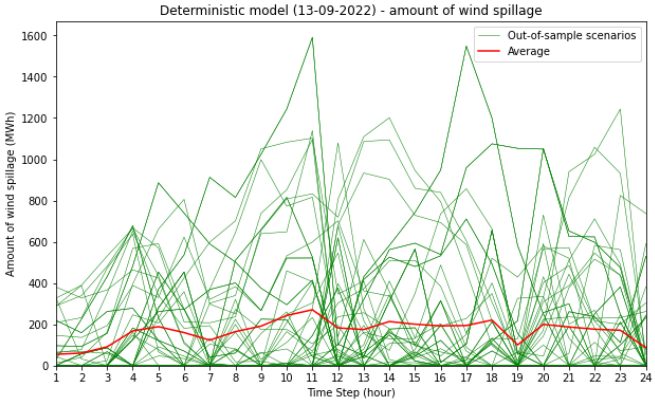
Deterministic model (13-09-2022) - amount of wind spillage
Out-of-sample scenarios
Average
Amount of wind spillage (MWh)
Time Step (hour)

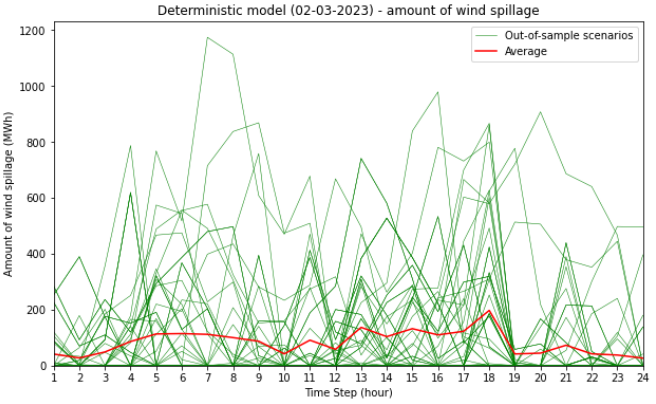
Deterministic model (02-03-2023) - amount of wind spillage
Out-of-sample scenarios
Average
Amount of wind spillage (MWh)
Time Step (hour)

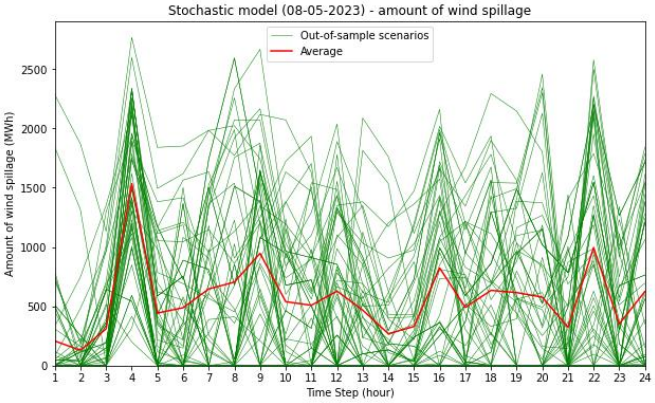
Stochastic model (08-05-2023) - amount of wind spillage
Out-of-sample scenarios
Average
Amount of wind spillage (MWh)
Time Step (hour)

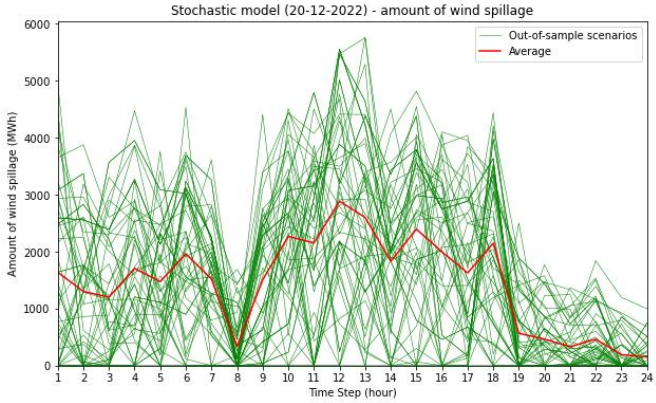
Stochastic model (20-12-2022) - amount of wind spillage
Out-of-sample scenarios
Average
Amount of wind spillage (MWh)
Time Step (hour)

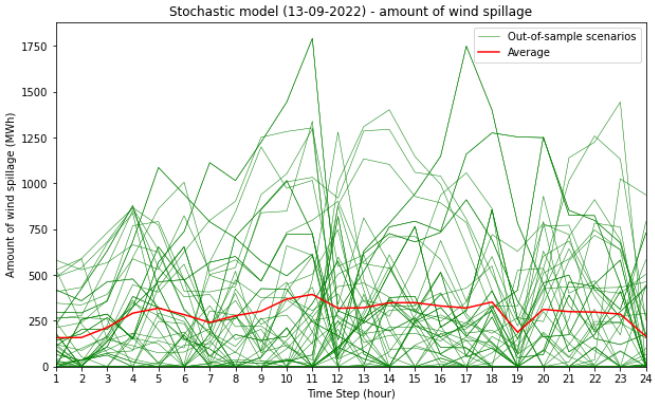
Stochastic model (13-09-2022) - amount of wind spillage
Out-of-sample scenarios
Average
Amount of wind spillage (MWh)
Time Step (hour)

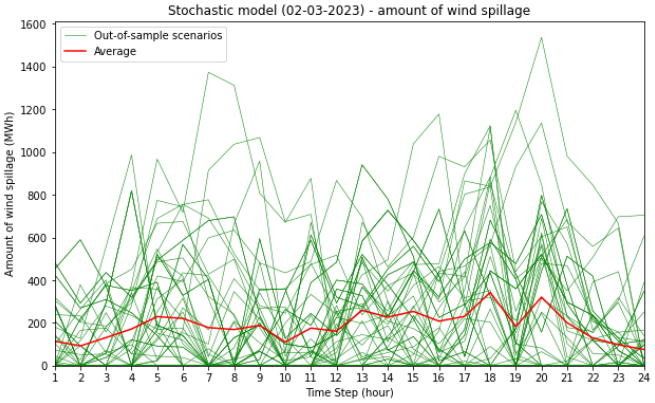
Stochastic model (02-03-2023) - amount of wind spillage
Out-of-sample scenarios
Average
Amount of wind spillage (MWh)
Time Step (hour)

D.3 In-sample analysis results – France

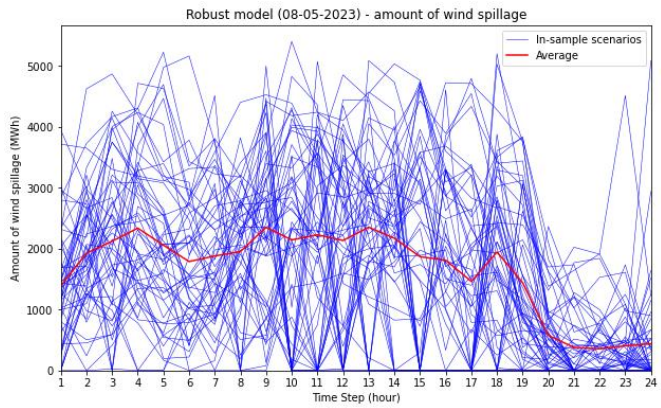

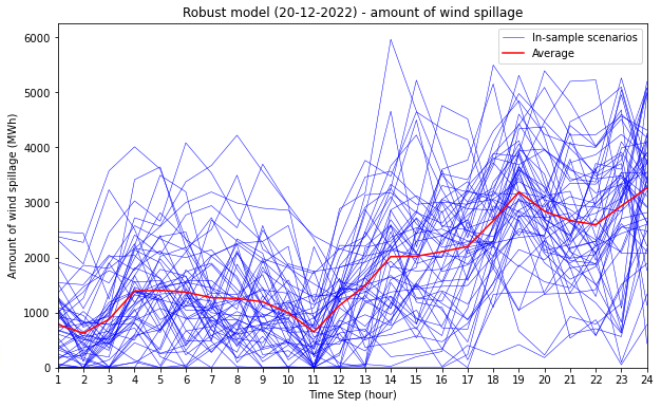

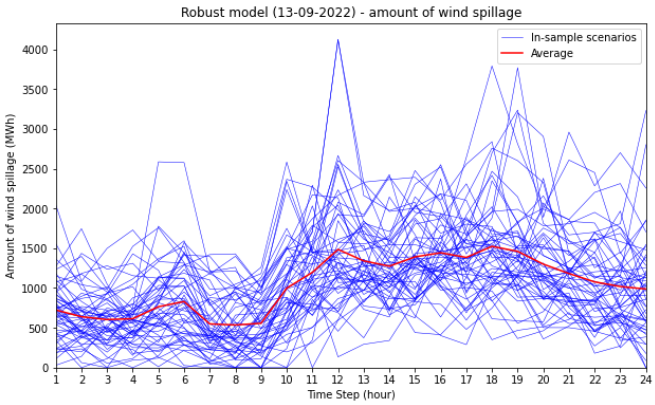

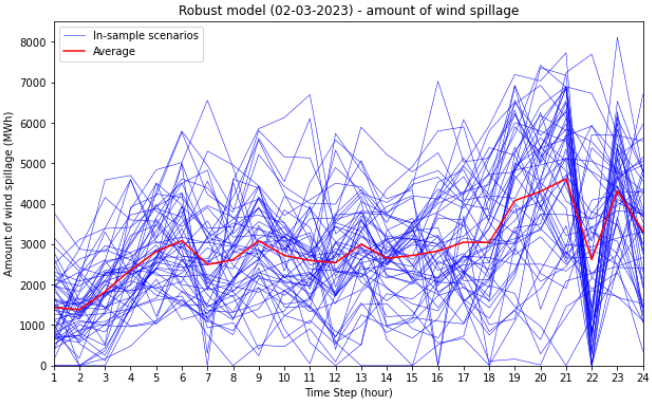

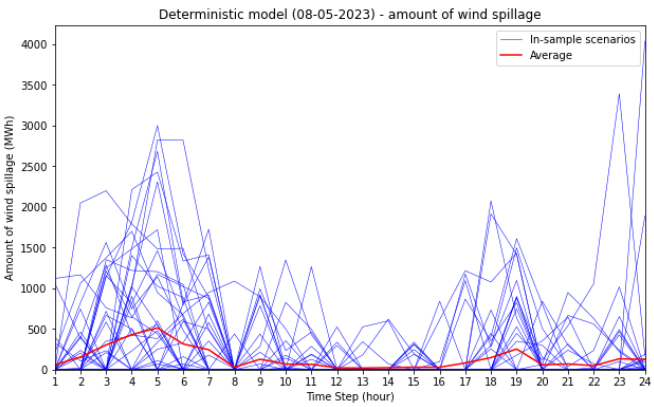

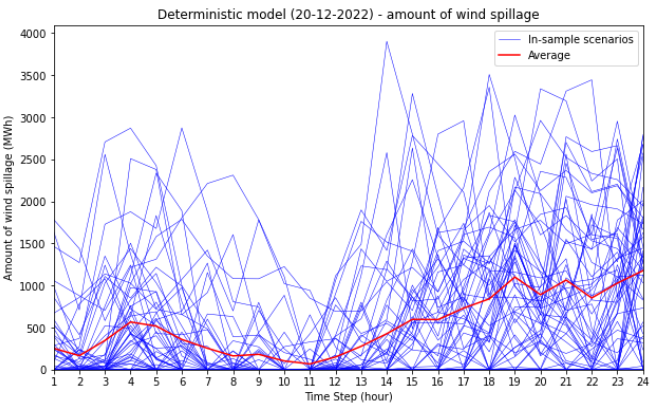

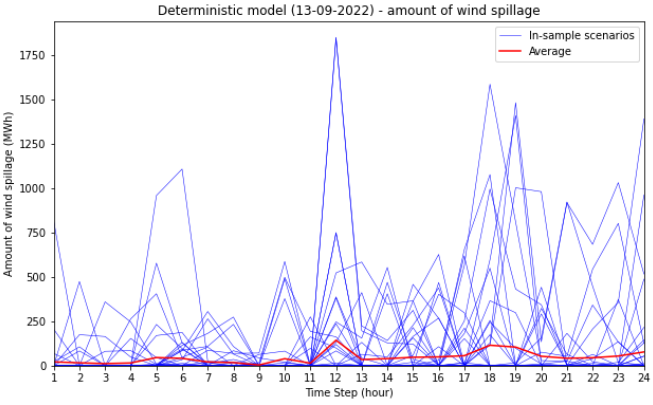

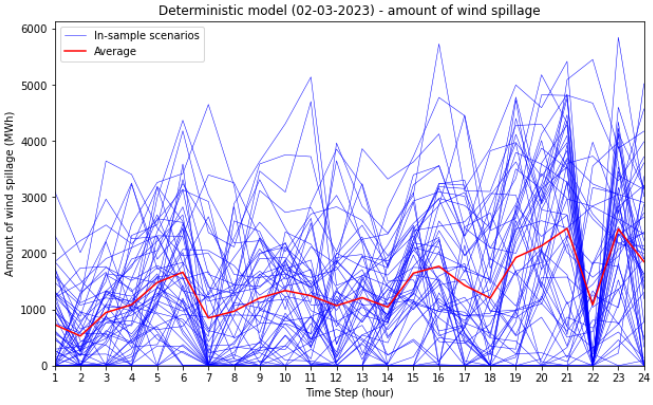

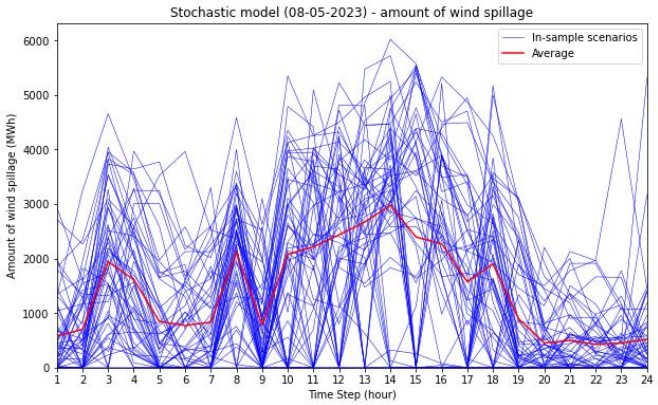

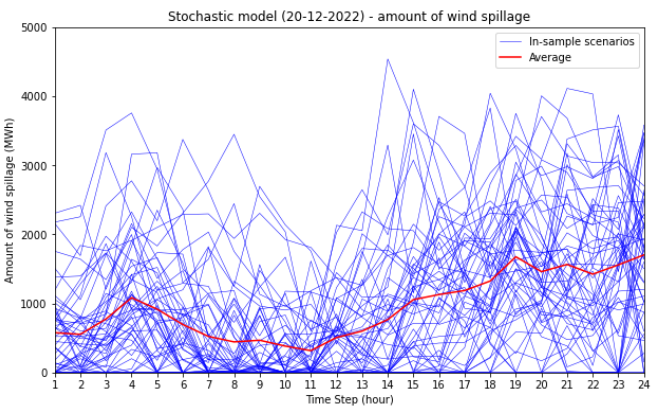

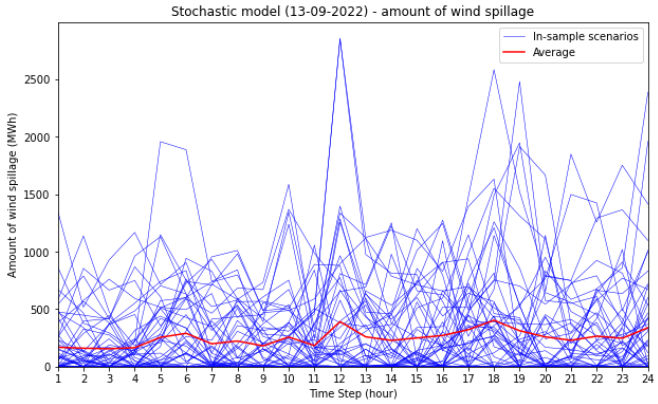

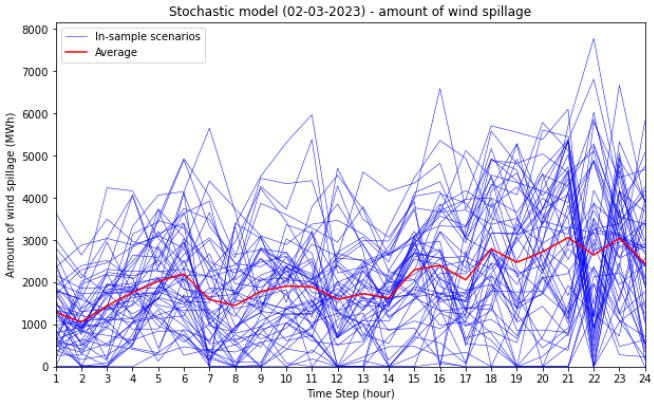

D.4 Out-of-sample analysis results – France

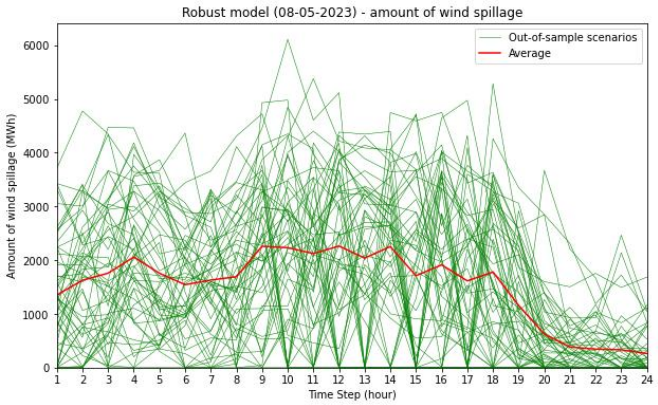

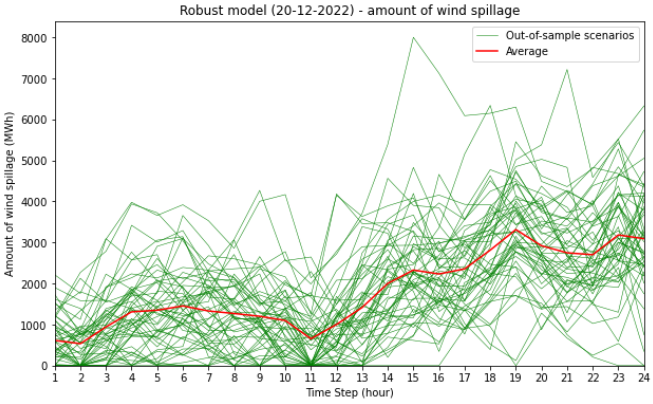

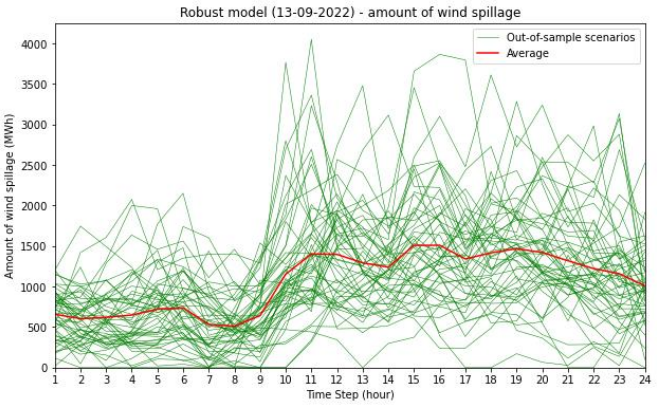

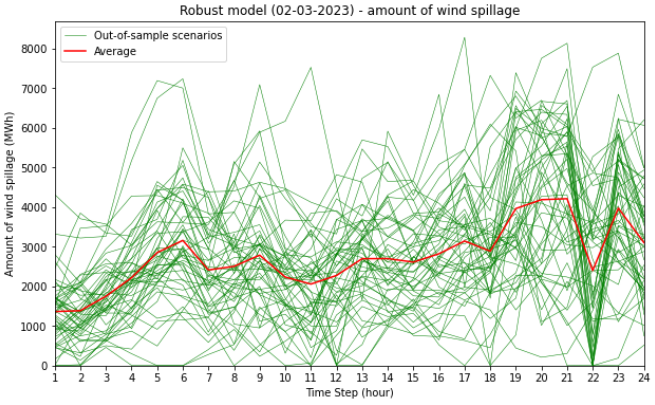

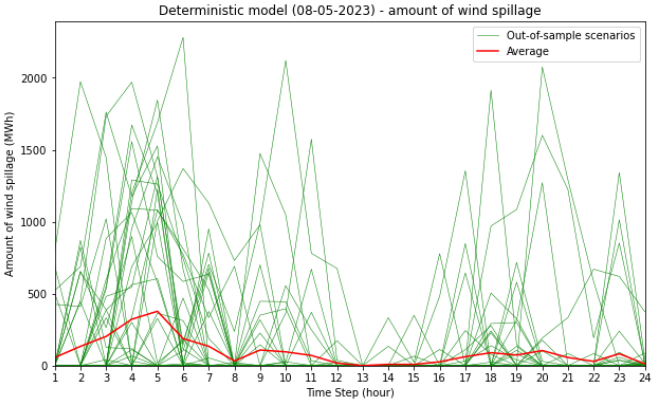
Deterministic model (08-05-2023) - amount of wind spillage
Out-of-sample scenarios
Average
Amount of wind spillage (MWh)
Time Step (hour)

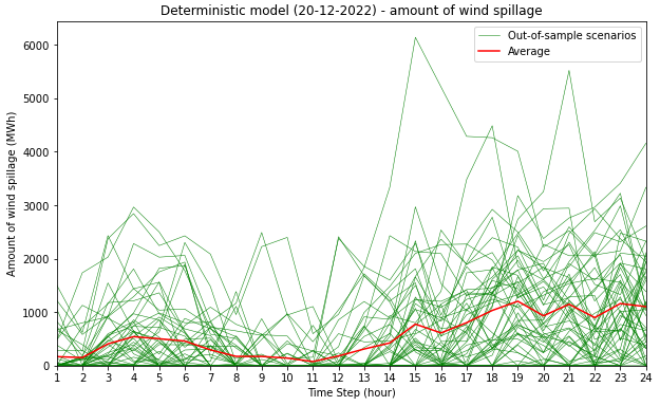
Deterministic model (20-12-2022) - amount of wind spillage
Out-of-sample scenarios
Average
Amount of wind spillage (MWh)
Time Step (hour)

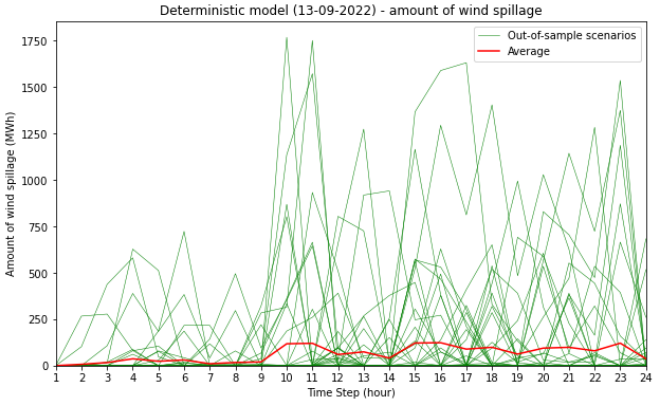
Deterministic model (13-09-2022) - amount of wind spillage
Out-of-sample scenarios
Average
Amount of wind spillage (MWh)
Time Step (hour)

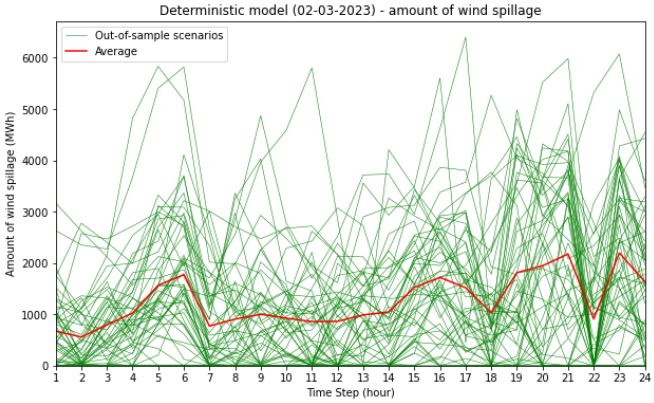
Deterministic model (02-03-2023) - amount of wind spillage
Out-of-sample scenarios
Average
Amount of wind spillage (MWh)
Time Step (hour)

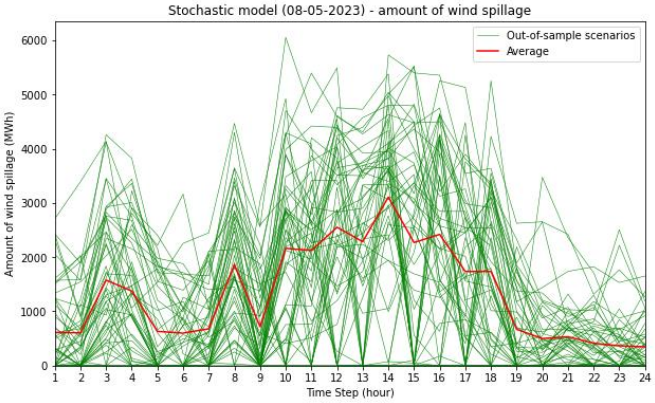
Stochastic model (08-05-2023) - amount of wind spillage
Out-of-sample scenarios
Average
Amount of wind spillage (MWh)
Time Step (hour)

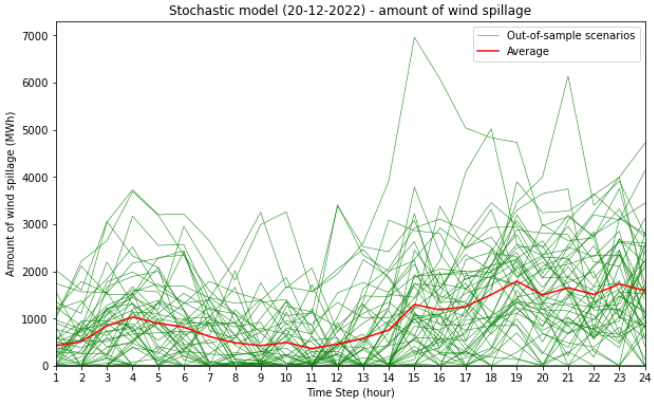
Stochastic model (20-12-2022) - amount of wind spillage
Out-of-sample scenarios
Average
Amount of wind spillage (MWh)
Time Step (hour)

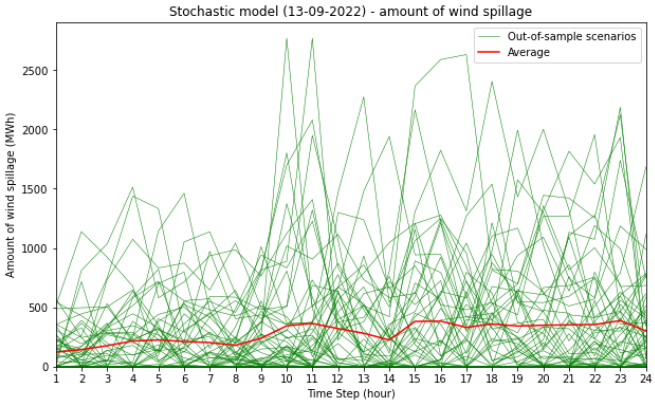
Stochastic model (13-09-2022) - amount of wind spillage
Out-of-sample scenarios
Average
Amount of wind spillage (MWh)
Time Step (hour)

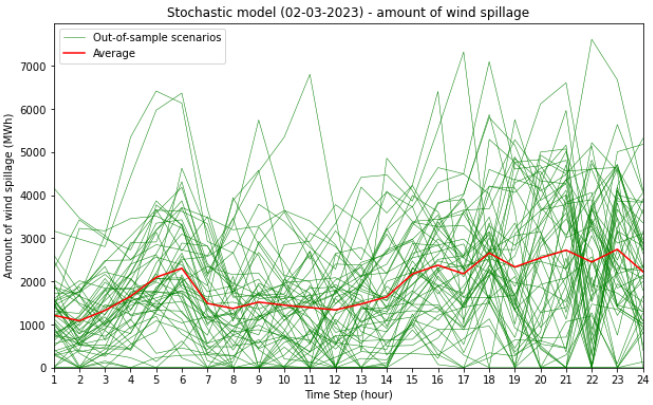
Stochastic model (02-03-2023) - amount of wind spillage
Out-of-sample scenarios
Average
Amount of wind spillage (MWh)
Time Step (hour)

D.5 In-sample analysis results – Germany

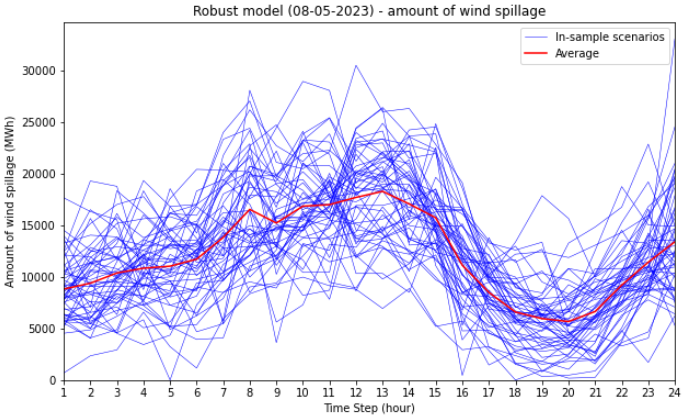

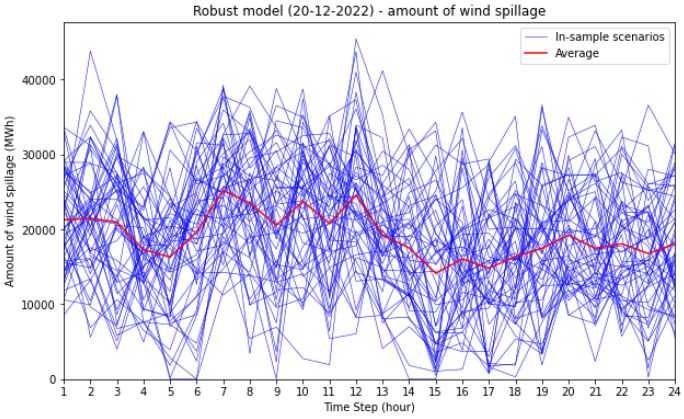

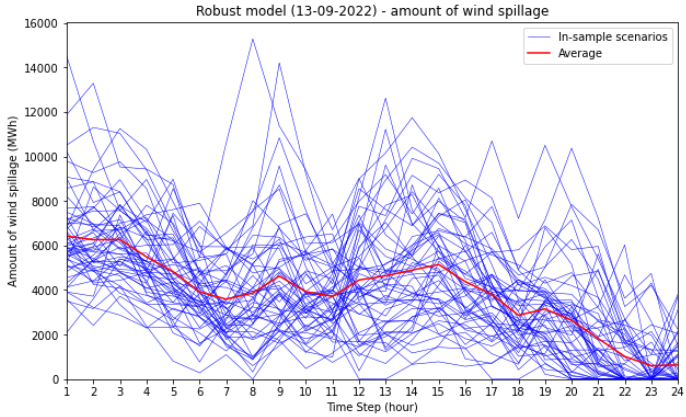

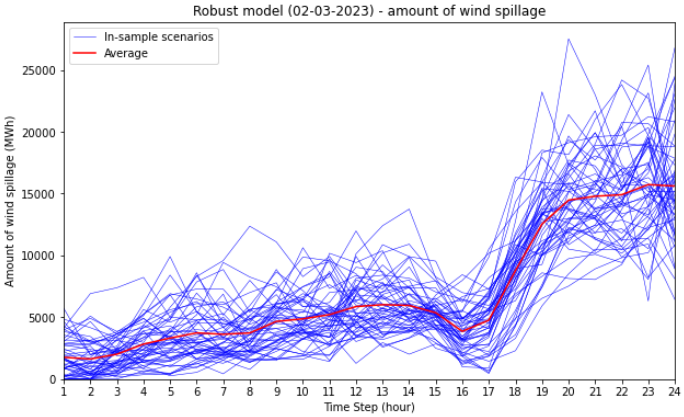

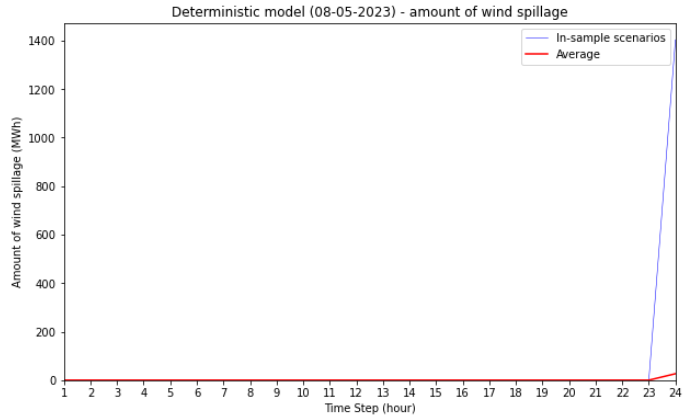

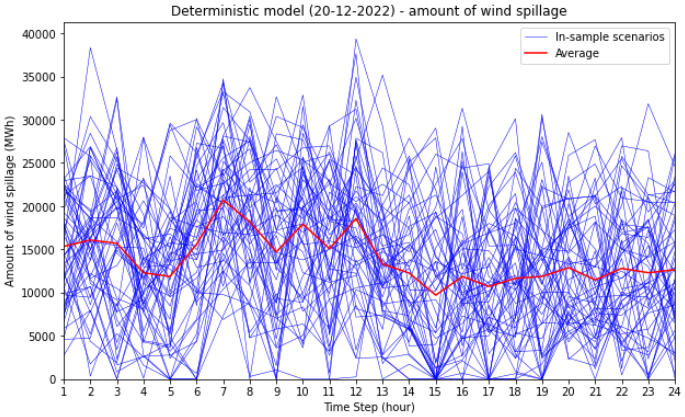

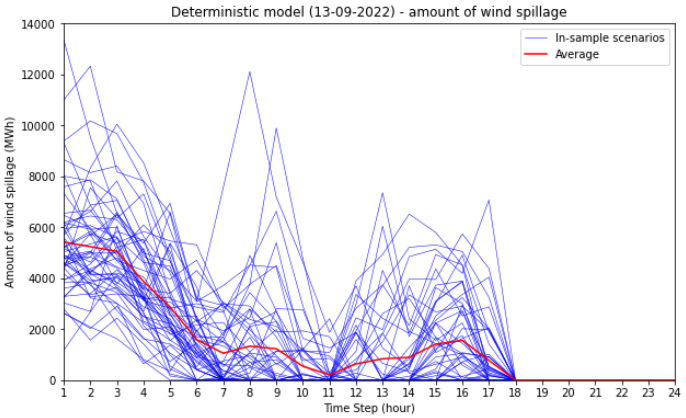

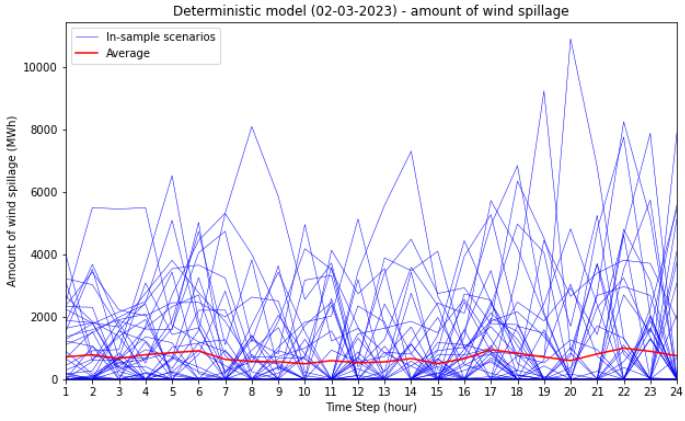

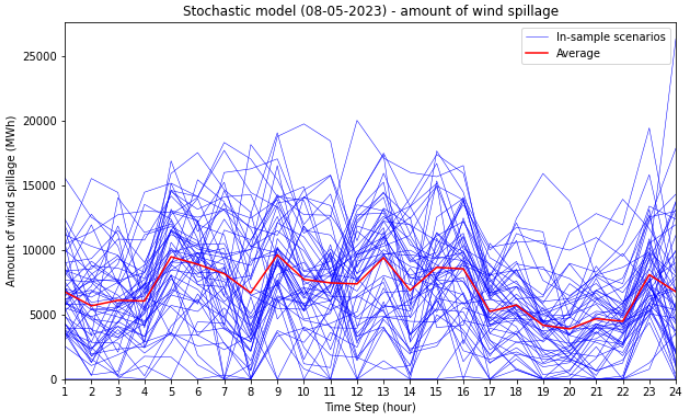

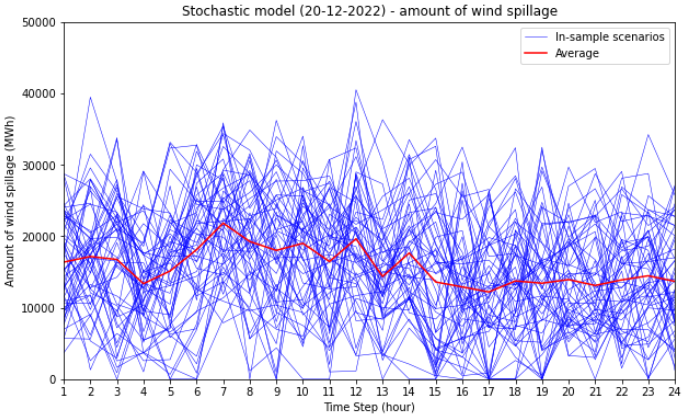

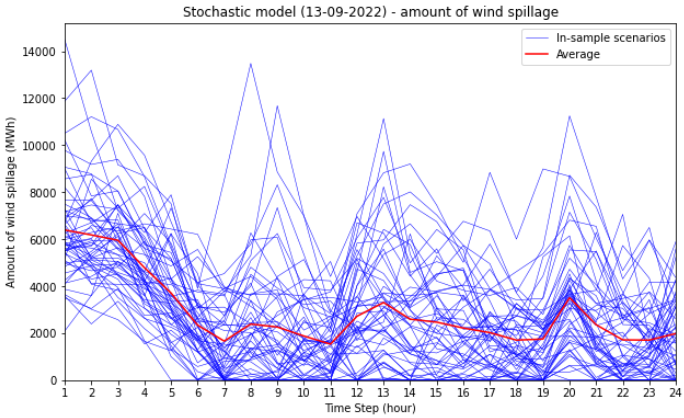

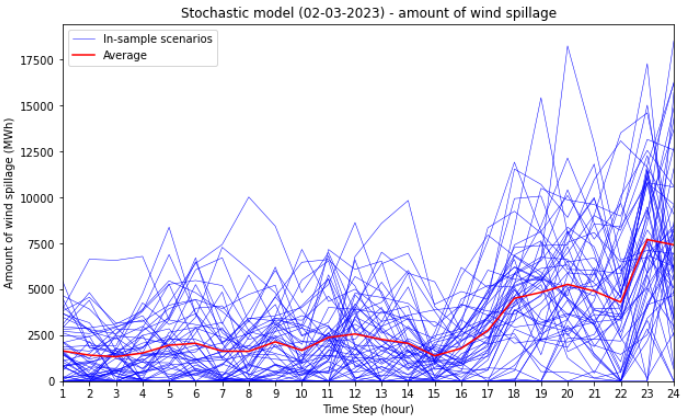

D.6 Out-of-sample analysis results – Germany

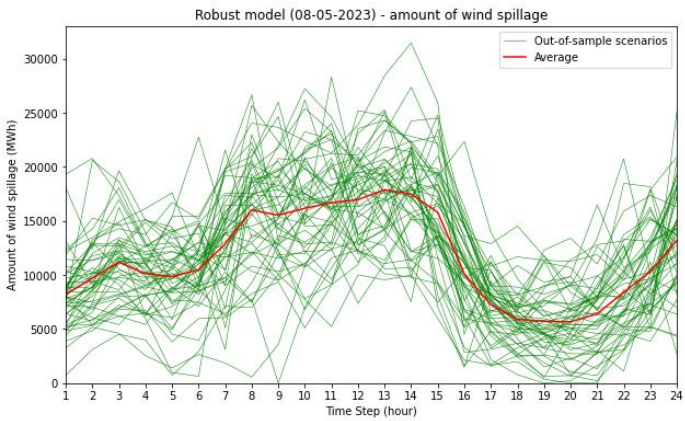

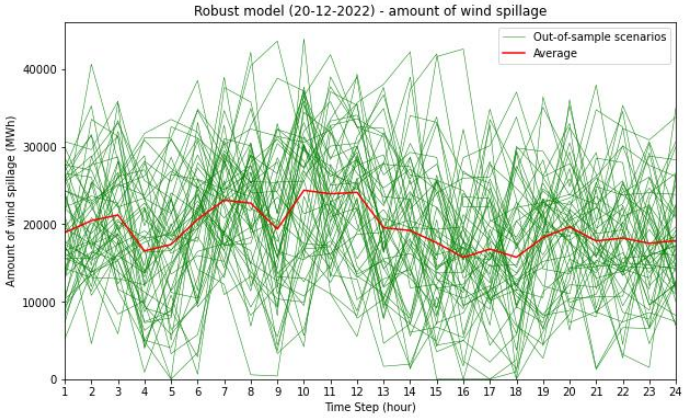

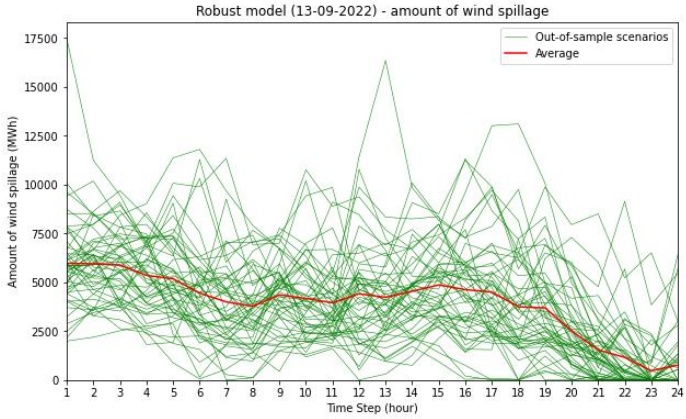

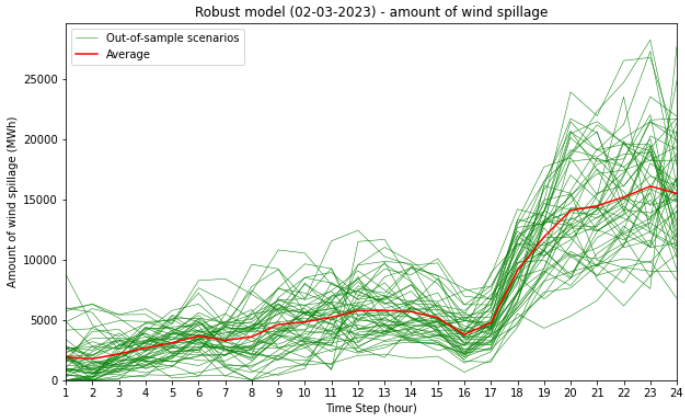

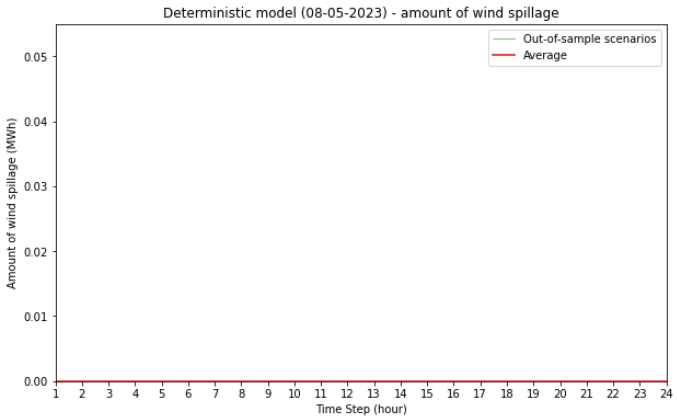
Deterministic model (08-05-2023) - amount of wind spillage
Out-of-sample scenarios
Average
Amount of wind spillage (MWh)
Time Step (hour)

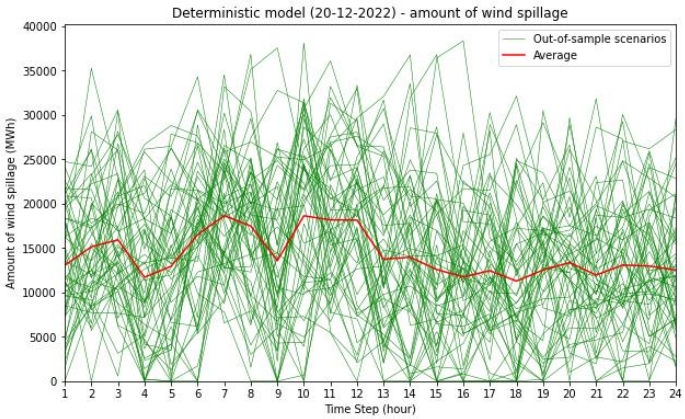
Deterministic model (20-12-2022) - amount of wind spillage
Out-of-sample scenarios
Average
Amount of wind spillage (MWh)
Time Step (hour)

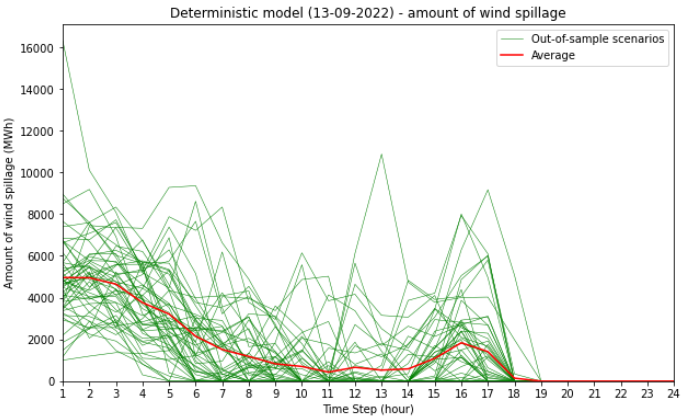
Deterministic model (13-09-2022) - amount of wind spillage
Out-of-sample scenarios
Average
Amount of wind spillage (MWh)
Time Step (hour)

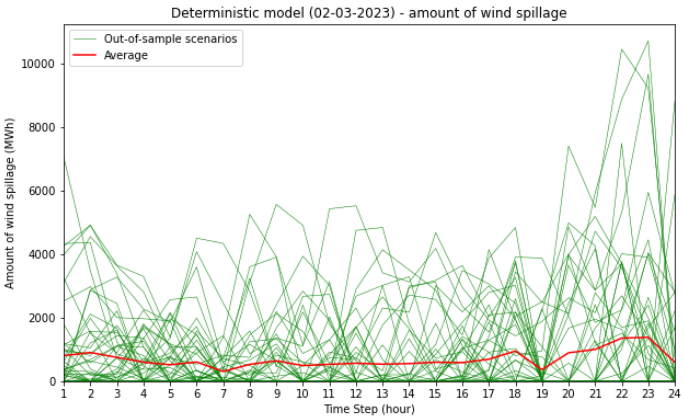
Deterministic model (02-03-2023) - amount of wind spillage
Out-of-sample scenarios
Average
Amount of wind spillage (MWh)
Time Step (hour)

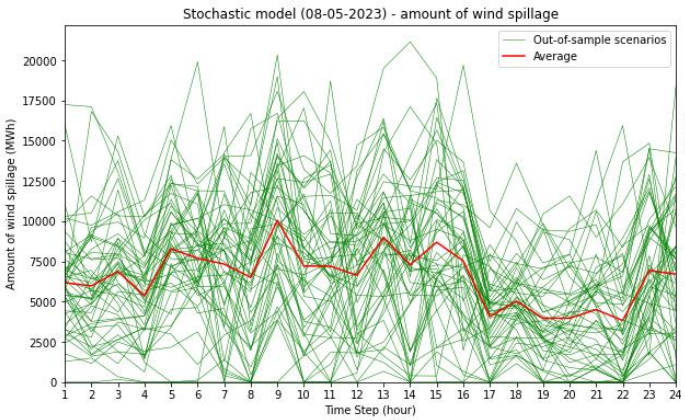
Stochastic model (08-05-2023) - amount of wind spillage
Out-of-sample scenarios
Average
Amount of wind spillage (MWh)
Time Step (hour)

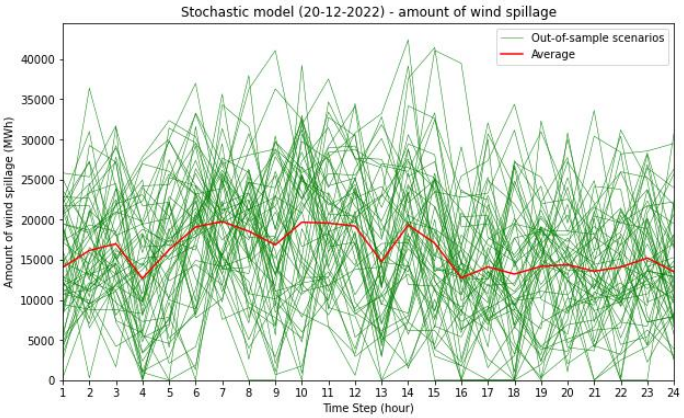
Stochastic model (20-12-2022) - amount of wind spillage
Out-of-sample scenarios
Average
Amount of wind spillage (MWh)
Time Step (hour)

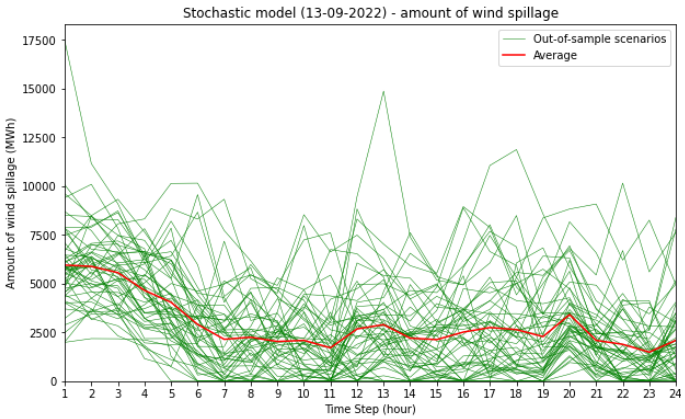
Stochastic model (13-09-2022) - amount of wind spillage
Out-of-sample scenarios
Average
Amount of wind spillage (MWh)
Time Step (hour)

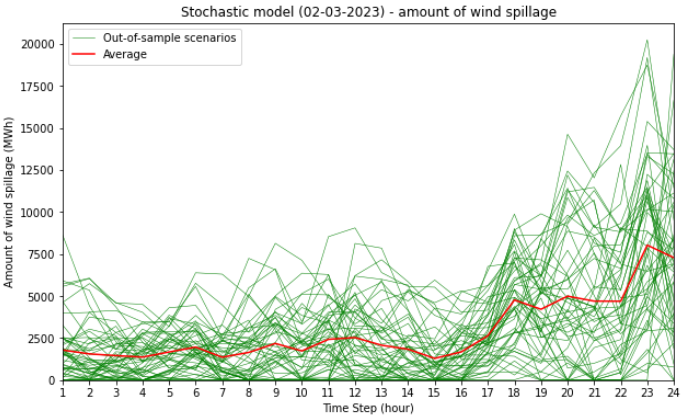
Stochastic model (02-03-2023) - amount of wind spillage
Out-of-sample scenarios
Average
Amount of wind spillage (MWh)
Time Step (hour)

Appendix E – Overview of deliveries

Content	File name
Meta data – [country]	*"Meta data – [country].xlsx"*
Deterministic model script code	*"DeterministicModel.py"*
Two-stage stochastic model script code	*"StochasticModel.py"*
Robust model script code	*"RobustModel.py"*
Model input data [date] – [country]	*"InputFinal – [country] [date].xlsx"*
Model input data sensitivity analysis	*"InputFinal - NL (20-12-2022) [in-sample size].xlsx"*
Case study results – [country]	*"Model Results – [country].xlsx"*
Sensitivity analysis results (in-sample size)	*"Model results - Sensitivity analysis (in-sample size).xlsx"*
Sensitivity analysis results (budget-of-uncertainty) – [country]	*"Model results – [country] - Sensitivity analysis (budget-of-uncertainty).xlsx"*
RESgen stochastic producer day ahead forecasts	*"[Stochastic producer].csv"*